

DISSERTATION

**EXAMINATION OF MOLECULAR GENETIC FACTORS
INVOLVED IN SENSITIVITY TO BREAST CANCER
FOLLOWING RADIATION EXPOSURE**

Submitted by

Abby J. Williams

Graduate Degree Program in Cell and Molecular Biology

In partial fulfillment of the requirements

For the Degree of Doctor of Philosophy

Colorado State University

Fort Collins, Colorado

Fall 2008

UMI Number: 3346475

INFORMATION TO USERS

The quality of this reproduction is dependent upon the quality of the copy submitted. Broken or indistinct print, colored or poor quality illustrations and photographs, print bleed-through, substandard margins, and improper alignment can adversely affect reproduction.

In the unlikely event that the author did not send a complete manuscript and there are missing pages, these will be noted. Also, if unauthorized copyright material had to be removed, a note will indicate the deletion.

UMI[®]

UMI Microform 3346475

Copyright 2009 by ProQuest LLC.

All rights reserved. This microform edition is protected against unauthorized copying under Title 17, United States Code.

ProQuest LLC
789 E. Eisenhower Parkway
PO Box 1346
Ann Arbor, MI 48106-1346

COLORADO STATE UNIVERSITY

October 31, 2008

WE HEREBY RECOMMEND THAT THE DISSERTATION PREPARED UNDER OUR SUPERVISION BY ABBY J. WILLIAMS ENTITLED EXAMINATION OF MOLECULAR GENETIC FACTORS INVOLVED IN SENSITIVITY TO BREAST CANCER FOLLOWING RADIATION EXPOSURE BE ACCEPTED AS FULFILLING IN PART THE REQUIREMENTS FOR THE DEGREE OF DOCTOR OF PHILOSOPHY.

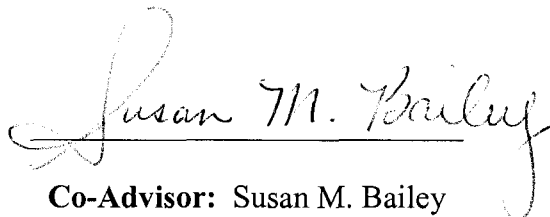
Committee on Graduate Work



Alice J. Sigurdson



Joel S. Bedford



Co-Advisor: Susan M. Bailey



Advisor: Robert L. Ullrich



Department Head: Paul Laybourn

ABSTRACT OF DISSERTATION

EXAMINATION OF MOLECULAR GENETIC FACTORS INVOLVED IN SENSITIVITY TO BREAST CANCER FOLLOWING RADIATION EXPOSURE

Understanding DNA repair is not only an important aspect of cell biology, but also has important implications for the field of carcinogenesis since cancer most likely occurs from genetic damage that occurs over one's lifetime. DNA repair needs to be accurate and efficient in order for a cell to maintain genomic stability, and defects in repair systems can result in radiosensitivity. Because radiation exposure, DNA repair deficiency and telomere malfunction are associated with cancer risk, we investigated Lymphoblastoid Cell Lines (LCLs) from breast cancer patients and controls for chromosomal radiosensitivity, relative telomere length, and gene expression changes. The importance of studying peripheral blood lymphocytes from cancer patients lies in the fact that minimally invasive techniques are lacking for the detection of individuals with high risk for cancer, and that telomere length has been proposed to be useful in this regard. Identification of radiosensitivity markers would be a valuable contribution for clinicians in hopes of avoiding excessive radiation or chemotherapy treatment given to patients.

Failure to adequately repair DNA damage can result in cell suicide or halting of cell cycle progression in an attempt to allow repair mechanisms to operate. If damage persists, a cell can be pushed toward transformation and the pathway of carcinogenesis. A second aspect of the current work was to study the Homologous Recombination double-strand break repair protein, Rad51D. The emerging interrelations

between DNA repair and telomere maintenance also prompted us to evaluate Rad51D's role in telomere function.

The final aspect of this research involved examination of how DNA repair related proteins are linked to the indirect effect of ionizing radiation exposure known as the bystander effect (BSE). We are the first to demonstrate that DNA-PKcs and ATM are required to generate, but not receive, a bystander signal. We also show that mouse embryonic fibroblasts do not generate bystander signals to neighboring cells, while their adult cell counterparts do.

Taken together, this work makes important contributions to our appreciation of the many and varied roles DNA repair related proteins play in maintenance of chromosomal integrity, proper telomere function, inhibition of carcinogenesis and now, regulation of the BSE.

Abby J. Williams
Graduate Degree Program in Cell and Molecular Biology
Colorado State University
Fort Collins, Colorado 80523
Fall 2008

ACKNOWLEDGEMENTS

This work would not have been possible without the contributions of so many. First I would like to thank my advisors, Dr. Robert Ullrich and Dr. Susan Bailey, for allowing me to work under their supervision and take advantage of their scientific expertise. I would also like to thank my committee members, Dr. Joel Bedford and Dr. Alice Sigurdson for supporting me throughout my graduate journey. It was an honor to have such a talented committee.

I am also grateful to several members of our laboratory who have also helped along the way. A special thank you goes to Dr. Tanner Hagelstrom and Dr. Kristin Askin for their collaboration with the bystander project, as well as always answering my questions when I was new to the lab. In addition, I'd like to thank Christine Battaglia for keeping the lab in order and for technical support. Thank you to Dr. Eli Williams for cytogenetic expertise, Dr. Ron Carsten for endless encouragement and new perspectives, and Phuong Le for traveling with me to scientific meetings and being so supportive.

I would also like to thank Dr. Edwin Goodwin for scientific and editorial advice. For collaborative efforts, I am thankful to Dr. Woody Wright, Dr. Michael Story and Dr. Douglas Pittman. A special thank you goes to Dr. Phil Smiraldo for collaborative work as well as scientific discussion and guidance.

To Jessica Goldstrohm and Julie Moreno, you have no idea how much your support and friendship has meant to me. Thank you for all the chat sessions and lunch breaks!

Finally, I would like to thank my family. My parents, Kraig and Martha Walker have always encouraged me to accomplish any goal I set in my mind. Thank you for always listening to me when times were rough. I want to thank my sister, Rachel, for supporting me throughout this time as well. I would like to especially thank my husband, Dustin, for putting up with my temporary insanity during this process. I am blessed to have many other friends and family members that have been right by my side every step of the way. Thank you for believing in me—I love you all dearly!

“A legitimate conflict between science and religion cannot exist. Science without religion is lame, religion without science is blind.”

-Albert Einstein, *Science, Philosophy and Religion: a Symposium, 1941*

DEDICATION

This work is dedicated to the love of my life, Dustin, for unlimited love and encouragement. We did it!

TABLE OF CONTENTS

Title	i
Signature Page	ii
Abstract	iii
Acknowledgements	v
Dedication	vii
Table of Contents	viii

Chapter 1. Introduction

<i>Introduction & Purpose</i>	2
<i>Breast Cancer</i>	5
Introduction	5
Lymphoblastoid cell lines from breast cancer patients & controls	7
<i>Ionizing Radiation</i>	12
Introduction	12
Bystander effect	12
IR and breast cancer	15
<i>Telomeres</i>	17
Introduction	17
Telomeres and breast cancer	21
Telomeres and IR	22
<i>DNA Double-strand break repair</i>	23
Introduction	23
DNA damage response	24
Non-homologous end joining	26
Homologous recombination	27
Rad51D	28
Homologous recombination and telomeres	32
DSB repair and IR	33
DSB repair and cancer treatment	34
<i>References</i>	36

Chapter 2. Materials & Methods

<i>Cell Culture</i>	49
Cell passage	50
Media	50
<i>Cytogenetic techniques</i>	51
Cell harvest	51
Slide preparation	53
Dropping slides	53
CO-FISH	53
FPG	57
G2 assay	58

Flow Cytometry Assays	59
Telomere flow FISH	59
γ H2AX foci flow.....	62
Bystander Effect experiments	64
Cell transfer assay	64
RNA isolation and gene expression	66
RNA isolation	66
Microarray analysis.....	66
Preparation of cDNA	68
Real Time PCR	69
Protein Analysis	72
Co-IP	72
Western blot.....	74
DNA Analysis	76
DNA isolation	76
PCR.....	76
DNA sequencing.....	78
Real Time PCR for telomere length	78
References	81

Chapter 3. Characterizing Lymphoblastoid Cell Lines from Breast Cancer Cases & Controls in the US Radiation Technologist Cohort: A Pilot Study.

Abstract.....	84
Introduction.....	85
Materials & Methods	87
Results.....	90
Discussion.....	97
References.....	104

Chapter 4. Characterizing the Role of RAD51D in Radiation Response in Human Cells and Telomere Maintenance in Rad51d-Deficient Mouse Cells.

Abstract.....	111
Introduction.....	112
Materials & Methods	115
Results.....	120
Discussion.....	128
References.....	135

Chapter 5. DNA-PKcs and ATM Influence Generation of Ionizing Radiation-Induced Bystander Signals.

Abstract.....	141
Introduction.....	142
Materials & Methods	145
Results.....	148
Discussion.....	159
References	166

Chapter 6. Mouse Embryonic Fibroblasts Fail to Generate a Radiation-Induced Bystander Response.

Abstract.....	171
Introduction.....	172
Materials & Methods	174
Results.....	176
Discussion.....	183
References	191

Chapter 7. Discussion

Introduction.....	195
LCLs	195
Rad51d.....	201
Bystander Effect.....	205
Conclusions & Future Directions.....	208
References.....	211

Appendices

I. List of Abbreviations	214
II. Summary of LCLs Patient Information	219
III. Microarray analysis design	220

Chapter 1

Introduction

Introduction & Purpose

Breast cancer is the most common cancer among women (besides skin cancer) in regards to incidence, accounting for more than 1 in 4 cancers diagnosed in US women (American Cancer Society, www.cancer.org Cancer facts and Figures, (Parkin 2004; Parkin *et al.* 2005)). Less than 10% of breast cancers are due to an inherited predisposition, for example from mutations in such genes as BRCA1 and BRCA2 (Claus *et al.* 1991; Rahman and Stratton 1998). This leaves a large percentage of breast cancers unexplained while certainly there are many contributing elements and risk factors such as parity, diet, age at menarche, to name a few. Our goal is to contribute new knowledge to this intricate puzzle by studying DNA repair mechanisms, radiation biology and telomere maintenance as they relate to carcinogenesis. Because breast cancer is an extremely complex and heterogeneous disease, one single diagnostic marker or treatment plan will not be sufficient for every woman. There is hope that identification of more informative markers will help individualize treatment plans and thus increase disease-free time and survival, as well as avoid over-treatment with excessive chemotherapy and radiation therapy, which can result in co-morbidities and secondary cancers.

A major focus of the present work was to characterize blood cell lines isolated from breast cancer patients and controls, all of whom belong to a radiation technologist cohort that has been studied for 25 years (Mohan *et al.* 2003; Sigurdson *et al.* 2003; Doody *et al.* 2006). We chose to investigate telomere length, response to radiation exposure and gene expression levels in 20 lymphoblastoid cell lines (LCLs) from these radiation technologists (10 breast cancer cases and 10 controls). Similar studies have previously reported the importance of each of these elements for possible screening

techniques, however to our knowledge, no one has combined multiple assays in the same study. This combination of endpoints provides an advantage to a more thorough understanding of the cellular changes that have occurred in each cell line. Interestingly, we observed a trend for longer telomeres and less radiation-induced damaged in the cases compared to the controls. These findings suggest that cells from breast cancer cases were able to proliferate with mutations, thus were capable of surviving and progressing toward the neoplastic phenotype, while damaged cells in the control set would undergo apoptosis and be lost.

Although it is unlikely that the cancer in any of the breast cancer patients involved in this study was due solely to their occupational radiation exposure (based on the multistep model of carcinogenesis in which multiple harmful mutations need to be acquired to fully progress toward cancer), it is still important to study low doses of ionizing radiation (IR) and identify markers of potentially sensitive individuals. It has been firmly established that IR can increase the risk of breast cancer at high doses and dose rates (Ronckers *et al.* 2005). However, most exposures are at low doses and dose rates where risks are not well defined. While the risk of cancer associated with *low* doses of ionizing radiation is not entirely clear at this time, it is believed that risk of cancer increases proportionally with increasing radiation dose received. Further, the impact of sensitive subpopulations on risks and the genetic differences that account for this sensitivity are not known. The relevance of low dose radiation exposures can be appreciated when considering not only occupational radiation exposure, but also diagnostic medical tests, frequent-flyer risks, space exploration and radiological terrorism (Brenner *et al.* 2003).

In addition to the direct effects of IR exposure, indirect effects such as the Bystander Effect (BSE) are also important considerations for both healthcare and radiological research. The BSE is observed when cells or tissues that are not directly hit with ionizing radiation behave as if they were, presumably via some signal(s) generated by a directly hit cell, which is then received by the non-hit cell. This phenomenon is not well understood, although it has been studied for a number of years. We evaluated the role of the DNA repair related proteins DNA-PKcs and ATM in the generation and/or reception of bystander signals to unirradiated cells and found that, at least in our system, both proteins are in fact necessary to generate (but not receive) a bystander response (Hagelstrom *et al.* 2008). In addition, we found that mouse embryonic fibroblasts (MEFs) do not generate a bystander signal, while “adult” mouse cells of the same genotype do (manuscript in preparation, see Chapter 6). Although these findings are perhaps surprising, conflicting reports and unanswered questions regarding the BSE and its mechanism(s) are currently common (for reviews see (Matsumoto *et al.* 2007; Morgan and Sowa 2007; Schwartz 2007)).

Finally, we investigated the role of the DSB repair protein Rad51d in telomere function, as it was shown to co-localize to telomeres via binding to TRF2 (Tarsounas *et al.* 2004). By using specific cytogenetic techniques, we evaluated telomere dysfunction in Rad51d-deficient MEFs and discovered that Rad51d is indeed needed to maintain genomic stability. Furthermore, gene expression levels of *RAD51D* and *EZH2* (the protein shown to down-regulate *RAD51D* and its related family members in breast cancer (Zeidler *et al.* 2005)) were assessed following IR exposure. The results show that *RAD51D* and *EZH2* respond in a similar manner to IR. Moreover, a low-penetrance

variant in *RAD51D* has been linked to breast cancer susceptibility (Rodriguez-Lopez *et al.* 2004), but no variant was found when 7 commonly studied immortalized human mammary epithelial cells lines were sequenced. Nevertheless, these results should not completely rule out the examination of this alternate allele because a much larger sample size would be necessary in order to unequivocally identify low-penetrance alleles.

This project emphasizes the relevance of interrelations between DNA repair, telomere maintenance, radiation effects and mammary carcinogenesis. Given that the results from this work only shed light on a fraction of the complexity of these fields, it remains certain that research in all of these areas must continue, not only for researchers to gain a better understanding of the underlying cellular mechanisms, but also to enhance the diagnosis and treatment of diseases related to each of these issues.

Breast Cancer

Introduction

Presently 12.3% (1 in 8) is the lifetime risk of developing breast cancer for a woman living in the US (www.cancer.org). Some risk factors include age, family history, race, radiation exposure at a young age, late menopause, hormone use and obesity (David Schottenfeld 2006). Breast cancer, as with most cancers, occurs when cells acquire sufficient genetic mutations to undergo transformation, no longer functioning under normal growth limitations. If not stopped, these transformed cells replicate, form a tumor and metastasize.

From 2000-2004 the median age at diagnosis of breast cancer was 61 years (www.cancer.org). Age is the most influential factor for breast cancer risk, followed by

family history. Interestingly, decreased telomere length, which also plays a role in tumorigenesis, correlates with increasing age as well (reviewed in (Aubert and Lansdorp 2008)). Additionally, high-dose radiation to the chest between the ages of 10 and 30 years also increases risk for breast cancer (Ronckers *et al.* 2005). Together these facts hint at a relationship between breast cancer, telomere function, and radiation. A woman's best chance at beating breast cancer is early detection and therefore, more improved and/or more options for screening methods would benefit all women. Therefore, we investigated radiosensitivity and telomere length in lymphoblastoid cell lines (LCLs) derived from breast cancer patients and controls.

Recently, breast cancer susceptibility alleles have been classified into three groups: rare high-penetrance alleles (such as BRCA1 and BRCA2), rare moderate-penetrance alleles (like ATM and PALB2) and common low-penetrance alleles (for example CASP8 and FGFR2), just to name a few (Stratton and Rahman 2008). Identifying more low-penetrance alleles would be highly beneficial, however obstacles arise when studying the relationship between genes and radiation in breast cancer, including the need for a large population to study who have been exposed to radiation as well as accurate estimates of dose to the breast and an appropriate control group (Ronckers *et al.* 2005). We have examined gene expression profiles (microarrays) of our LCLs to examine what role genetics may play in these samples. Although this pilot study has added to our overall understanding of breast cancer following IR exposure, additional factors need to be considered for clinical applications such as cost of materials, reproducibility of the assay, time to complete the assay and variability from human causes.

Lymphoblastoid Cell Lines from Breast Cancer Patients & Controls

Since the 1980s the National Cancer Institute (in collaboration with the University of Minnesota and the American Registry of Radiologic Technologists (ARRT)) has studied a nation-wide group of radiation technologists (Mohan *et al.* 2003; Sigurdson *et al.* 2003; Doody *et al.* 2006). This cohort, the United States Radiologic Technologists (USRT), is of particular interest since most human radiation studies to date involve high, acute doses of radiation, e.g. the Atomic bomb survivors or nuclear accidents like Chernobyl. In contrast, the radiation technologists were more likely exposed to chronic low doses of radiation. The USRT originally contained about 143,000 participants (not all of them were used in every study conducted), the majority of which were white women, with roughly 41% beginning their work as a radiation technologist before the age of 20 years and with the current mean age being approximately 55 years (Boice *et al.* 1992; Doody *et al.* 1998; Sigurdson *et al.* 2003; Bhatti *et al.* 2008). Criteria for participation in the study included ARRT certification for a minimum of 2 years during the years of 1926-1982 and residency in the U.S. (Boice *et al.* 1992; Doody *et al.* 1998). Of the study population (143,000 technologists), 92% were certified in radiography, 3% in nuclear medicine, 0.5% in radiation therapy and 4% in some combination of these categories (Boice *et al.* 1992). Questionnaires have been mailed to members of the cohort that provided information on work experience, personal diagnostic procedures, cancer risk factors, cancer diagnoses and other health and life-style information such as alcohol and tobacco use as well as reproductive history (Boice *et al.* 1992; Sigurdson *et al.* 2003; Sigurdson *et al.* 2007).

Several studies related to this cohort have been completed and most revealed an increased risk for cancer including breast cancer, leukemia, melanoma, thyroid, and basal cell carcinoma, specifically for those who were employed prior to the 1950s (Freedman *et al.* 2003; Sigurdson *et al.* 2003; Linet *et al.* 2005; Yoshinaga *et al.* 2005; Doody *et al.* 2006). In addition, SNP studies revealed a decreased risk of breast cancer with D302H in *CASP8* and an increased risk of breast cancer associated with *IL1a* in A114S (interleukin-1 α) (Sigurdson *et al.* 2007) as well as a SNP in *WRN* and 3 separate SNPs in *PRKDC* (the gene encoding DNA-PKcs) showing association with breast dose and risk of breast cancer in the USRT cohort (Bhatti *et al.* 2008). The COMET assay was also performed on LCLs from the USRT for breast plus other cancer, early-onset breast, thyroid cancer, long-lived cancer free, and cancer-free control groups, resulting in an association of increased endogenous DNA damage with increased cancer risk, which the authors relate to a reduced ability to regulate endogenous damage (Sigurdson *et al.* 2005).

Other countries besides the USA have also studied health effects in radiation workers. Medical diagnostic x-ray workers in China had significantly elevated risks for leukemia, skin cancer, breast cancer, lung cancer, bladder cancer and esophageal cancer, likely due to occupational exposure, as evaluated by cancer incidence from 1950 to 1995 (Wang *et al.* 2002). A study of British radiologists (1897-1997) revealed a 41% excess risk of cancer mortality if one was registered with a radiological society for more than 40 years. However, similar to the USRT cohort, there was no increase of cancer mortality for those first registered after 1954 (Berrington *et al.* 2001). In contrast, an examination of two radiotherapy departments in Denmark found no significant increased risk for

cancer among the staff, however the accumulated doses were relatively low and the number of participants was lower than other investigations (Andersson *et al.* 1991).

Even though the primary limitation to all radiation worker studies is the lack of exact radiation dose to the breast (or other areas of interest), there is some dose information available for the USRT since dosimetry badges were introduced around 1960 and dose estimates have been calculated based on work history, available film badge readings and chromosome translocation frequencies in PBLs (Simon *et al.* 2006; Bhatti *et al.* 2007). Several key advantages surround this study including the very large number of participants, the large percentage of women, the wide variety of radiation workers included, the long-term follow-up and the fairly detailed patient information based on medical records and questionnaires. Potential complications to keep in mind are the fact that patients need to have responded to the questionnaires, live to the time of survey and, for our studies, the fact that the LCLs were made post-diagnosis is a limitation to keep in mind.

We have studied twenty (20) Lymphoblastoid Cell Lines (LCLs) from early-onset breast cancer patients and controls (10 of each), all of whom were radiation technologists from the USRT cohort and none of whom carry BRCA mutations. These are peripheral blood lymphocytes (PBLs) that have been transformed with Epstein Barr virus (EBV) to maintain cell growth in culture. Although this is of possible concern, LCLs in early stages with normal diploid karyotypes possess little to no telomerase activity and are believed to be relatively normal; however they can become immortalized/tumorigenic but this may take 100 population doublings or more and results in aneuploidy, strong telomerase activity and other characteristics (Sugimoto *et al.* 2004). Thus, we performed

all LCL experiments at low passage (less than 15). We have evaluated relative telomere lengths via Telomere Flow FISH, chromosome radiosensitivity (the relative susceptibility of cells, tissues, or organisms to the damaging effects of radiation) via the G2 Assay, and gene expression changes via microarray analysis. While our sample size is small, this work is one of the first to evaluate PBLs from radiation workers using numerous endpoints and serves as a pilot study providing preliminary evidence for future, larger studies.

Previous publications have explored telomere length in blood cells, however to our knowledge, none of them have included radiation technologists. It is interesting that small doses of radiation received by these women may be a factor in development of breast cancer. Peripheral blood lymphocytes (PBLs) are widely used to evaluate radiosensitivity of normal tissues because normal cells are generally less heterogeneous than tumor populations and generally laboratory assays are more successful with normal cell samples (West 1995). Additional advantages include minimal invasiveness to obtain samples (blood draw), analysis is quick and results are reproducible, making these types of studies attractive for both the laboratory and the clinic (Bourguignon *et al.* 2005). In addition, previous studies have shown increased chromosome damage following X-irradiation in lymphocytes of breast cancer patients compared to controls (Baeyens *et al.* 2002), providing promise for use of PBLs in radiosensitivity screening.

Our microarray results indicate that VIPR2 (Vasoactive intestinal peptide receptor 2) is down-regulated in the LCLs of the breast cancer cases compared to the controls. VIPR2, also called VPAC2, is a G-protein coupled receptor found in the membrane of a variety cells (Wei and Mojsov 1996; Reubi 2000; Vaudry *et al.* 2000). Both pituitary

adenylate cyclase activating polypeptide (PACAP) and vasoactive intestinal peptide (VIP) can bind to these receptors. These homologous peptides function as neurotransmitters and neuroendocrine hormones, often as anti-inflammatory factors (Calvo *et al.* 1996; Gonzalez-Rey and Delgado 2005).

It is known that VIPR1/2 receptors are present in both normal and tumorigenic mammary epithelial cells (Garcia-Fernandez *et al.* 2005). VIPR receptors are often over-expressed in a variety of human tumors but specifically VIPR1 over-expression predominates in breast cancer (Reubi 2000; Reubi *et al.* 2000; Schulz *et al.* 2004). The over-expression of these receptors has been utilized in the clinic since VIP analogs have been used for PET imaging of breast cancers as well as for chemotherapeutic agents in both breast and lung cancer (Moody and Gozes 2007; Zhang *et al.* 2007).

Currently it is not clear exactly how VIPR1/VIPR2 expression is regulated in the immune system, however the presence of VIP binding sites in human primary T cells, LCLs and peripheral blood mononuclear cells has been shown (Beed *et al.* 1983; Wiik *et al.* 1988; Ottaway *et al.* 1990; O'Dorisio *et al.* 1992). Cells of the immune system also produce VIP (Leceta *et al.* 1996). It is known that when VIP binds to VIPR, cAMP production is stimulated in human lymphocytes, which then activates protein kinase A (PKA); this has specifically been demonstrated in PBLs (O'Dorisio *et al.* 1981; Ottaway *et al.* 1983; Guerrero *et al.* 1984; Calvo *et al.* 1986). Active PKA can affect different signaling pathways and can have a wide variety of effects on the cell, including changes in proliferation and cell cycle progression, among others. Exactly what changes and specific transcriptional regulation occurs in lymphocytes (and other cell types for that matter) as a result of these signaling networks is still under investigation.

Ionizing Radiation

Introduction

Ionizing radiation (IR) can be defined as energy with both wave-like and particle-like properties that is capable of ionization, the process of adding or removing one or more electrons from atoms, creating ions (Hall 2006). There are several different kinds of IR, but for these studies, gamma-rays from a ^{137}Cs source were used, which are high energy, low Linear Energy Transfer (LET), meaning they are very penetrating and disperse their energy at a low rate along their track, or pathway. In simple terms, IR causes DNA damage, which can cause cell death or help initiate carcinogenesis. The energy deposited by IR causes damage through both direct mechanisms (direct interaction with DNA) and by indirect mechanisms (interaction with water in the cell and creation reactive oxygen species (ROS) that can then damage DNA) (Hall 2006). Some DNA lesions caused by IR include base damage, single-strand breaks (SSBs), and one of the most detrimental types of damage, double-strand breaks (DSBs).

The Bystander Effect

The bystander effect (BSE) is the process by which a directly irradiated cell communicates its distress to a neighboring, non-irradiated cell, which then displays an effect. It has been proposed that the bystander signal is either ROS (Narayanan *et al.* 1997; Kashino *et al.* 2007), NOS (Shao *et al.* 2003), or cytokines (Shareef *et al.* 2007), that function either through gap junctions (Azzam *et al.* 1998; Azzam *et al.* 2001) or through media (Lehnert *et al.* 1997; Mothersill and Seymour 1998). While several biological endpoints are used to study the BSE, including micronuclei formation,

clonogenic survival, apoptosis, and sister chromatid exchange (SCE) (M'Kacher *et al.*), we used SCE as an evaluation of the BSE because they provide results promptly and accurately. Most importantly, SCE levels are not affected by direct low LET radiation.

SCE are thought to represent genomic instability and can be measured by the Fluorescence Plus Geimsa (FPG) technique developed by Wolff and Perry (Perry and Wolff 1974). This method works by utilizing bromodeoxyuridine (BrdU), a thymidine analogue. Cells cultured in the presence of BrdU will incorporate it into newly synthesized DNA strands. When cells reach a second round of replication in the presence of BrdU, again newly synthesized DNA will incorporate the analogue and at this point, the sister chromatids will be distinguishable by their BrdU substitutions. One chromatid will have an unsubstituted strand and a substituted strand, while the other chromatid will contain BrdU substitutions in both strands. Differential staining can be visualized by FPG, which degrades DNA strands substituted with BrdU using UV and a hot salt solution and results in “harlequin” stained chromosomes. The chromatid with one BrdU substituted and one unsubstituted DNA strand will stain more darkly with Geimsa compared to the doubly substituted chromatid, which will appear lighter in color since it had more degradation due to more BrdU being present. A “color switch” indicates a SCE has occurred (Figure 1).

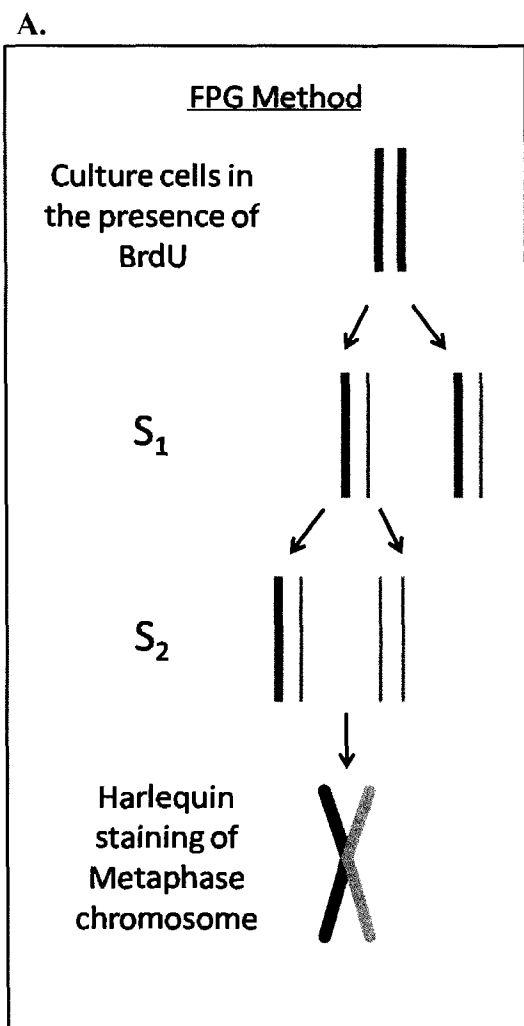
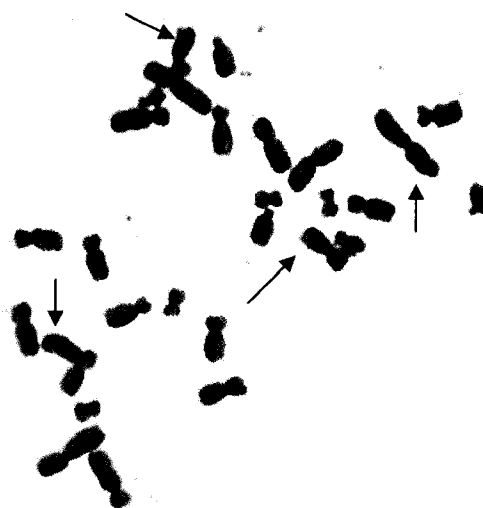


Figure 1. FPG. A. Diagram of the FPG process. Green strands are newly synthesized and incorporate BrdU. After two rounds of replication the sister chromatids are differentially substituted with BrdU. B. Partial human metaphase spread showing harlequin staining and several SCEs.

B.



Presently it is uncertain what the mechanism of the BSE is, thus it warrants further exploration. Due to our interest in radiation and carcinogenesis, as well as DNA repair, we investigated the role of various DNA repair proteins in the BSE. First we studied DNA-dependent Protein Kinase catalytic subunit (DNA-PKcs) and Ataxia Telangiectasia Mutated (ATM: see Double-strand break repair section) using a novel cell transfer assay we developed (Hagelstrom *et al.* 2008). We discovered that human AT^{-/-} cells can receive a bystander signal from neighboring cells but they cannot generate one. We also showed that cells from the wild-type C57BL/6 mouse (wild-type DNA-PKcs) generate a bystander signal in response to IR, whereas cells from the BALB/c mouse

(DNA-PKcs deficient) did not generate a bystander response in unirradiated neighboring cells. It has been demonstrated by numerous investigators that various DNA repair related proteins may have roles in the induction of the BSE. For example, Chinese hamster ovary (CHO) cells deficient in Rad51C, Rad51D, XRCC2, XRCC3 and BRCA2 did not appear to induce a BSE following treatment with low doses of alpha particles (Nagasawa *et al.* 2008). Additionally, like many aspects of the BSE, contradictory reports exist claiming both that p53 status does not affect the production of or response to bystander signals (Kadhim *et al.* 1996; Zhang *et al.* 2008) and also that when p53 is mutated, no BSE is observed (Ryan *et al.* 2008). Results from our cell transfer work suggest that p53 is needed to generate a bystander signal as no BSE is observed from p53^{-/-} mouse cell transfer experiments (see chapter 6).

During our investigation of the relationship between DNA repair proteins and the BSE we discovered that mouse embryonic fibroblasts (MEFs) are not capable of producing a bystander response in our system. A variety of MEFs and their genotypically corresponding “adult” fibroblasts were used to demonstrate that while irradiated primary adult mouse fibroblast donor cells could produce an increase in SCE frequency in human fibroblasts recipient cells, none of the MEFs could produce an effect.

IR and breast cancer

It is important to study IR not only to increase our understanding, but also because it is capable of increasing cancer risks and is a major tool in the diagnosis and treatment of breast cancer. It is known from various animal and human studies that the mammary gland is especially sensitive to the effects of radiation exposure. Exactly why

this is true is not understood but likely it is a result of the interaction of multiple factors including the type of radiation received, the dose and dose-rate of the radiation, fractionated vs. non-fractionated exposures, age at exposure and certainly genetic elements, just to name a few.

Currently, the most informative data regarding human breast cancer induction from IR exposure comes from studies of the Hiroshima and Nagasaki atomic bomb survivors, which suggest that excess risk of breast cancer is proportional to the radiation dose received (Land *et al.* 2003; Ronckers *et al.* 2005). These studies also re-emphasize that radiation-related breast cancer risk is much higher among women exposed at a younger age (adolescence or childhood) compared to women exposed at older ages (Land *et al.* 2003). An analysis that pooled 8 cohorts of women previously exposed to radiation (either A-bomb survivors or from diagnostic or therapeutic procedures) illustrated again the importance of age at radiation exposure and cancer risk and also suggested that women with some benign breast conditions may have a larger risk for radiation-related breast cancer (Preston *et al.* 2002). These authors also suggest that radiation-associated breast cancers occur at the same ages as spontaneous breast cancers (Preston *et al.* 2002). Still, one must remember that although radiation exposure at any age increases cancer risk, age at exposure, genetic predisposition and likely environmental factors as well, contribute to risk of developing breast cancer.

More recent evidence suggests that women with mutations in the DNA repair related genes p53, PTEN, CHEK2, ATM, NBS1, BRIP1, and PALB2 (in addition to BRCA1 and BRCA2) may be more susceptible to radiation-induced breast cancer compared to women without these mutations (Bernstein *et al.* 2006; Broeks *et al.* 2007;

Cardis *et al.* 2007). Previous studies have also shown that patients with bilateral breast cancer showed statistically higher amounts of γ -radiation-induced chromatid breaks (G2 assay) in their lymphocytes when compared to controls (Rubio *et al.* 2002). Furthermore, evidence for heritability of this radiosensitivity has been reported after completing the G2 assay on radiosensitive or normal individuals and their first-degree relatives (Roberts *et al.* 1999). Taken together, these data support the notion that some women may be more susceptible to damage from radiation, particularly when a family history and/or DNA repair related mutations are present.

We used the G2 chromosome assay to evaluate radiosensitivity of our USRT cohort LCLs. The G2 assay assesses chromatid-type aberrations following a fairly low dose of radiation given to PBLs (in this case LCLs). Several investigations previously utilized this method and demonstrated associations between breast cancer and increased chromosomal radiosensitivity (Roberts *et al.* 1999; Scott *et al.* 1999; Baeyens *et al.* 2002).

Telomeres

Introduction

Telomeres are the capping structures at the ends of linear chromosomes that allow cells to discriminate between the natural chromosome ends and broken DNA ends (DSBs) (de Lange 2002; de Lange 2005; Rodier *et al.* 2005). More specifically, mammalian telomeres consist of tandem arrays of 5'-TTAGGG-3' repeats as well as a plethora of telomere-binding and telomere-associated proteins (Ferreira *et al.* 2004; Rodier *et al.* 2005). Three proteins bind directly to telomeric DNA (in mammals), TRF1

(Telomere Repeat Factor), TRF2 and POT1 (Protection of Telomeres) (Figure 2). Other proteins, both with telomere and/or DNA repair functions, then bind to these proteins, building complex structures at the end of chromosomes. In addition, a 3' single-stranded overhang exists that, in one current structural model, loops back and invades into the double-stranded DNA and forms a t-loop (Griffith *et al.* 1999; de Lange 2002; de Lange 2005). Human telomeres are approximately 5-15kb in length but shorten as aging occurs, primarily due to the end replication problem (Levy *et al.* 1992; Allsopp *et al.* 1995), but also from direct damage, oxidative stress or mutated/deficient telomeric proteins (Blackburn 1990; de Lange 2002; Espejel *et al.* 2002; Jaco *et al.* 2004; Rodier *et al.* 2005; Richter and von Zglinicki 2007). Dysfunctional (shortened) telomeres are thought to contribute to tumorigenesis predominantly by promoting genetic instability, through inappropriate fusion events, allowing progressively malignant phenotypes to surface (Rodier *et al.* 2005; Bailey and Murnane 2006).

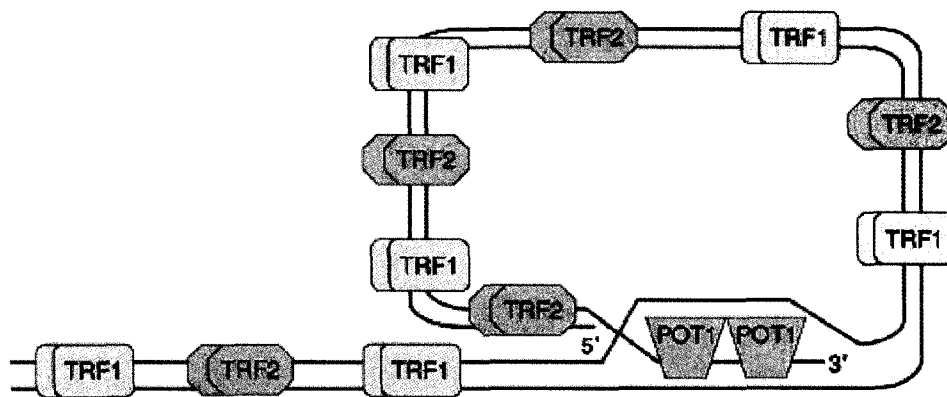


Figure 2. Schematic of a mammalian telomere. This simplified diagram illustrates the end-capping function of telomeres, composed of both DNA and proteins. *Image from (Rodier et al. 2005).*

Interestingly, some DNA repair proteins are now emerging as having roles in telomere function as well (d'Adda di Fagagna *et al.* 2004; Slijepcevic and Al-Wahiby 2005). This is noteworthy since normal telomeres protect the ends of chromosomes from being recognized as DSBs and thus prevent improper initiation of DNA repair mechanisms. Previously our lab has shown the importance of DSB repair proteins (especially DNA-PKcs) in telomere end-capping function independent of shortening (Bailey *et al.* 1999; Bailey *et al.* 2004). Together this information illustrates the significance of telomeres because of their relationship to DNA repair and carcinogenesis, as well as their potential role as markers in the clinic.

One way to study telomere function is by utilizing Chromosome Orientation Fluorescence *in situ* Hybridization (CO-FISH) (Bailey *et al.* 1996; Bailey *et al.* 2004). CO-FISH is a strand-specific modification of FISH and is a powerful laboratory tool. By growing cell cultures in the presence of BrdU, newly synthesized strands of DNA are targeted for degradation while the original parental strands are left largely intact and serve as the template for binding of complementary probes (Bailey *et al.* 2004). For our objectives, CO-FISH has provided insight into leading-strand versus lagging-strand telomere dysfunction. Figure 3 provides an illustration and brief description of the CO-FISH process. For more detailed information, see Chapter 2: Materials & Methods.

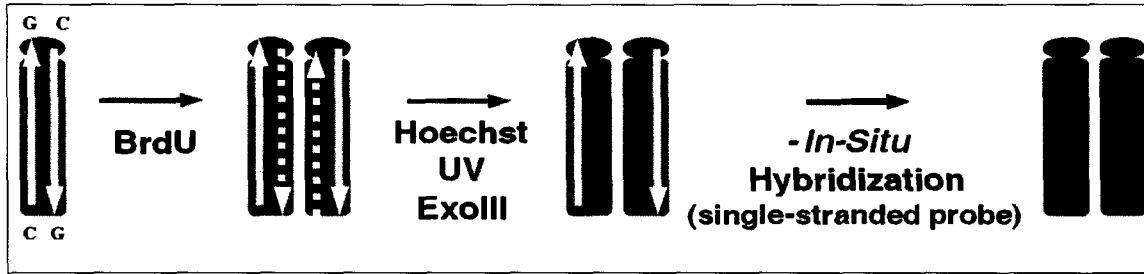


Figure 3. CO-FISH. Since BrdU is incorporated only into the newly synthesized DNA strand (dotted yellow line), treatment of metaphase spreads with Hoeschst dye and UV light creates nicks at those sights, which are then digested by Exonuclease III. DNA probes can then be used to target either the leading-strand telomere or the lagging-strand telomere, depending on the sequence of the probe. *Image courtesy of SM Bailey.*

There are numerous ways to evaluate telomere lengths in the laboratory including Quantitative FISH (Q-FISH), Telomere Flow FISH, Real-Time PCR, Single telomere length analysis (STELA) and Terminal Restriction Fragment (TRF) lengths (Cawthon 2002; Baird 2005). We attempted to utilize the Real-Time PCR method (Cawthon 2002) for telomere length analysis in the LCLs since it is quantitative and can be completed relatively quickly, making it ideal for numerous samples. However, attempts by various individuals in our laboratory have produced inconsistent results. The assay worked in the sense that the Real-Time PCR produced data, but the PCR efficiency was very low and the results were extremely variable. It should be noted that other investigators obtained reasonable results using this method (Nordfjall *et al.* 2005; Shen *et al.* 2007; Trkova *et al.* 2007; O'Callaghan *et al.* 2008), nevertheless we concluded that this method is unreliable in our hands. We instead used Telomere Flow FISH, with much improved results, which are discussed in Chapter 3.

Telomeres and Breast Cancer

Many investigations into the relationship between breast cancer and telomere length show promising results for telomeres as prognostic indicators. It has been shown that shorter telomeres were present in breast carcinomas that had metastasized compared to carcinomas that had not metastasized, supporting a relationship between telomere length (shortening) and tumor aggressiveness (Griffith *et al.* 1999). In addition, in invasive breast carcinoma, reduced levels of telomeric DNA were associated with aneuploidy, which serves as a marker for genetic instability (Griffith *et al.* 1999). Despite having active telomerase, the enzyme responsible for lengthening telomeric DNA, most human carcinomas, including that of the breast, still have trouble maintaining adequate telomere length (Dahse *et al.* 1997). Poor clinical outcome has also been associated with telomere shortening not only in breast cancer but also in cases of lung cancer, neuroblastoma, leukemia and endometrial cancer (Dahse *et al.* 1997), strengthening the potential use of telomeres as markers in a variety of cancers. Furthermore, by measuring telomeric DNA content (TC), Jeffrey Griffith's laboratory has shown that TC is associated with stage and prognosis in breast cancer and is predictive of breast cancer-free survival interval (Fordyce *et al.* 2006; Heaphy *et al.* 2007). Interestingly, other studies have shown that distinct telomere shortening occurs in ductal carcinoma *in situ* (DCIS), the stage prior to invasive ductal carcinoma (IDC), suggesting that telomere loss in IDC is not due to further cell proliferation but rather occurs at the pre-invasive level and thus may help initiate invasiveness (Meeker *et al.* 2004; Meeker *et al.* 2004). Similar results also revealed telomere shortening in the secretory ducts of normal breast terminal duct lobular units (TDLU), from which most breast cancers are

thought to arise, while this shortening was not observed in tissues that breast cancer rarely arises from (Meeker *et al.* 2004). Previous reports also reveal increased mRNA expression levels of the telomere-binding proteins TRF1 and TRF2 in non-cancerous tissues compared to cancer samples (Saito *et al.* 2002). An increase in dicentric chromosomes and telomeric associations (TA) in peripheral blood lymphocytes of patients with breast cancer has also been reported as significantly increased compared to controls (Paz-y-Mino *et al.* 1997), supporting our investigation of LCLs and telomere length. Finally, Fordyce, et al., show that telomere DNA content is associated with tumor size, nodal involvement, TNM stage, 5-year overall survival, and 5-year disease-free survival in breast cancer, which may be useful to physicians for preliminary staging prior to treatment (Fordyce *et al.* 2006). Collectively these results emphasize the value of evaluating telomeres in breast cancer staging.

Telomeres and IR

Telomeres may act as sensors that relate to a cell's ability to respond to genotoxic stress, including IR, which further integrates telomeres into the link between radiosensitivity and predisposition to cancer (Slijepcevic 2004). Several reports have linked shorter telomeres with increased radiosensitivity. For example, studies of murine lymphoma cells revealed a major reduction in telomere length in radiosensitive cells compared to radioresistant cells and similarly, shorter telomeres in lymphocytes from breast cancer patients are linked with greater sensitivity to IR (McIlrath *et al.* 2001). Analysis of human fibroblasts demonstrates that cells with shorter telomeres display increased radiosensitivity versus younger fibroblasts with longer telomeres (Rubio *et al.*

2002). In addition, studies from *Terc*^{+/+} and *Terc*^{-/-} MEFs revealed reduced cell survival, increased chromosome aberrations, and delayed DNA repair capability in *Terc*^{-/-} MEFs with critically shortened telomeres, illustrating that telomere dysfunction and sensitivity to IR may reduce DNA repair (Wong *et al.* 2000). In contrast, although their work with *mTR*^{-/-} mice supports the idea that mice with shorter telomeres are hypersensitive to radiation, other authors argue that DNA DSB repair is not affected by shortened telomeres given that G5 *mTR*^{-/-} mice show normal levels of SCE as well as normal V(D)J recombination (Goytisolo *et al.* 2000).

One explanation is that increased radiosensitivity may be due to accelerated telomere shortening as a result of heightened oxidative stress, which can result following IR exposure and the presence of free radicals. Telomere loss due to oxidative damage was shown to often make more of a contribution to overall telomere loss than just the end-replication problem, thus showing a dependency for telomere shortening on stress conditions (von Zglinicki 2002; Houben *et al.* 2008). Taken together, these reports support a link between telomere shortening and radiosensitivity (for reviews see (Genesca *et al.* 2006; Ayouaz *et al.* 2008)).

DNA Double-Strand Break Repair

Introduction

DNA double-strand breaks can occur in the cell from both endogenous sources, such as reactive oxygen species (ROS), programmed rearrangements (V(D)J recombination) or from physical stress on the chromosome itself, as well as from exogenous sources including ionizing radiation, chemical mutagens, and

chemotherapeutics (Khanna and Jackson 2001). There are two main pathways for double-strand break (DSB) repair in mammalian systems: Non-Homologous End Joining (NHEJ) and Homologous Recombination (HR) (Figure 4). NHEJ primarily occurs during the G1 and early S phase of the cell cycle and is often referred to as error prone. HR is utilized during the late S and G2 phases of the cell cycle when a sister chromatid is present for use as a template and is considered error-free. The importance of studying DNA repair stems from evidence that deficiencies in DNA repair or DNA damage responses lead to increased cancer risk.

DNA Damage Response (ATM & γ H2AX)

Cellular response to IR depends on a wide variety of factors including cell cycle checkpoint control, signal transduction mechanisms and DSB repair, thus making DNA damage response genes important regulators of radiosensitivity—the relative susceptibility of cells, tissues, or organisms to the damaging effects of radiation. The ATM protein is a key player in a very large signaling network that has roles in checkpoint functions and coordinating repair of DSBs, among other things (Rotman and Shiloh 1999). One function of ATM lies in the phosphorylation of the histone variant H2AX at serine 139 in response to DSBs (reviewed in (Pilch *et al.* 2003; Fillingham *et al.* 2006)). This phosphorylation state, referred to as γ H2AX, can occur up to hundreds of kilobases surrounding a DSB and is believed to initiate recruitment of DNA repair proteins (reviewed in (Pilch *et al.* 2003; Fillingham *et al.* 2006)). Interestingly, some mutations in ATM are also associated with increased risk for breast cancer (Swift *et al.* 1991; Easton 1994).

γ H2AX foci have been correlated with the number of DNA DSBs produced by IR, making them a useful tool for DSB detection (Sedelnikova *et al.* 2002). Furthermore, γ H2AX levels decrease as DSBs are rejoined, thus allowing investigations into DNA repair kinetics and radiosensitivity with previous reports show that the rate of γ H2AX loss following IR treatment is slower and the number of cells with remaining γ H2AX foci is higher in more radiosensitive cell lines (MacPhail *et al.* 2003; Banath *et al.* 2004; Olive and Banath 2004; Taneja *et al.* 2004). It should be noted, however, that some cell lines with increased levels of chromosomal rearrangements demonstrated higher background levels of γ H2AX and that these types of excess endogenous levels can hinder accurate results when incorporating γ H2AX into experimental designs (Yu *et al.* 2006).

Just as γ H2AX has a role in damage response pathways, it has also been linked to the Fanconi anemia/BRCA pathway as a response to stalled replication forks (Bogliolo *et al.* 2007). γ H2AX has also been used recently in both mouse and human studies to distinguish between *Atm*^{+/+}, *Atm*^{+/-} and *Atm*^{-/-} genotypes using a low dose rate assay, showing the value in this technique in identifying even mildly radiosensitive individuals (Kato *et al.* 2006; Kato *et al.* 2006). Interestingly, elevated levels of γ H2AX foci in untreated melanoma cells compared to melanocytes has been reported and further co-localization of these foci with TRF1 in these melanoma cells suggests the presence of dysfunctional telomeres that may induce a DNA damage response (Warters *et al.* 2005). γ H2AX also occurs in telomeric regions following TRF2 inhibition, implying that dysfunctional telomeres are now recognized as DSBs (d'Adda di Fagagna *et al.* 2003; Takai *et al.* 2003). Telomere uncapping or dysfunction can, in fact, activate ATM and initiate a DNA damage response, just like a DSB (Guo *et al.* 2007).

We chose to evaluate radiation response in LCLs via γ H2AX foci formation measured by flow cytometry as a measure of radiosensitivity, however the results were inconsistent. Thus we utilized results from the G2 assay for this work.

Non-Homologous End Joining

During NHEJ, the Ku70/80 heterodimer binds to the ends of broken DNA, followed by the binding of DNA-PKcs (catalytic subunit), activating its protein kinase activity (Collis *et al.* 2005). The Ku70/Ku80 heterodimer and DNA-PKcs together make up DNA-PK. DNA ends are processed as needed and the ligaseIV/XRCC4 complex seals the DNA together. More recently, additional proteins have been identified that have roles in this process including XLF/cernunnos, a nuclease called Artemis, the MRN complex (Mre11/Rad50/NBS1) and even ATM (Ma *et al.* 2002; Buck *et al.* 2006). For a detailed review, see (van Gent and van der Burg 2007; Weterings and Chen 2008).

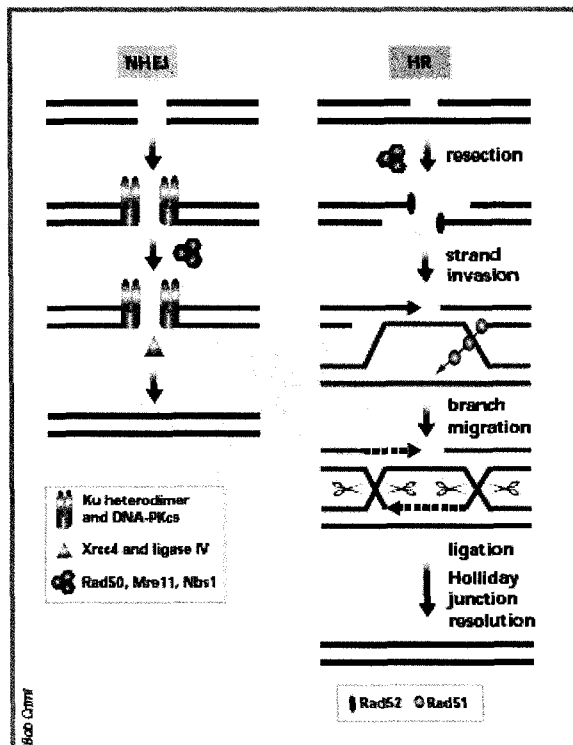


Figure 4. Non-Homologous End Joining compared to Homologous Recombination. NHEJ simply rejoins DSB ends while HR uses homologous sequences for repair. *Image from (Khanna and Jackson 2001).*

Homologous Recombination

HR, a type of homology directed repair, is crucial not only for repairing DNA DSBs but also plays important roles in bypassing stalled replication forks and DNA interstrand crosslink (ICLs) repair (Li and Heyer 2008). In addition, HR is absolutely required for creating antigen diversity via V(D)J recombination, genetic diversity via meiosis and for normal lymphocyte development (Caddle *et al.* 2008). The overall result of HR is accurate repair of DSBs using homologous sequences as templates. The main proteins involved in HR include Rad51 and five Rad51 paralogs known as XRCC2, XRCC3 (XRCC = X-ray cross-complementing), Rad51B, Rad51C and Rad51D (Thacker 2005).

Eukaryotic Rad51 is a structural and functional homolog of *E. Coli* RecA, with both having ATPase activity (Pittman *et al.* 1998). Following resection of a DNA break to create a 3' single-stranded overhang, Rad51, the central player in HR, forms a nucleoprotein filament on the single-strand ends of a DSB and catalyzes strand exchange between the damaged DNA and the matching homolog, perhaps with the help of Rad52 and Rad54 (Thacker and Zdzienicka 2004; Arnold *et al.* 2006). Interestingly, BRCA2 plays a role in targeting Rad51 to the DNA as well as in facilitating oligomerization of Rad51 monomers (Pellegrini *et al.* 2002). DNA synthesis occurs next, followed by branch migration and resolution of the cross-over structure. It should be noted that the detailed molecular events of these stages involving the various Rad51 paralogs are still under investigation (Thacker 2005).

As with any process in the cell, there are consequences for errors that occur during HR since recombination between misaligned sequences can result in insertions,

deletions, inversions, or translocations. In addition, recombination between homologous chromosomes can cause loss of heterozygosity (LOH), which often results in loss of tumor suppressor gene functions that can spur the initiation of carcinogenesis (Loree *et al.* 2006). It is interesting that people who are born predisposed to spontaneously high levels of recombination are prone to cancer (Bishop and Schiestl 2000), again supporting links between DNA repair malfunctions and carcinogenesis.

Rad51d

Rad51d (also known as Rad51L3 or Trad) is a Rad51 family member that has roles in DSB repair, genetic recombination and telomere maintenance (Tarsounas *et al.* 2004). We know that RAD51D directly interacts with XRCC2 and that this complex in humans forms nucleoprotein filaments along single-stranded DNA and catalyzes homologous pairing between ssDNA and dsDNA (Braybrooke *et al.* 2000; Kurumizaka *et al.* 2002). In addition, the RAD51D-XRCC2 heterodimer is able to stimulate BLM activity, a RecQ helicase mutated in Bloom's syndrome resulting in a predisposition to cancer, to disrupt synthetic Holliday junctions (Braybrooke *et al.* 2003). Together these data suggest that Rad51d is involved in at least two features of HR, strand invasion and possibly Holliday junction resolution (Smiraldo *et al.* 2005). We also know that Rad51d co-localizes to telomeres by binding to TRF2 (Tarsounas *et al.* 2004), thus making Rad51d a recent example of a DNA repair protein likely to have telomere functions as well.

Since Rad51d deficient human and mouse cells fail to proliferate and a mouse knock-out is embryonic lethal, we have utilized mouse embryonic fibroblasts (MEFs)

created in Douglas L. Pittman's laboratory by Phillip Smiraldo (Smiraldo *et al.* 2005). These MEFs are Rad51d-deficient as well as p53 deficient, which was necessary in order to rescue the cell phenotype. Dr. Smiraldo's previous studies characterize these cells as having elevated chromosomal instability, increased centrosome fragmentation, decreased levels of Rad51-foci formation, hypersensitivity to the DNA damaging agents MMC, cisplatin, and methyl methanesulfonate, decreased telomere length and increased chromosome end-to-end fusions (Tarsounas *et al.* 2004; Smiraldo *et al.* 2005). Despite these findings, we may be unaware of the true value of this protein since it has been shown in *Arabidopsis* that a mutant version of Rad51D increases the plant's susceptibility to pathogen infection, showing this protein's function in both defense gene transcription as well as HR (Durrant *et al.* 2007). These results further support the idea that Rad51d is needed to maintain genomic stability and therefore is deserving of further investigation into its precise role.

Intriguingly, our interest in breast cancer and RAD51D was brought together by a report that a missense variant in the human RAD51D gene may be a low-penetrance allele in families that are high-risk for breast cancer (Rodriguez-Lopez *et al.* 2004). This variant, E233G, was found in low frequency among the control population and test groups and further, all cases carrying E233G belonged to breast cancer families (BRCA1/2-negative) (Rodriguez-Lopez *et al.* 2004). However, it should be noted that a more recent evaluation of this variant in family studies of Australian women reported no association between E233G and breast cancer risk but mentioned that larger studies could be used to assess if there is a *small* risk of breast cancer associated with this variant (Dowty *et al.* 2007). On the other hand, this study did suggest that E233G is associated

with a *slight* increase in breast cancer risk and that the proportion of variant carriers in the Australian Breast Cancer Family Study (ABCFS) increased with increasing family history, even though both observations were not statistically significant (Dowty *et al.* 2007). Variants like these tie easily into the idea that breast cancer is caused by a wide variety of low-penetrance susceptibility alleles, as discussed previously, many of which have yet to be identified.

It has been shown that RAD51D and the other Rad51 paralogs are down-regulated in many cancers, including that of the breast, due to the up-regulation of EZH2 (Zeidler *et al.* 2005; Ding and Kleer 2006). EZH2, Enhancer of Zeste 2, is a polycomb group protein that functions in the maintenance of heritable transcription patterns (Laible *et al.* 1997). Specifically, this protein is a histone methyltransferase which acts as an epigenetic repressor by tightly compacting the DNA, making it “closed” to protein access. Like *Rad51d*, disruption of *Ezh2* in mice causes embryonic lethality, likely because EZH2 is needed for the derivation of pluripotent Embryonic Stem cells (and proper B cell development) (O'Carroll *et al.* 2001; Su *et al.* 2003). It should be taken into consideration that the polycomb group proteins silence over 1,000 genes in human embryonic fibroblasts, the majority of which are involved in embryonic development or cell fate (Bracken *et al.* 2006). Interestingly, brand new evidence shows that EZH2 is recruited to the sites of DSBs, with a potential role in returning chromatin back to its original state following completion of repair (O'Hagan *et al.* 2008). Moreover, the observation that condensed chromatin is much less susceptible to DSB induction by gamma-radiation than decondensed, active chromatin regions has newly been reported (Falk *et al.* 2008). Lastly, we know that some histone-modifying proteins (i.e. the Sir

family of proteins) participate in telomeric silencing in yeast (Martin *et al.* 1999).

Together these data further highlight the connection between DNA repair, carcinogenesis, telomere maintenance and radiation response at the cellular, or more precisely, the DNA level.

As mentioned above, it has been suggested that EZH2 contributes to mammary carcinogenesis by down-regulation of the Rad51 paralogs which leads to decreased DNA repair via HR (Zeidler *et al.* 2005). Interestingly, Kleer *et al.*, reported EZH2 over-expression in invasive carcinoma of the breast compared to normal mammary epithelium and that this over-expression not only promotes transformation of breast epithelial cells but also is linked with invasive and metastatic tumors compared to normal breast tissue (Kleer *et al.* 2003). It has also been reported that EZH2 is up-regulated in DCIS, atypical ductal hyperplasia and even normal breast epithelial cells from women with elevated breast cancer risk (Ding and Kleer 2006). Not only does this hold diagnostic value for breast cancer, but elevated levels of EZH2 have also been reported in bladder carcinoma, endometrial cancer, prostate cancer, and lymphoma, (reviewed in (Zeidler and Kleer 2006)). This protein transactivates genes commonly targeted by estrogen and directly interacts with estrogen receptor α , providing yet another link between EZH2 and breast cancer (Shi *et al.* 2007). In addition, loss of p16(INK4A) in primary human mammary epithelial cells leads to EZH2 up-regulation (Reynolds *et al.* 2006) and activated p53 suppresses EZH2 (Tang *et al.* 2004), demonstrating roles for EZH2 in cell cycle progression as well as initiation of carcinogenesis.

Because of these reports, we chose to evaluate changes in gene expression of *RAD51D* and *EZH2* following radiation exposure. It appears that both genes respond similarly to IR, as both are up-regulated at 2 and 8 hours post-IR.

Homologous Recombination and Telomeres

Not only is HR important for repairing DNA DSBs or bypassing stalled replication forks, but it also plays a role in telomere protection and elongation in mammalian cells. As discussed earlier, telomeres must be maintained at a proper length in order to maintain their protective role. If they become too short to function properly, there are two pathways cells can use to counter-act this problem: the use of the enzyme telomerase, a reverse transcriptase that elongates the G-rich telomere strand, or Alternative Lengthening of Telomeres (ALT), a recombination-based elongation method (Kim *et al.* 1994; Bryan *et al.* 1995; Bryan *et al.* 1997). One (or both) of these methods are usually activated in tumor cells, but are not generally used in normal somatic cells (Shay and Bacchetti 1997).

ALT is telomere specific and utilizes an HR-based mechanism to replicate telomeric DNA, but the exact mechanism has yet to be elucidated. Although ALT is usually limited to tumor cells, it illustrates yet another role for HR in the cell. On the other hand, it has been argued that HR-assisted capping during the G2 phase of the cell cycle, immediately following DNA (and therefore telomere) replication, is essential to reconstruct the protective t-loop, thus preventing a DNA damage response in the following cell cycle's G1 phase (Cesare and Reddel 2008). Thus, not only is the

regulation of HR important for accurate DNA repair, but also for proper telomere replication and function.

DSB Repair and IR

A major aspect of DSB repair disorders is a predisposition to tumorigenesis (O'Driscoll and Jeggo 2006). This is well illustrated in studies of defects in X-ray Cross Complementing (XRCC) genes. XRCC2 and XRCC3 genes are Rad51 paralogs whose functions are not entirely clear and XRCC1 has been identified as BRCA2 (Thacker and Zdzienicka 2003; Thacker 2005). As their name suggests, discovery of the XRCC genes came from the observations that these genes help protect mammalian cells from damage caused by IR (West 2003). Animal studies that disrupt XRCC genes important in NHEJ lead to increased lymphoid tumors whereas disruptions affecting XRCC genes that function in HR lead to breast cancer (West 2003) and similar effects are observed in human diseases resulting from mutations in specific XRCC genes, showing the importance of DNA repair both in radiation protection and tumorigenesis. Furthermore, studies with rat mammary gland show that following radiation exposure, Rad51 protein levels, as well as other repair proteins, increased (Loree *et al.* 2006). This is logical given that DSBs result from IR exposure and thus DSB repair proteins would be needed to start the repair process. DSBs caused by radiation, or any other mechanism, can be repaired by either HR or NHEJ.

DSB Repair and Cancer Treatment

We know that both breast cancer susceptibility genes BRCA1 and BRCA2 interact with Rad51 and thus have roles in DNA repair via HR (Venkitaraman 2002). As mentioned earlier, we also know that defects in XRCC genes involved in HR can lead to breast cancer (West 2003) and that the E233G variant in *RAD51D* is potentially linked to breast cancer risk (Rodriguez-Lopez *et al.* 2004). Although breast cancer is a complex disease, these data emphasize important links between HR repair and carcinogenesis.

Various studies illustrate the value of targeting DNA repair mechanisms for treatment modalities. For example, a new drug called Tirapazamine is a cytotoxin that targets hypoxic cells in solid tumors and may be a particularly effective treatment of HR-defective tumors as these types of cells are more sensitive to the drug (Evans *et al.* 2008). Another and perhaps more elegant example is the potential use of poly-ADP ribose polymerase (PARP) inhibitors in BRCA1 and BRCA2 heterozygous mutation carriers. These tumors have decreased HR ability because of the mutated BRCA1/2 function and blocking PARP, which is required for the other repair pathways base excision repair and single-strand break repair, enhances the dependence on HR and therefore increases tumor cell killing (Bryant *et al.* 2005). There are numerous PARP inhibitors as well as Chk1 and Chk2 (cell cycle regulators activated via DNA damage by ATM/ATR) inhibitors currently in clinical trials (reviewed in (O'Connor *et al.* 2007).

Cells that lack HR are mildly sensitive to radiation but are highly sensitive to DNA-crosslinking agents (Thompson and Schild 2001)—targeted therapies in this situation could be exploited via production of DNA crosslinks. The ATPase motif in *RAD51D* is essential for interstrand crosslink repair (ICL) (Gruver *et al.* 2005) therefore

possible treatments could rely on mutating the ATPase motif in RAD51D or other RAD51 paralogs in tumor cells and then inducing ICLs. These are just a few examples of cancer therapies based on DNA repair mechanisms, but as knowledge in this field continues to expand, one can assume that the possibilities for cancer treatments will only grow.

References

- Allsopp, RC, Chang E, Kashefi-Azham M, Rogaev EI, Piatyszek MA, Shay JW and Harley CB (1995). *Telomere shortening is associated with cell division in vitro and in vivo* Exp Cell Res 220(1): 194-200.
- Andersson, M, Engholm G, Ennow K, Jessen KA and Storm HH (1991). *Cancer risk among staff at two radiotherapy departments in Denmark* Br J Radiol 64(761): 455-60.
- Arnold, K, Kim MK, Frerk K, Edler L, Savelyeva L, Schmezer P and Wiedemeyer R (2006). *Lower level of BRCA2 protein in heterozygous mutation carriers is correlated with an increase in DNA double strand breaks and an impaired DSB repair* Cancer Lett.
- Aubert, G and Lansdorp PM (2008). *Telomeres and aging* Physiol Rev 88(2): 557-79.
- Ayouaz, A, Raynaud C, Heride C, Revaud D and Sabatier L (2008). *Telomeres: hallmarks of radiosensitivity* Biochimie 90(1): 60-72.
- Azzam, EI, de Toledo SM, Gooding T and Little JB (1998). *Intercellular communication is involved in the bystander regulation of gene expression in human cells exposed to very low fluences of alpha particles* Radiat Res 150(5): 497-504.
- Azzam, EI, de Toledo SM and Little JB (2001). *Direct evidence for the participation of gap junction-mediated intercellular communication in the transmission of damage signals from alpha -particle irradiated to nonirradiated cells* Proc Natl Acad Sci U S A 98(2): 473-8.
- Baeyens, A, Thierens H, Claes K, Poppe B, Messiaen L, De Ridder L and Vral A (2002). *Chromosomal radiosensitivity in breast cancer patients with a known or putative genetic predisposition* Br J Cancer 87(12): 1379-85.
- Bailey, SM, Brenneman MA, Halbrook J, Nickoloff JA, Ullrich RL and Goodwin EH (2004). *The kinase activity of DNA-PK is required to protect mammalian telomeres* DNA Repair (Amst) 3(3): 225-33.
- Bailey, SM, Goodwin EH and Cornforth MN (2004). *Strand-specific fluorescence in situ hybridization: the CO-FISH family* Cytogenet Genome Res 107(1-2): 14-7.
- Bailey, SM, Goodwin EH, Meyne J and Cornforth MN (1996). *CO-FISH reveals inversions associated with isochromosome formation* Mutagenesis 11(2): 139-44.
- Bailey, SM, Meyne J, Chen DJ, Kurimasa A, Li GC, Lehnert BE and Goodwin EH (1999). *DNA double-strand break repair proteins are required to cap the ends of mammalian chromosomes* Proc Natl Acad Sci U S A 96(26): 14899-904.
- Bailey, SM and Murnane JP (2006). *Telomeres, chromosome instability and cancer* Nucleic Acids Res 34(8): 2408-17.
- Baird, DM (2005). *New developments in telomere length analysis* Exp Gerontol 40(5): 363-8.
- Banath, JP, Macphail SH and Olive PL (2004). *Radiation sensitivity, H2AX phosphorylation, and kinetics of repair of DNA strand breaks in irradiated cervical cancer cell lines* Cancer Res 64(19): 7144-9.
- Beed, EA, O'Dorisio MS, O'Dorisio TM and Gaginella TS (1983). *Demonstration of a functional receptor for vasoactive intestinal polypeptide on Molt 4b T lymphoblasts* Regul Pept 6(1): 1-12.

- Bernstein, JL, Teraoka SN, John EM, Andrulis IL, Knight JA, Lapinski R, Olson ER, Wolitzer AL, Seminara D, Whittemore AS and Concannon P (2006). *The CHEK2*1100delC allelic variant and risk of breast cancer: screening results from the Breast Cancer Family Registry* Cancer Epidemiol Biomarkers Prev 15(2): 348-52.
- Berrington, A, Darby SC, Weiss HA and Doll R (2001). *100 years of observation on British radiologists: mortality from cancer and other causes 1897-1997* Br J Radiol 74(882): 507-19.
- Bhatti, P, Preston DL, Doody MM, Hauptmann M, Kampa D, Alexander BH, Petibone D, Simon SL, Weinstock RM, Bouville A, Yong LC, Freedman DM, Mabuchi K, Linet MS, Edwards AA, Tucker JD and Sigurdson AJ (2007). *Retrospective biodosimetry among United States radiologic technologists* Radiat Res 167(6): 727-34.
- Bhatti, P, Struewing JP, Alexander BH, Hauptmann M, Bowen L, Mateus-Pereira LH, Pineda MA, Simon SL, Weinstock RM, Rosenstein M, Stovall M, Preston DL, Linet MS, Doody MM and Sigurdson AJ (2008). *Polymorphisms in DNA repair genes, ionizing radiation exposure and risk of breast cancer in U.S. Radiologic technologists* Int J Cancer 122(1): 177-82.
- Bishop, AJ and Schiestl RH (2000). *Homologous recombination as a mechanism for genome rearrangements: environmental and genetic effects* Hum Mol Genet 9(16): 2427-334.
- Blackburn, EH (1990). *Telomeres: structure and synthesis* J Biol Chem 265(11): 5919-21.
- Bogliolo, M, Lyakhovich A, Callen E, Castella M, Cappelli E, Ramirez MJ, Creus A, Marcos R, Kalb R, Neveling K, Schindler D and Surralles J (2007). *Histone H2AX and Fanconi anemia FANCD2 function in the same pathway to maintain chromosome stability* Embo J 26(5): 1340-51.
- Boice, JD, Jr., Mandel JS, Doody MM, Yoder RC and McGowan R (1992). *A health survey of radiologic technologists* Cancer 69(2): 586-98.
- Bourguignon, MH, Gisone PA, Perez MR, Michelin S, Dubner D, Giorgio MD and Carosella ED (2005). *Genetic and epigenetic features in radiation sensitivity. Part II: implications for clinical practice and radiation protection* Eur J Nucl Med Mol Imaging 32(3): 351-68.
- Bracken, AP, Dietrich N, Pasini D, Hansen KH and Helin K (2006). *Genome-wide mapping of Polycomb target genes unravels their roles in cell fate transitions* Genes Dev 20(9): 1123-36.
- Braybrooke, JP, Li JL, Wu L, Caple F, Benson FE and Hickson ID (2003). *Functional interaction between the Bloom's syndrome helicase and the RAD51 paralog, RAD51L3 (RAD51D)* J Biol Chem 278(48): 48357-66.
- Braybrooke, JP, Spink KG, Thacker J and Hickson ID (2000). *The RAD51 family member, RAD51L3, is a DNA-stimulated ATPase that forms a complex with XRCC2* J Biol Chem 275(37): 29100-6.
- Brenner, DJ, Doll R, Goodhead DT, Hall EJ, Land CE, Little JB, Lubin JH, Preston DL, Preston RJ, Puskin JS, Ron E, Sachs RK, Samet JM, Setlow RB and Zaider M (2003). *Cancer risks attributable to low doses of ionizing radiation: assessing what we really know* Proc Natl Acad Sci U S A 100(24): 13761-6.

- Broeks, A, Braaf LM, Huseinovic A, Nooijen A, Urbanus J, Hogervorst FB, Schmidt MK, Klijn JG, Russell NS, Van Leeuwen FE and Van 't Veer LJ (2007). *Identification of women with an increased risk of developing radiation-induced breast cancer: a case only study* Breast Cancer Res 9(2): R26.
- Bryan, TM, Englezou A, Dalla-Pozza L, Dunham MA and Reddel RR (1997). *Evidence for an alternative mechanism for maintaining telomere length in human tumors and tumor-derived cell lines* Nat Med 3(11): 1271-4.
- Bryan, TM, Englezou A, Gupta J, Bacchetti S and Reddel RR (1995). *Telomere elongation in immortal human cells without detectable telomerase activity* Embo J 14(17): 4240-8.
- Bryant, HE, Schultz N, Thomas HD, Parker KM, Flower D, Lopez E, Kyle S, Meuth M, Curtin NJ and Helleday T (2005). *Specific killing of BRCA2-deficient tumours with inhibitors of poly(ADP-ribose) polymerase* Nature 434(7035): 913-7.
- Buck, D, Malivert L, de Chasseval R, Barraud A, Fondaneche MC, Sanal O, Plebani A, Stephan JL, Hufnagel M, le Deist F, Fischer A, Durandy A, de Villartay JP and Revy P (2006). *Cernunnos, a novel nonhomologous end-joining factor, is mutated in human immunodeficiency with microcephaly* Cell 124(2): 287-99.
- Caddle, LB, Hasham MG, Schott WH, Shirley BJ and Mills KD (2008). *Homologous recombination is necessary for normal lymphocyte development* Mol Cell Biol 28(7): 2295-303.
- Calvo, JR, Guerrero JM, Molinero P, Blasco R and Goberna R (1986). *Interaction of vasoactive intestinal peptide (VIP) with human peripheral blood lymphocytes: specific binding and cyclic AMP production* Gen Pharmacol 17(2): 185-9.
- Calvo, JR, Pozo D and Guerrero JM (1996). *Functional and molecular characterization of VIP receptors and signal transduction in human and rodent immune systems* Adv Neuroimmunol 6(1): 39-47.
- Cardis, E, Hall J and Tavtigian SV (2007). *Identification of women with an increased risk of developing radiation-induced breast cancer* Breast Cancer Res 9(3): 106.
- Cawthon, RM (2002). *Telomere measurement by quantitative PCR* Nucleic Acids Res 30(10): e47.
- Cesare, AJ and Reddel RR (2008). *Telomere uncapping and alternative lengthening of telomeres* Mech Ageing Dev 129(1-2): 99-108.
- Claus, EB, Risch N and Thompson WD (1991). *Genetic analysis of breast cancer in the cancer and steroid hormone study* Am J Hum Genet 48(2): 232-42.
- Collis, SJ, DeWeese TL, Jeggo PA and Parker AR (2005). *The life and death of DNA-PK* Oncogene 24(6): 949-61.
- d'Adda di Fagagna, F, Reaper PM, Clay-Farrace L, Fiegler H, Carr P, Von Zglinicki T, Saretzki G, Carter NP and Jackson SP (2003). *A DNA damage checkpoint response in telomere-initiated senescence* Nature 426(6963): 194-8.
- d'Adda di Fagagna, F, Teo SH and Jackson SP (2004). *Functional links between telomeres and proteins of the DNA-damage response* Genes Dev 18(15): 1781-99.
- Dahse, R, Fiedler W and Ernst G (1997). *Telomeres and telomerase: biological and clinical importance* Clin Chem 43(5): 708-14.
- David Schottenfeld, JFF (2006). Cancer Epidemiology and Prevention, Oxford University Press.
- de Lange, T (2002). *Protection of mammalian telomeres* Oncogene 21(4): 532-40.

- de Lange, T (2005). *Shelterin: the protein complex that shapes and safeguards human telomeres* Genes Dev 19(18): 2100-10.
- Ding, L and Kleer CG (2006). *Enhancer of Zeste 2 as a marker of preneoplastic progression in the breast* Cancer Res 66(19): 9352-5.
- Doody, MM, Freedman DM, Alexander BH, Hauptmann M, Miller JS, Rao RS, Mabuchi K, Ron E, Sigurdson AJ and Linet MS (2006). *Breast cancer incidence in U.S. radiologic technologists* Cancer 106(12): 2707-15.
- Doody, MM, Mandel JS, Lubin JH and Boice JD, Jr. (1998). *Mortality among United States radiologic technologists, 1926-90* Cancer Causes Control 9(1): 67-75.
- Dowty, JG, Lose F, Jenkins MA, Chang JH, Chen X, Beesley J, Dite GS, Southey MC, Byrnes GB, Tesoriero A, Giles GG, Hopper JL and Spurdle AB (2007). *The RAD51D E233G variant and breast cancer risk: population-based and clinic-based family studies of Australian women* Breast Cancer Res Treat.
- Durrant, WE, Wang S and Dong X (2007). *Arabidopsis SNI1 and RAD51D regulate both gene transcription and DNA recombination during the defense response* Proc Natl Acad Sci U S A 104(10): 4223-7.
- Easton, DF (1994). *Cancer risks in A-T heterozygotes* Int J Radiat Biol 66(6 Suppl): S177-82.
- Espejel, S, Franco S, Sgura A, Gae D, Bailey SM, Taccioli GE and Blasco MA (2002). *Functional interaction between DNA-PKcs and telomerase in telomere length maintenance* Embo J 21(22): 6275-87.
- Evans, JW, Chernikova SB, Kachnic LA, Banath JP, Sordet O, Delahoussaye YM, Treszezamsky A, Chon BH, Feng Z, Gu Y, Wilson WR, Pommier Y, Olive PL, Powell SN and Brown JM (2008). *Homologous recombination is the principal pathway for the repair of DNA damage induced by tirapazamine in mammalian cells* Cancer Res 68(1): 257-65.
- Falk, M, Lukasova E and Kozubek S (2008). *Chromatin structure influences the sensitivity of DNA to gamma-radiation* Biochim Biophys Acta.
- Ferreira, MG, Miller KM and Cooper JP (2004). *Indecent exposure: when telomeres become uncapped* Mol Cell 13(1): 7-18.
- Fillingham, J, Keogh MC and Krogan NJ (2006). *GammaH2AX and its role in DNA double-strand break repair* Biochem Cell Biol 84(4): 568-77.
- Fordyce, CA, Heaphy CM, Bisoffi M, Wyaco JL, Joste NE, Mangalik A, Baumgartner KB, Baumgartner RN, Hunt WC and Griffith JK (2006). *Telomere content correlates with stage and prognosis in breast cancer* Breast Cancer Res Treat.
- Freedman, DM, Sigurdson A, Rao RS, Hauptmann M, Alexander B, Mohan A, Morin Doody M and Linet MS (2003). *Risk of melanoma among radiologic technologists in the United States* Int J Cancer 103(4): 556-62.
- Garcia-Fernandez, MO, Collado B, Bodega G, Cortes J, Ruiz-Villaespesa A, Carmena MJ and Prieto JC (2005). *Pituitary adenylate cyclase-activating peptide/vasoactive intestinal peptide receptors in human normal mammary gland and breast cancer tissue* Gynecol Endocrinol 20(6): 327-33.
- Genesca, A, Martin M, Latre L, Soler D, Pampalona J and Tusell L (2006). *Telomere dysfunction: a new player in radiation sensitivity* Bioessays 28(12): 1172-80.
- Gonzalez-Rey, E and Delgado M (2005). *Role of vasoactive intestinal peptide in inflammation and autoimmunity* Curr Opin Investig Drugs 6(11): 1116-23.

- Goytisolo, FA, Samper E, Martin-Caballero J, Finnon P, Herrera E, Flores JM, Bouffler SD and Blasco MA (2000). *Short telomeres result in organismal hypersensitivity to ionizing radiation in mammals* J Exp Med 192(11): 1625-36.
- Griffith, JD, Comeau L, Rosenfield S, Stansel RM, Bianchi A, Moss H and de Lange T (1999). *Mammalian telomeres end in a large duplex loop* Cell 97(4): 503-14.
- Griffith, JK, Bryant JE, Fordyce CA, Gilliland FD, Joste NE and Moyzis RK (1999). *Reduced telomere DNA content is correlated with genomic instability and metastasis in invasive human breast carcinoma* Breast Cancer Res Treat 54(1): 59-64.
- Gruver, AM, Miller KA, Rajesh C, Smiraldo PG, Kaliyaperumal S, Balder R, Stiles KM, Albala JS and Pittman DL (2005). *The ATPase motif in RAD51D is required for resistance to DNA interstrand crosslinking agents and interaction with RAD51C* Mutagenesis 20(6): 433-40.
- Guerrero, JM, Prieto JC, Calvo JR and Goberna R (1984). *Activation of cyclic AMP-dependent protein kinase by VIP in blood mononuclear cells* Peptides 5(2): 371-3.
- Guo, X, Deng Y, Lin Y, Cosme-Blanco W, Chan S, He H, Yuan G, Brown EJ and Chang S (2007). *Dysfunctional telomeres activate an ATM-ATR-dependent DNA damage response to suppress tumorigenesis* Embo J 26(22): 4709-19.
- Hagelstrom, RT, Askin KF, Williams AJ, Ramaiah L, Desaintes C, Goodwin EH, Ullrich RL and Bailey SM (2008). *DNA-PKcs and ATM influence generation of ionizing radiation-induced bystander signals* Oncogene.
- Hall, EJ (2006). Radiobiology for the Radiologist.
- Heaphy, CM, Baumgartner KB, Bisoffi M, Baumgartner RN and Griffith JK (2007). *Telomere DNA content predicts breast cancer free survival interval* Clin Cancer Res 13(23): 7037-43.
- Houben, JM, Moonen HJ, van Schooten FJ and Hageman GJ (2008). *Telomere length assessment: biomarker of chronic oxidative stress?* Free Radic Biol Med 44(3): 235-46.
- Jaco, I, Munoz P and Blasco MA (2004). *Role of human Ku86 in telomere length maintenance and telomere capping* Cancer Res 64(20): 7271-8.
- Kadhim, MA, Walker CA, Plumb MA and Wright EG (1996). *No association between p53 status and alpha-particle-induced chromosomal instability in human lymphoblastoid cells* Int J Radiat Biol 69(2): 167-74.
- Kashino, G, Prise KM, Suzuki K, Matsuda N, Kodama S, Suzuki M, Nagata K, Kinashi Y, Masunaga S, Ono K and Watanabe M (2007). *Effective suppression of bystander effects by DMSO treatment of irradiated CHO cells* J Radiat Res (Tokyo) 48(4): 327-33.
- Kato, TA, Nagasawa H, Weil MM, Genik PC, Little JB and Bedford JS (2006). *gamma-H2AX foci after low-dose-rate irradiation reveal atm haploinsufficiency in mice* Radiat Res 166(1 Pt 1): 47-54.
- Kato, TA, Nagasawa H, Weil MM, Little JB and Bedford JS (2006). *Levels of gamma-H2AX Foci after low-dose-rate irradiation reveal a DNA DSB rejoining defect in cells from human ATM heterozygotes in two at families and in another apparently normal individual* Radiat Res 166(3): 443-53.
- Khanna, KK and Jackson SP (2001). *DNA double-strand breaks: signaling, repair and the cancer connection* Nat Genet 27(3): 247-54.

- Kim, NW, Piatyszek MA, Prowse KR, Harley CB, West MD, Ho PL, Coviello GM, Wright WE, Weinrich SL and Shay JW (1994). *Specific association of human telomerase activity with immortal cells and cancer* Science 266(5193): 2011-5.
- Kleer, CG, Cao Q, Varambally S, Shen R, Ota I, Tomlins SA, Ghosh D, Sewalt RG, Otte AP, Hayes DF, Sabel MS, Livant D, Weiss SJ, Rubin MA and Chinnaiyan AM (2003). *EZH2 is a marker of aggressive breast cancer and promotes neoplastic transformation of breast epithelial cells* Proc Natl Acad Sci U S A 100(20): 11606-11.
- Kurumizaka, H, Ikawa S, Nakada M, Enomoto R, Kagawa W, Kinebuchi T, Yamazoe M, Yokoyama S and Shibata T (2002). *Homologous pairing and ring and filament structure formation activities of the human Xrcc2*Rad51D complex* J Biol Chem 277(16): 14315-20.
- Laible, G, Wolf A, Dorn R, Reuter G, Nislow C, Lebersorger A, Popkin D, Pillus L and Jenuwein T (1997). *Mammalian homologues of the Polycomb-group gene Enhancer of zeste mediate gene silencing in Drosophila heterochromatin and at S. cerevisiae telomeres* Embo J 16(11): 3219-32.
- Land, CE, Tokunaga M, Koyama K, Soda M, Preston DL, Nishimori I and Tokuoka S (2003). *Incidence of female breast cancer among atomic bomb survivors, Hiroshima and Nagasaki, 1950-1990* Radiat Res 160(6): 707-17.
- Leceta, J, Martinez C, Delgado M, Garrido E and Gomariz RP (1996). *Expression of vasoactive intestinal peptide in lymphocytes: a possible endogenous role in the regulation of the immune system* Adv Neuroimmunol 6(1): 29-36.
- Lehnert, BE, Goodwin EH and Deshpande A (1997). *Extracellular factor(s) following exposure to alpha particles can cause sister chromatid exchanges in normal human cells* Cancer Res 57(11): 2164-71.
- Levy, MZ, Allsopp RC, Futcher AB, Greider CW and Harley CB (1992). *Telomere end-replication problem and cell aging* J Mol Biol 225(4): 951-60.
- Li, X and Heyer WD (2008). *Homologous recombination in DNA repair and DNA damage tolerance* Cell Res 18(1): 99-113.
- Linnet, MS, Freedman DM, Mohan AK, Doody MM, Ron E, Mabuchi K, Alexander BH, Sigurdson A and Hauptmann M (2005). *Incidence of haematopoietic malignancies in US radiologic technologists* Occup Environ Med 62(12): 861-7.
- Loree, J, Koturbash I, Kutanzi K, Baker M, Pogribny I and Kovalchuk O (2006). *Radiation-induced molecular changes in rat mammary tissue: possible implications for radiation-induced carcinogenesis* Int J Radiat Biol 82(11): 805-15.
- M'Kacher, R, Bennaceur-Griscelli A, Girinsky T, Koscielny S, Delhommeau F, Dossou J, Violot D, Leclercq E, Courtier MH, Beron-Gaillard N, Assaf E, Ribrag V, Bourhis J, Feneux D, Bernheim A, Parmentier C and Carde P (2007). *Telomere shortening and associated chromosomal instability in peripheral blood lymphocytes of patients with Hodgkin's lymphoma prior to any treatment are predictive of second cancers* Int J Radiat Oncol Biol Phys 68(2): 465-71.
- Ma, Y, Pannicke U, Schwarz K and Lieber MR (2002). *Hairpin opening and overhang processing by an Artemis/DNA-dependent protein kinase complex in nonhomologous end joining and V(D)J recombination* Cell 108(6): 781-94.

- MacPhail, SH, Banath JP, Yu TY, Chu EH, Lambur H and Olive PL (2003). *Expression of phosphorylated histone H2AX in cultured cell lines following exposure to X-rays* Int J Radiat Biol 79(5): 351-8.
- Martin, SG, Laroche T, Suka N, Grunstein M and Gasser SM (1999). *Relocalization of telomeric Ku and SIR proteins in response to DNA strand breaks in yeast* Cell 97(5): 621-33.
- Matsumoto, H, Hamada N, Takahashi A, Kobayashi Y and Ohnishi T (2007). *Vanguards of paradigm shift in radiation biology: radiation-induced adaptive and bystander responses* J Radiat Res (Tokyo) 48(2): 97-106.
- McIlrath, J, Bouffler SD, Samper E, Cuthbert A, Wojcik A, Szumiel I, Bryant PE, Riches AC, Thompson A, Blasco MA, Newbold RF and Slijepcevic P (2001). *Telomere length abnormalities in mammalian radiosensitive cells* Cancer Res 61(3): 912-5.
- Meeker, AK, Hicks JL, Gabrielson E, Strauss WM, De Marzo AM and Argani P (2004). *Telomere shortening occurs in subsets of normal breast epithelium as well as in situ and invasive carcinoma* Am J Pathol 164(3): 925-35.
- Meeker, AK, Hicks JL, Iacobuzio-Donahue CA, Montgomery EA, Westra WH, Chan TY, Ronnett BM and De Marzo AM (2004). *Telomere length abnormalities occur early in the initiation of epithelial carcinogenesis* Clin Cancer Res 10(10): 3317-26.
- Mohan, AK, Hauptmann M, Freedman DM, Ron E, Matanoski GM, Lubin JH, Alexander BH, Boice JD, Jr., Doody MM and Linet MS (2003). *Cancer and other causes of mortality among radiologic technologists in the United States* Int J Cancer 103(2): 259-67.
- Moody, TW and Gozes I (2007). *Vasoactive intestinal peptide receptors: a molecular target in breast and lung cancer* Curr Pharm Des 13(11): 1099-104.
- Morgan, WF and Sowa MB (2007). *Non-targeted bystander effects induced by ionizing radiation* Mutat Res 616(1-2): 159-64.
- Mothersill, C and Seymour CB (1998). *Cell-cell contact during gamma irradiation is not required to induce a bystander effect in normal human keratinocytes: evidence for release during irradiation of a signal controlling survival into the medium* Radiat Res 149(3): 256-62.
- Nagasawa, H, Wilson PF, Chen DJ, Thompson LH, Bedford JS and Little JB (2008). *Low doses of alpha particles do not induce sister chromatid exchanges in bystander Chinese hamster cells defective in homologous recombination* DNA Repair (Amst) 7(3): 515-22.
- Narayanan, PK, Goodwin EH and Lehnert BE (1997). *Alpha particles initiate biological production of superoxide anions and hydrogen peroxide in human cells* Cancer Res 57(18): 3963-71.
- Nordfjall, K, Larefalk A, Lindgren P, Holmberg D and Roos G (2005). *Telomere length and heredity: Indications of paternal inheritance* Proc Natl Acad Sci U S A 102(45): 16374-8.
- O'Callaghan, N, Dhillon V, Thomas P and Fenech M (2008). *A quantitative real-time PCR method for absolute telomere length* Biotechniques 44(6): 807-9.
- O'Carroll, D, Erhardt S, Pagani M, Barton SC, Surani MA and Jenuwein T (2001). *The polycomb-group gene Ezh2 is required for early mouse development* Mol Cell Biol 21(13): 4330-6.

- O'Connor, MJ, Martin NM and Smith GC (2007). *Targeted cancer therapies based on the inhibition of DNA strand break repair* *Oncogene* 26(56): 7816-24.
- O'Dorisio, MS, Hermina NS, O'Dorisio TM and Balcerzak SP (1981). *Vasoactive intestinal polypeptide modulation of lymphocyte adenylate cyclase* *J Immunol* 127(6): 2551-4.
- O'Dorisio, MS, Shannon BT, Mulne AF, Zwick D, Grossman NJ and Ruymann FB (1992). *Vasoactive intestinal peptide receptor expression on human lymphoblasts* *Am J Pediatr Hematol Oncol* 14(2): 144-50.
- O'Driscoll, M and Jeggo PA (2006). *The role of double-strand break repair - insights from human genetics* *Nat Rev Genet* 7(1): 45-54.
- O'Hagan, HM, Mohammad HP and Baylin SB (2008). *Double strand breaks can initiate gene silencing and SIRT1-dependent onset of DNA methylation in an exogenous promoter CpG island* *PLoS Genet* 4(8): e1000155.
- Olive, PL and Banath JP (2004). *Phosphorylation of histone H2AX as a measure of radiosensitivity* *Int J Radiat Oncol Biol Phys* 58(2): 331-5.
- Ottaway, CA, Bernaerts C, Chan B and Greenberg GR (1983). *Specific binding of vasoactive intestinal peptide to human circulating mononuclear cells* *Can J Physiol Pharmacol* 61(7): 664-71.
- Ottaway, CA, Lay TE and Greenberg GR (1990). *High affinity specific binding of vasoactive intestinal peptide to human circulating T cells, B cells and large granular lymphocytes* *J Neuroimmunol* 29(1-3): 149-55.
- Parkin, DM (2004). *International variation* *Oncogene* 23(38): 6329-40.
- Parkin, DM, Bray F, Ferlay J and Pisani P (2005). *Global cancer statistics, 2002* *CA Cancer J Clin* 55(2): 74-108.
- Paz-y-Mino, C, Sanchez ME, Del Pozo M, Baldeon MA, Cordova A, Gutierrez S, Penaherrera MS, Neira M, Ocampo L and Leone PE (1997). *Telomeric association in women with breast and uterine cervix cancer* *Cancer Genet Cytogenet* 98(2): 115-8.
- Pellegrini, L, Yu DS, Lo T, Anand S, Lee M, Blundell TL and Venkitaraman AR (2002). *Insights into DNA recombination from the structure of a RAD51-BRCA2 complex* *Nature* 420(6913): 287-93.
- Perry, P and Wolff S (1974). *New Giemsa method for the differential staining of sister chromatids* *Nature* 251(5471): 156-8.
- Pilch, DR, Sedelnikova OA, Redon C, Celeste A, Nussenzweig A and Bonner WM (2003). *Characteristics of gamma-H2AX foci at DNA double-strand breaks sites* *Biochem Cell Biol* 81(3): 123-9.
- Pittman, DL, Weinberg LR and Schimenti JC (1998). *Identification, characterization, and genetic mapping of Rad51d, a new mouse and human RAD51/RecA-related gene* *Genomics* 49(1): 103-11.
- Preston, DL, Mattsson A, Holmberg E, Shore R, Hildreth NG and Boice JD, Jr. (2002). *Radiation effects on breast cancer risk: a pooled analysis of eight cohorts* *Radiat Res* 158(2): 220-35.
- Rahman, N and Stratton MR (1998). *The genetics of breast cancer susceptibility* *Annu Rev Genet* 32: 95-121.
- Reubi, JC (2000). *In vitro evaluation of VIP/PACAP receptors in healthy and diseased human tissues. Clinical implications* *Ann N Y Acad Sci* 921: 1-25.

- Reubi, JC, Laderach U, Waser B, Gebbers JO, Robberecht P and Laissue JA (2000). *Vasoactive intestinal peptide/pituitary adenylate cyclase-activating peptide receptor subtypes in human tumors and their tissues of origin* *Cancer Res* 60(11): 3105-12.
- Reynolds, PA, Sigaroudinia M, Zardo G, Wilson MB, Benton GM, Miller CJ, Hong C, Fridlyand J, Costello JF and Tlsty TD (2006). *Tumor suppressor p16INK4A regulates polycomb-mediated DNA hypermethylation in human mammary epithelial cells* *J Biol Chem* 281(34): 24790-802.
- Richter, T and von Zglinicki T (2007). *A continuous correlation between oxidative stress and telomere shortening in fibroblasts* *Exp Gerontol* 42(11): 1039-42.
- Roberts, SA, Spreadborough AR, Bulman B, Barber JB, Evans DG and Scott D (1999). *Heritability of cellular radiosensitivity: a marker of low-penetrance predisposition genes in breast cancer?* *Am J Hum Genet* 65(3): 784-94.
- Rodier, F, Kim SH, Nijjar T, Yaswen P and Campisi J (2005). *Cancer and aging: the importance of telomeres in genome maintenance* *Int J Biochem Cell Biol* 37(5): 977-90.
- Rodriguez-Lopez, R, Osorio A, Ribas G, Pollan M, Sanchez-Pulido L, de la Hoya M, Ruibal A, Zamora P, Arias JI, Salazar R, Vega A, Martinez JI, Esteban-Cardenosa E, Alonso C, Leton R, Urioste Azcorra M, Miner C, Armengod ME, Carracedo A, Gonzalez-Sarmiento R, Caldes T, Diez O and Benitez J (2004). *The variant E233G of the RAD51D gene could be a low-penetrance allele in high-risk breast cancer families without BRCA1/2 mutations* *Int J Cancer* 110(6): 845-9.
- Ronckers, CM, Erdmann CA and Land CE (2005). *Radiation and breast cancer: a review of current evidence* *Breast Cancer Res* 7(1): 21-32.
- Rotman, G and Shiloh Y (1999). *ATM: a mediator of multiple responses to genotoxic stress* *Oncogene* 18(45): 6135-44.
- Rubio, MA, Kim SH and Campisi J (2002). *Reversible manipulation of telomerase expression and telomere length. Implications for the ionizing radiation response and replicative senescence of human cells* *J Biol Chem* 277(32): 28609-17.
- Ryan, LA, Smith RW, Seymour CB and Mothersill CE (2008). *Dilution of irradiated cell conditioned medium and the bystander effect* *Radiat Res* 169(2): 188-96.
- Saito, K, Yagihashi A, Nasu S, Izawa Y, Nakamura M, Kobayashi D, Tsuji N and Watanabe N (2002). *Gene expression for suppressors of telomerase activity (telomeric-repeat binding factors) in breast cancer* *Jpn J Cancer Res* 93(3): 253-8.
- Schulz, S, Rocken C, Mawrin C, Weise W, Hollt V and Schulz S (2004). *Immunocytochemical identification of VPAC1, VPAC2, and PAC1 receptors in normal and neoplastic human tissues with subtype-specific antibodies* *Clin Cancer Res* 10(24): 8235-42.
- Schwartz, JL (2007). *Variability: the common factor linking low dose-induced genomic instability, adaptation and bystander effects* *Mutat Res* 616(1-2): 196-200.
- Scott, D, Barber JB, Spreadborough AR, Burrill W and Roberts SA (1999). *Increased chromosomal radiosensitivity in breast cancer patients: a comparison of two assays* *Int J Radiat Biol* 75(1): 1-10.

- Sedelnikova, OA, Rogakou EP, Panyutin IG and Bonner WM (2002). *Quantitative detection of (125)IdU-induced DNA double-strand breaks with gamma-H2AX antibody* Radiat Res 158(4): 486-92.
- Shao, C, Stewart V, Folkard M, Michael BD and Prise KM (2003). *Nitric oxide-mediated signaling in the bystander response of individually targeted glioma cells* Cancer Res 63(23): 8437-42.
- Shareef, MM, Cui N, Burikhanov R, Gupta S, Satishkumar S, Shajahan S, Mohiuddin M, Rangnekar VM and Ahmed MM (2007). *Role of tumor necrosis factor-alpha and TRAIL in high-dose radiation-induced bystander signaling in lung adenocarcinoma* Cancer Res 67(24): 11811-20.
- Shay, JW and Bacchetti S (1997). *A survey of telomerase activity in human cancer* Eur J Cancer 33(5): 787-91.
- Shen, J, Terry MB, Gurvich I, Liao Y, Senie RT and Santella RM (2007). *Short telomere length and breast cancer risk: a study in sister sets* Cancer Res 67(11): 5538-44.
- Shi, B, Liang J, Yang X, Wang Y, Zhao Y, Wu H, Sun L, Zhang Y, Chen Y, Li R, Zhang Y, Hong M and Shang Y (2007). *Integration of estrogen and Wnt signaling circuits by the polycomb group protein EZH2 in breast cancer cells* Mol Cell Biol 27(14): 5105-19.
- Sigurdson, AJ, Bhatti P, Doody MM, Hauptmann M, Bowen L, Simon SL, Weinstock RM, Linet MS, Rosenstein M, Stovall M, Alexander BH, Preston DL, Struewing JP and Rajaraman P (2007). *Polymorphisms in apoptosis- and proliferation-related genes, ionizing radiation exposure, and risk of breast cancer among U.S. Radiologic Technologists* Cancer Epidemiol Biomarkers Prev 16(10): 2000-7.
- Sigurdson, AJ, Doody MM, Rao RS, Freedman DM, Alexander BH, Hauptmann M, Mohan AK, Yoshinaga S, Hill DA, Tarone R, Mabuchi K, Ron E and Linet MS (2003). *Cancer incidence in the US radiologic technologists health study, 1983-1998* Cancer 97(12): 3080-9.
- Sigurdson, AJ, Hauptmann M, Alexander BH, Doody MM, Thomas CB, Struewing JP and Jones IM (2005). *DNA damage among thyroid cancer and multiple cancer cases, controls, and long-lived individuals* Mutat Res 586(2): 173-88.
- Simon, SL, Weinstock RM, Doody MM, Neton J, Wenzl T, Stewart P, Mohan AK, Yoder RC, Hauptmann M, Freedman DM, Cardarelli J, Feng HA, Bouville A and Linet M (2006). *Estimating historical radiation doses to a cohort of U.S. radiologic technologists* Radiat Res 166(1 Pt 2): 174-92.
- Slijepcevic, P (2004). *Is there a link between telomere maintenance and radiosensitivity?* Radiat Res 161(1): 82-6.
- Slijepcevic, P and Al-Wahiby S (2005). *Telomere biology: integrating chromosomal end protection with DNA damage response* Chromosoma.
- Smiraldo, PG, Gruver AM, Osborn JC and Pittman DL (2005). *Extensive chromosomal instability in Rad51d-deficient mouse cells* Cancer Res 65(6): 2089-96.
- Stratton, MR and Rahman N (2008). *The emerging landscape of breast cancer susceptibility* Nat Genet 40(1): 17-22.
- Su, IH, Basavaraj A, Krutchinsky AN, Hobert O, Ullrich A, Chait BT and Tarakhovsky A (2003). *Ezh2 controls B cell development through histone H3 methylation and Igh rearrangement* Nat Immunol 4(2): 124-31.

- Sugimoto, M, Tahara H, Ide T and Furuichi Y (2004). *Steps involved in immortalization and tumorigenesis in human B-lymphoblastoid cell lines transformed by Epstein-Barr virus* Cancer Res 64(10): 3361-4.
- Swift, M, Morrell D, Massey RB and Chase CL (1991). *Incidence of cancer in 161 families affected by ataxia-telangiectasia* N Engl J Med 325(26): 1831-6.
- Takai, H, Smogorzewska A and de Lange T (2003). *DNA damage foci at dysfunctional telomeres* Curr Biol 13(17): 1549-56.
- Taneja, N, Davis M, Choy JS, Beckett MA, Singh R, Kron SJ and Weichselbaum RR (2004). *Histone H2AX phosphorylation as a predictor of radiosensitivity and target for radiotherapy* J Biol Chem 279(3): 2273-80.
- Tang, X, Milyavsky M, Shats I, Erez N, Goldfinger N and Rotter V (2004). *Activated p53 suppresses the histone methyltransferase EZH2 gene* Oncogene 23(34): 5759-69.
- Tarsounas, M, Munoz P, Claas A, Smiraldi PG, Pittman DL, Blasco MA and West SC (2004). *Telomere maintenance requires the RAD51D recombination/repair protein* Cell 117(3): 337-47.
- Thacker, J (2005). *The RAD51 gene family, genetic instability and cancer* Cancer Lett 219(2): 125-35.
- Thacker, J and Zdzienicka MZ (2003). *The mammalian XRCC genes: their roles in DNA repair and genetic stability* DNA Repair (Amst) 2(6): 655-72.
- Thacker, J and Zdzienicka MZ (2004). *The XRCC genes: expanding roles in DNA double-strand break repair* DNA Repair (Amst) 3(8-9): 1081-90.
- Thompson, LH and Schild D (2001). *Homologous recombinational repair of DNA ensures mammalian chromosome stability* Mutat Res 477(1-2): 131-53.
- Trkova, M, Prochazkova K, Krutilkova V, Sumerauer D and Sedlacek Z (2007). *Telomere length in peripheral blood cells of germline TP53 mutation carriers is shorter than that of normal individuals of corresponding age* Cancer 110(3): 694-702.
- van Gent, DC and van der Burg M (2007). *Non-homologous end-joining, a sticky affair* Oncogene 26(56): 7731-40.
- Vaudry, D, Gonzalez BJ, Basille M, Yon L, Fournier A and Vaudry H (2000). *Pituitary adenylate cyclase-activating polypeptide and its receptors: from structure to functions* Pharmacol Rev 52(2): 269-324.
- Venkitaraman, AR (2002). *Cancer susceptibility and the functions of BRCA1 and BRCA2* Cell 108(2): 171-82.
- von Zglinicki, T (2002). *Oxidative stress shortens telomeres* Trends Biochem Sci 27(7): 339-44.
- Wang, JX, Zhang LA, Li BX, Zhao YC, Wang ZQ, Zhang JY and Aoyama T (2002). *Cancer incidence and risk estimation among medical x-ray workers in China, 1950-1995* Health Phys 82(4): 455-66.
- Warters, RL, Adamson PJ, Pond CD and Leachman SA (2005). *Melanoma cells express elevated levels of phosphorylated histone H2AX foci* J Invest Dermatol 124(4): 807-17.
- Wei, Y and Mojsos S (1996). *Tissue specific expression of different human receptor types for pituitary adenylate cyclase activating polypeptide and vasoactive intestinal polypeptide: implications for their role in human physiology* J Neuroendocrinol 8(11): 811-7.

- West, CM (1995). *Invited review: intrinsic radiosensitivity as a predictor of patient response to radiotherapy* Br J Radiol 68(812): 827-37.
- West, SC (2003). *Molecular views of recombination proteins and their control* Nat Rev Mol Cell Biol 4(6): 435-45.
- Weterings, E and Chen DJ (2008). *The endless tale of non-homologous end-joining* Cell Res 18(1): 114-24.
- Wiik, P, Opstad PK, Knardahl S and Boyum A (1988). *Receptors for vasoactive intestinal peptide (VIP) on human mononuclear leucocytes are upregulated during prolonged strain and energy deficiency* Peptides 9(1): 181-6.
- Wong, KK, Chang S, Weiler SR, Ganesan S, Chaudhuri J, Zhu C, Artandi SE, Rudolph KL, Gottlieb GJ, Chin L, Alt FW and DePinho RA (2000). *Telomere dysfunction impairs DNA repair and enhances sensitivity to ionizing radiation* Nat Genet 26(1): 85-8.
- Yoshinaga, S, Hauptmann M, Sigurdson AJ, Doody MM, Freedman DM, Alexander BH, Linet MS, Ron E and Mabuchi K (2005). *Nonmelanoma skin cancer in relation to ionizing radiation exposure among U.S. radiologic technologists* Int J Cancer 115(5): 828-34.
- Yu, T, MacPhail SH, Banath JP, Klovov D and Olive PL (2006). *Endogenous expression of phosphorylated histone H2AX in tumors in relation to DNA double-strand breaks and genomic instability* DNA Repair (Amst) 5(8): 935-46.
- Zeidler, M and Kleer CG (2006). *The Polycomb group protein Enhancer of Zeste 2: its links to DNA repair and breast cancer* J Mol Histol 37(5-7): 219-23.
- Zeidler, M, Varambally S, Cao Q, Chinnaiyan AM, Ferguson DO, Merajver SD and Kleer CG (2005). *The Polycomb group protein EZH2 impairs DNA repair in breast epithelial cells* Neoplasia 7(11): 1011-9.
- Zhang, K, Aruva MR, Shanthly N, Cardi CA, Patel CA, Rattan S, Cesarone G, Wickstrom E and Thakur ML (2007). *Vasoactive intestinal peptide (VIP) and pituitary adenylate cyclase activating peptide (PACAP) receptor specific peptide analogues for PET imaging of breast cancer: In vitro/in vivo evaluation* Regul Pept 144(1-3): 91-100.
- Zhang, Y, Zhou J, Held KD, Redmond RW, Prise KM and Liber HL (2008). *Deficiencies of double-strand break repair factors and effects on mutagenesis in directly gamma-irradiated and medium-mediated bystander human lymphoblastoid cells* Radiat Res 169(2): 197-206.

Chapter 2

Materials & Methods

Cell culture

Multiple cell lines were utilized in this research, each with their own media and care. In each section a more detailed description will cover the particular cell line being used. All cell culture was performed in a sterile hood and maintained in incubators at 37°C with 5% CO₂.

Cells were obtained as follows: 5C normal human dermal fibroblasts (Cascade Biologics #C-004-5C), human ATM^{-/-} fibroblasts (AG04450), human LCLs (NIH), human MCF10A (ATCC #CRL-10317). All of the human mammary carcinoma cells BT-20, BT-483, DU4475, HBL100, MCF7, MDA231, MDA330, T47D and ZR75-1 were obtained from the Tissue Culture Core Facility at The University of Colorado Health Science Center (contact: Lori Sherman).

Mouse cells were obtained as follows: p53^{-/-} mouse kidneys (Taconic #p53N4-M), MEF CF-1 (ATCC #SCRC-1040), CF-1 mouse kidneys (Charles River Laboratories), MEF C57BL/6 (ATCC, #SCRC-1008), C57BL/6J mouse (Jackson Laboratory), BALB/cByJ mouse (Jackson Laboratory), SCID mouse (Jackson Laboratory), C.B6 and B6.C congenics were created in our laboratory, MEF Rad51D^{-/-} were kindly provided by Phillip Smiraldo and Douglas Pittman (Smiraldo *et al.* 2005), MEF Artemis and Artemis mouse ear/tail snips were kindly provided by JoAnn Sekiguchi (Rooney *et al.* 2002), and MEF LigIV^{-/-} cells were kindly provided by Penny Jeggo.

Cell Passage

To passage fibroblasts, media was aspirated off the cells using a vacuum. Approximately 1.5ml of 0.25% Trypsin-EDTA was added to the cells and the flask was rinsed briefly. The Trypsin solution was then aspirated and 1.5ml fresh Trypsin was added to the cells and allowed to sit until the fibroblasts became detached from the flask. Approximately 4-5 ml of media was added to the flask and the entire cells/Trypsin-EDTA/media solution was placed into a 15 ml centrifuge tube. The cells were pelleted in a centrifuge at 1000 rpm for 5 minutes. The supernatant was aspirated and the cells were re-suspended in new media. If desired, cells were counted using a Coulter Counter and seeded at a desired concentration. Alternatively, cells in the media/trypsin mixture were immediately distributed into new flasks without centrifuging. Media was added to flasks to bring to total volume of 12 ml for a T-75 flask or 5 ml for a T-25 flask. For Freezing and thawing cell cultures, see protocols in Appendix A.

To passage lymphoblasts, a desired amount of cells in mL was taken out of the stock T-75 flask and placed into a new T-75 flask. Fresh media was added to a total of 12-15mL. Alternatively, all cells in the stock flask were centrifuged at 1000rpm, resuspended in approximately 5mL of fresh media and then divided into new flasks as desired. Again, fresh media was added to total 12-15mL per T-75 flask.

Media

Fibroblasts: Most fibroblasts lines were grown in T-75 flasks using α MEM media with 10% fetal bovine serum (FBS; Hyclone #SV30014.03) and 0.5% Penicillin/Streptomycin (pen/strep; Hyclone #SV30010).

Lymphoblastoid Cell Lines (LCLs): lymphoblast lines were grown in T-75 flasks using RPMI 1640 media with L-glutamine with 15% FBS and 0.5% Pen/Strep. These cells grow in *suspension* (otherwise known as anchorage independent).

Human Breast Cancer Lines:

- BT-20: Cells were grown in Earle's Balanced Saline Solution/MEM (EBSS/MEM or Earle's MEM) with 1% non-essential amino acids, 10% FBS, 1% 100mM sodium pyruvate and 0.5% pen/strep.
- MCF7, HBL100, MDA231, MDA330, and ZR75-1: Cells were grown in Earle's MEM with 5% FBS, and 0.5% pen/strep.
- MCF10A: Cells were grown in 1:1 DMEM:Ham's F12 media with 5% FBS, 20ng/mL Epidermal Growth Factor (EGF), 0.5ug/mL Hydrocortisone, 0.1ug/mL Cholera toxin, 10ug/mL Insulin, and 1% pen/strep.
- DU4475: Cells were grown in RPMI 1640 media (with L-glutamine) with 15% FBS and 0.5% Pen/Strep. (Note: These cells grow in *suspension* and 10% FBS is all that is required for these cells.)

Cytogenetic Techniques

Cell harvest

Note: Cell cultures that grow in suspension do not need to be trypsinized like these protocols call for.

Fibroblasts: Add 20µl (alternatively add 10ul) of colcemid (0.1 to 0.2 µg/ml) for every 1 ml of media in the culture approximately 2-4 hours before intended harvest time. The longer the colcemid is in culture, the more metaphases will be present; however, the longer the colcemid is in culture, the quality of the metaphases will go down. At the time of harvest, pour off the media into a 15mL conical tube. Add about 1ml of trypsin-EDTA 0.25% in Hank's balanced salt solution (Hyclone) to the flask and rinse the flask. Then

pour the trypsin into the same conical tube and add another 1 mL of trypsin to the cells. Visualize the cells under a phase microscope, after trypsinizing the cells should appear rounded up and detached from the flask. Pipette approximately 5 ml of media into flask and pipette up and down to rinse all the cells off the flask. Remove the media/trypsin/cell solution and place in the same conical tube.

Centrifuge the conical tubes for 5 minutes at 1000 rpm. Aspirate the media/trypsin off the cells being careful not to remove the cell pellet. Loosen the cell pellet by flicking the tube, resuspend the pellet in 4 ml of 75mM KCl by and vortex at medium speed if needed or gently invert the tube to ensure there are no clumps of cells. Let the tubes sit for 15 minutes at room temperature.

Add 1 ml of Carnoy's fixative a.k.a "fix" (see solutions for fix preparation) to the tubes and invert. Centrifuge the conical tubes for 5 minutes at 1000 rpm. Aspirate the supernatant and add 4 ml of fix drop-wise to the tubes while vortexing. Let the solution sit at room temperature for 10 minutes (or longer) and spin again. Wash by adding new fix to the pellet while vortexing, let sit for 10 minutes, and centrifuge. Repeat again and proceed to dropping slides or store the cells in fix at 4°C. Once slides have been made, store left over cells in fix at -20°C.

Harvest Solutions:

Hypotonic solution (0.075 KCl): Measure 5.59 g of KCl and add dH₂O to a final volume of 1 L. Filter-sterilize and store the solution at room temperature.

Fix (Carnoy's fixative): Fix is a 3:1 methanol/acetic acid solution. Using the plunger pipettes, pump 15 ml of methanol into an Erlenmeyer flask and follow with 5 ml of glacial acetic acid and mix well by swirling. Always use fresh fix. Fix more than a few hours old will have additional compounds not desired for this procedure.

Colcemid: Gibco #15212-012, stock is 10ug/mL

Slide Cleaning & Preparation

Fischer Premium Slides were placed into slide racks and placed in glass chambers. A 1:1 methanol/ethanol solution was added, approximately 50 ml, or enough to fully cover the slides. A cover was placed on the chamber and left at room temperature overnight. The next day, the methanol/ethanol solution was aspirated off, and the slides were rinsed 3X with ddH₂O. After the final water rinse, the water was poured off and the slides were stored for later use in at -20°C.

Dropping slides

Slides for cytogenetic analysis were all prepared using Fischer Premium Slides Frosted. Slides were stored at -20°C and rinsed 3X with ddH₂O before use and placed on ice. After cell harvest, the cell pellets were washed 2X using 3:1 methanol/acetic acid fix. After the final wash, cells were centrifuged at 1000 rpm for 5 minutes and the supernatant was aspirated using a vacuum. Fix was added to the pellet in an amount in order to make the solution “slightly milky”. Approximately 3 drops of the cell solution was dropped onto a Fischer Premium Slide and steamed over a water bath for approximately 10 seconds. The slide was then dried on a warming tray until dry. The slides were visualized on a Zeiss phase microscope to check for metaphase spreads.

CO-FISH

Chromosome Orientation- Fluorescence *In Situ* Hybridization was done according to S.M. Bailey’s method (Bailey *et al.* 1996; Bailey *et al.* 2004).

Irradiation:

If radiation is a desired part of the CO-FISH process, cell cultures are allowed to become confluent in a T-25 flask. The cells are then irradiated, one flask with 0 Gy and one flask with 1 Gy, with a sealed-source Mark I ^{137}Cs γ -irradiator (J.L. Shepherd and Associates). 24 hours later the cultures are split to allow cell growth in the presence of BrdU as described subsequently.

Fixing steps:

Slides with metaphase spreads that were obtained from cells grown for one round of replication in the presence of 2×10^{-5} M 5'-bromo-2'-deoxyuridine (BrdU, Sigma #B5002-1G) were used for these experiments. Slides were prepared by soaking in RNase A (100 $\mu\text{g}/\text{ml}$ H_2O) for 10 minutes in a 37°C water bath. Slides were then rinsed in PBS. Slides were fixed in 3% formaldehyde/PBS solution for 10 minutes at room temperature. Next, slides were dehydrated in a cold ethanol series (75%, 85%, and 100% ethanol) for 2 minutes each. Then the slides were air dried.

Hybridization steps:

After the slides have dried, they are stained with Hoescht 33258 by placing 50 μl of the Hoescht 33258 into 50 ml of 2x SSC (0.5 $\mu\text{g}/\text{ml}$ 2X SSC) for 15 minutes at room temperature. The slides are then flooded with 50 μl of 2x SSC and coverslip is placed on the slide. Using a Stratalinker 2400 (Stratagene #400075), expose the slides to 365 nm UV for 30 minutes. The coverslips are then removed and rinsed with H_2O and air dried. An Exonuclease III solution (Promega) is prepared while drying (0.5 μl of enzyme, 45 μl

of H₂O, and 5 µl buffer (50 mM Tris-HCl, 5 mM MgCl₂, and 5 mM dithiothreitol, pH 8.0)) and applied at 50 µl per slide and a coverslip is mounted. This was allowed to sit at room temperature for 10 minutes. The slides are then rinsed with H₂O and air dried. After drying, the slides are placed in a Coplin jar filled with 70% formamide/2x SSC solution heated in a H₂O bath at 70°C for 1 minute (be sure to heat the Coplin jar in the H₂O bath at the same time, placing a cold Coplin jar in a hot water bath will cause breakage). After 1 minute, remove the slides from the hot solution and immediately place in a fresh cold ethanol series. Let the slides soak in each ethanol solution (75%, 85%, and 100%) for 2 minutes each. Let the slides air dry. Apply 20 µl of hybridization solution to each slide and coverslip (see below for description of hybridization solution). Add 10 µl of H₂O to each hole in the hybridization chambers and place slides in them. Let hybridize for approximately 2 hours at 37° C in the dark (times may vary depending on results).

Rinsing steps:

After hybridization, remove slides from hybridization chambers and place in 70% formamide/ 2x SSC at 29° with shaking for 15 minutes. Wash slides with PN buffer for 5 minutes at room temperature. Mount slides with approximately 12µl of Vectashield antifade-DAPI. Store the slides at 4°C in the dark for future examination.

Alternative staining:

It may be desired to incorporate anti-BrdU staining to the slides for extra security that CO-FISH has worked properly. After the 70% formamide/2x SSC at 29°C wash,

rinse for 1 minute in PN buffer. Add 20 μ l of anti-BrdU probe (see below for description) to each slide and place in hybridization chambers. Incubate at 37°C for 30 minutes. Remove from chamber and place in PN buffer for 5 minutes, and mount with Vectashield/DAPI as above.

Image Analysis:

Images were analyzed and captured using a Zeiss Axioskop2 Plus microscope equipped with a Photometrics Coolsnap ES2 camera and Metavue 7.1 software.

Solutions for CO-FISH:

Note: most of these solutions can be used a few times before they need to be made fresh again.

RNAse A: Ribonuclease A (Sigma): Add 0.005 g of RNAse A to 50 ml of dH₂O, thoroughly dissolve. Store at 4°C when not in use.

3% formaldehyde solution: Use 4.05 ml of 37% Formaldehyde from Fischer Scientific in a Coplin jar. Bring the volume up to 50 ml total with PBS (see description of PBS below).

PBS (Phosphate buffered solution): Dissolve 8 g of NaCl (Fischer Scientific), 0.2g of KCl, 1.44 g of Na₂HPO₄ (Merck), and 0.24 g of KH₂PO₄ (Fischer Scientific) in 800 ml of dH₂O. Adjust the pH to 7.4 with HCl (Aldrich) using an Orion pH meter. Add dH₂O to make final volume 1 L. Filter sterilize and store at room temperature.

Hoescht 33258 (Fisher #AC22989-1000): Make working solution by dissolving Hoescht 33258 to a final concentration of 500 μ g/ml of H₂O. It is very light sensitive, so keep covered in aluminum foil.

70% formamide/2x SSC (for wash and denature steps): Add 5 ml of 2x SSC, 10ml of dH₂O, and 35 ml of 37% formamide to a Coplin jar.

20X SSC (standard sodium citrate): For a final volume a concentration of 3 M

NaCl and 0.3 M Na citrate (Fischer Scientific) is needed. Add 87.66g NaCl and 44.12g NaCitrate and dissolve in dH₂O. Final volume should be 500 ml. Filter sterilize and store at room temperature.

2X SSC: Take 100 ml of 20X SSC stock solution and add 900 ml of dH₂O. Store at room temperature.

Working Probe solution: Take 1 µl of stock PNA-Cy3 probe (Applied Biosystems) and add to 99 µl of dH₂O. Heat at 50° C for 30 minutes at store at -20° C.

Hybridization solution: For approximately 2 slides, add 35 µl of formamide, 12µl Tris-HCl (12 µM), 2.5 µl KCl (5 µM), 0.5 µl MgCl₂ (1 µM), and lastly, 3.3 µl of working probe solution. Denature probe right before use by heating for 5 minutes at 70° C and immediately placing on ice until use.

PN buffer: make 1L of 0.1M Na₂HPO₄ in water. Add to this 50mL of 0.1M NaH₂PO₄ and 1mL of Triton X-100.

FPG

Fluorescence plus Giemsa (FPG) was performed according to (Perry and Wolff 1974). Slides are initially stained with 50 µl of Hoescht 33258 in 50 ml of 2x SSC (see above for description) for 15 minutes at room temperature. The slides are then rinsed with ddH₂O and air dried. Mount the slides with 50 µl 2X SSC and coverslip (see above description for coverslips). Expose slides to 365 nm UV light in a Stratalinker 3000 for 30 minutes. Remove coverslips and place in a Coplin jar of 2X SSC at 60° C, in a water bath, for 30 minutes. Do not let the slides dry in between. Take the slides out of the water bath and rinse with ddH₂O very well, at least 5 rinses. Stain the slides with 5% Giemsa for approximately 10 minutes. The amount of time will determine the coloration and contrast on the slides.

FPG solutions:

Hoescht 33258: Make working solution by dissolving Hoescht 33258 to a final concentration of 500 μ g/ml in H₂O. It is very light sensitive, so keep covered in aluminum foil.

2x SSC: Take 100 ml of 20x SSC stock solution and add 900 ml of dH₂O. Store at room temperature.

5% Giemsa: Take 2 ml of Modified Giemsa Stain from Sigma, and place in a 50ml conical tube. Add 38 ml of dH₂O, mix well. This is a 1:20 dilution to make the working solution.

G2 Assay

The G2 assay is designed to measure radiation sensitivity at the chromosome level. This method simply evaluates chromatid-type damage in chromosomes from the G2 phase of the cell cycle in cell cultures following radiation treatment. The basis for this protocol comes from David Scott's laboratory (Scott *et al.* 1999) but T.C. Hsu also contributed to the development of this assay (Wei *et al.* 1996; Wu *et al.* 2005).

Non-confluent cell cultures were irradiated with either 0 Gy or 0.5 Gy of γ -radiation. 30 minutes after radiation treatment, colcemid was added to a final concentration of 0.1 μ g/mL. 1 hour after the addition of colcemid, cells were harvested on ice (as described above) and fixed with 3:1 Methanol:Acetic Acid. Slides were then prepared (as described above). Finally, slides were stained with 5% Geimsa for about 10 minutes and analyzed for chromatid-type aberrations and telomere associations. A minimum of 25 metaphases were scored for each cell line.

G2 Assay Analysis

A student's t-test was used to compare cases as a group to controls as a group. Logistic regression was performed to estimate if the results of the G2 assay could predict case/control status using SigmaStat 3.5 (Systat Software, Inc).

G2 Assay Solutions:

5% Geimsa: Take 2 ml of Modified Giemsa Stain from Sigma, and place in a 50ml conical tube. Add 38 ml of dH₂O, mix well. This is a 1:20 dilution to make the working solution.

Sealed-source Mark I ¹³⁷Cs γ -irradiator (J.L. Shepherd and Associates)

Flow Cytometry Assays

Telomere Flow FISH

Preparing & Fixing Cells

The majority of this protocol came from (Rufer *et al.* 1998). Non-confluent LCLs were harvested by simply pouring cells into 15mL conical tubes and centrifuging at 1000rpm for 5min. Cells were counted using a Beckman Coulter Counter and then frozen down as normal (see appendix for protocol) with all samples having the same number of cells, usually 2 million. While cells were counted, the remaining cell population was kept on ice. Extra cells were kept aside for various controls. The number of cells was adjusted to be the same for all samples and the cells were frozen and stored at -80°C until the next steps can be carried out.

Hybridization with Telomere Probe

Cells were quickly thawed as usual and washed 2X with PBS (see appendix for thawing protocol). Next cells were resuspended in 300ul of hybridization mixture with the Tel-C PNA probe conjugated to FITC (with AND without telomere probe for “DNA only” controls--see below for details) and heated for 10min in an 80°C water bath. Then cells were allowed to hybridize with the probe at room temperature by placing on a rocking platform in the dark for 1.5-2.5 hours. Cells were then washed with approximately 1mL of wash solution (see below), spun down, and resuspended in approximately 500ul DNA staining solution. Cells were filtered through 30um filters (GCAT #04-0041-2316) to eliminate clumps, which can damage the flow cytometry machine, and allowed to sit for at least 20min before analysis.

Flow Cytometry Parameters

A 488nm excitation laser on a MoFlo Flow Cytometer (Dako) equipped with Summit software was used to collect flow cytometry data. The voltage for FITC was set at 665 with a gain of 8 (linear) while the PI HV was 400 with a gain of 1 (linear). Controls include unstained cells, cells that had “DNA only” stain and had no processing as well as CHO A_L cells “DNA only” and a CHO A_L “telomere” sample.

Flow Cytometry Analysis

Relative telomere length was calculated for each patient by subtracting the average FITC intensity of the “DNA only” sample from the average FITC intensity of the

corresponding “telomere sample”, both of which are gated on the G0/G1 population of cells to adjust for DNA content. Summit 4.0 Software (Dako Cytomation) was used for analysis.

Telomere Flow FISH solutions:

PBS

Hybridization Solution: Mix 210ul of formamide (Fisher), 6ul 1M Tris-HCl pH 7.1, 0.0015g Bovine Serum Albumin (BSA, Sigma), 22.66ul Tel-C PNA FITC working probe solution and 61.34ul H₂O for each sample. This gives a solution with final concentrations of 70% formamide, 20mM Tris-HCl, 0.5% BSA and 50nM PNA telomere probe.

For “DNA only” controls, mix the above solution except replace the Tel-C PNA probe with H₂O.

Working Tel-C PNA Solution: Dilute the stock PNA solution (6.62 X 10⁻⁵M or 356ug/mL, Applied Biosystems) 1:100 with H₂O. The PNA sequence is: Flu-OO-CCC-TAA-CCC-TAA-CCC-TAA and the working solution is 6.62 X 10⁻⁷M.

Wash Solution: Mix 700ul of formamide (Fisher), 10ul 1M Tris-HCl and 290ul H₂O for each sample. This gives final concentrations of 70% formamide and 10mM Tris-HCl.

DNA Staining Solution: Mix 10ul of stock PI (Propidium Iodide), 10ul of stock RNase A and 980ul PBS. This makes 1mL, make as much as you need for the number of samples you have. The final concentrations are 10ug/mL PI and 1ug/mL RNase A.

Stock PI: 1mg/ml in PBS pH 7, store at 4°C, in dark (MP Biomedicals #19545825)

Stock RNase A: Mix 0.005g of RNase A (Sigma #R5503) in 50 mL H₂O for a final concentration of 100ug/mL. Store at 4°C.

γ H2AX Foci Flow

Irradiation, Preparing & Fixing Cells

This protocol comes from Zhang et al., with slight modifications (Zhang *et al.* 2005). 5mL of non-confluent LCLs were irradiated in T-25 flasks at a dose rate of 10cGy per hour for 24 hr from a ^{137}Cs source which gave a total dose of 2.4Gy γ -radiation. 0Gy and 2.4Gy samples were harvested as stated above and a portion of cells was set aside for counting.

Working quickly to fix the cells as soon as the irradiation was complete, cells were fixed in 1% EM grade paraformaldehyde/PBS vortexed immediately (a single cell suspension is needed) and placed on ice for 15min. Cells were then centrifuged at 1000rpm for 5 min and resuspended in 3mL ice cold PBS, then 7mL of 100% ultra pure cold EtOH was added slowly while vortexing (final concentration of 70% EtOH). Make sure there are no clumps of cells. Cells can now be stored at -20°C until the process can be continued. Cells should be left on ice or stored at 4°C for at least 30 min before moving to the next step if the cells will not be stored at -20°C

Applying Antibodies for H2AX foci

Stored cells were pelleted in the centrifuge at 1000rpm for 5min. Next cells were transferred to 1.5mL microcentrifuge tubes and resuspended in permeabilization buffer (see below) for 20-30 minutes on ice. Cells were pelleted again and resuspended in 200ul primary antibody for p-H2AX ser139 (mouse monoclonal antibody, Upstate # 05-636, 200ug/ul stock) diluted 1:200 in TBFP and allowed to hybridize at room temperature in the dark with rocking for 1.5-2 hr. Next, the cells were centrifuged at 10,000rpm for 5min and washed with 1mL PBS and centrifuged again. 200ul of secondary antibody

diluted 1:200 in TBFP (goat anti-mouse IgG conjugated to AlexaFluor488, Molecular Probes/Invitrogen #A11029, 2mg/mL stock) was then hybridized to the cells on ice for 30 min in the dark. Finally, the cells were resuspended in DNA staining solution, filtered through 30um filters (GCAT #04-0041-2316) and allowed to incubate for at least 20min before analysis.

Flow Cytometry Parameters

A 488nm excitation laser on a MoFlo Flow Cytometer (Dako) equipped with Summit software was used to collect flow cytometry data. The voltage for FITC was set at 665 with a gain of 8 (linear) while the PI HV was 400 with a gain of 1 (linear). Controls include unstained cells, cells that had “DNA only” stain and had no processing as well as CHO A_L cells “DNA only”, a CHO A_L “ γ H2AX” sample, a primary antibody with PI only, a secondary antibody with PI only and a primary secondary antibody only sample.

Flow Cytometry Analysis

Relative γ H2AX intensity was calculated for each patient by subtracting the average FITC/Alexa488 intensity of the “DNA only” sample from the average FITC/Alexa488 intensity of the corresponding “ γ H2AX sample”, both of which are gated on the G0/G1 population of cells to adjust for DNA content. Summit 4.0 Software (Dako Cytomation) was used for analysis.

H2AX Foci Flow Solutions:

PBS

1% paraformaldehyde: Mix 100ul of 10% paraformaldehyde (Fisher #NC9895083) with 900ul PBS to make a 1% paraformaldehyde solution.

TBFP: Mix 5ul Tween (FRESH each time), 0.01g BSA (Fisher), 10ul FBS and 985ul PBS for each sample. The final concentrations are 0.5% Tween, 1% BSA, and 1% FBS.

Permeabilization buffer: Mix 2.5ul Triton X-100 (FRESH each time, brand) and 997.5ul PBS. The final concentration of Triton X-100 is 0.25%.

DNA Staining Solution: Mix 10ul of stock PI (Propidium Iodide), 10ul of stock RNase A and 980ul PBS. This makes 1mL, make as much as you need for the number of samples you have. The final concentrations are 10ug/mL PI and 1ug/mL RNase A.

Stock PI: 1mg/ml in PBS pH 7, store at 4°C, in dark (MP Biomedicals #19545825)

Stock RNase A: Mix 0.005g of RNase A (Sigma #R5503) in 50mL H₂O for a final concentration of 100ug/mL. Store at 4°C.

Bystander Effect Experiments

Cell Transfer Assay

Preparation of recipient cells: Recipient cells were grown up prior to the experiment and were in log phase growth. The day of the experiment, the cells were trypsinized and centrifuged at 1000 rpm for 5 minutes. They were then re-suspended in PBS and counted using a Beckman Coulter Counter. Approximately 400,000 recipient cells were then added to a T-75 flask, and 12 ml of α MEM was added to the flask. Donor cells were then added as quickly as possible (see below).

Preparation of donor cells: The donor cells were grown up in α MEM and were in log phase growth before use. The day of the experiment, the donor cells were irradiated using a sealed-source Mark I ^{137}Cs γ -irradiator (J.L. Shepherd and Associates) for a total dose of 1 Gy. After irradiation, cells were trypsinized and centrifuged down at 1000 rpm for 5 minutes. Cells were re-suspended in sterile PBS and counted using a Beckman Coulter Counter. Donor cells were then seeded into flasks containing the recipient cells at dilutions of either 1:100 or 1:1000 donor to recipients. BrdU was added to the culture at a concentration of $1-2 \times 10^{-5}\text{M}$. The entire culture was allowed to grow for approximately two rounds of replication, harvested, and slides were prepared. FPG and cytogenetic analysis on the slides then allowed visualization of G-SCE.

BSE Statistical Analyses

Metaphases were blinded and scored for either G-SCE. Standard deviations were calculated and used to determine standard error of the mean (SEM) for the error bars. Statistical analysis on SCE can be difficult as several assumptions must be made. The first is that the SCE's are independent of each other, in that, one particular cell was not hypersensitive compared to the others. This also leads to the assumption that SCE follow a Poisson distribution. Finally, it must be assumed that DNA content scales similarly with chromosome number (unless it is confirmed using flow cytometry). Given the characteristics, it seems safe to make these assumptions. For most lines, SCE was calculated on a per chromosome basis as to avoid any issues with chromosome number variation between metaphases. For the bystander data, SCE per metaphase was used as only the normal human fibroblast cell line was used, and it has a fairly stable

chromosome number. Also, with matching controls in every experiment, it is safe to analyze on a per metaphase basis.

RNA Isolation & Gene Expression Techniques

RNA Isolation

RNA was harvested from LCLs as well as 5C normal human fibroblasts and human mammary MCF10A epithelial cells. An RNA isolation kit from Qiagen was used. Briefly, cells were harvested and washed once with PBS if trypsin was used during the harvest. Cells were lysed, added to a column, washed and eluted with RNase-free H₂O. RNA concentration was determined using a Nanodrop Spectrophotometer and stored at -20°C for short term and -80°C for long term.

RNA from LCLs was shipped to Michael Story's lab for microarray analysis while 5C and MCF10A RNA was made into cDNA and used for Real-Time PCR.

RNA isolation materials & reagents:

RNeasy Mini Kit (Qiagen #74106)
QIAshredder Kit (Qiagen #79656)
Beta-Mercaptoethanol (BME)
70% ethanol made with RNase free H₂O

Microarrays with Telomere/DNA repair genes

Genomic RNA was isolated from low passage LCLs using an RNeasy kit (Qiagen). The probes found on the array were designed by the Wright lab in consultation with Operon Biotechnologies (Huntsville, AL) based upon subtelomeric DNA sequences

provided by Harold Reithman of the Wistar Institute in 2003

(http://www.wistar.org/research_facilities/riethman/research.htm). These 70-mer probes were designed to survey a large number of subtelomeric genes and putative genes. The oligos represent 180 genes from duplicated subtelomeric regions: 271 genes from single-copy subtelomeres, 92 randomly selected control genes, 12 “typical” control genes, 60 non-telomeric genes known to change with cellular age, 48 telomere-related genes and 90 miscellaneous “interesting” genes.

Most of these genes are identified with the ends of telomeres or are telomere responsive. Many are putative genes and may not be expressed at all, or, are expressed at very specific times in the life of a cell. Therefore, one may see little to no expression signal for these genes.

The slide has 2 grids of 2,304 spots representing each gene spotted in triplicate. Slides used are Full Moon Matrix II 3-D slides and were printed using a MicroGrid II print robot. Labeling and hybridization was performed using a Perkin Elmer (Waltham, MA) MicroMax Hybridization Kit (indirect labeling) according to the manufacturer’s protocol. Total RNA (10ug) was used. All samples were compared to a reference RNA signal (Stratagene Universal Reference RNA).

After washing and drying, the slides were immediately scanned on an Axon (Molecular Devices, Sunnyvale, CA) GenePix 4300 Scanner. Data was downloaded onto BRB-ArrayTools (NCI, Bethesda, MD).

Microarray materials & reagents:

RNeasy kit (Qiagen)
Full Moon Matrix II 3-D slides
MicroMax RNA labeling Kit (Perkin Elmer)
Universal Reference RNA (Stratagene)
Axon GenePix 4300 Scanner (Molecular Devices)

Microarray analysis:

Data was downloaded onto BRB-ArrayTools (NCI, Bethesda, MD), background corrected and normalized within and across arrays. Gene selections were performed using the SAM algorithm within BRB ArrayTools using a false discovery rate of 10% and a fold-change cutoff of 2.

Preparation of cDNA

cDNA was made by using a Verso cDNA kit (ABgene #ab1453) and experiments were performed in a bench-top hood specifically for PCR work. 4ul of 5X buffer, 2ul of dNTP, 1ul of 3:1 random hexamers:oligo dT were mixed together and spun down for each sample. Then 1ul of Versomax enzyme (times the number of samples) was added, gently mixed and centrifuged briefly. Next, 8ul of this master mix solution was added to each well of the PCR tubes. Then the proper amount of H₂O (to total 12ul with amount of RNA) was added to each well. Finally, the appropriate amount of ul of RNA was added to each well so that every sample contained 1ug of RNA total and the cells were briefly centrifuged. Every PCR reaction should total 20ul.

Next the PCR samples were placed in a PCR machine (either a Hybaid or a BioRad Icyler) and went through the following protocol:

Hold 42°C for 30 minutes

Hold 95°C for 2 minutes
Hold 4°C

PCR tubes were then briefly centrifuged and cDNA was stored at -20°C. cDNA concentration is assumed to be a 1:1 ratio from the RNA used so a concentration of 1 µg in 20 µl was assumed for the cDNA. This gives a concentration of 0.05 µg/µl or 50 ng/µl.

cDNA materials & reagents:

Verso cDNA kit (ABgene #ab1453)
DNase, RNase free H₂O
Hybaid PCR machine

Real Time PCR

For Rad51D and EZH2 analysis following IR in 5C and MCF10A cells

Cells were irradiated with either 0Gy or 5Gy radiation from a sealed-source Mark I ¹³⁷Cs γ-irradiator (J.L. Shepherd and Associates) and RNA was harvested as described above at 0, 2, 4, 8 and 24 hr post-irradiation. Both confluent and log-phase cells were used and both of these experiments were repeated 3 times, starting with irradiating new flasks of cells. The housekeeping gene used was TFRC (transferrin receptor) and I did not observe any changes in the housekeeping following radiation exposure. In addition, I found at least one other investigator that also used TFRC as a housekeeping gene after IR (Sorensen *et al.* 2005).

Keep all reagents on ice, keep SYBR green in the dark, & perform real time PCR in the PCR hood. cDNA (usually a total amount of 10, 12.5 or 15ng was used) and primers were diluted to appropriate concentrations (see materials below). For each well, 10 µl of Sybr green, 5 µl of primers and 5 µl of cDNA was used. In a 96-well plate,

aliquots of 10ul Sybr green were added to each well being used. Next, the appropriate primers were added followed by the appropriated cDNA. The PCR plate was then sealed carefully and the plate was centrifuged at approximately 1500rpm in the dark for no more than 5min. Each reaction was done in triplicate and water replaced cDNA in the control wells. The plate was then placed in the BioRad Icycler and was analyzed under the following protocol:

PCR protocol

1. 95°C for 3 min
2. 95°C for 15 min
3. 45 cycles of
 - a. 95°C for 10 sec
 - b. 55°C for 45 sec-With data collection and real-time analysis enabled
4. 95°C for 1 min
5. 55°C for 1 min
6. 80 cycles of
 - a. 55°C for 10 sec-increase setpoint temperature after cycle 2 by 0.5°C
-melt curve data collection and analysis enabled

Plates were stored at -20°C when PCR was complete.

Real time PCR materials & reagents:

Primers

- EZH2 10X stock (Qiagen #QT00054614) (1X final concentration)
 - Rad51D 10X stock (Qiagen #QT00021168) (1X final concentration)
 - TRFC 50uM stock (Sigma Genosys) (100nM final concentration)
- F: 5' CGCTGGTCAGTTCGTGATTA 3'
R: 5' GCATTCCCGAAATCTGTTGT 3'
100uM stock for both → mix to make 50uM stock of mixed F & R

96 well Real-time PCR plates

Optical seals for real-time PCR plates

QPCR 2X SYBR Green Fluorescein Mix (Thermo Scientific #ab-1219/b)

DNase, RNase free H₂O

BioRad Icycler thermal cycler

Icycler iQ software version 3.1

PCR reaction	cDNA
10ul Sybr green	•loaded 1ug RNA so assume 1000ng
5ul primers	cDNA made in 20ul = 50ng/ul
<u>5ul cDNA</u>	1ul cDNA
20ul rxn	<u>19ul H₂O</u>
	20ul → load 5ul per well = 12.5ng
Rad51D & EZH2 primers	TFRC primers
2ul 10X primers	50mM (mixed F & R) → 10uM (1:5)
<u>3ul H₂O</u>	1ul TFRC stock
5ul per well	<u>4ul H₂O</u>
	5ul of 10uM primers, then:
	0.4ul 10uM primers
	<u>4.6ul H₂O</u>
	5ul per well

Real Time PCR

For VIPR2 in LCLs to confirm microarray results

The same procedures were followed as listed above, however only 500ng of RNA was used in the creation of cDNA (instead of 1ug). Therefore, the concentration of the cDNA created should be 25ng/ul. 12.5ng of cDNA was used in the Real Time reaction. The same protocol as listed above was used in the icycler. I used the exact same RNA samples that were used for the microarray analysis and the same housekeeping gene as listed above.

Real time PCR materials & reagents:

Primers

- VIPR2 10X stock (Qiagen #QT00073388) (1X final concentration)
 - TRFC 50uM stock (Sigma Genosys) (same as above)
- And other reagents as listed above

Real Time PCR analysis & statistical methods

The Livak method was used to normalize results to the housekeeping gene and to compare unirradiated and irradiated samples (Livak and Schmittgen 2001). One way ANOVA with Tukey's post-test was performed for statistical significance using Prism 4.0c software (GraphPad Software, Inc.).

Protein Analysis

Co-Immunoprecipitation

Co-IP was performed using the ProFound Mammalian Co-Immunoprecipitation Kit from Pierce. Whole cell lysates were extracted from human log-phase 5C and MCF10A cells and all steps were performed in a sterile laminar flow hood. The first part of the Co-IP is antibody immobilization in which antibody coupling gel is applied to a column. 200ul of gel slurry is added to the column and centrifuged for 1min at 3,000rpm. The flow through is discarded and the gel is then washed with 400ul of coupling buffer 3 times. Finally the antibody for the protein of interest is added to the gel along with sodium cyanoborohydride and the tube with the gel/antibody mixture in it is incubated over night with end-over-end mixing at 4°C.

The next day, the tube is centrifuged and washed with 400ul coupling buffer. Then 400ul of quenching buffer is added, centrifuged and the flow through discarded. Another 400ul of quenching buffer is added along with sodium cyanoborohydride and incubated for 30min. Next the gel is washed 2 times with wash solution and then 2 times

with coupling buffer. At this point the gels can be stored for later use or the protocol can be continued.

Now the 5C and MCF10A cells are lysed and diluted if needed in coupling buffer. Lysates are added to a gel with antibody and one without to serve as a control for non-specific binding. The gel columns with protein lysates are incubated over night with end-over-end mixing.

The tubes are centrifuged the next day and it is optional to save the flow through for further analysis. 400ul of Co-IP buffer are added to the tubes, gently mixed and centrifuged. This is repeated 2 more times and these flow-through samples can be saved as washes 1, 2 and 3.

The next part of this process is the elution of the Co-IP complex. Elution buffer is simply added to the gel columns, gently mixed and centrifuged. This is repeated 2 more times and these flow through samples are saved as elution 1, 2 and 3.

It is optional at this point to add 400ul of elution buffer and 100ul of loading dye to the gel. This mixture is then transferred to a new tube after mixing and heated at 95°C for 4min. The mixture is then put back onto the column and centrifuged. This sample is the gel boil sample and can be used if the Co-IP complex is not eluted easily. All of the samples listed in this procedure can be evaluated via SDS PAGE and western blot, but the most important samples are the elutions.

Co-IP materials & reagents:

Mammalian Co-IP Kit (Pierce #23605)
Primary Rad51D Antibody (Chemicon #MAB3698)
Primary EZH2 Antibody (Cell Signaling Technology #3147)
Primary human 5C cells
Human MCF10A cells

SDS PAGE & Western Blot

The elutions and other sample of interest from above are now run on an SDS PAGE gel. We like to use BioRad 10% TrisHCl gels. 20ul of each elution plus 5ul of 4X loading dye are added to each lane of the gel after heat treatment at 95°C for 4min. A protein ladder with known molecular weights is also included in one lane. The SDS gel is run at 200V for 37min.

Next the SDS gel is transferred to a PVDF membrane (Immobilon-FL). This membrane must be soaked in 100% methanol prior to use and gloves should be worn to avoid fingerprints on the membrane. The transfer is done at 100V for 1 hr and 15min at room temperature with spinning and an ice pack in the chamber.

The membrane is then blocked with 5% milk in TBS for 1 hr at room temperature with gentle shaking. The membrane should then be rinsed with 1X TBST and the primary antibody can now be applied. Usually the primary antibody is diluted 1:1000 in TBST with 1% milk. Incubate the membrane with the primary antibody solution, in this case with antibodies for Rad51D and EZH2, for 1 hr at room temperature with gentle shaking.

Then the membrane should be rinsed 4 times for 5min each with TBST to remove any excess primary antibody. Next the membrane can be incubated at room temperature for 1 hr with the secondary antibody. This consists of 10 mL Odyssey blocking buffer, 10ul of Tween 20, 10ul of 10% SDS and a 1:10,000 dilution of goat anti-mouse IgG. This is light sensitive to be sure to prepare the solution in the dark and keep the membrane covered in foil during the incubation.

Finally, the membrane is rinsed again 4 times for 5 min each with TBST, in the dark. Lastly, wash the membrane once with TBS. The membrane can be kept in the TBS in the dark for up to 24 hr for imaging. Image the membrane using the Odyssey scanner.

SDS and Western blot materials & reagents:

Precast 10% TrisHCl gel (BioRad #161-1155)
Instant non-fat dry milk
Transfer membrane, immobilon-FL (Millipore #IPFL20200)
Power source
Gel boxes
Filter paper (BioRad #1703932)
Precision Plus Dual color standard marker (BioRad #161-0374)
Odyssey blocking buffer (Li-cor Biosciences #927-40000)
Goat anti-mouse IgG Alexafluor 680 (Invitrogen #A21058) (secondary antibody)
Rad51D monoclonal antibody (Chemicon #MAB3698) (primary antibody)
EZH2 monoclonal antibody (Cell Signaling Technology #3147) (primary antibody)

5X TBS: Mix 12.1g of TrisBase and 146.1g NaCl in about 800mL of water. Adjust the pH to 7.5 and bring the final volume up to 1L with additional water. Dilute with water to 1X TBS before using.

TBST: Dilute 5X TBS to make 1L of 1X TBS and add 1mL of Tween-20 for a final concentration of 0.1% Tween-20.

5X Running buffer: Mix 15g of TrisBase, 72g of Glycine and 5g of SDS in 1L of water. Dilute with water to a concentration of 1X before using.

Transfer buffer: Make this fresh each time. Dissolve 3.03g of TrisBase, and 14.4g of Glycine in about 600mL of water. Add 200mL of Methanol. Bring the total volume up to 1L with more water. Try to keep this cold before the transfer begins.

Block solution: For 5% block solution, add 0.75g of instant non-fat dry milk to 15mL of 1X TBS.

1° antibody solution: Add 0.15g of milk to 1X TBST. Then add 15ul of primary Rad51D antibody and 15ul of primary EZH2 antibody.

2° antibody solution: In the dark, mix together 10mL of Odyssey blocking buffer,

10ul of Tween-20, 10ul of 10% SDS and 1ul of goat anti-mouse Alexa 680. This results in the following final concentrations: 0.1% Tween-20 and 0.01% SDS.

DNA Isolation and Rad51D SNP Analysis

DNA Isolation

DNA was isolated using a Qiagen kit. Briefly, cells were centrifuged and lysed followed by proteinase treatment. DNA mixture was added to a column, washed and then eluted into H₂O. DNA concentration was measured with a Nanodrop Spectrophotometer and stored at -20°C.

DNA isolation materials & reagents:

DNeasy Tissue Kit (Qiagen #69506)
PBS
100% EtOH

PCR for Rad51D variant detection

The following reagents were mixed: 2.5ul 10X PCR buffer, 0.5ul dNTP, 0.75ul MgCl₂, 1.25ul 10uM primers, 0.5ul Taq polymerase, and 18.5ul H₂O for each DNA sample. Aliquot 24ul of this mixture to the PCR tubes. Add 1ul of DNA for each sample to the tubes. This is for a total amount of 50ng of DNA, however if DNA samples are not at this same concentration, adjust the DNA volume and then correspondingly adjust the H₂O volume. Briefly spin down tubes and place them in the PCR machine, using the following protocol:

PCR protocol:

- a. 36 cycles of:
 - i. 94°C for 45 sec
 - ii. 60°C for 30 sec
 - iii. 72°C for 1.5 min
- b. 72°C for 10 min
- c. 4°C Hold

The purity of the PCR product was examined by gel electrophoresis, using a 1.5% agarose gel. If PCR products were “dirty”, they were cleaned up by Ethanol precipitation. To 30ul of PCR product, the following was added: 3ul of 3M Sodium Acetate, 60ul of 100% cold ethanol. The solution was then mixed well and placed at -80°C for 1 hour. The tubes were then centrifuged and the DNA pellets were washed with 70% ethanol and centrifuged again. The pellets were allowed to air dry and then resuspended in 16ul of H₂O.

Rad51D PCR materials & Reagents:

PCR 1X reaction

- 1 ul DNA (for 50ng total, can be adjusted)
- 2.5 ul 10X PCR buffer
- 0.5 ul dNTP
- 0.75ul MgCl₂
- 1.25 ul 10uM primers
- 0.5 ul Taq
- 18.5 ul H₂O
- 25 ul reaction

Primers (Ordered from Sigma Genosys)

- F1: 5' CTGTGAAGGTGGTGGTTGTG 3'
- F3: 5' GGAAGTGTGAAGGTGGTGGT 3'
- R1: 5' TCGATGGTGTCCAGGAGAAT 3'
- 100uM stock for each

Taq DNA polymerase 5U/ul (Invitrogen #18038-042)

- 10X PCR buffer
- 50mM MgCl₂

dNTP Mix, 10uM each (Fermentas #R0191)

Rad51D Variant DNA Sequencing

To detect the presence of the E233G SNP in Rad51D, DNA samples and primer F1 (at a concentration of 19ng/ul) was shipped to Davis Sequencing according to their instructions.

Real Time PCR for Telomere Length

Telomere Real Time PCR

This protocol was taken from Dr. Cawthon with minor changes, and here is designed for use with human samples, although a similar protocol for mouse samples is available (Cawthon 2002). Enough working solution (10uM) of primers was prepared for the amount of reactions and all primers were diluted as needed (see materials below). Primer master mixes were mixed and stored on ice. DNA was also freshly diluted to 1ng/ul and kept on ice. The “S” reaction and “T” reactions need to be performed separately so either the PCR plate was divided in half or 2 separate plates were used. Using the PCR hood and working in the dark because the Sybr green is light sensitive, 10ul of Sybr green master mix were added to each well on a PCR plate. Next, 5ul of the correct primers (S primers first) were added to the wells. Finally, 5ul of the appropriate DNA samples (or H₂O for controls) was added to each well. The plate was sealed, briefly centrifuged, put into the PCR Icyler machine and went through the following protocol. Immediately after the “S” run completed, the “T” run was performed the same

way, including the same plate set-up so samples are in the same well position for each run, using the following protocol.

PCR Protocol:

S profile:

1. 95°C for 15 min
2. 45 cycles of
 - a. 95°C for 15 sec
 - b. 58°C for 20 sec
 - c. 72°C for 20 sec
3. 95°C for 1 min
4. 60°C for 1 min
5. 80 cycles of
 - a. 60°C for 10 sec
 - increase setpoint temperature after cycle 2 by 0.5°C
 - melt curve data collection and analysis enabled

T profile:

1. 95°C for 15 min
2. 30 cycles of
 - a. 95°C for 15 sec
 - b. 56°C for 1 min
 - With data collection and real-time analysis enabled
3. 95°C for 1 min
4. 60°C for 1 min
5. 80 cycles of
 - a. 60°C for 10 sec
 - increase setpoint temperature after cycle 2 by 0.5°C
 - melt curve data collection and analysis enabled

Real time PCR materials & reagents:

Primers (Ordered from Sigma Genosys):

-Single copy gene, beta-globin, 100uM stock

•Hbg1 5' GCTTCTGACACAACCTGTGTTCACTAGC 3'

•Hbg2 5' CACCAACTTCATCCACGTTCCACC 3'

-Telomeres, 100uM stock

•Tel 1b

5' CGGTTTGTGGGTTTGGGTTTGGGTTTGGGTTTGGGTT 3'

•Tel 2b

5' GGCTTGCCTTACCCTTACCCTTACCCTTACCCTTACCCT 3'

96 well Real-time PCR plates
Optical seals for real-time PCR plates
QPCR 2X SYBR Green Fluorescein Mix (Thermo Scientific #ab-1219/b)
DNase, RNase free H₂O
BioRad Icyler thermal cycler
Icyler iQ software version 3.1

PCR reaction
10ul sybr green
5ul DNA (total 5ng)
5ul primers
20ul total

S primer mix:
0.6 ul (10um) hgb1
1.4 ul (10um) hgb2
3.0 ul H2O
5.0 ul total (each well)

T primer mix:
2 ul (1um) Tel1b
1.8 ul (10um) Tel2b
1.2 ul H2O
5.0 ul total (each well)

Final concentrations of primers:
300 nM hgb1 100 nM tel 1b
700 nM hgb2 900 nM tel 2b

References

- Bailey, SM, Goodwin EH and Cornforth MN (2004). *Strand-specific fluorescence in situ hybridization: the CO-FISH family* Cytogenet Genome Res 107(1-2): 14-7.
- Bailey, SM, Goodwin EH, Meyne J and Cornforth MN (1996). *CO-FISH reveals inversions associated with isochromosome formation* Mutagenesis 11(2): 139-44.
- Cawthon, RM (2002). *Telomere measurement by quantitative PCR* Nucleic Acids Res 30(10): e47.
- Livak, KJ and Schmittgen TD (2001). *Analysis of relative gene expression data using real-time quantitative PCR and the 2(-Delta Delta C(T)) Method* Methods 25(4): 402-8.
- Perry, P and Wolff S (1974). *New Giemsa method for the differential staining of sister chromatids* Nature 251(5471): 156-8.
- Rooney, S, Sekiguchi J, Zhu C, Cheng HL, Manis J, Whitlow S, DeVido J, Foy D, Chaudhuri J, Lombard D and Alt FW (2002). *Leaky Scid phenotype associated with defective V(D)J coding end processing in Artemis-deficient mice* Mol Cell 10(6): 1379-90.
- Rufer, N, Dragowska W, Thornbury G, Roosnek E and Lansdorf PM (1998). *Telomere length dynamics in human lymphocyte subpopulations measured by flow cytometry* Nat Biotechnol 16(8): 743-7.
- Scott, D, Barber JB, Spreadborough AR, Burrill W and Roberts SA (1999). *Increased chromosomal radiosensitivity in breast cancer patients: a comparison of two assays* Int J Radiat Biol 75(1): 1-10.
- Smiraldo, PG, Gruver AM, Osborn JC and Pittman DL (2005). *Extensive chromosomal instability in Rad51d-deficient mouse cells* Cancer Res 65(6): 2089-96.
- Sorensen, BS, Hao J, Overgaard J, Vorum H, Honore B, Alsner J and Horsman MR (2005). *Influence of oxygen concentration and pH on expression of hypoxia induced genes* Radiother Oncol 76(2): 187-93.
- Wei, Q, Spitz MR, Gu J, Cheng L, Xu X, Strom SS, Kripke ML and Hsu TC (1996). *DNA repair capacity correlates with mutagen sensitivity in lymphoblastoid cell lines* Cancer Epidemiol Biomarkers Prev 5(3): 199-204.
- Wu, X, Zheng YL and Hsu TC (2005). *Mutagen-induced chromatid breakage as a marker of cancer risk* Methods Mol Biol 291: 59-67.
- Zhang, Y, Lim CU, Williams ES, Zhou J, Zhang Q, Fox MH, Bailey SM and Liber HL (2005). *NBS1 knockdown by small interfering RNA increases ionizing radiation mutagenesis and telomere association in human cells* Cancer Res 65(13): 5544-53.

Chapter 3

Characterizing Lymphoblastoid Cell Lines from Breast Cancer Cases and Controls in the US Radiologic Technologist Cohort: A Pilot Study

Characterizing Lymphoblastoid Cell Lines from Breast Cancer Cases and Controls in the US Radiologic Technologist Cohort: A Pilot Study.

Abby J. Williams¹, Alice J. Sigurdson², Michael Story³, Robert L. Ullrich¹, and Susan M. Bailey¹.

¹Department of Environmental and Radiological Health Sciences, Colorado State University, Fort Collins, CO 80523

²Radiation Epidemiology Branch, Division of Cancer Epidemiology and Genetics, National Cancer Institute, NIH, DHHS, Bethesda, MD, USA

³Department of Radiation Oncology, University of Texas Southwestern Medical Center, Dallas, TX 75390

Abstract

Occupational and diagnostic exposure to ionizing radiation is of concern regarding cancer risk, especially pertaining to tissues with known radiosensitivity such as the female mammary gland. We have studied twenty (20) Lymphoblastoid Cell Lines (LCLs) from early-onset breast cancer patients and controls (10 each), all of whom were Radiologic Technologists from the US Radiation Technologist (USRT) cohort. We performed the G2 chromosomal radiosensitivity assay, microarray analysis to evaluate gene expression, and Telomere Flow FISH to assess relative telomere lengths in all 20 cell lines. The cases on average displayed a trend for fewer chromatid-type aberrations following radiation exposure, longer telomeres and lower expression levels of VIPR2 compared to the controls. Our results suggest that breast cancer cases are more radioresistant (i.e., less radiosensitive), perhaps facilitating the accumulation of persistent mutations, while the more radiosensitive nature of the controls leads to cell killing and elimination of damaged cells. While our sample size is small, this work is one of the first to combine multiple endpoints in the study of PBLs from breast cancer patients with hopes of identifying screening criteria and serves as a pilot study that may provoke future, larger studies of radiation-induced breast cancer.

Introduction

Breast cancer is a leading cause of death among women today. Ionizing radiation (IR) is a known carcinogen, prompting concern regarding personal exposures, which can range from radiation therapy to mammograms. While the risk of cancer associated with *low* doses of ionizing radiation is not entirely clear, it is believed that the risk of cancer increases with increasing radiation dose received (Land *et al.* 2003; Ronckers *et al.* 2005). The relevance of exposures to low doses of radiation is readily apparent from everyday lifestyle, which can involve diagnostic medical tests, occupational radiation exposure, frequent-flyer risks, space exploration and radiological terrorism (Brenner *et al.* 2003).

Since the 1980s the NCI has studied cancer incidence in a cohort of US Radiologic Technologists (USRT) that is of particular interest due to their potential exposure to chronic, low doses of ionizing radiation (IR), rather than primarily to acute high doses that have been primarily studied in the Japanese atomic bomb survivors (Mohan *et al.* 2003; Sigurdson *et al.* 2003; Doody *et al.* 2006). The USRT originally contained about 143,000 participants, the majority of which were white women, with roughly 41% beginning their work as a radiation technologist before the age of 20 years and with the current mean age being approximately 55 years (Boice *et al.* 1992; Doody *et al.* 1998; Sigurdson *et al.* 2003; Bhatti *et al.* 2008). Questionnaires have been mailed to members of the cohort that provide information on work experience, personal diagnostic procedures, cancer risk factors, cancer diagnoses and other health and life-style information such as alcohol and tobacco use as well as reproductive history (Boice *et al.* 1992; Sigurdson *et al.* 2003; Sigurdson *et al.* 2007). An increased risk of breast cancer,

basal cell carcinoma, melanoma, and leukemia has been observed in these radiologic technologists, specifically those who were employed prior to the 1950s (Freedman *et al.* 2003; Sigurdson *et al.* 2003; Linet *et al.* 2005; Yoshinaga *et al.* 2005; Doody *et al.* 2006).

Previous studies have shown increased chromosome damage following X-irradiation in lymphocytes of breast cancer patients compared to controls (Baeyens *et al.* 2002) and other reports utilizing the G2 chromosomal radiosensitivity assay also demonstrate a correlation between women with breast cancer and increased radiosensitivity of PBLs (Roberts *et al.* 1999; Scott *et al.* 1999). Additionally, shorter telomeres, the capping structures that protect the ends of linear chromosomes, have been associated with breast cancer patients compared to controls (Griffith *et al.* 1999; Meeker *et al.* 2004; Fordyce *et al.* 2006). Moreover, poor clinical outcome has been associated with telomere shortening not only in breast cancer but also in cases of lung cancer, neuroblastoma, leukemia and endometrial cancer (Dahse *et al.* 1997).

Although the primary limitation to the USRT study (as with most early radiation worker studies) is the lack of exact radiation dose to the breast (or other areas of interest), some dose information is available given that dosimetry badges were introduced around 1960 and dose estimates were calculated based on work history, available film badge readings and chromosome translocation frequencies in PBLs (Simon *et al.* 2006; Bhatti *et al.* 2007). Several key advantages surround the USRT study including the very large number of participants and large percentage of women, the wide variety of radiation workers included, the long-term follow-up and the fairly detailed patient information based on medical records and questionnaires.

In the present study, we evaluated G2 chromosomal radiation response, relative telomere lengths, and gene expression in 20 LCLs from the USRT cohort, 10 of which are early-onset breast cancer cases without BRCA mutations and 10 represent age-matched controls. Our findings reveal a trend suggesting that chromosomal radiosensitivity was lower in cases compared to controls (i.e., cases were radioresistant), telomere length on average was longer in cases, and Vasoactive Intestinal Peptide Receptor 2 (VIPR2) expression was lower in cases compared to controls, although no differences reached statistical significance, likely due to our sample size.

Materials & Methods

USRT Cohort. Details of the US Radiologic Technologists cohort have been described previously (Boice *et al.* 1992; Doody *et al.* 1998). Briefly, participants had to be residents of the US and certified for a minimum of two years by the American Registry of Radiologic Technologists between the years of 1926-1982. Blood samples were taken from cohort members and lymphoblasts transformed using Epstein-Barr virus, thus forming cell lines (Lymphoblastoid Cell Lines; LCLs). Low passage LCLs were used to minimize effects of *in vitro* culture.

Cell Culture. The LCLs were cultured in RPMI1640 media supplemented with 15% fetal bovine serum and antibiotics. Cells were counted using a Z2 Cell Counter (Coulter Beckman, Fullerton, CA).

G2 Assay. The G2 chromosomal radiosensitivity assay has previously been described (Wei *et al.* 1996; Scott *et al.* 1999; Wu *et al.* 2005). Briefly, log-phase cultures were

irradiated with either 0 or 0.5 Gy IR from a sealed-source Mark I ^{137}Cs γ -irradiator (J.L. Shepherd and Associates), incubated for 30 min, then Colcemid (Gibco) was added at a final concentration of 0.2 $\mu\text{g/ml}$. Cultures were harvested 1 hour later. Cells were suspended in 0.075M KCl for 20 minutes on ice, then fixed with 3:1 methanol: acetic acid, and slides were prepared using standard cytogenetic techniques. Slides were stained with 5% Geimsa for 10 min at room temperature. A minimum of 25 metaphase spreads were scored for chromatid-type aberrations (indicative of exposure in G2) using a Zeiss Axioskop2 Plus microscope equipped with a Photometrics Coolsnap ES2 camera and Metavue 7.1 software. Primarily chromatid gaps (less than the width of a chromatid) and breaks (larger than the width of a chromatid) were scored with samples blinded to the viewer.

Telomere Flow FISH. This method has been described previously (Rufer *et al.* 1998). LCLs were harvested, washed with PBS, counted and adjusted to contain the same number of cells. Cultures were stored at -80°C until the day of flow cytometry analysis when cells were quickly thawed, washed 2 times with PBS and resuspended in a hybridization mixture consisting of 70% formamide, 20mM TrisHCl pH 7.1, 0.5% BSA, and 50nM Telomere PNA Tel-C (CCCTAA)₃ probe conjugated to FITC (Applied Biosystems). Samples were heated to 80°C for 10 min to denature and then incubated at room temperature for 2 hours (for hybridization). Cells were washed with 70% formamide/10mM TrisHCl pH 7.1 and resuspended in Propidium Iodide (PI; MP Biomedicals) with RNase A (Sigma). Samples were run on a MoFlo Flow Cytometer

(Dako) using a 488nm excitation laser at 110mW and Summit Software. Voltage for FITC was set at 665 with a gain of 8 (linear). PI HV was 400, gain of 1 (linear).

Microarray Analysis. Genomic RNA was isolated from low passage LCLs using an RNeasy kit (Qiagen). The probes found on the array were designed by the Wright and Shay laboratory (UTSW, Dallas, TX) in consultation with Operon Biotechnologies (Huntsville, AL) based upon subtelomeric DNA sequences provided by Harold Reithman of the Wistar Institute in 2003. The oligos represent 180 genes from duplicated subtelomeric regions, 271 genes from single-copy subtelomeres, 92 randomly selected control genes, 12 “typical” control genes, 60 non-telomeric genes known to change with cellular age, 48 telomere-related genes and 90 miscellaneous “interesting” genes.

Slides used are Full Moon Matrix II 3-D slides and were printed using a MicroGrid II print robot. Labeling and hybridization was performed using a Perkin Elmer (Waltham, MA) MicroMax Hybridization Kit (indirect labeling) according to the manufacturer’s protocol. Total RNA (10ug) was used. All samples were compared to a reference RNA signal (Stratagene Universal Reference RNA).

After washing and drying, the slides were immediately scanned on an Axon (Molecular Devices, Sunnyvale, CA) GenePix 4300 Scanner. Data was downloaded onto BRB-ArrayTools (NCI, Bethesda, MD), background corrected and normalized within and across arrays. Gene selections were performed using the SAM algorithm within BRB ArrayTools using a false discovery rate of 10% and a fold-change cutoff of 2.

Statistical Analysis. For both the G2 Assay and Telomere Flow FISH a student's t-test was performed to calculate significant differences between cases and controls. Error bars represent standard error of the means. In addition, unconditional logistic regression was performed using MINITAB Student Release 14 to adjust for confounding factors of age at blood draw and radiation dose to breast tissue and determine if any endpoints used here are predictive of case versus control status.

Results

We evaluated G2 chromosomal radiosensitivity, relative telomere lengths and microarray gene expression analysis on 20 LCLs from members of the USRT cohort (10 cases and 10 controls). As a measure of repair, γ H2AX foci formation (a phosphorylated histone variant that marks the sites of DNA double-strand breaks (Olive and Banath 2004)) was also evaluated following radiation exposure via flow cytometry, but data was inconsistent (Supplementary data). Information summarizing patient information is shown in Table 1.

G2 Assay: Less chromosomal radiosensitivity in breast cancer cases vs controls

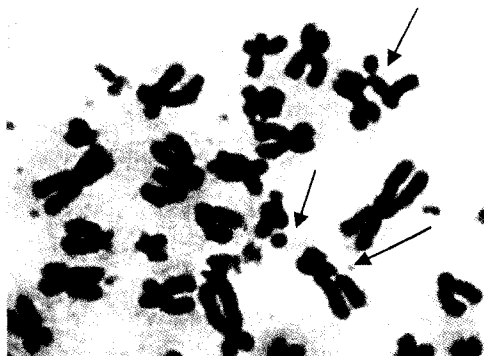


Figure 1. A partial metaphase spread from an LCL following the G2 Assay. The red arrows indicates a chromatid break and the blue arrow points towards a chromatid gap.

The G2 assay measures chromosomal radiosensitivity, observed as chromatid-type aberrations, which are indicative of exposure in G2. Both chromatid-type gaps and breaks were scored (Figure 1) and an average per cell was calculated for both the cases and controls. Overall, chromatid-type aberrations were higher in controls compared to cases, though not reaching statistical significance; controls averaged 2.0 chromatid breaks+gaps per cell, cases 1.77 per cell (Figure 2A). A distribution graph was created from average chromatid gaps+breaks for individual LCLs to illustrate that there were no outliers to skew the data (Figure 2B). It is interesting to note that each time the G2 assay was performed, the standard deviation was greater for chromatid gaps plus breaks within the cases compared to the controls. The controls as a group also had higher levels of chromatid gaps as well as chromatid breaks when the aberration types were analyzed separately (Figure 2C), however, again this did not reach statistical significance. Taken together, these results demonstrate a range of individual radiosensitivity and response to IR, with cases tending to display a more radioresistant (less radiosensitive) phenotype.

A.

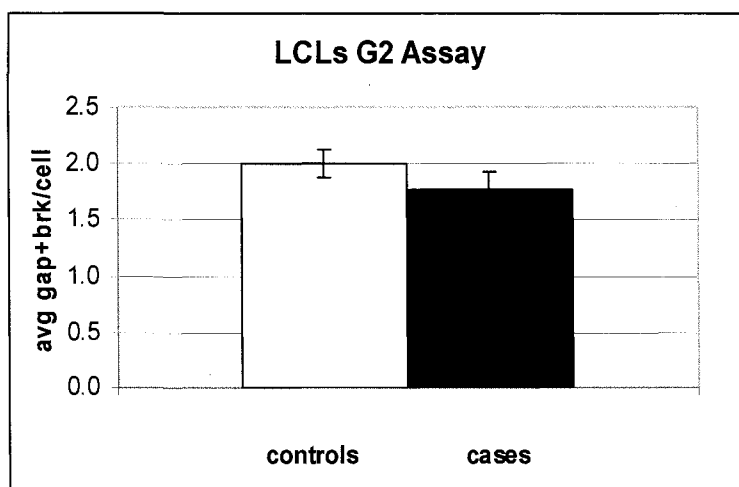
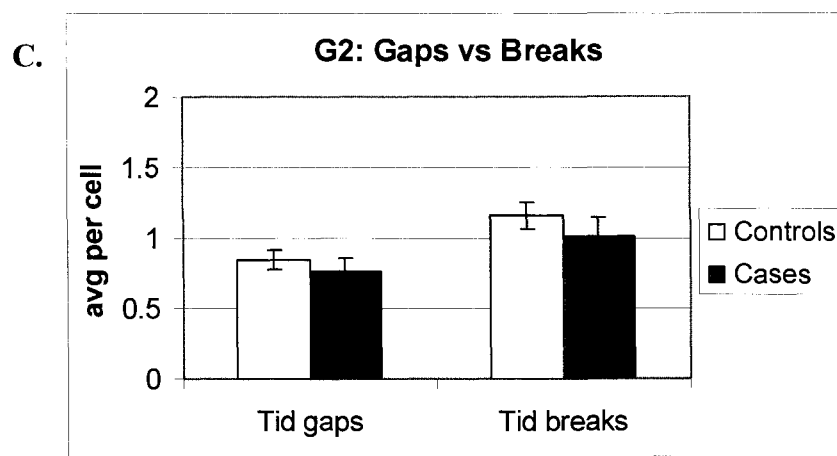
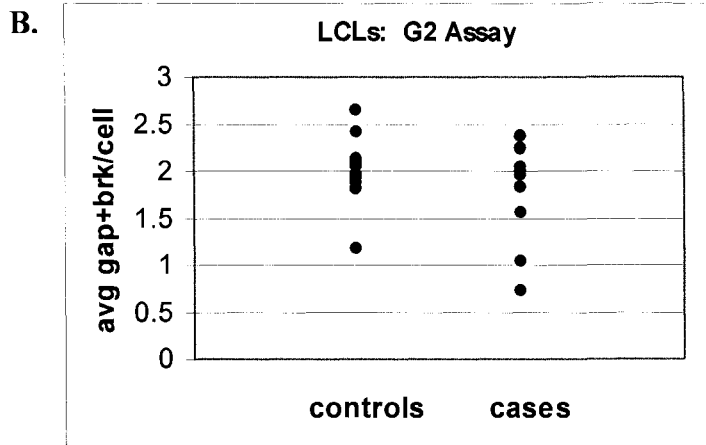


Figure 2. G2 Assay Results. A. Average chromatid gaps & breaks per cell for breast cancer cases compared to controls. ($p = 0.2784$) B. Distribution of chromatid gaps+breaks for individual LCLs. C. Average chromatid gaps compared to average chromatid breaks for cases and controls.



Longer telomere lengths in breast cancer cases compared to controls

Relative telomere lengths were assessed by performing telomere FISH and analyzing fluorescence intensity via flow cytometry (Flow FISH). With no adjustments for age (telomeres shorten with age), the telomeres were longer on average in the cases compared to the controls (Figure 3A). Even with adjustments for age, cases still have longer telomeres compared to controls, but this may be due to our small sample size (Figure 3B).

It should also be noted that LCL #9, #16 and #20 had two distinct telomere peaks and LCL #4 had three distinct telomere peaks, while all the other LCLs only had one. It

has previously been demonstrated that inheritance plays a role in telomere length settings, which could explain these various telomere length sub-populations (Nordfjall *et al.* 2005; Njajou *et al.* 2007). Since Flow FISH provides an average relative telomere length based on the whole population of telomeres, concerns of aneuploidy arise that could skew the data. However, no signs of aneuploidy were observed in the DNA histograms from the flow cytometry. As an additional precaution, preparations of various LCLs were made onto slides and metaphase chromosomes counted, confirming that these cell lines are indeed diploid (data not shown). We were also concerned that EBV transformation may influence telomere maintenance, but it has been shown that early passage diploid cells remain telomerase negative (Sugimoto *et al.* 2004).

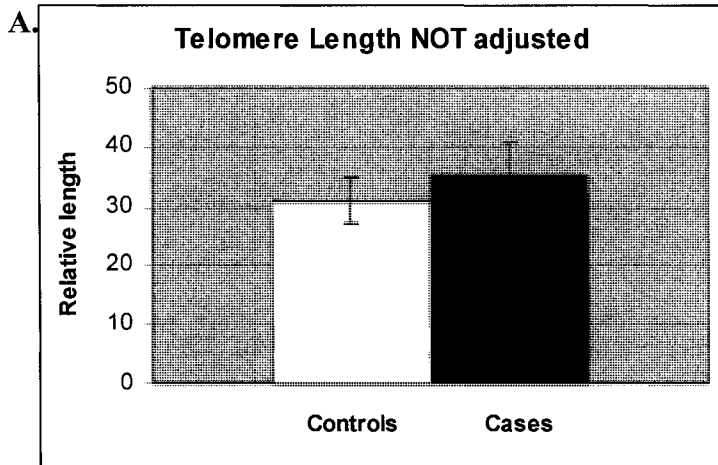
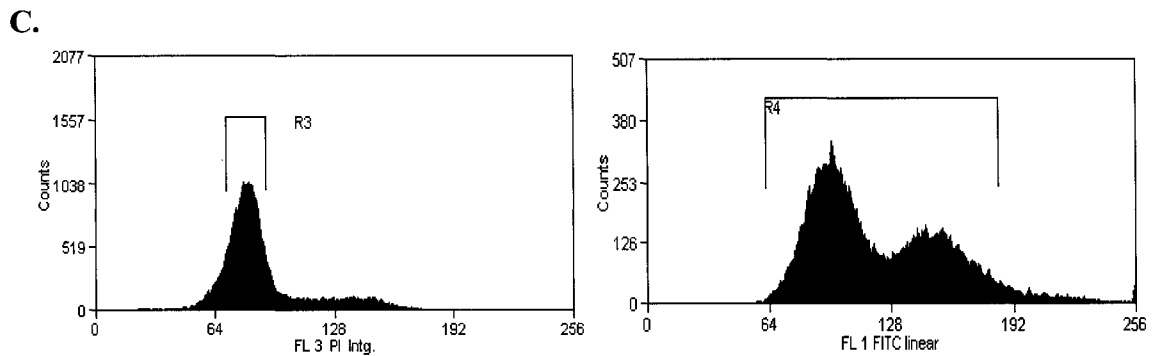
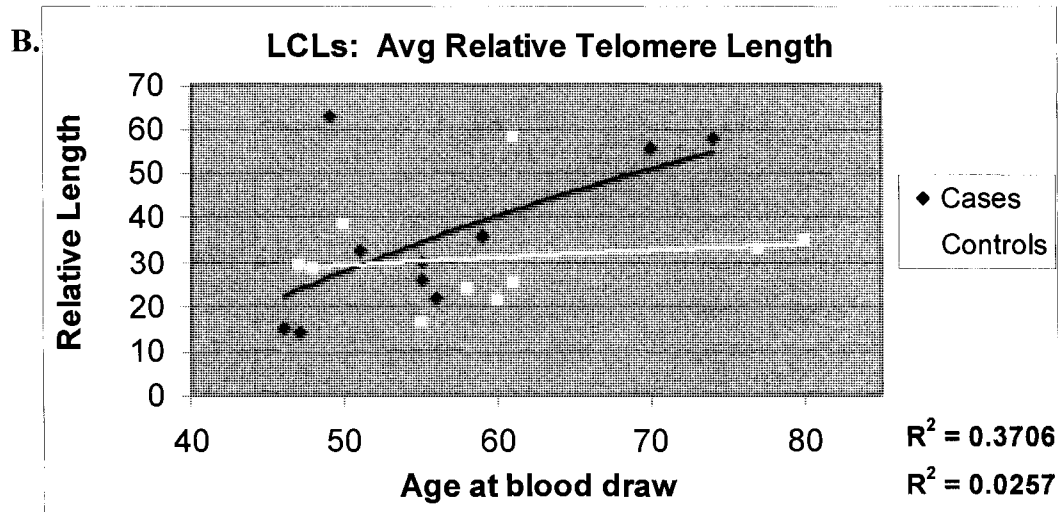


Figure 3. Relative telomere lengths for LCLs.

A. Simple average length in cases vs controls, without adjusting for age. **B.** Relative telomere lengths for each LCL plotted against the age in which the patient's blood was drawn. **C.** Example of an LCL with multiple telomere sub-populations. The DNA histogram is shown on the left (red) and the fluorescence for the telomere probe is shown on the right (green)



VIPR2 expression is down-regulated in breast cancer cases vs controls

Results from our microarray analysis of gene expression revealed that Vasoactive Intestinal Peptide Receptor 2 (VIPR2; also known as VPAC2) is down-regulated in the cases compared to the controls (Figure 4A), showing a fold-change of 0.422605 between cases and controls (Figure 4B). We utilized Real Time PCR to confirm/test these results, which show that (TBD).

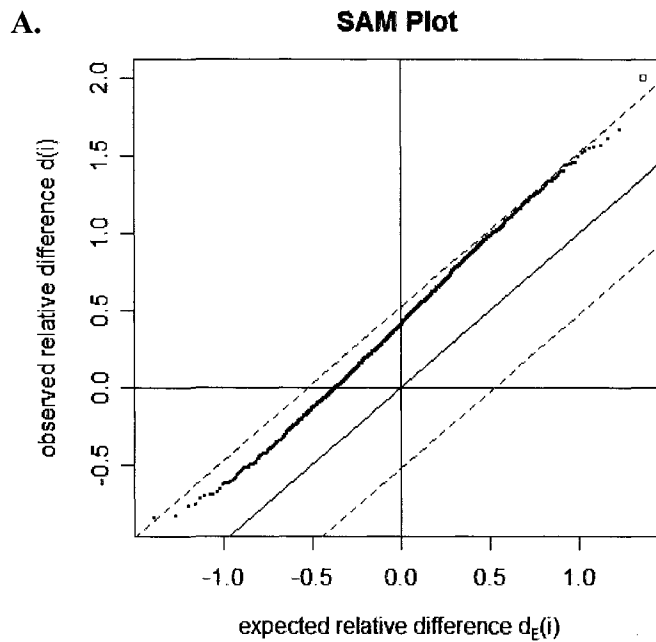


Figure 4. Microarray results. **A.** Vasoactive Intestinal Peptide Receptor 2 (VIPR2) is down-regulated in the cases compared to the controls. VIPR2 is represented by the red square. **B.** The geometric means of ratios in class 1 (cases) is the log ratio of probe binding to reference RNA binding. This is the same for class 2 (controls). The fold change is the ratio of ratios, case/control.

B.

Geom mean of ratios class one	Geom mean of ratios class 2	Fold change	Unique ID	Corresponding gene
0.25207	0.5964672	0.422605	AI025211	VIPR2

Predictive value of telomere length & G2 chromosomal radiosensitivity

We find that none of the endpoints evaluated here are strictly predictive of case vs. control status, however the small sample size means the power to detect significant differences is low. Logistic regression shows that no endpoints are statistically significant regardless of whether the data was analyzed as categorical or continuous (Figure 5). We chose dose estimates that were constructed with a lag time of 10 years, the average accepted latency time for solid cancers (Land 1987).

Logistic Regression Analysis (Continuous)			
Predictor	Odds Ratio	95% CI	
		Lower	Upper
Age	0.95	0.86	1.05
Telo	1.02	0.96	1.09
Age	0.90	0.78	1.05
Dose	3.01	0.31	29.30
Telo	1.02	0.95	1.08
Dose	1.12	0.29	4.37
G2	0.47	0.07	3.02
Age	0.87	0.73	1.03
Dose	3.40	0.36	32.46
G2	0.19	0.02	2.14
Telo	1.04	0.96	1.12

Logistic Regression Analysis (Categorical)			
Predictor	Odds Ratio	95% CI	
		Lower	Upper
Longest telo as referent group			
Telo 1	0.375	0.039	3.605
Telo 2	0.563	0.068	4.672
Longest telo as referent group			
Telo 1	0.213	0.015	3.049
Telo 2	0.326	0.028	3.743
Age	0.942	0.842	1.054

Figure 5. Logistic regression for G2 assay results & relative telomere lengths. No endpoints used indicate predictive ability for case/control status whether analyzing the data as continuous or categorical.

Summary of LCLs Patient Information

Patient	Status	Age at Blood Draw	Estimated Dose to Breast* (Rad)	Age at Breast Diagnosis 1	Age at Diagnosis 2	Type of Diagnosis 2	Age at Diagnosis 3	Type of Diagnosis 3	Race
1	Case	74	2.419	31	38	Thyroid	44	Breast	white
2	Case	55	0	22	36	Skin Melanoma	37	Skin Melanoma	white
3	Case	51	0.019	31	x	x	x	x	white
4	Case	70	0	33	35	Breast	x	x	white
5	Case	56	0	26	x	x	x	x	white
6	Case	59	0.853	33	63	Breast	x	x	white
7	Case	49	0	30	x	x	x	x	white
8	Case	47	0.033	32	33	Lung & Bronchus	46	Breast	white
9	Case	46	0	28	44	Breast	x	x	white
10	Case	55	0.589	33	x	x	x	x	white
11	Control	58	0.072	x	x	x	x	x	white
12	Control	47	0.052	49	x	x	x	x	white
13	Control	50	0.163	x	x	x	x	x	white
14	Control	48	0	x	x	x	x	x	white
15	Control	55	0.061	x	x	x	x	x	white
16	Control	80	1.74	x	x	x	x	x	white
17	Control	61	0.053	x	x	x	x	x	white
18	Control	60	0.068	x	x	x	x	x	white
19	Control	61	0	x	x	x	x	x	white
20	Control	77	1.115	x	x	x	x	x	white

*with lag time of 10 years

Table 1. Patient information for all LCLs used. Age at blood draw, additional cancers, estimated radiation dose to the breast tissue and race for all 20 patients is reported here.

Discussion

A concern for radiation workers is unavoidable occupational IR exposure and associated cancer risk. Everyday life on planet earth involves exposure to low doses of radiation. A primary concern for radiation oncologists is to identify radiosensitive individuals prior to treatment, therefore relevant markers are important to enhance the assessment of individual cancer susceptibility. We demonstrate a trend for higher levels

of chromatid-type damage (G2 chromosomal radiosensitivity) in the group of controls compared to the cases, though not at a level of statistical significance; this is in contrast to the majority of reports that utilize similar protocols (Roberts *et al.* 1999; Scott *et al.* 1999; Baeyens *et al.* 2002; Scott 2004). This observation may hint at more radiosensitivity in the controls, thus more cell killing and elimination from the population, while the more radioresistant nature of the cases allows damaged cells to survive, acquire additional mutations and continue advancing towards tumorigenesis. Indeed, evaluating apoptotic response in these cells would provide more information to test this hypothesis. It should be noted that our observation of higher levels of chromatid-type damage (i.e. G2 chromosomal radiosensitivity) in the controls does associate with the presence of shorter telomere lengths, consistent with previous investigations that have documented a relationship between decreased telomere length and increased radiosensitivity (Goytisolo *et al.* 2000; McIlrath *et al.* 2001; Cabuy *et al.* 2005). In addition, previous work demonstrates that age has no influence on chromosomal radiosensitivity of either cases or controls (Scott *et al.* 1999; Scott *et al.* 2003).

We report a trend for longer relative telomere lengths in LCLs of breast cancer patients compared to controls, analyzed by Telomere Flow FISH. Telomeres have shown promise as prognostic indicators in the clinic based on a demonstrated relationship between shorter telomeres and breast cancer susceptibility by various investigators (Meeker and Argani 2004; Shen *et al.* 2007). However, it has recently been reported by another group that significantly longer telomeres were associated with breast cancer cases compared to controls (Svenson *et al.* 2008), supporting our finding of a tendency for longer telomeres in our cases vs. controls. In addition, abnormally long telomeres have

been identified in the LCLs of a subset of clinically radiosensitive cancer patients (Sprung *et al.* 2008). Together, these results support our findings, and although the differences we find are not statistically significant, it is beneficial to note that no difference in blood telomere lengths between breast cancer patients and controls were observed in another study that used TRFs (terminal restriction fragments), a method that utilizes southern blotting to measure telomeres (Barwell *et al.* 2007). A recent study with sample sizes similar to ours (n=20 controls, n=24 cases total, n=13 age-matched cases) did observe shorter telomeres in the PBLs from breast cancer cases compared to controls, but this finding was not statistically significant either (Iwasaki *et al.* 2008). These results support our finding in the sense that our sample sizes were similar and neither outcome was able to produce a significant difference between breast cancer cases and controls, for telomere lengths.

It should also be noted that LCL #9, 16 and 20 had two distinct telomere peaks and LCL #4 had three distinct telomere peaks while all the other LCLs only had one—2 of these were diagnosed with breast cancer and 2 were not. One might wonder if EBV-transformation may be affecting telomere regulation in these LCLs, however many genes of interest were investigated via microarray technology and only one gene was potentially different between cases and controls, suggesting that EBV has not greatly disturbed cellular regulation in these cell lines at the low passage we investigated. We also know that telomere lengths are heterogeneous and inherited (Nordfjall *et al.* 2005; Njajou *et al.* 2007), therefore it is probable that these women simply have multiple sub-populations of telomere length. On the other hand, it is interesting to note that the 2 cases with multiple telomere populations were among those cases that were diagnosed with a second cancer

(Table 1). It is not necessary for all telomeres to become critically shortened or uncapped in order to initiate carcinogenesis, therefore investigations into individual telomere lengths among these LCLs could provide additional insight into the existence of different telomere lengths between breast cancer cases and controls. It is possible that these two cancer patients have longer telomere lengths at the population level, but a few short individual telomeres that could confer radiosensitivity.

Finally, we observed decreased expression of *VIPR2* in the LCLs of cases compared to controls. *VIPR2*, also called *VPAC2*, is a G-protein coupled receptor found in the membrane of a variety of cells (Wei and Mojsov 1996; Reubi *et al.* 2000; Vaudry *et al.* 2000). It is known that *VIPR1/2* receptors are present in both normal and tumorigenic mammary epithelial cells (Garcia-Fernandez *et al.* 2005). Interestingly, *VIPR* receptors are often over-expressed in a variety of human tumors, however *VIPR1* over-expression has been shown to predominate in breast cancer (Reubi 2000; Reubi *et al.* 2000; Schulz *et al.* 2004). *VIPR2* has not been as extensively studied in lymphocytes.

Given that *VIPR2* is a G-protein coupled receptor, down-regulation potentially has many functional implications. If there are fewer of these receptors in the PBLs of a patient, this could lead to initiation (or inhibition) of different signaling pathways compared to the presence of normal amounts of this receptor and in turn, have different downstream effects on the cell. We speculate that *VIPR2* down-regulation in lymphocytes may play a role in tumor progression; less *VIPR2* expression results in a lack of immune response to tumorigenic cells, thus contributing to progression of the cancer. Western blots investigating *VIPR2* protein levels in these LCLs would be informative.

We know that VIP (a peptide that binds to VIPR2) activates cAMP which then activates PKA. We also know that PKA can affect a number of substrates in lymphocytes, including NF κ B, MAPK, CREB and phospholipases, that then modify immune function (Torgersen *et al.* 2002). Lymphocytes with decreased VIPR2 receptors may function in the sense that they are alive and present in the body, but they may not contribute to elimination of tumor cells via anti-infection/anti-inflammatory activities. This is particularly interesting for breast cancer as it has been shown that higher amounts of B lymphocytes in lymph nodes correlates with increased disease stage (Wernicke 1975; Morton *et al.* 1986). On the other hand, it is known that NF κ B activates anti-apoptotic gene expression (Wang *et al.* 1998; Chen *et al.* 2000). If NF κ B is down-regulated as a downstream effect of lower *VIPR2* expression, then anti-apoptotic responses would not be activated, thus favoring a pro-apoptotic state in lymphocytes. In this scenario, the presence of fewer lymphocytes in breast cancer cases may allow tumors to evade an immune response altogether, again contributing to tumor progression. It should be taken into consideration that evidence exists for roles of NF κ B in both promotion and inhibition of cancer development (reviewed in (Karin 2006)), however NF κ B does play a role in regulating cell proliferation, cell survival, cell immunity and inflammation and therefore should be further studied in this context (reviewed in (Cortes Sempere *et al.* 2008)).

In addition, lower levels of adenylate cyclase (the enzyme that activates cAMP) have been observed in the lymphocytes of gastrointestinal cancer patients compared to lymphocytes from healthy individuals (Berstein *et al.* 1995). Perhaps an investigation of cAMP levels in our LCLs would provide similar results. Furthermore, studies regarding

NF κ B regulation in our breast cancer cases and controls may be beneficial. It may also be worthwhile to perform additional microarrays, Real Time PCR, or western blotting to evaluate potential differences in *RAD51D* and *EZH2*. Because the microarrays used here were made prior to our collaboration, these genes were not included in this report (see chapter 4).

It should be noted that the majority of these women diagnosed with breast cancer from whom the LCLs came have survived multiple cancers. Perhaps these patients are actually resistant to radiation treatment and have the ability to overcome the hardship of cancer treatment and go into remission. It may be that this ability to survive multiple cancers is genetic and thus further investigations are warranted. Future studies may need to include a new set of LCLs both to repeat these studies as well as examine other aspects of carcinogenesis besides an early-onset phenotype.

Although the USRT LCLs were collected post-diagnosis (and likely post-treatment), it has been shown that no difference in the amount of DNA damage assessed by the Alkaline Comet assay is observed in LCLs collected before compared to collection after breast cancer diagnosis (Bhatti *et al.* 2008). In addition, other reports have also used LCLs to study telomere length and radiosensitivity, (Meijer *et al.* 1999; Trenz *et al.* 2005; Sprung *et al.* 2008). Here we show a trend that chromosomal radiosensitivity is lower, relative telomere lengths are longer, and *VIPR2* expression is down-regulated in USRT LCLs from breast cancer cases compared to controls. None of the techniques used were able to predict the case-control status of the radiation technologists at a level of statistical significance, however larger studies are necessary for confirmation of these results. It seems likely that multiple end points used in combination will be key for successful

identification of cancer susceptible or radiosensitive individuals given the complex nature of environmental factors, genetic susceptibility and proper molecular regulation in carcinogenesis.

Acknowledgements

The authors wish to thank Woody Wright (University of Texas Southwestern Medical Center) for providing the microarray chips and Leslie Armstrong-Lea (Colorado State University) for flow cytometry technical assistance.

References

- Baeyens, A, Thierens H, Claes K, Poppe B, Messiaen L, De Ridder L and Vral A (2002). *Chromosomal radiosensitivity in breast cancer patients with a known or putative genetic predisposition* Br J Cancer 87(12): 1379-85.
- Barwell, J, Pangon L, Georgiou A, Docherty Z, Kesterton I, Ball J, Camplejohn R, Berg J, Aviv A, Gardner J, Kato BS, Carter N, Paximadas D, Spector TD and Hodgson S (2007). *Is telomere length in peripheral blood lymphocytes correlated with cancer susceptibility or radiosensitivity?* Br J Cancer 97(12): 1696-700.
- Berstein, LM, Pravosudov IV and Kryukova OG (1995). *Hormonal regulation of adenylate cyclase activity in circulating lymphocytes and its interrelationship with hormone sensitivity of tumor tissue in colorectal cancer patients* Neoplasma 42(2): 57-61.
- Bhatti, P, Preston DL, Doody MM, Hauptmann M, Kampa D, Alexander BH, Petibone D, Simon SL, Weinstock RM, Bouville A, Yong LC, Freedman DM, Mabuchi K, Linet MS, Edwards AA, Tucker JD and Sigurdson AJ (2007). *Retrospective biodosimetry among United States radiologic technologists* Radiat Res 167(6): 727-34.
- Bhatti, P, Sigurdson AJ, Thomas CB, Iwan A, Alexander BH, Kampa D, Bowen L, Doody MM and Jones IM (2008). *No evidence for differences in DNA damage assessed before and after a cancer diagnosis* Cancer Epidemiol Biomarkers Prev 17(4): 990-4.
- Bhatti, P, Struewing JP, Alexander BH, Hauptmann M, Bowen L, Mateus-Pereira LH, Pineda MA, Simon SL, Weinstock RM, Rosenstein M, Stovall M, Preston DL, Linet MS, Doody MM and Sigurdson AJ (2008). *Polymorphisms in DNA repair genes, ionizing radiation exposure and risk of breast cancer in U.S. Radiologic technologists* Int J Cancer 122(1): 177-82.
- Boice, JD, Jr., Mandel JS, Doody MM, Yoder RC and McGowan R (1992). *A health survey of radiologic technologists* Cancer 69(2): 586-98.
- Brenner, DJ, Doll R, Goodhead DT, Hall EJ, Land CE, Little JB, Lubin JH, Preston DL, Preston RJ, Puskin JS, Ron E, Sachs RK, Samet JM, Setlow RB and Zaider M (2003). *Cancer risks attributable to low doses of ionizing radiation: assessing what we really know* Proc Natl Acad Sci U S A 100(24): 13761-6.
- Cabuy, E, Newton C, Joksic G, Woodbine L, Koller B, Jeggo PA and Slijepcevic P (2005). *Accelerated telomere shortening and telomere abnormalities in radiosensitive cell lines* Radiat Res 164(1): 53-62.
- Chen, C, Edelstein LC and Gelinas C (2000). *The Rel/NF-kappaB family directly activates expression of the apoptosis inhibitor Bcl-x(L)* Mol Cell Biol 20(8): 2687-95.
- Cortes Sempere, M, Rodriguez Fanjul V, Sanchez Perez I and Perona R (2008). *The role of the NFkappaB signalling pathway in cancer* Clin Transl Oncol 10(3): 143-7.
- Dahse, R, Fiedler W and Ernst G (1997). *Telomeres and telomerase: biological and clinical importance* Clin Chem 43(5): 708-14.
- Doody, MM, Freedman DM, Alexander BH, Hauptmann M, Miller JS, Rao RS, Mabuchi K, Ron E, Sigurdson AJ and Linet MS (2006). *Breast cancer incidence in U.S. radiologic technologists* Cancer 106(12): 2707-15.

- Doody, MM, Mandel JS, Lubin JH and Boice JD, Jr. (1998). *Mortality among United States radiologic technologists, 1926-90* Cancer Causes Control 9(1): 67-75.
- Fordyce, CA, Heaphy CM, Bisoffi M, Wyaco JL, Joste NE, Mangalik A, Baumgartner KB, Baumgartner RN, Hunt WC and Griffith JK (2006). *Telomere content correlates with stage and prognosis in breast cancer* Breast Cancer Res Treat.
- Freedman, DM, Sigurdson A, Rao RS, Hauptmann M, Alexander B, Mohan A, Morin Doody M and Linet MS (2003). *Risk of melanoma among radiologic technologists in the United States* Int J Cancer 103(4): 556-62.
- Garcia-Fernandez, MO, Collado B, Bodega G, Cortes J, Ruiz-Villaespesa A, Carmena MJ and Prieto JC (2005). *Pituitary adenylate cyclase-activating peptide/vasoactive intestinal peptide receptors in human normal mammary gland and breast cancer tissue* Gynecol Endocrinol 20(6): 327-33.
- Goytisolo, FA, Samper E, Martin-Caballero J, Finnon P, Herrera E, Flores JM, Bouffler SD and Blasco MA (2000). *Short telomeres result in organismal hypersensitivity to ionizing radiation in mammals* J Exp Med 192(11): 1625-36.
- Griffith, JK, Bryant JE, Fordyce CA, Gilliland FD, Joste NE and Moyzis RK (1999). *Reduced telomere DNA content is correlated with genomic instability and metastasis in invasive human breast carcinoma* Breast Cancer Res Treat 54(1): 59-64.
- Iwasaki, T, Robertson N, Tsigani T, Finnon P, Scott D, Levine E, Badie C and Bouffler S (2008). *Lymphocyte telomere length correlates with in vitro radiosensitivity in breast cancer cases but is not predictive of acute normal tissue reactions to radiotherapy* Int J Radiat Biol 84(4): 277-84.
- Karin, M (2006). *Nuclear factor-kappaB in cancer development and progression* Nature 441(7092): 431-6.
- Land, CE (1987). *Temporal distributions of risk for radiation-induced cancers* J Chronic Dis 40 Suppl 2: 45S-57S.
- Land, CE, Tokunaga M, Koyama K, Soda M, Preston DL, Nishimori I and Tokuoka S (2003). *Incidence of female breast cancer among atomic bomb survivors, Hiroshima and Nagasaki, 1950-1990* Radiat Res 160(6): 707-17.
- Linet, MS, Freedman DM, Mohan AK, Doody MM, Ron E, Mabuchi K, Alexander BH, Sigurdson A and Hauptmann M (2005). *Incidence of haematopoietic malignancies in US radiologic technologists* Occup Environ Med 62(12): 861-7.
- McIlrath, J, Bouffler SD, Samper E, Cuthbert A, Wojcik A, Szumiel I, Bryant PE, Riches AC, Thompson A, Blasco MA, Newbold RF and Slijepcevic P (2001). *Telomere length abnormalities in mammalian radiosensitive cells* Cancer Res 61(3): 912-5.
- Meeker, AK and Argani P (2004). *Telomere shortening occurs early during breast tumorigenesis: a cause of chromosome destabilization underlying malignant transformation?* J Mammary Gland Biol Neoplasia 9(3): 285-96.
- Meeker, AK, Hicks JL, Gabrielson E, Strauss WM, De Marzo AM and Argani P (2004). *Telomere shortening occurs in subsets of normal breast epithelium as well as in situ and invasive carcinoma* Am J Pathol 164(3): 925-35.
- Meijer, AE, Zhivotovsky B and Lewensohn R (1999). *Epstein-Barr virus-transformed lymphoblastoid cell lines of ataxia telangiectasia patients are defective in X-ray-induced apoptosis* Int J Radiat Biol 75(6): 709-16.

- Mohan, AK, Hauptmann M, Freedman DM, Ron E, Matanoski GM, Lubin JH, Alexander BH, Boice JD, Jr., Doody MM and Linet MS (2003). *Cancer and other causes of mortality among radiologic technologists in the United States* Int J Cancer 103(2): 259-67.
- Morton, BA, Ramey WG, Paderon H and Miller RE (1986). *Monoclonal antibody-defined phenotypes of regional lymph node and peripheral blood lymphocyte subpopulations in early breast cancer* Cancer Res 46(4 Pt 2): 2121-6.
- Njajou, OT, Cawthon RM, Damcott CM, Wu SH, Ott S, Garant MJ, Blackburn EH, Mitchell BD, Shuldiner AR and Hsueh WC (2007). *Telomere length is paternally inherited and is associated with parental lifespan* Proc Natl Acad Sci U S A 104(29): 12135-9.
- Nordfjall, K, Larefalk A, Lindgren P, Holmberg D and Roos G (2005). *Telomere length and heredity: Indications of paternal inheritance* Proc Natl Acad Sci U S A 102(45): 16374-8.
- Olive, PL and Banath JP (2004). *Phosphorylation of histone H2AX as a measure of radiosensitivity* Int J Radiat Oncol Biol Phys 58(2): 331-5.
- Reubi, JC (2000). *In vitro evaluation of VIP/PACAP receptors in healthy and diseased human tissues. Clinical implications* Ann N Y Acad Sci 921: 1-25.
- Reubi, JC, Laderach U, Waser B, Gebbers JO, Robberecht P and Laissue JA (2000). *Vasoactive intestinal peptide/pituitary adenylate cyclase-activating peptide receptor subtypes in human tumors and their tissues of origin* Cancer Res 60(11): 3105-12.
- Roberts, SA, Spreadborough AR, Bulman B, Barber JB, Evans DG and Scott D (1999). *Heritability of cellular radiosensitivity: a marker of low-penetrance predisposition genes in breast cancer?* Am J Hum Genet 65(3): 784-94.
- Ronckers, CM, Erdmann CA and Land CE (2005). *Radiation and breast cancer: a review of current evidence* Breast Cancer Res 7(1): 21-32.
- Rufer, N, Dragowska W, Thornbury G, Roosnek E and Lansdorp PM (1998). *Telomere length dynamics in human lymphocyte subpopulations measured by flow cytometry* Nat Biotechnol 16(8): 743-7.
- Schulz, S, Rocken C, Mawrin C, Weise W, Hollt V and Schulz S (2004). *Immunocytochemical identification of VPAC1, VPAC2, and PAC1 receptors in normal and neoplastic human tissues with subtype-specific antibodies* Clin Cancer Res 10(24): 8235-42.
- Scott, D (2004). *Chromosomal radiosensitivity and low penetrance predisposition to cancer* Cytogenet Genome Res 104(1-4): 365-70.
- Scott, D, Barber JB, Spreadborough AR, Burrill W and Roberts SA (1999). *Increased chromosomal radiosensitivity in breast cancer patients: a comparison of two assays* Int J Radiat Biol 75(1): 1-10.
- Scott, D, Spreadborough AR and Roberts SA (2003). *Less G(2) arrest in irradiated cells of breast cancer patients than in female controls: a contribution to their enhanced chromosomal radiosensitivity?* Int J Radiat Biol 79(6): 405-11.
- Shen, J, Terry MB, Gurvich I, Liao Y, Senie RT and Santella RM (2007). *Short telomere length and breast cancer risk: a study in sister sets* Cancer Res 67(11): 5538-44.
- Sigurdson, AJ, Bhatti P, Doody MM, Hauptmann M, Bowen L, Simon SL, Weinstock RM, Linet MS, Rosenstein M, Stovall M, Alexander BH, Preston DL, Struewing

- JP and Rajaraman P (2007). *Polymorphisms in apoptosis- and proliferation-related genes, ionizing radiation exposure, and risk of breast cancer among U.S. Radiologic Technologists* Cancer Epidemiol Biomarkers Prev 16(10): 2000-7.
- Sigurdson, AJ, Doody MM, Rao RS, Freedman DM, Alexander BH, Hauptmann M, Mohan AK, Yoshinaga S, Hill DA, Tarone R, Mabuchi K, Ron E and Linet MS (2003). *Cancer incidence in the US radiologic technologists health study, 1983-1998* Cancer 97(12): 3080-9.
- Simon, SL, Weinstock RM, Doody MM, Neton J, Wenzl T, Stewart P, Mohan AK, Yoder RC, Hauptmann M, Freedman DM, Cardarelli J, Feng HA, Bouville A and Linet M (2006). *Estimating historical radiation doses to a cohort of U.S. radiologic technologists* Radiat Res 166(1 Pt 2): 174-92.
- Sprung, CN, Davey DS, Withana NP, Distel LV and McKay MJ (2008). *Telomere length in lymphoblast cell lines derived from clinically radiosensitive cancer patients* Cancer Biol Ther 7(5): 638-44.
- Sugimoto, M, Tahara H, Ide T and Furuichi Y (2004). *Steps involved in immortalization and tumorigenesis in human B-lymphoblastoid cell lines transformed by Epstein-Barr virus* Cancer Res 64(10): 3361-4.
- Svenson, U, Nordfjall K, Stegmayr B, Manjer J, Nilsson P, Tavelin B, Henriksson R, Lenner P and Roos G (2008). *Breast cancer survival is associated with telomere length in peripheral blood cells* Cancer Res 68(10): 3618-23.
- Torgersen, KM, Vang T, Abrahamsen H, Yaqub S and Tasken K (2002). *Molecular mechanisms for protein kinase A-mediated modulation of immune function* Cell Signal 14(1): 1-9.
- Trenz, K, Schutz P and Speit G (2005). *Radiosensitivity of lymphoblastoid cell lines with a heterozygous BRCA1 mutation is not detected by the comet assay and pulsed field gel electrophoresis* Mutagenesis 20(2): 131-7.
- Vaudry, D, Gonzalez BJ, Basille M, Yon L, Fournier A and Vaudry H (2000). *Pituitary adenylate cyclase-activating polypeptide and its receptors: from structure to functions* Pharmacol Rev 52(2): 269-324.
- Wang, CY, Mayo MW, Korneluk RG, Goeddel DV and Baldwin AS, Jr. (1998). *NF-kappaB antiapoptosis: induction of TRAF1 and TRAF2 and c-IAP1 and c-IAP2 to suppress caspase-8 activation* Science 281(5383): 1680-3.
- Wei, Q, Spitz MR, Gu J, Cheng L, Xu X, Strom SS, Kripke ML and Hsu TC (1996). *DNA repair capacity correlates with mutagen sensitivity in lymphoblastoid cell lines* Cancer Epidemiol Biomarkers Prev 5(3): 199-204.
- Wei, Y and Mojsov S (1996). *Tissue specific expression of different human receptor types for pituitary adenylate cyclase activating polypeptide and vasoactive intestinal polypeptide: implications for their role in human physiology* J Neuroendocrinol 8(11): 811-7.
- Wernicke, M (1975). *Quantitative morphologic assessment of immunoreactivity in regional lymph nodes of patients with carcinoma of the breast* Surg Gynecol Obstet 140(6): 919-24.
- Wu, X, Zheng YL and Hsu TC (2005). *Mutagen-induced chromatid breakage as a marker of cancer risk* Methods Mol Biol 291: 59-67.
- Yoshinaga, S, Hauptmann M, Sigurdson AJ, Doody MM, Freedman DM, Alexander BH, Linet MS, Ron E and Mabuchi K (2005). *Nonmelanoma skin cancer in relation to*

Supplementary Data

γ H2AX foci were analyzed in all twenty LCLs, however results were inconsistent and therefore no accurate conclusions can be made (Figure S1). Cultures of each cell line were exposed to either 0 Gy or a total dose of 2.4Gy gamma-radiation, from a low dose rate of 10cGy/hour for a period of 24 hours. Cultures were removed from the irradiator and immediately fixed for further processing.

Briefly cells were fixed, hybridized with a primary antibody for γ H2AX and a secondary antibody conjugated to FITC. Finally, DNA was stained with PI and fluorescence was analyzed using a MoFlo Flow Cytometer (Dako) and Summit software.

γ H2AX foci via flow cytometry

sample	status	Run #1	Run #2	Run #3
0.017	Case	16.27	11.52	4.63
0.06	Case	-8.05	-9.01	-24.98
10595	Case	-25.98	17.34	-10.16
10600	Case	70.78	20.69	35.54
10603	Case	-4.36	13.25	-160
10727	Case	-26.74	24.81	-43.38
10748	Case	-32.84	27.28	3.6
10759	Case	-36.03	4.83	-9.01
10782	Case	-12.87	11.91	19.69
10789	Case	3.94	-5.21	-5.04
15020	Control	-69.35	2.86	-134.16
15021	Control	-19.2	26.24	8.88
15035	Control	-53.48	0.52	-49.44
15044	Control	-64.93	21.51	-20.37
15050	Control	18.37	-12.73	-291.55
15102	Control	5.6	58.67	-15.25
15127	Control	-15.36	22.95	8.23
15149	Control	-6.94	10.16	-2.24
15152	Control	7.16	15.19	49.85
15172	Control	-24.44	11.74	32.95

Figure S1. γ H2AX foci via flow cytometry. Using a low-dose rate assay developed by Kato et al., average fluorescence intensity was calculated for γ H2AX foci by subtracting the unirradiated sample from the irradiated sample for each individual LCL (2.4 Gy – 0 Gy). Results were extremely variable and not reproducible and therefore not used for the analysis of the LCL properties.

Chapter 4

Characterizing the Role of Human *RAD51D* in Radiation Response and Telomere Maintenance in Rad51d-Deficient Mouse Cells

Characterizing the Role of Human *Rad51D* in Radiation Response and Telomere Maintenance in Rad51d-Deficient Mouse Cells

Abby J. Williams^{1*}, Phillip G. Smiraldo^{2*}, Robert L. Ullrich¹, Susan M. Bailey¹ and Douglas L. Pittman³.

¹Department of Environmental and Radiological Health Sciences, Colorado State University, Fort Collins, CO 80523

²Department of Cell Biology, University of Texas Southwestern Medical Center, Dallas, TX 75390

³South Carolina College of Pharmacy, University of South Carolina, Columbia, SC 29208

*These authors contributed equally to this work.

Abstract

Telomeres are DNA-protein structures at the terminal ends of all eukaryotic chromosomes that allow the cell to distinguish chromosome ends from damaged DNA and protect the ends of chromosomes from degradation and fusion. Telomeric DNA is composed of double-stranded repetitive sequences followed by a single-stranded overhanging tail on the 3' terminus, which is required for proper telomere function. Here, we investigated the length of the 3' overhang using non-denatured/denatured in gel hybridization of DNA from primary mouse embryonic fibroblasts deficient for Rad51d. The Rad51d-deficient cells had an approximate 40 percent increase in overhang signal intensity compared to controls. Furthermore, analysis via Chromosome Orientation Fluorescence *In Situ* Hybridization (CO-FISH) revealed elevated levels of detached centromeres, chromatid fusions and T-SCE in Rad51d-deficient cells compared to controls. In addition, Real Time PCR following ionizing radiation (IR) treatment of human cells revealed *RAD51D* to be elevated 2 and 8 hours after IR treatment, likely as an effect of cytogenetic damage. These results imply that *RAD51D* is required for the regulation of telomeric overhang length and identify a precise telomeric role of Rad51D in maintaining genome stability.

Introduction

Telomeres are nucleoprotein structures at the ends of linear eukaryotic chromosomes that stabilize chromosomal termini and allow cells to distinguish natural chromosome ends from DNA double-stranded breaks (DSBs) (de Lange 2005). In humans, telomeres are comprised of 5-15 kb of double stranded, tandemly repeated, hexameric sequence; the strand running 5' to 3' towards the chromosome end contains the sequence TTAGGG, which is referred to as the G-rich strand. The telomeric G-rich strand is longer than the complementary C-rich strand, thus forming a single-stranded 3' overhanging tail at the terminus of each telomere (Zakian 1995; Chakhparonian and Wellinger 2003). The 3' overhang serves as a substrate for telomerase, the specialized reverse transcriptase responsible for adding telomere repeats de novo (Greider and Blackburn 1987), and is also required for the binding of telomeric single-stranded binding proteins (POT1 in mammals) that function to control telomerase activity and to protect chromosome ends from degradation and fusion (Wei and Price 2003).

Telomeric proteins are thought to stabilize chromosome ends by remodeling telomere DNA into Holliday junction-like structures referred to as t-loops (Griffith *et al.* 1999). This protective conformation forms when the single-stranded, G-rich overhang invades duplex telomeric DNA and pairs with the complementary C-rich strand. *In vitro*, TRF2 binds duplex telomeric DNA and helps remodel linear telomeres into t-loops (Griffith *et al.* 1999; Stansel *et al.* 2001). Additionally, reduction of POT1 by RNA interference (RNAi) caused loss of the telomeric overhanging tail, increased levels of telomere fusions and senescence (Veldman *et al.* 2004; Hockemeyer *et al.* 2005; Yang *et al.* 2005). Combined, these data emphasize the importance of maintaining telomere

stability and suggest a fundamental requirement for the 3' single-strand overhang in telomere protection.

Although *in vitro* purified TRF2 protein is capable of reconfiguring telomeres into t-loop structures, the reaction is not efficient, suggesting that *in vivo*, TRF2 is assisted by other factors that promote strand invasion of the single-stranded tail during the process of t-loop formation (Griffith *et al.* 1999; Stansel *et al.* 2001; de Lange 2005). RAD51D, a protein required for DNA repair by homologous recombination (HR) was recently demonstrated to function at telomeres (Tarsounas *et al.* 2004). The RAD51D protein has DNA-stimulated ATPase activity (Braybrooke *et al.* 2000; Braybrooke *et al.* 2003) and can promote homologous pairing between single- and double-stranded DNA (Kurumizaka *et al.* 2002; Yokoyama *et al.* 2004), making it a candidate for assisting in t-loop formation. Loss of RAD51D conferred extensive chromosome instability, increased telomere fusions, and accelerated telomere attrition (Takata *et al.* 2001; Tarsounas *et al.* 2004; Smiraldo *et al.* 2005).

Telomere length has also been correlated with radiosensitivity, as shorter telomeres seem to enhance sensitivity to radiation exposure. For example, studies of murine lymphoma cells revealed a major reduction of telomere length in radiosensitive cells compared to radioresistant cells. Similarly, shorter telomeres in lymphocytes from breast cancer patients correlate with greater sensitivity to IR (McIlrath *et al.* 2001). In addition, analysis of human fibroblasts demonstrates that older cells with shorter telomeres display increased radiosensitivity versus younger fibroblasts with longer telomeres (Rubio *et al.* 2002). Based on these observations, we sought to investigate the response of *RAD51D* expression following exposure to radiation.

It has been reported that a variant in *Rad51D* may play a role in breast cancer susceptibility as well (Rodriguez-Lopez *et al.* 2004; Dowty *et al.* 2007). Therefore, we determined if this variant, E233G, was present in a variety of human mammary carcinoma lines commonly used in the laboratory. Furthermore, reports also demonstrate that the histone methyltransferase protein EZH2 is up-regulated in many cancers, including that of the breast, and that EZH2 down-regulates the Rad51 paralogs, including RAD51D (Zeidler *et al.* 2005; Ding and Kleer 2006). EZH2, Enhancer of Zeste 2, is a polycomb group protein that functions in the maintenance of heritable transcription patterns (Laible *et al.* 1997). It has been suggested that this protein contributes to mammary carcinogenesis by down-regulation of the Rad51 paralogs which leads to decreased DNA repair via HR (Zeidler *et al.* 2005; Zeidler and Kleer 2006). We therefore investigated whether or not EZH2 and RAD51D physically bind to each other by performing Co-IP experiments.

To further characterize the roles of Rad51D, we examined relative expression levels of *RAD51D* (and *EZH2*) at various time points following exposure to IR in both log phase and contact-inhibited human cells. To examine the role of Rad51D at telomeres in mice, we analyzed the relative length of the 3' single-strand overhang as well as cytogenetic characteristics of Rad51d-deficient mouse embryonic fibroblasts (MEFs). Rad51d-deficient cells had an approximate 40 percent increase in overhang signal intensity compared to controls as well as elevated frequencies of chromosome aberrations and T-SCE. These data demonstrate that Rad51d is required for the regulation of the extreme telomere termini, specifically, the length of the 3' telomeric

overhang, for maintaining genomic stability and for suppressing extensive SCE in telomeric regions, thus serving to help maintain genomic stability.

Materials & Methods

Plug preparation and electrophoresis. Primary mouse embryonic fibroblasts (MEFs) were generated as described and grown in DMEM supplemented with 7.5% fetal bovine serum, 7.5% newborn calf serum, and antibiotics (Smiraldo *et al.* 2005). Sub-confluent cultures of primary (< passage 5) MEFs (two independent homozygous wild-type, one *Rad51d*^{+/-} *Trp53*^{+/-}, two independent *Trp53*^{-/-}, and two independent *Rad51d*^{-/-} *Trp53*^{-/-} cell lines) were trypsinized, counted by hemacytometer, pelleted by centrifugation for 6 minutes at 100 RCF, and washed in 1xPBS. After washing, cells were pelleted by centrifugation for 5 minutes at 100 RCF and resuspended in 1% low melt agarose at 45°C and 1.6×10^6 cells cast into 40µL plug molds. After casting, plugs were incubated overnight at 37°C in a lithium dodecyl sulfate (LDS) solution containing 1% LDS, 100mM EDTA pH8.0, and 10mM Tris pH 8.0 (2.5mls per plug). Plugs were then washed twice in a 20% NDS solution containing 6.8mM N-laurylsarcosine, 127mM EDTA, and 2mM Tris (two hours per wash) at room temperature (2.5mls per plug). DNA plugs to be digested by restriction enzyme were washed twice in TE (one hour per wash) at room temperature (2mls per plug). Plugs were then incubated twice (one hour per incubation) in 1x MboI restriction enzyme buffer at room temperature (200µL per plug). Each plug was then incubated in 150µL of 1x MboI buffer with 30U of MboI at 37°C overnight. The following morning, 20 additional units of MboI were added to each tube and incubated at 37°C for 4 hours. DNA plugs were prepared for electrophoresis by

washing twice in TE (one hour per wash) at room temperature and once in 0.5xTBE electrophoresis running buffer (one hour) at room temperature. Plugs were loaded into a 1% agarose gel and DNA fragments separated by pulsed field gel electrophoresis (CHEF-DR II apparatus, BioRad) at 6v/cm for 20 hours with an initial pulse time of 1second and a final pulse time of 10 seconds (chamber temperature maintained at 14°C).

In-gel hybridization. Following electrophoresis, the DNA was stained with ethidium bromide for photography and gels were dried at 50°C for 45 minutes in preparation for three successive hybridizations. The dried gels were prehybridized in 20 mM NaH₂PO₄, 0.1% SDS, 5x Denhardt's solution, and 5xSSC for one hour at 55°C, and first hybridized with the [γ -³²P]ATP end-labeled oligonucleotide (TTAGGG)₄ overnight at 55°C in prehybridization solution. Gels were then washed three times for 20 min in 4xSSC at room temperature and three times for 20 min in 4xSSC, 0.1%SDS at 57°C. Gels were exposed to phosphorimager screens overnight, developed using a Typhoon 8600 Variable Mode Imager (Molecular Dynamics, Amersham Pharmacia Biotech), and radioactive signals quantified (excluding signals from DNA that remained in the wells) using ImageQuant[®] version 5.2 for Windows. For the second hybridization, gels were prehybridized for one hour at 55°C, hybridized with the [γ -³²P]ATP end-labeled oligonucleotide (CCCTAA)₄ overnight at 55°C, washed, and exposed to phosphorimager screens overnight, developed, and radioactive signals quantitated. Dried gels were then alkali denatured in 0.6 M NaCl, 0.2 M NaOH for one hour at room temperature, neutralized in 1.5 M NaCl, 0.5 M Tris, for one hour at room temperature, and rinsed in ddH₂O for 30 min at room temperature. For the third hybridization, gels were

prehybridized for one hour at 55°C, hybridized with the [γ - 32 P]ATP end-labeled oligonucleotide (TTAGGG)₄ overnight at 55°C, and washed. Gels were exposed to phosphorimager screens for 5 hours and radioactive signals quantified. Telomere lengths were estimated from radioactive signals of alkali denatured gels hybridized with the end labeled (TTAGGG)₄ oligonucleotide, as described (Harley *et al.* 1990).

Relative G-strand overhang lengths were determined by the following equation, $RS_N / [(TL_C / TL_E) * RS_D]$, where RS_N is the radioactive signal from native gels hybridized with the (CCCTAA)₄ oligonucleotide, TL_C is the estimated telomere lengths of the control (homozygous wild-type) cells, TL_E is the estimated telomere lengths of the experimental (*Rad51*^{d^{-/-}} *Trp53*^{+/-}, *Trp53*^{-/-}, or *Rad51*^{d^{-/-}} *Trp53*^{-/-}) cells, and RS_D is the total radioactive signal from the denatured gels hybridized with the (TTAGGG)₄ oligonucleotide. Statistical significance of the experimental data was determined using SPSS[®] version 11.5 for Windows by ANOVA. Follow-up comparisons were performed using the Tukey HSD post hoc test.

Chromosome Orientation-FISH (CO-FISH). Confluent MEFs were irradiated with 0 Gy or 1Gy from a sealed-source Mark I ¹³⁷Cs γ -irradiator (J.L. Shepherd and Associates) and allowed 24 hr for repair. Cultures were then split and grown in the presence of 2 x 10⁻⁵ M 5'-bromo-2'-deoxyuridine (BrdU, Sigma) for one round of replication. Cells were harvested and slides were prepared using standard cytogenetic techniques. CO-FISH has been described previously in detail (Bailey *et al.* 2004). Briefly, slides were treated with RNase A 100 μ g/ml H₂O) at 37° C. Slides were then rinsed in PBS and fixed in 3% formaldehyde/PBS solution for 10 minutes at room temperature. Next, slides were

dehydrated in a cold ethanol series, then stained with Hoescht 33258 and exposed to 365 nm UV light. Following an Exonuclease III treatment (Promega), slides were heated in 70% formamide/2x SSC at 70°C and again subjected to the cold ethanol series. Finally, slides were hybridized with a PNA-TelG probe (Applied Biosystems) conjugated to Cy3, rinsed and mounted with Vectashield antifade and DAPI.

Images were analyzed and captured using a Zeiss Axioskop2 Plus microscope equipped with a Photometrics Coolsnap ES2 camera and Metavue 7.1 software. Slides were blinded and scored for chromosomal and telomeric aberrations. Standard deviations were calculated and used to determine the standard error of the mean (SEM) to generate error bars. A student's T-test was calculated to determine statistical significance and all conditions were repeated twice. If results were not significantly different, data was pooled.

Sequencing for E233G variant. Several human mammary carcinoma lines were obtained from the Tissue Culture Core Facility at The University of Colorado Health Science Center: BT-20, BT-483, DU4475, HBL100, MCF7, MDA231, MDA330, T47D and ZR75-1. DNA was harvested using a Qiagen kit and PCR was performed using the following primers designed from the NCBI website: F1: 5'CTGTGAAGGTGGTGGTTGTG3' R1: 5'TCGATGGTGTCCAGGAGAAT3'. PCR products were then shipped to Davis Sequencing.

Real time PCR. Both confluent and exponentially growing flasks of primary normal human dermal fibroblasts (5C; Cascade Biologics) and immortalized mammary epithelial

MCF10A (ATCC) cell cultures were irradiated with either 0 Gy or 5 Gy radiation from a sealed-source Mark I ¹³⁷Cs γ -irradiator (J.L. Shepherd and Associates) and RNA was harvested 0, 2, 4, 8 and 24 hr post-irradiation. RNA was isolated using a Qiagen kit and cDNA was then generated using a Verso cDNA kit (ABgene #ab1453). 2X Sybr Green Fluorescein Mix (Thermo Scientific) was used for real time PCR assays. 12.5ng of cDNA was added to the Sybr green in a 96-well plate. The housekeeping gene used was TFRC (Transferrin Receptor) (F: 5' CGCTGGTCAGTTCGTGATTA 3' and R: 5' GCATTCCCGAAATCTGTTGT 3') with final primer concentration of 100nM. Rad51D and EZH2 primers were diluted to a final concentration of 1X (Qiagen). Each reaction was performed in triplicate and run in a BioRad Icyler. Ct values were normalized to the housekeeping gene and $\Delta\Delta$ Ct was calculated for each time point using the Livak method to compare the unirradiated samples with the irradiated samples (Livak and Schmittgen 2001). One-way ANOVA with Tukey's post-test was performed for statistical analysis using Prism 4.0c (GraphPad Software, Inc.) using data from three independent experiments.

Results

3' single-stranded telomeric overhangs are elongated in Rad51d-deficient MEFs

Rad51d is essential for maintaining chromosome and telomere stability. Here, we report the relative length of the 3' single-stranded, telomeric overhangs in Rad51d-deficient primary mouse embryonic fibroblasts (MEFs) compared to homozygous wild-type, *Rad51d*^{+/-} *Trp53*^{+/-}, or *Trp53*^{-/-} MEFs by utilizing the non-denaturing/denaturing in-gel hybridization technique. Following electrophoresis, native gels containing non-denatured DNA were first probed with a radioactively labeled (TTAGGG)₄ oligonucleotide. Because this probe is identical to the sequence of the telomeric 3' overhang, no signal above background was observed in lanes containing DNA (data not shown) demonstrating that the DNA in the gel was not nicked or denatured during electrophoresis. The possibility that probe hybridization failed was ruled out because the (TTAGGG)₄ oligonucleotide was successfully used for a subsequent hybridization (see below). The same gel was then hybridized with a radioactively labeled (CCCTAA)₄ oligonucleotide which produced overhang signals for all genotypes (Figure 1A). Before electrophoresis, if the plugs containing genomic DNA were pretreated with the single-strand-specific DNA nuclease, mung bean nuclease, overhang signals were absent (data not shown), demonstrating that the radioactively labeled (CCCTAA)₄ oligonucleotide was binding to the single-stranded, telomeric 3' overhangs. Although DNA from the same number of cells of each genotype was used in these experiments, the intensity of the overhang signals of *Rad51d*^{-/-} *Trp53*^{-/-} MEFs could not be directly compared to the intensity of the overhang signals of control cells because *Rad51d*-deficient cells have a high level of hypo- and hyperploidy.

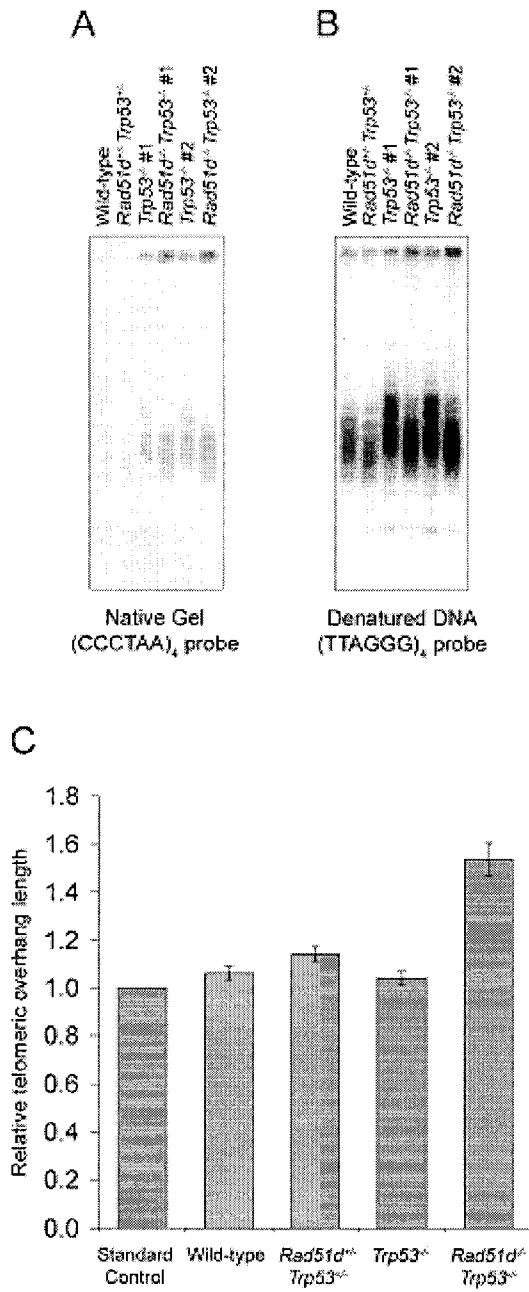


Figure 1. Comparison of relative telomeric 3' overhang lengths in primary mouse embryonic fibroblasts (MEFs). Radioactively labeled oligonucleotide in-gel hybridizations to MboI digested genomic DNA isolated from primary MEFs. **A.** Native gel hybridized with (CCCTAA)₄ probe. **B.** The DNA from the same gel was alkali denatured and hybridized with (TTAGGG)₄ probe. **C.** Relative G-strand overhang lengths were determined by the following equation, $RS_N / [(TL_C / TL_E) * RS_D]$, where RS_N is the radioactive signal from native gels hybridized with the (CCCTAA)₄ oligonucleotide, TL_C is the estimated telomere lengths of the control (homozygous wild-type) cells, TL_E is the estimated telomere lengths of the experimental (*Rad51d*^{+/-} *Trp53*^{+/-}, *Trp53*^{-/-}, or *Rad51d*^{-/-} *Trp53*^{-/-}) cells, and RS_D is the total radioactive signal from the denatured gels hybridized with the (TTAGGG)₄ oligonucleotide. Telomere lengths were estimated from radioactive signals of alkali denatured gels hybridized with the (TTAGGG)₄ oligonucleotide, as described (Harley *et al.* 1990). Error bars are the standard error of the mean from at least three independent experiments.

To normalize the overhang signal to DNA content, the DNA in the same gel was alkali denatured, hybridized with a radioactively labeled (TTAGGG)₄ oligonucleotide, and total radioactive signal quantified for each sample. Differences of telomere lengths among samples were taken into consideration when calculating the relative length of the telomeric 3' overhangs (Figure 1C) (Materials and Methods). No significant difference in the relative length of the telomeric overhangs was observed when comparing homozygous wild-type, heterozygous *Rad51d*^{+/-} *Trp53*^{+/-}, or *Trp53*^{-/-} cells ($p > 0.05$). However, a 1.4-fold increase in relative length of the telomeric overhangs in the mutant *Rad51d*^{-/-} *Trp53*^{-/-} primary MEFs was significantly different compared to controls (homozygous wild-type vs. *Rad51d*^{-/-} *Trp53*^{-/-} $p \leq 0.001$, *Rad51d*^{+/-} *Trp53*^{+/-} vs. *Rad51d*^{-/-} *Trp53*^{-/-} $p = 0.001$, *Rad51d*^{-/-} *Trp53*^{-/-} vs. *Trp53*^{-/-} $p \leq 0.001$). These results demonstrate that Rad51d is required for proper maintenance of the telomeric 3' overhangs in mammalian cells.

Increased chromosomal aberrations in Rad51d-deficient MEFs

We also confirm increased levels of chromosome aberrations in *Trp53*^{-/-} *Rad51d*^{-/-} MEFs compared to *Trp53*^{-/-} MEFs as seen previously (Smiraldo *et al.* 2005). Increased levels of dicentrics, chromatid breaks, chromatid fusions and detached centromeres were observed in *Rad51d*^{-/-} MEFs (Figures 2 and 3). No telomere signals were present at the points of fusion for either the dicentrics or chromatid fusions, suggesting no telomere uncapping occurs without Rad51d. T-SCE levels were elevated in *Rad51D*^{-/-} MEFs compared to controls (Figure 4), suggesting that Rad51D normally participates in regulating T-SCE, but is not necessary to execute an SCE in telomeric regions of DNA.

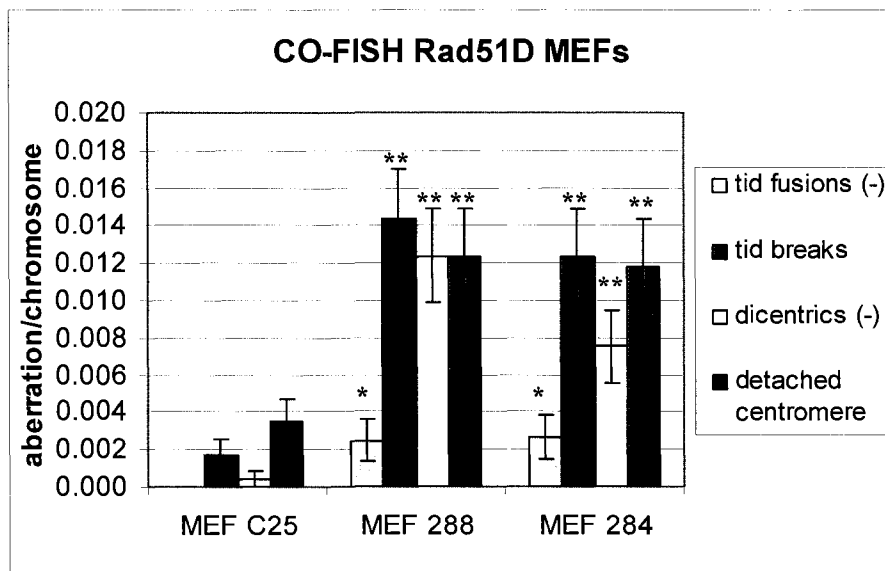
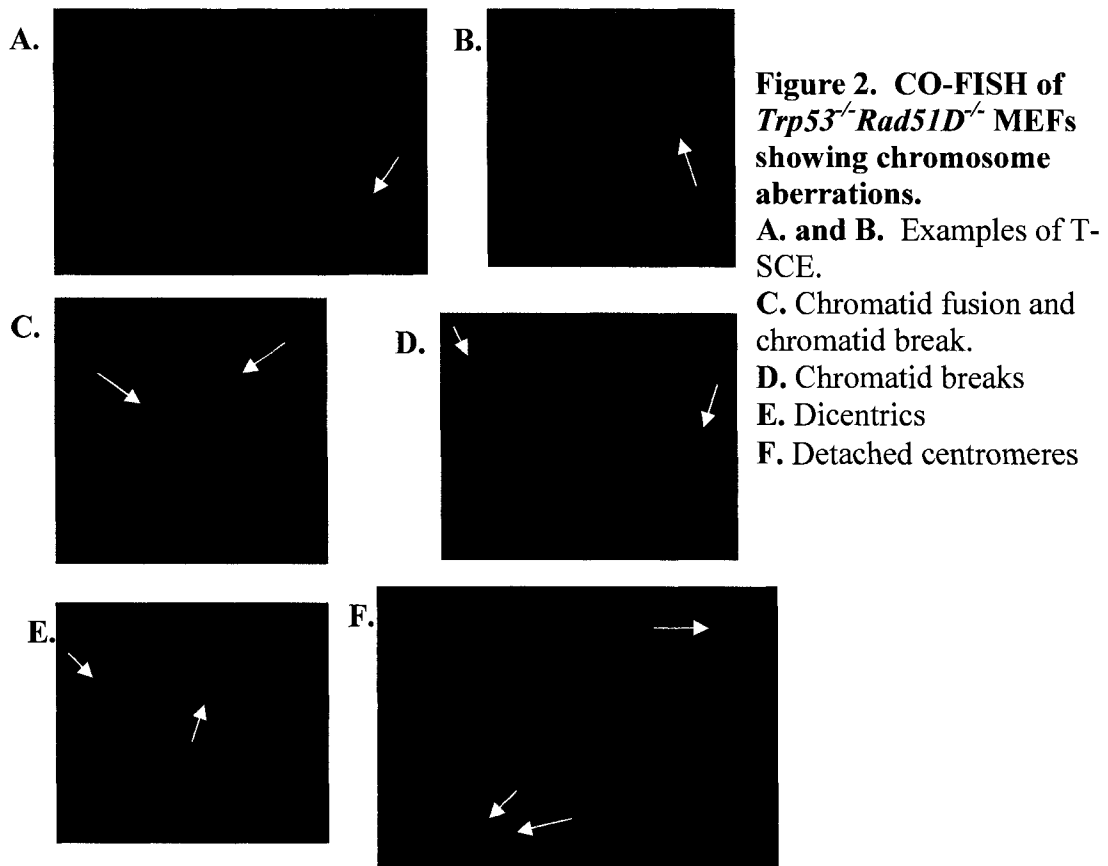


Figure 3. Elevated chromosome aberrations in *Rad51D*^{-/-} MEFs. Chromatid fusions, chromatid breaks, dicentric and detached centromeres are all significantly increased in *Trp53*^{-/-} *Rad51D*^{-/-} cells (MEF 284 & 288) compared to *Trp53*^{-/-} (MEF C25) cells. (*p<0.05, **p<0.01)

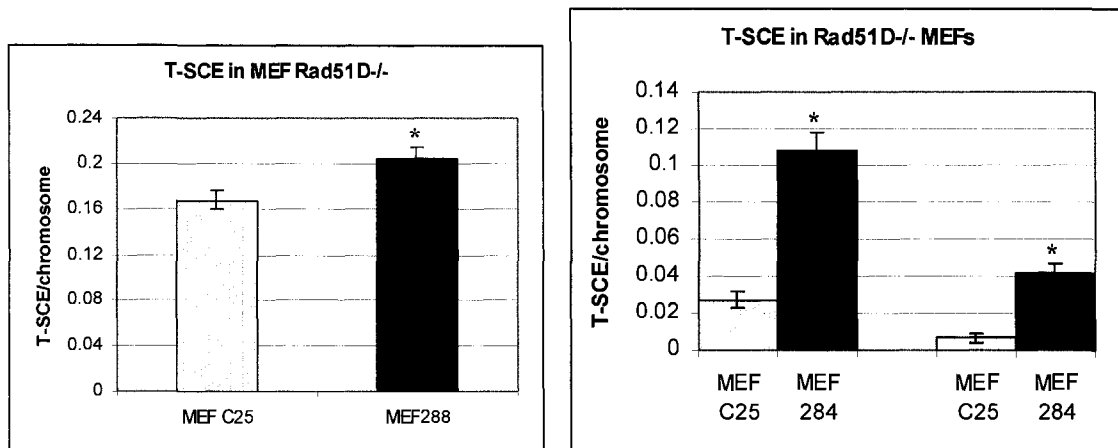


Figure 4. T-SCE levels Rad51D-deficient MEFs. T-SCE frequencies are significantly elevated in *Trp53^{-/-}Rad51D^{-/-}* (MEF 284 & 288) compared to *Trp53^{-/-}* control (MEF C25) cells. *p<0.05

Telomere CO-FISH was also performed with irradiated MEFs. The number of dicentric chromosomes did increase in *Rad51D^{-/-}* MEFs with radiation treatment (Figure 5). However, detached centromeres were not influenced by radiation (data not shown), suggesting that these are spontaneous events. No increase in chromatid break or fusion frequencies were seen following radiation (data not shown), suggesting the majority of cells were in G1 at the time of exposure.

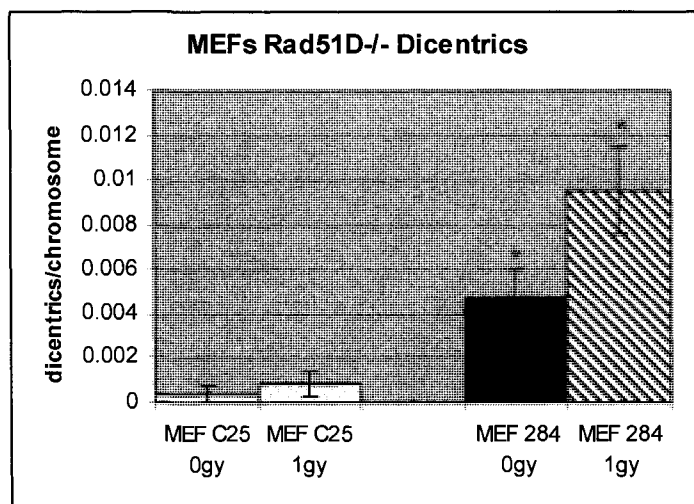


Figure 5. Dicentric chromosomes after radiation treatment in Rad51D-deficient MEFs. The level of dicentrics was significantly increased in *Trp53^{-/-}Rad51D^{-/-}* cells (MEF 284) following exposure to radiation and compared to *Trp53^{-/-}* control (MEF C25) cells. *p<0.05

No RAD51D E233G Variant Found in Mammary Epithelial Cell Lines

It has been suggested that RAD51D may also have roles in carcinogenesis as the variant E233G in *RAD51D* may be a low-penetrance breast cancer susceptibility allele (Rodriguez-Lopez *et al.* 2004). We sequenced DNA from 8 human mammary epithelial lines to determine whether or not this specific variant was present. None of the eight lines sequenced had this variant (Table 1), which may not be surprising considering the need for large sample sizes in order to accurately detect SNPs.

Cell Line	E233G variant
MCF10A	no
MCF-7	no
MDA231	no
MDA330	no
HBL100	no
ZR75-1	no
DU4475	no
BT-20	no

Table 1. DNA sequencing of mammary epithelial cell lines.
No cell line contains the *RAD51D* variant E233G.

EZH2 & RAD51D Respond Similarly to IR

It has been shown that Rad51D and other Rad51 paralogs are down-regulated in breast cancer due to the over-expression of EZH2. We investigated *RAD51D* and *EZH2* gene expression changes following exposure to radiation using Real Time PCR in both normal human fibroblasts (5C HDF) and epithelial cells (MCF10A). In log phase 5C HDF cells, expression of both *RAD51D* and *EZH2* increased 2 hours after radiation, but then decreased to roughly background levels, increasing slightly again at 8 hours (Figure

6A). In log-phase MCF10A cells, relative expression of *RAD51D* and *EZH2* also increased at both 2 and 8 hours after radiation, although these changes are not statistically significant (Figure 6B).

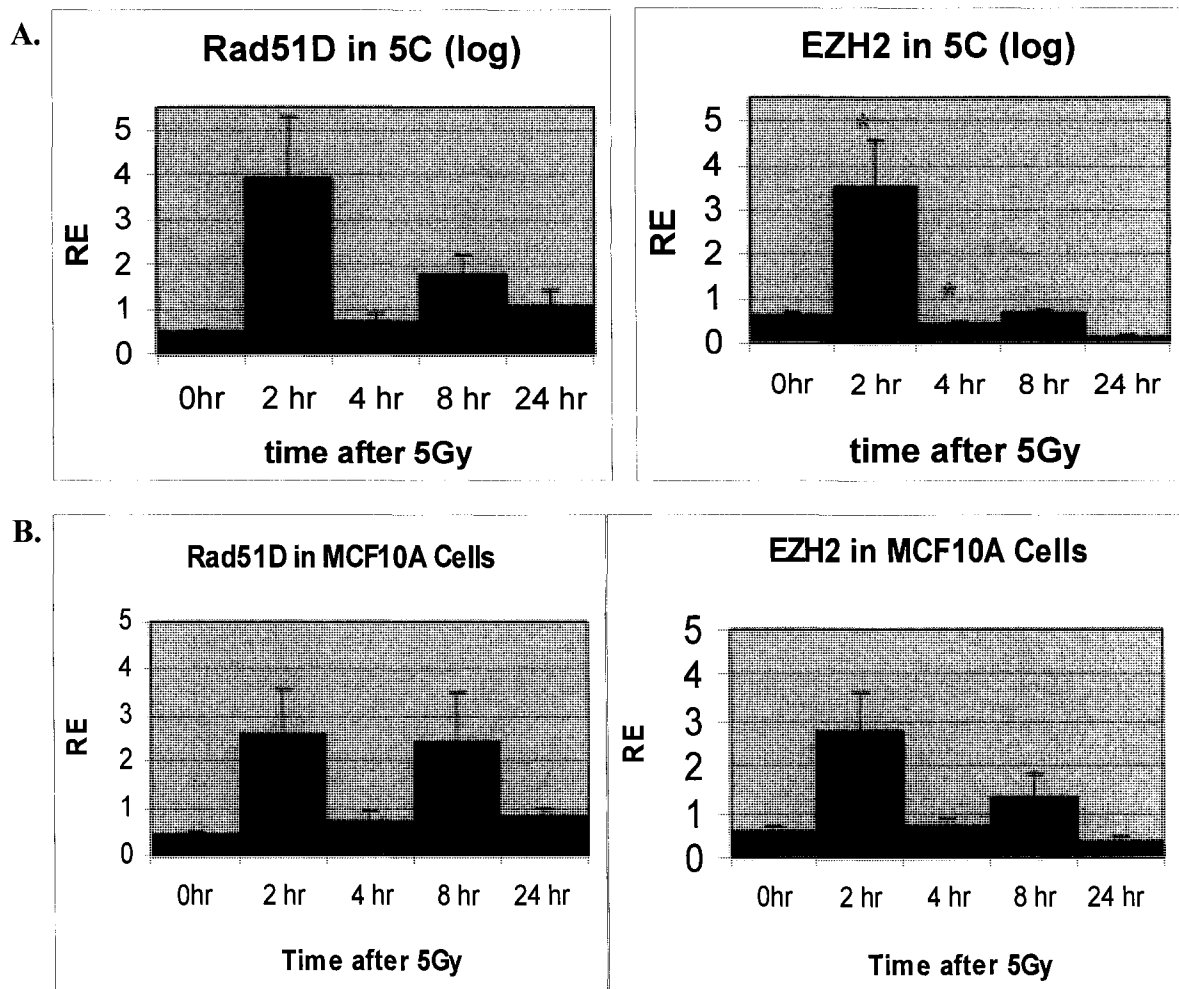


Figure 6. Real Time PCR after IR exposure to log-phase cells. **A.** In 5C HDF cells, both *RAD51D* and *EZH2* expression increases 2 hours after radiation and then falls back down to levels similar to background with a slight increase seen again at 8 hours. **B.** In MCF10A cells a similar trend is seen. (RE: relative expression). * $p < 0.05$

To determine if these changes were cell cycle related, we performed the same experiment using contact-inhibited 5C HDF and MCF10A cells. *RAD51D* and *EZH2* gene expression changes in non-cycling cells were not as dramatic as those seen in log-phase cultures (Figure 7A and 7B). In addition, the relative expression of *RAD51D* seems to be most prominent at 8 hours post-IR in both the 5C and MCF10A cells (Figure 7). The relative expression of *RAD51D* appears to change more dramatically than *EZH2* in both cell types as well.

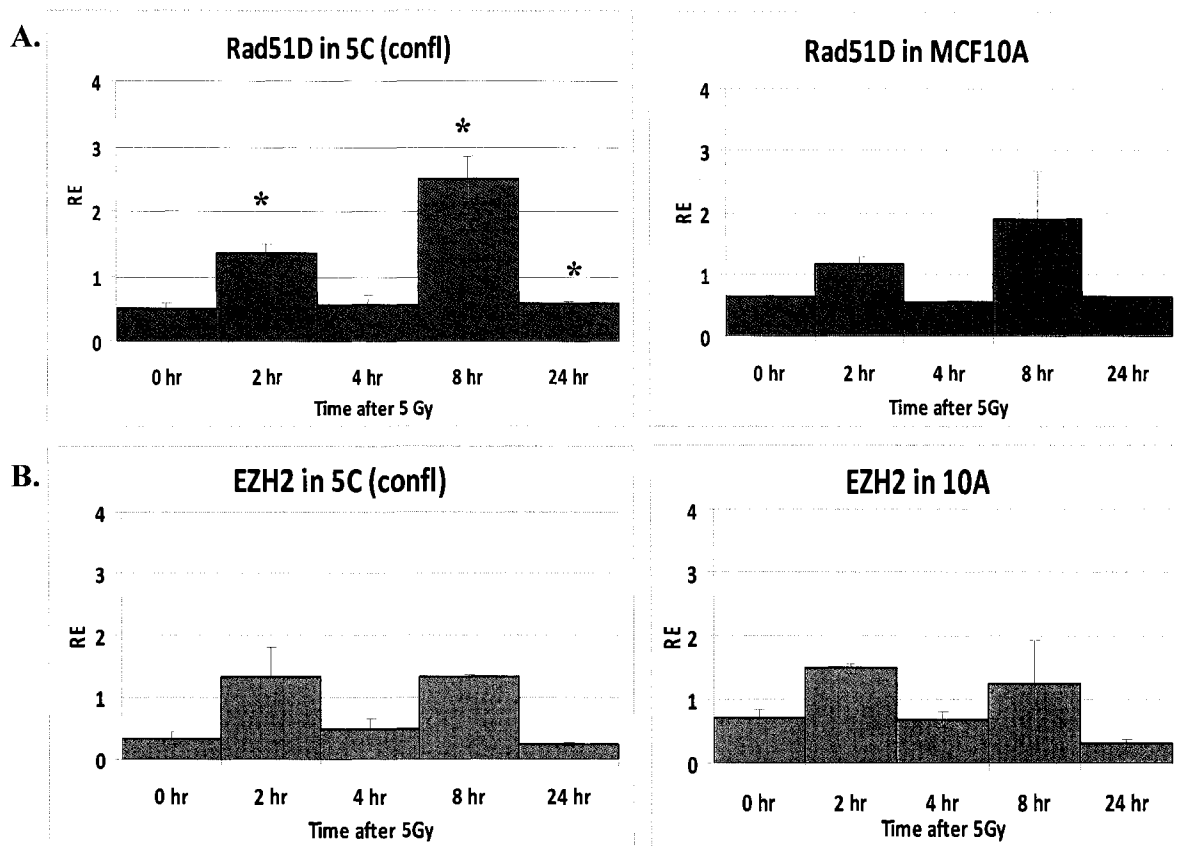


Figure 7. Real Time PCR after IR exposure to contact-inhibited cells. A. In 5C HDF an increase in relative expression is seen at 2 and 8 hours post-IR for both *EZH2* and *RAD51D*. B. In MCF10A cells the same general trend is observed. (RE: relative expression). * $p < 0.05$

Discussion

Telomeres function in a number of biological pathways including protection of chromosome ends from degradation and DNA repair mechanisms, meiotic chromosome segregation, and chromatin silencing (Zakian 1995; Greider 1996). It has also been proposed that telomeres play a role in preventing unlimited cell division through what has been termed the “end-replication problem” (Harley 1991). With each round of cellular division, telomeres gradually shorten, eventually triggering senescence thus placing a limitation on the number of cellular divisions a cell may undergo. If telomeres are left unprotected, chromosome ends become vulnerable to enzymatic degradation and/or can be recognized by DNA repair pathways that fuse chromosomes together. One model of telomeric-end protection involves formation of structures termed t-loops, in which the extreme terminal 3′ single-stranded overhang invades the duplex telomeric DNA (Griffith *et al.* 1999). Thus, maintenance of the 3′ overhang is critical for telomere protection in regard to this telomere capping mechanism. Here, we demonstrate that the length of telomeric 3′ single-stranded overhangs are approximately 40 percent longer in primary mouse embryonic fibroblasts deficient for Rad51d compared to control cells, suggesting Rad51d plays a role in regulating the length of the ss-overhang.

Previous studies have demonstrated extensive chromosome instability in mouse and chicken cells deficient for *Rad51d* (Takata *et al.* 2001; Smiraldo *et al.* 2005). In mammals, RAD51D also functions at telomeres; in its absence, decreased duplex telomere lengths and increased telomere fusions were observed (Tarsounas *et al.* 2004). Rad51d belongs to a family of RAD51-like proteins that functions to repair damaged DNA by homologous recombination in vertebrates (Thacker 1999; Thompson and Schild

2002; West 2003). When a panel of chicken DT40 knockout cell lines possessing deletions of individual genes involved in homologous recombination (HR) or non-homologous end joining (NHEJ) DNA repair pathways were investigated for telomere dysfunction, depletion of Rad51 conferred an approximate 1.5-fold increase in the relative telomeric 3' overhang signal intensity (Wei *et al.* 2002). Interestingly, this increased signal is comparable to that observed in Rad51d-deficient primary mouse embryonic fibroblasts. In mammalian cells, there is no evidence that RAD51 plays a role in telomere maintenance (Tarsounas *et al.* 2004), except in cells that can maintain telomere length in the absence of telomerase by the alternative lengthening of telomeres (ALT) pathway (Yeager *et al.* 1999). This suggests that Rad51d in mammals, and Rad51 in *Gallus gallus* (chicken), may perform similar processing functions at telomeres in a species-specific manner. It has also been demonstrated that other repair proteins play roles in regulating proper telomere function including, but not limited to, DNA-PKcs and Ku (Bailey *et al.* 1999). Such data emphasize the complex nature of the regulation of DNA repair processes and telomere maintenance by some of the same proteins.

Because overall duplex telomere lengths are decreased in Rad51d-deficient cells, we speculate that the increased length of telomeric 3' ss-overhangs observed in this study result from deregulated enzymatic degradation of the C-rich telomeric strand, as opposed to inappropriate elongation of the G-rich strand by telomerase. Several lines of evidence suggest that a 5' to 3' exonuclease activity normally acts at telomeres. First, newly created telomeres replicated by leading strand synthesis are blunt ended. However, single-stranded G-rich tails are observed at all chromosome ends in cells lacking detectable levels of telomerase (Dionne and Wellinger 1996; Makarov *et al.* 1997;

Hemann and Greider 1999). Second, with each population doubling, it has been estimated that human cells grown in culture lose approximately 100bp (Harley *et al.* 1990; Counter *et al.* 1992). This rate of shortening is faster than that expected from the end replication problem of lagging strand synthesis, suggesting that telomere processing occurs following DNA replication. Although the nuclease responsible for such degradation has not been identified, this process is tightly regulated; the C-rich telomeric strand nearly always ends with the sequence ATC-5' (Sfeir *et al.* 2005). The data presented in this study suggest Rad51d is involved in regulating the processing of telomere ends. If excessive 5' to 3' nuclease degradation of the C-rich strand occurs in the absence of Rad51d, elongated 3' ss-overhangs would be generated. Accelerated telomere attrition would occur as these cells divide, consistent with previous studies demonstrating decreased telomere lengths in Rad51d-deficient cells.

To further examine Rad51d's telomeric role, we utilized CO-FISH. Increased levels of chromatid fusions and chromatid breaks were observed, suggesting on-going instability among the Rad51d-deficient background since chromatid-type aberrations occur in G2 of the cell cycle immediately preceding the cell harvest. No telomere signal was seen at the point of chromatid fusions, suggesting that telomere uncapping is not occurring—perhaps due to the elongated ss-overhangs present in these cells. Telomere shortening could explain the chromatid fusions since critically shortened telomeres are unstable and often fuse with other unstable chromosome ends (uncapped telomeres or DSBs), as well as the fact that shorter telomeres are known to exist in these MEFs (Tarsounas *et al.* 2004). In addition, increased numbers of dicentric chromosomes and detached centromeres were also seen. Centromere aberrations were also previously

observed in these cells (Smiraldo *et al.* 2005), implying that Rad51d possibly plays a role in facilitating replication through euchromatin-heterochromatin junctions. Telomere CO-FISH following IR exposure revealed an increase in dicentrics in the Rad51d-deficient cells. IR is known to cause DNA damage (DSBs) that then can be mis-repaired, forming aberrations including dicentrics (reviewed in (Bailey and Bedford 2006)). Further results demonstrate that spontaneous genomic SCE (G-SCE) levels are unchanged (Smiraldo *et al.* 2005) while T-SCE levels are elevated in Rad51d^{-/-} MEFs, implying that Rad51d is not needed for T-SCE to occur. More importantly, Rad51d preferentially regulates SCE recombination in telomeric DNA. However it should be noted that non-mammalian DT40 Rad51d^{-/-} (chicken) cells do have decreased levels of SCE (Takata *et al.* 2001). Based on these observations, it seems likely that Rad51d has a role in suppressing excessive SCE, at least in telomeric DNA, which is equally as important for maintaining genomic stability as suppressing chromosomal aberrations. Similar reports of HR proteins and SCE have previously been described (Hagelstrom *et al.*, 2008, unpublished data and (Sonoda *et al.* 1999; Helleday 2003; Nagasawa *et al.* 2005)).

Due to reports that EZH2 down-regulates RAD51D in various cancers, we investigated expression changes in *RAD51D* and *EZH2* following exposure to IR in both human immortalized mammary epithelial and human primary dermal fibroblast cells. The overall trends are similar in both cell types and for both genes, with increases in relative expression at 2 and 8 hours post-IR. These results indicate that *EZH2* and *RAD51D* respond to IR in a similar manner, however further studies will be necessary to evaluate the details of underlying mechanisms regulating this response. Analysis of protein levels and Co-Immunoprecipitation studies may provide clues to this regulation.

Interestingly, *RAD51* was shown to be up-regulated 4 hours after (but not 24 hours after) 5 Gy of gamma-radiation in human TK6 cells but did not show a significant increase after receiving a dose of 10 Gy or 20 Gy at either time point analyzed (Akerman *et al.* 2005). Although these authors did observe an increase in expression, microarrays were used, which differ from our study and furthermore, they did not include a 0 hour time point in their analysis. Nonetheless, this increase in *RAD51* is encouraging since *RAD51D* is closely related to *RAD51*. Another paralog, *RAD51C*, was also slightly elevated after IR treatment (5 Gy) in normal human lymphoblastoid cells (Rieger and Chu 2004).

It was recently reported that EZH2 is recruited to sites of DNA damage and may function in returning chromatin to its initial state following completion of repair processes (O'Hagan *et al.* 2008). This may suggest that the changes in relative expression levels following radiation treatment are due to the presence of EZH2 at DNA damage sites. It has been demonstrated in yeast that the Sir family of proteins (histone deacetylases) help regulate chromatin silencing in telomeric regions as well as DSB repair (Tsukamoto *et al.* 1997; Martin *et al.* 1999). In fact, following initiation of a DNA damage response, Sir2-4 are actually recruited from the telomeres to DSBs (Boulton and Jackson 1998). It may be that EZH2 is needed throughout the genome to signal the completion of the DNA repair process or to participate in regulating which sites are repaired, or in what order they are repaired. Perhaps *RAD51D* assists in the repair of telomeric DNA damage, specifically by restoring the protective t-loop structure after the repair process has concluded. A more likely reason for the increase of this protein is the

need for RAD51D to help repair interstrand cross-links (ICLs) (Smiraldo *et al.* 2005), which also result from IR exposure.

Following a report of a variant in the *RAD51D* gene that may be a low-penetrance breast cancer susceptibility allele (Rodriguez-Lopez *et al.* 2004), we sequenced DNA for the presence of this variant in several commonly studied human breast epithelial lines; MCF10A, MCF-7, MDA231, MDA330, HBL100, ZR75-1, DU4475 and BT-20. None of these lines contained the E233G variant in *RAD51D*. This is perhaps not surprising since large studies are needed for detection of Single Nucleotide Polymorphisms (SNPs). Nevertheless, further investigation is required in order to either validate or refute E233G as a breast cancer susceptibility allele.

In summary, these data demonstrate that RAD51D is necessary for maintaining genomic instability, the normal length of the telomeric 3' ss-overhang, and suppression of T-SCE in mice. In the absence of RAD51D, telomeric 3' ss-overhang signal intensities were approximately 40 percent higher compared to controls, and T-SCE and chromosomal aberration levels were elevated. In addition, Rad51D and EZH2 gene expression levels respond similarly to IR, regardless of the cell type or cell cycle state. We know from previous studies that the length of the telomeric 3' ss-overhang is proportional the rate of telomere shortening (cells with long overhangs lose more telomeric repeats with each cell division (Huffman *et al.* 2000)), which gives insight as to why overall telomere lengths are decreased in the absence of RAD51D. Although it is not known if RAD51D acts alone or as part of a protein complex at telomeres, future investigations of protein interactions involving Rad51d and telomere-specific proteins

will further define the role of Rad51d at chromosome ends and in maintaining genome stability.

References

- Akerman, GS, Rosenzweig BA, Domon OE, Tsai CA, Bishop ME, McGarrity LJ, Macgregor JT, Sistare FD, Chen JJ and Morris SM (2005). *Alterations in gene expression profiles and the DNA-damage response in ionizing radiation-exposed TK6 cells* Environ Mol Mutagen 45(2-3): 188-205.
- Bailey, SM and Bedford JS (2006). *Studies on chromosome aberration induction: what can they tell us about DNA repair?* DNA Repair (Amst) 5(9-10): 1171-81.
- Bailey, SM, Goodwin EH and Cornforth MN (2004). *Strand-specific fluorescence in situ hybridization: the CO-FISH family* Cytogenet Genome Res 107(1-2): 14-7.
- Bailey, SM, Meyne J, Chen DJ, Kurimasa A, Li GC, Lehnert BE and Goodwin EH (1999). *DNA double-strand break repair proteins are required to cap the ends of mammalian chromosomes* Proc Natl Acad Sci U S A 96(26): 14899-904.
- Boulton, SJ and Jackson SP (1998). *Components of the Ku-dependent non-homologous end-joining pathway are involved in telomeric length maintenance and telomeric silencing* Embo J 17(6): 1819-28.
- Braybrooke, JP, Li JL, Wu L, Caple F, Benson FE and Hickson ID (2003). *Functional interaction between the Bloom's syndrome helicase and the RAD51 paralog, RAD51L3 (RAD51D)* J Biol Chem 278(48): 48357-66.
- Braybrooke, JP, Spink KG, Thacker J and Hickson ID (2000). *The RAD51 family member, RAD51L3, is a DNA-stimulated ATPase that forms a complex with XRCC2* J Biol Chem 275(37): 29100-6.
- Chakhparonian, M and Wellinger RJ (2003). *Telomere maintenance and DNA replication: how closely are these two connected?* Trends Genet 19(8): 439-46.
- Counter, CM, Avilion AA, LeFeuvre CE, Stewart NG, Greider CW, Harley CB and Bacchetti S (1992). *Telomere shortening associated with chromosome instability is arrested in immortal cells which express telomerase activity* Embo J 11(5): 1921-9.
- de Lange, T (2005). *Shelterin: the protein complex that shapes and safeguards human telomeres* Genes Dev 19(18): 2100-10.
- Ding, L and Kleer CG (2006). *Enhancer of Zeste 2 as a marker of preneoplastic progression in the breast* Cancer Res 66(19): 9352-5.
- Dionne, I and Wellinger RJ (1996). *Cell cycle-regulated generation of single-stranded G-rich DNA in the absence of telomerase* Proc Natl Acad Sci U S A 93(24): 13902-7.
- Dowty, JG, Lose F, Jenkins MA, Chang JH, Chen X, Beesley J, Dite GS, Southey MC, Byrnes GB, Tesoriero A, Giles GG, Hopper JL and Spurdle AB (2007). *The RAD51D E233G variant and breast cancer risk: population-based and clinic-based family studies of Australian women* Breast Cancer Res Treat.
- Greider, CW (1996). *Telomere length regulation* Annu Rev Biochem 65: 337-65.
- Greider, CW and Blackburn EH (1987). *The telomere terminal transferase of Tetrahymena is a ribonucleoprotein enzyme with two kinds of primer specificity* Cell 51(6): 887-98.
- Griffith, JD, Comeau L, Rosenfield S, Stansel RM, Bianchi A, Moss H and de Lange T (1999). *Mammalian telomeres end in a large duplex loop* Cell 97(4): 503-14.

- Harley, CB (1991). *Telomere loss: mitotic clock or genetic time bomb?* *Mutat Res* 256(2-6): 271-82.
- Harley, CB, Futcher AB and Greider CW (1990). *Telomeres shorten during ageing of human fibroblasts* *Nature* 345(6274): 458-60.
- Helleday, T (2003). *Pathways for mitotic homologous recombination in mammalian cells* *Mutat Res* 532(1-2): 103-15.
- Hemann, MT and Greider CW (1999). *G-strand overhangs on telomeres in telomerase-deficient mouse cells* *Nucleic Acids Res* 27(20): 3964-9.
- Hockemeyer, D, Sfeir AJ, Shay JW, Wright WE and de Lange T (2005). *POT1 protects telomeres from a transient DNA damage response and determines how human chromosomes end* *Embo J* 24(14): 2667-78.
- Huffman, KE, Levene SD, Tesmer VM, Shay JW and Wright WE (2000). *Telomere shortening is proportional to the size of the G-rich telomeric 3'-overhang* *J Biol Chem* 275(26): 19719-22.
- Kurumizaka, H, Ikawa S, Nakada M, Enomoto R, Kagawa W, Kinebuchi T, Yamazoe M, Yokoyama S and Shibata T (2002). *Homologous pairing and ring and filament structure formation activities of the human Xrcc2*Rad51D complex* *J Biol Chem* 277(16): 14315-20.
- Laible, G, Wolf A, Dorn R, Reuter G, Nislow C, Lebersorger A, Popkin D, Pillus L and Jenuwein T (1997). *Mammalian homologues of the Polycomb-group gene Enhancer of zeste mediate gene silencing in Drosophila heterochromatin and at S. cerevisiae telomeres* *Embo J* 16(11): 3219-32.
- Livak, KJ and Schmittgen TD (2001). *Analysis of relative gene expression data using real-time quantitative PCR and the 2(-Delta Delta C(T)) Method* *Methods* 25(4): 402-8.
- Makarov, VL, Hirose Y and Langmore JP (1997). *Long G tails at both ends of human chromosomes suggest a C strand degradation mechanism for telomere shortening* *Cell* 88(5): 657-66.
- Martin, SG, Laroche T, Suka N, Grunstein M and Gasser SM (1999). *Relocalization of telomeric Ku and SIR proteins in response to DNA strand breaks in yeast* *Cell* 97(5): 621-33.
- McIlrath, J, Bouffler SD, Samper E, Cuthbert A, Wojcik A, Szumiel I, Bryant PE, Riches AC, Thompson A, Blasco MA, Newbold RF and Slijepcevic P (2001). *Telomere length abnormalities in mammalian radiosensitive cells* *Cancer Res* 61(3): 912-5.
- Nagasawa, H, Peng Y, Wilson PF, Lio YC, Chen DJ, Bedford JS and Little JB (2005). *Role of homologous recombination in the alpha-particle-induced bystander effect for sister chromatid exchanges and chromosomal aberrations* *Radiat Res* 164(2): 141-7.
- O'Hagan, HM, Mohammad HP and Baylin SB (2008). *Double strand breaks can initiate gene silencing and SIRT1-dependent onset of DNA methylation in an exogenous promoter CpG island* *PLoS Genet* 4(8): e1000155.
- Rieger, KE and Chu G (2004). *Portrait of transcriptional responses to ultraviolet and ionizing radiation in human cells* *Nucleic Acids Res* 32(16): 4786-803.
- Rodriguez-Lopez, R, Osorio A, Ribas G, Pollan M, Sanchez-Pulido L, de la Hoya M, Ruibal A, Zamora P, Arias JI, Salazar R, Vega A, Martinez JI, Esteban-Cardenosa E, Alonso C, Leton R, Urioste Azcorra M, Miner C, Armengod ME, Carracedo A,

- Gonzalez-Sarmiento R, Caldes T, Diez O and Benitez J (2004). *The variant E233G of the RAD51D gene could be a low-penetrance allele in high-risk breast cancer families without BRCA1/2 mutations* Int J Cancer 110(6): 845-9.
- Rubio, MA, Kim SH and Campisi J (2002). *Reversible manipulation of telomerase expression and telomere length. Implications for the ionizing radiation response and replicative senescence of human cells* J Biol Chem 277(32): 28609-17.
- Sfeir, AJ, Chai W, Shay JW and Wright WE (2005). *Telomere-end processing the terminal nucleotides of human chromosomes* Mol Cell 18(1): 131-8.
- Smiraldo, PG, Gruver AM, Osborn JC and Pittman DL (2005). *Extensive chromosomal instability in Rad51d-deficient mouse cells* Cancer Res 65(6): 2089-96.
- Sonoda, E, Sasaki MS, Morrison C, Yamaguchi-Iwai Y, Takata M and Takeda S (1999). *Sister chromatid exchanges are mediated by homologous recombination in vertebrate cells* Mol Cell Biol 19(7): 5166-9.
- Stansel, RM, de Lange T and Griffith JD (2001). *T-loop assembly in vitro involves binding of TRF2 near the 3' telomeric overhang* Embo J 20(19): 5532-40.
- Takata, M, Sasaki MS, Tachiiri S, Fukushima T, Sonoda E, Schild D, Thompson LH and Takeda S (2001). *Chromosome instability and defective recombinational repair in knockout mutants of the five Rad51 paralogs* Mol Cell Biol 21(8): 2858-66.
- Tarsounas, M, Munoz P, Claas A, Smiraldo PG, Pittman DL, Blasco MA and West SC (2004). *Telomere maintenance requires the RAD51D recombination/repair protein* Cell 117(3): 337-47.
- Thacker, J (1999). *A surfeit of RAD51-like genes?* Trends Genet 15(5): 166-8.
- Thompson, LH and Schild D (2002). *Recombinational DNA repair and human disease* Mutat Res 509(1-2): 49-78.
- Tsukamoto, Y, Kato J and Ikeda H (1997). *Silencing factors participate in DNA repair and recombination in Saccharomyces cerevisiae* Nature 388(6645): 900-3.
- Veldman, T, Etheridge KT and Counter CM (2004). *Loss of hPot1 function leads to telomere instability and a cut-like phenotype* Curr Biol 14(24): 2264-70.
- Wei, C and Price M (2003). *Protecting the terminus: t-loops and telomere end-binding proteins* Cell Mol Life Sci 60(11): 2283-94.
- Wei, C, Skopp R, Takata M, Takeda S and Price CM (2002). *Effects of double-strand break repair proteins on vertebrate telomere structure* Nucleic Acids Res 30(13): 2862-70.
- West, SC (2003). *Molecular views of recombination proteins and their control* Nat Rev Mol Cell Biol 4(6): 435-45.
- Yang, Q, Zheng YL and Harris CC (2005). *POT1 and TRF2 cooperate to maintain telomeric integrity* Mol Cell Biol 25(3): 1070-80.
- Yeager, TR, Neumann AA, Englezou A, Huschtscha LI, Noble JR and Reddel RR (1999). *Telomerase-negative immortalized human cells contain a novel type of promyelocytic leukemia (PML) body* Cancer Res 59(17): 4175-9.
- Yokoyama, H, Sarai N, Kagawa W, Enomoto R, Shibata T, Kurumizaka H and Yokoyama S (2004). *Preferential binding to branched DNA strands and strand-annealing activity of the human Rad51B, Rad51C, Rad51D and Xrcc2 protein complex* Nucleic Acids Res 32(8): 2556-65.
- Zakian, VA (1995). *Telomeres: beginning to understand the end* Science 270(5242): 1601-7.

- Zeidler, M and Kleer CG (2006). *The Polycomb group protein Enhancer of Zeste 2: its links to DNA repair and breast cancer* J Mol Histol 37(5-7): 219-23.
- Zeidler, M, Varambally S, Cao Q, Chinnaiyan AM, Ferguson DO, Merajver SD and Kleer CG (2005). *The Polycomb group protein EZH2 impairs DNA repair in breast epithelial cells* Neoplasia 7(11): 1011-9.

Chapter 5

DNA-PKcs and ATM Influence Generation of Ionizing Radiation-Induced Bystander Signals

DNA-PKcs and ATM Influence Generation of Ionizing Radiation-Induced Bystander Signals

R. Tanner Hagelstrom^{1*}, Kristin F. Askin^{1*}, Abby J. Williams^{1*}, Lila Ramaiah¹, Christian Desaintes², Edwin H. Goodwin³, Robert L. Ullrich¹, and Susan M. Bailey¹⁺.

¹Department of Environmental and Radiological Health Sciences, Colorado State University, Fort Collins, CO 80523

²Laboratory of Radiobiology, SCK·CEN (Studiecentrum voor kernenergie-Centre d'étude de l'énergie nucléaire), Boeretang 200, B-2400 MOL, Belgium

³KromaTiD Inc., Fort Collins, CO 80523

*These authors contributed equally to this work.

+Corresponding author. E-mail: sbailey@colostate.edu

Phone: (970) 491-2944

Keywords: DNA-PKcs, ATM, Ionizing Radiation, Bystander Effect

Running Title: DNA-PKcs and ATM influence bystander signaling

Abstract. The phenomenon by which irradiated cells influence non-irradiated neighboring cells, referred to as the bystander effect (BSE), is not well understood in terms of the underlying pathways involved. We sought to enlighten connections between DNA damage repair and the BSE. Utilizing sister chromatid exchange (M'Kacher *et al.*) frequencies as a marker of the BSE, we performed cell transfer strategies that enabled us to distinguish between generation versus reception of a bystander signal. We find that DNA-dependent Protein Kinase catalytic subunit (DNA-PKcs) and Ataxia Telangectasia Mutated (Panta *et al.*) are necessary for the generation of such a bystander signal in normal human cells following gamma (γ)-ray exposure, but are not required for its reception. Importantly, we also show that directly irradiated human cells do not respond to receipt of a bystander signal, helping to explain why the BSE is a low dose phenomenon. These studies provide the first evidence for a role of the DNA damage response proteins DNA-PKcs and ATM specifically in the generation of a bystander signal and inter-cellular signaling.

Introduction

Newly emerging insight into the mechanistic basis of carcinogenesis supports the concept that the genetic effects of low-dose radiation cancer risks are considerably more complex than one might imagine based on linear no-threshold extrapolations from the high-dose radiation received by Japanese atomic-bomb survivors. The observation of a low dose ionizing radiation (IR) induced bystander effect (BSE), i.e., irradiated cells signaling their distress to, and stimulating a response in, non-irradiated neighbors and inducing an effect is a case in point.

The BSE occurs when a directly irradiated cell generates and transmits a signal, such as reactive oxygen species (ROS) (Kashino *et al.* 2007), nitric oxide species (NOS) (Shao *et al.* 2006), or cytokines (Banaz-Yasar *et al.* 2007) either through gap junctions (Azzam *et al.* 1998; Azzam *et al.* 2001) or through media (Lehnert *et al.* 1997; Mothersill and Seymour 1998) to a neighboring non-irradiated cell. Given that the multiple markers that have been used to study the BSE, i.e., micronuclei formation (Yang *et al.* 2007), clonogenic survival (O'Neill-Mehlenbacher *et al.* 2007), apoptosis (Grifalconi *et al.* 2007), and sister chromatid exchange (M'Kacher *et al.*) (Nagasawa *et al.* 2005) (Figure 1), are themselves considered to be detrimental, it has been assumed that the BSE is harmful to neighboring cells. However, it has also been proposed that the BSE may actually be beneficial at a tissue level; cells exposed to a bystander signal are more radioresistant to subsequent IR-induced damage indicative of an adaptive response (Iyer and Lehnert 2002). It is also noteworthy that of these markers, only SCE frequency is not significantly influenced by direct low LET (e.g., gamma-ray) radiation exposure (Ardito *et al.* 1980), making SCE an attractive marker of the BSE.

Given numerous studies demonstrating the importance of DNA repair proteins in directly irradiated cells, we sought to examine what, if any, role they might play in the BSE. We focused on the repair proteins DNA-PKcs (DNA-dependent Protein Kinase catalytic subunit) and ATM (Ataxia Telangectasia Mutated). DNA-PK is a primary component of the Non-Homologous End-Joining (NHEJ) DSB repair pathway, consisting of the Ku 70/80 hetero-dimer and DNA-PKcs (Collis *et al.* 2005). DNA-PK is critical for DSB repair and for V(D)J recombination (Jeggo *et al.* 1995). It has also been shown that DNA-PK is important for the protection of mammalian telomeres by helping to maintain effective end-capping and preventing inappropriate fusions (Bailey *et al.* 1999; Bailey *et al.* 2001; Bailey *et al.* 2004). Like DNA-PKcs, ATM is a member of the phosphoinositide 3-kinase-like kinase (PIKK) family. ATM plays a critical role in the early detection of IR-induced DSBs (Barzilai *et al.* 2002) and is responsible for phosphorylation of numerous proteins involved in cell-cycle control, apoptosis and DNA repair (Lavin and Kozlov 2007).

Previous studies investigating how DNA repair status influences the BSE include several by Nagasawa *et al.*, who demonstrated that cells deficient in DNA repair proteins tend to exhibit large bystander responses following alpha-particle irradiation (Nagasawa *et al.* 2005). These authors speculated that cells experiencing defective repair of DNA damage induced by direct irradiation, display an increased bystander response likely due to increased production of ROS (Nagasawa and Little 2002). These early experiments were not capable of determining whether the role of these proteins was in the generation or in the reception of the bystander signal. Later, media transfer experiments revisited the role of several DNA repair proteins in generation of the bystander signal; here it was

concluded that these proteins played no role in the BSE (Mothersill *et al.* 2004).

However, media transfer experiments inherently limit the role of short-lived ROS, which many believe to be a crucial contributor to the BSE.

In the current study, we designed cell transfer strategies to assess the role of DNA-PKcs and ATM in the generation and/or reception of the IR-induced BSE following γ -ray exposure. Cells were divided into two groups, donors (irradiated) and recipients (non-irradiated). The donor cells were either un-irradiated (control) or exposed to 1 Gy of 137 Cesium γ -rays (treated), rinsed and then co-cultured with the recipient cells at a dilution of either 1:100 or 1:1000. Cells were harvested after two cell cycles in the presence of bromodeoxyuridine (BrdU) in order to facilitate visualization and analyses of SCE frequencies in unirradiated recipient cells as a marker of the BSE. Utilizing both mouse and human cell lines deficient in either DNA-PKcs or ATM and normal human fibroblasts, and by altering which was the donor, we assessed how DNA-PKcs and ATM influence the generation and/or reception of bystander signals.



Figure 1. Sister Chromatid Exchange (SCE). Partial human fibroblast (5C HDF) metaphase chromosome spread illustrating FPG harlequin staining (100x). A “color switch” (arrows) indicates an SCE has occurred.

Materials and Methods

Cell Lines and Cell Culture. Kidney tissue from 8–12 week old female C57BL/6, BALB/c, SCID, or congenic mice were minced, and digested in 199 medium containing collagenase (Worthington Type III; 200 units/ml) at 37°C for 3–5 h with gentle agitation. Disaggregated cells were washed 6x in phosphate buffered saline (PBS) containing 0.5% fetal bovine serum (FBS) and cultured in α -MEM medium (15% FBS, penicillin/streptomycin). Media was changed after 3 days of incubation. Low passage neonatal Human Dermal Fibroblasts (HDF C-004-5C; Cascade Biologics) were grown in α -MEM supplemented with 10% fetal bovine serum and antibiotics. Cells were counted using a Coulter Counter (Coulter Beckman, Fullerton, CA) and 4×10^5 human fibroblasts were plated into T-75 flasks, then co-cultured with 1:100 dilutions of either 0 Gy or 1 Gy γ -irradiated, exponentially growing donor cells. Donor cells were not allowed to near confluency and included human ATM^{-/-} (AG04450), DNA-PKcs deficient (BALB/c mouse), wild-type DNA-PKcs (C57BL/6 mouse), or congenic DNA-PKcs (manuscript in preparation). Irradiations were performed using a sealed-source Mark I ¹³⁷Cs γ -irradiator (J.L. Shepherd and Associates). 5'-bromo-2'-deoxyuridine (BrdU; Sigma) was added to cultures at a final concentration of 2×10^{-5} M and cells were allowed to grow for two rounds of cell division. Colcemid (Invitrogen) was added at a final concentration of 0.2 μ g/ml and cells were harvested approximately 2-3 hours later. Cells were trypsinized, centrifuged, then resuspended in 0.075M KCl for 15 minutes at room temperature and then fixed with 3:1 methanol: acetic acid.

C.B6-*Prkdc* and B6.C-*Prkdc*^{BALB} congenic mouse strains. Two strains congenic for the common allele (C57BL/6) and BALB/c variant allele of *Prkdc* were generated (manuscript in preparation) using the parental strains C57BL/6J (B6) and BALB/cByJ (C) (both obtained from Jackson Laboratory). For the congenic strain C.B6-*Prkdc*, B6CByF1 females were mated with C.B6 males to produce the N2 generation. Subsequent generations N2 – N10 were repeatedly backcrossed to BALB/cByJ mice. For congenic strain B6.C-*Prkdc*^{BALB}, CByB6F1 females were mated with B6 males to produce the N2 generation. Subsequent generations N2 – N10 were repeatedly backcrossed to C57BL/6J mice. In both congenic strains, progeny were selected for backcross mating if they carried donor *Prkdc* sequence as determined by PCR/RFLP (Yu *et al.* 2001). Additionally, a marker-directed breeding strategy (speed congenics) was adopted at backcross generations N8 – N12 which selected against progeny carrying background donor genome (Weil *et al.* 1997). Microsatellite markers polymorphic between B6.C and C.B6 were used to select backcross progeny whose genome contained the least donor sequence at loci other than *Prkdc*. Mice at backcross N10 or later were intercrossed and progeny homozygous for the donor *Prkdc* allele were selected for inbreeding. Mouse colonies were maintained at the Colorado State University Painter Center.

SCE Staining and Analysis. Slides of metaphase chromosomes were prepared using standard cytogenetic techniques, then stained using the Fluorescence Plus Giemsa technique (Perry and Wolff 1974) in order to obtain harlequin staining and to visualize SCE. Briefly, slides were stained with Hoescht 33258 (Thermo Sci Acros Organics) for

15 minutes at room temperature, rinsed with distilled water and exposed to UV light (365nm; Stratalinker) for 25 minutes. Slides are then soaked in 2x SSC at 60°C for 30 minutes. Following thorough rinses with distilled water, slides are allowed to air dry, and then stained with 5% Giemsa for 10 minutes. Images were analyzed and captured using a Zeiss Axioskop2 Plus microscope equipped with a Photometrics Coolsnap ES2 camera and Metavue 7.1 software.

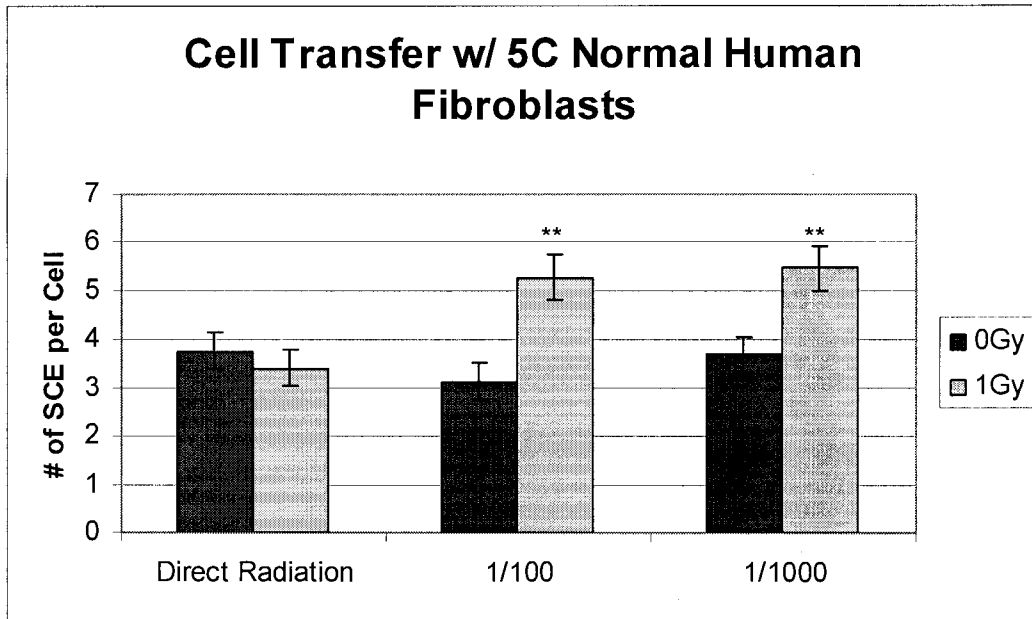
Statistical Analysis. Slides were blinded and scored by independent investigators for SCE. Standard deviations were calculated and used to determine the standard error of the mean (SEM) to generate error bars. A student's T-test was calculated to determine statistical significance. All conditions were repeated at least twice, and each experiment was scored by at least two individuals. If results were not significantly different, data was pooled. Results from additional experiments are provided as supplemental data (table).

Results

SCE frequencies in primary normal human dermal fibroblasts (5C HDF), both with and without exposure to 1Gy of direct γ -irradiation (^{137}Cs), were determined. It has been reported previously that direct low LET IR exposure does not significantly enhance SCE frequency (Ardito *et al.* 1980), which we confirmed here. 5C HDF's did not display elevated SCE frequencies subsequent to direct γ -irradiation as compared to the 0 Gy controls; SCE frequencies were 3.76 SCE/ metaphase (0 Gy) and 3.4 SCE/ metaphase (1 Gy) (Figure 2A), with no statistically significant difference between sample means.

We designed a cell transfer approach that utilizes SCE frequencies as a marker of the IR-induced BSE, and importantly facilitates discrimination between generation versus receipt of bystander signals. A small number of irradiated cells (donors) were added to a non-irradiated cell population (recipients). Immediately following IR exposure (1 Gy ^{137}Cs γ -rays), human fibroblast (5C HDF) donor cells were pelleted and rinsed in PBS to remove any remaining media. Donor cells were then diluted either 1:100 or 1:1000 and added to non-irradiated recipient cells (5C HDF). The co-culture was collected following two rounds of replication in the presence of BrdU and scored for SCE (vast majority were non-irradiated recipient cells). Our results revealed a significant elevation in SCE frequency in the samples whose donor cells were irradiated compared to the control samples whose donors were not irradiated (Figure 2A). The 1:100 dilutions displayed a frequency of 3.14 SCE/ metaphase (0 Gy) and 5.28 SCE/ metaphase (1 Gy). The 1:1000 dilutions displayed a frequency of 3.68 SCE/ metaphase (0 Gy) and 5.48 SCE/ metaphase (1 Gy). Frequency histograms (Figure 2B) illustrate that this is a general increase, rather than being limited to a subset of cells. It is also interesting to note that there was a

A.



B.

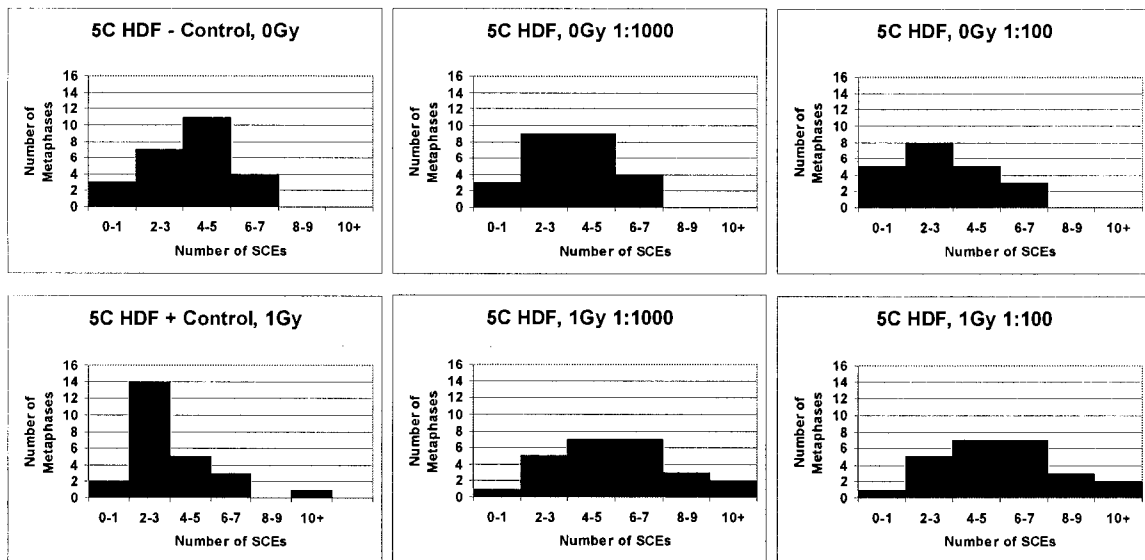


Figure 2A. Direct Irradiation versus BSE. Following γ -ray direct irradiation (no cell transfer), human fibroblasts (5C HDF) show no significant increase in SCE frequency. Using 5C HDFs as both donor (1 Gy), and recipient (0 Gy) bystander cells at 1:100 and 1:1000 dilutions, significant, and similar, increases in SCE levels were observed. **B.** The distributions of SCE number per metaphase illustrate an overall increase in SCE levels. * $\geq 95\%$ confidence, ** $\geq 99\%$ confidence.

similar increase in SCE frequency for both the 1:100 and 1:1000 dilutions, which is consistent with previous reports that the BSE appears to operate by an “on/off” mechanism (Nagasawa and Little 1992; Lehnert *et al.* 1997; Hu *et al.* 2006). Therefore, only the 1:100 dilution cell transfer method was utilized in subsequent experiments.

We confirmed that direct IR (γ -ray) exposure did not elevate SCE frequencies in our experimental system. These results imply that directly irradiated cells are refractory to the bystander signal. To test this hypothesis, we repeated the experiments outlined above, with addition of irradiated recipient cells (5C HDF) to the protocol (Figure 3). As seen previously, SCE frequencies did not increase in directly irradiated cells; 4.2 SCE/ metaphase (0 Gy) and 4.03 SCE/ metaphase (1 Gy) (Figure 3A). Also as expected, an increase in SCE frequency was observed when irradiated donor cells were added to non-irradiated recipient cells; 3.9 SCE/ metaphase (0 Gy) and 5.03 SCE/ metaphase (1 Gy) (Figure 3A.) However, there was no significant increase in SCE when irradiated donor cells were added to irradiated recipient cells; 4.08 SCE/ metaphase (0 Gy) and 3.88 SCE/ metaphase (1 Gy). This result supports the hypothesis that directly irradiated cells are refractory to the BSE, i.e., they are unable to either receive or respond to a bystander signal once they have activated the mechanism to generate bystander signals.

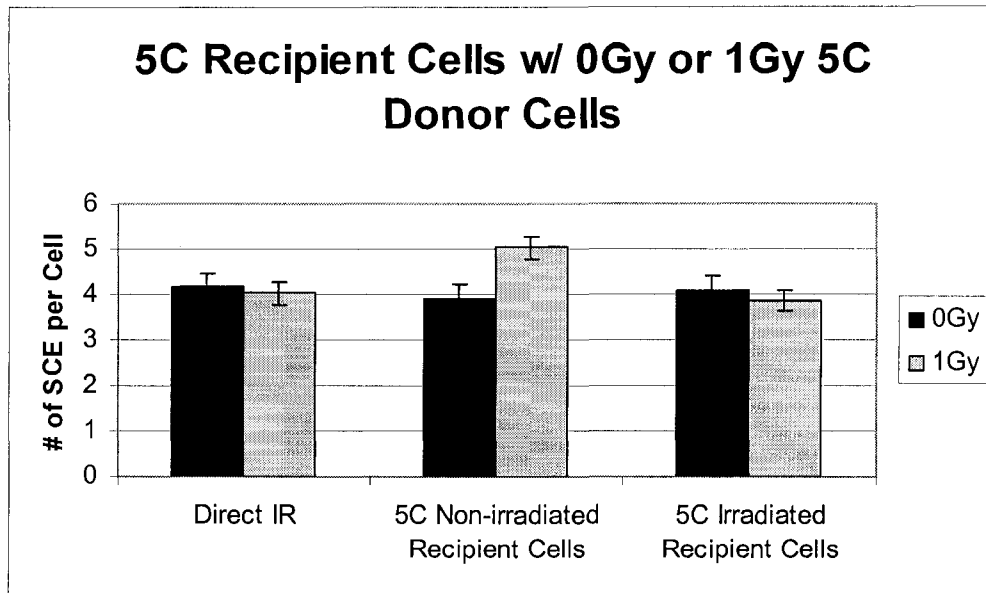


Figure 3A. Irradiated cells are refractory to bystander signals. Direct irradiation does not increase SCE levels. Irradiated donor cells (5C HDF) induce an increase in SCE frequency in non-irradiated recipient cells (5C HDF). When recipient cells were irradiated (1 Gy), they were no longer able to respond to the bystander signal.

We recognized the unavoidable reality that some, although very few, directly irradiated cells were scored as bystander cells in our cell transfer approach. Although we repeatedly determined that SCE frequencies do not increase in directly irradiated 5C HDFs (Fig 2A and 3A), we sought to further ensure that only bystander, non-hit cells were scored for SCE. Therefore, mouse cells, whose chromosome morphology is clearly distinguishable from human, were used as the irradiated donor cells and 5C HDFs were used as the non-irradiated recipient cells. Wild-type C57BL/6 mouse donor cells were irradiated and cultured with non-irradiated 5C HDF recipient cells. A significant increase in SCE frequency was observed in the 5C HDF recipients; 3.72 SCE/ metaphase (0 Gy) and 5.33 SCE/ metaphase (1Gy) ($p < 0.05$) (Figure 4A).

To examine the role of DNA-PKcs in the generation and/or reception of bystander signals in our system, we utilized BALB/c primary mouse kidney fibroblasts, which

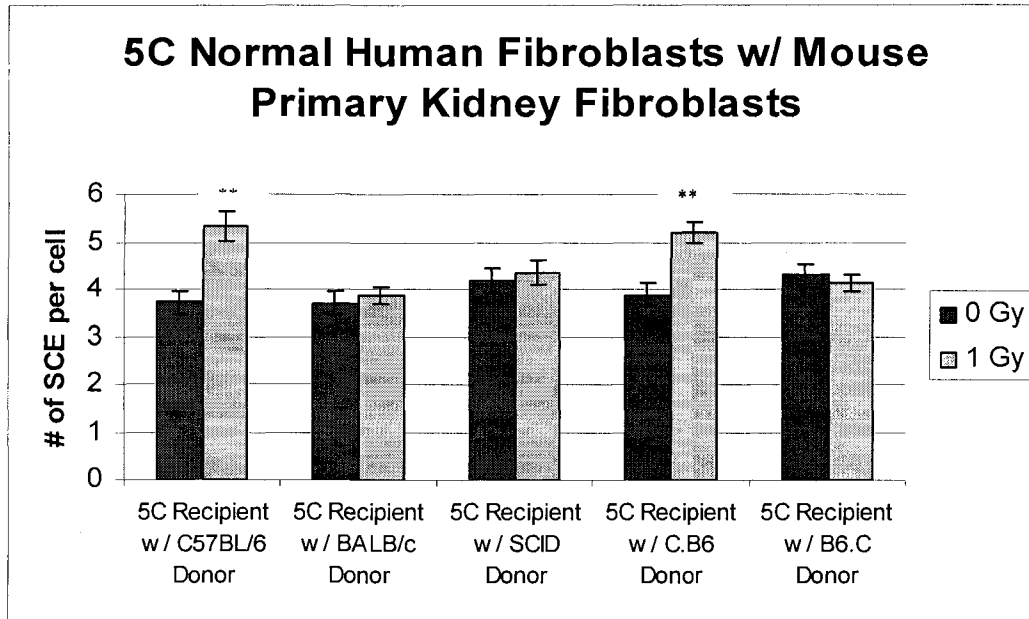
contain a hypomorphic variant of DNA-PKcs that results in reduced expression and kinase activity (Okayasu *et al.* 2000). Irradiated BALB/c donor cells were added to non-irradiated 5C HDF recipient cells. No significant increase in SCE frequency was observed in the 5C HDF recipient cells; 3.70 SCE/ metaphase (0Gy) and 3.86 SCE/ metaphase (1Gy) (Figure 4A), suggesting that DNA-PKcs is required for generation of the bystander signal. While background frequencies varied slightly (common with SCE), all trends were consistent (see supplementary Table 1 for additional SCE data demonstrating consistent trends).

Next, we utilized severe combined immunodeficiency (SCID) primary mouse kidney fibroblasts. SCID mice have a truncated version of DNA-PKcs and are essentially null for activity (Blunt *et al.* 1996). Again, no significant increase in SCE was seen when irradiated SCID donor cells were added to non-irradiated 5C HDF recipient cells; 4.18 SCE/ metaphase (0 Gy) and 4.36 SCE/ metaphase (1 Gy) (Figure 4A).

To further define a role for DNA-PKcs in the generation of bystander signals, additional transfer experiments were performed using a congenic mouse model recently created in our laboratory (manuscript in preparation). B6.C-*Prkdc*^{BALB} mice have a C57BL/6 wild type genetic background with the BALB/c variant allele of the *Prkdc* gene, while C.B6-*Prkdc* mice have a BALB/c genetic background with the C57BL/6 wild type *Prkdc* gene. Consistent with our C57BL/6 results, SCE frequencies were significantly increased when irradiated C.B6 donor cells (wild type *Prkdc*) were added to the 5C HDF recipient cells; 3.88 SCE/ metaphase (0Gy) and 5.19 SCE/ metaphase (1Gy) (Figure 4A). SCE frequencies were also evaluated in 5C HDF recipient cells using the B6.C strain

(*Prkdc^{BALB}*) as the irradiated donor cells. Consistent with our BALB/c results, no significant increase in SCE frequency was observed; 4.29 SCE/ metaphase (0 Gy) and

A.



B.

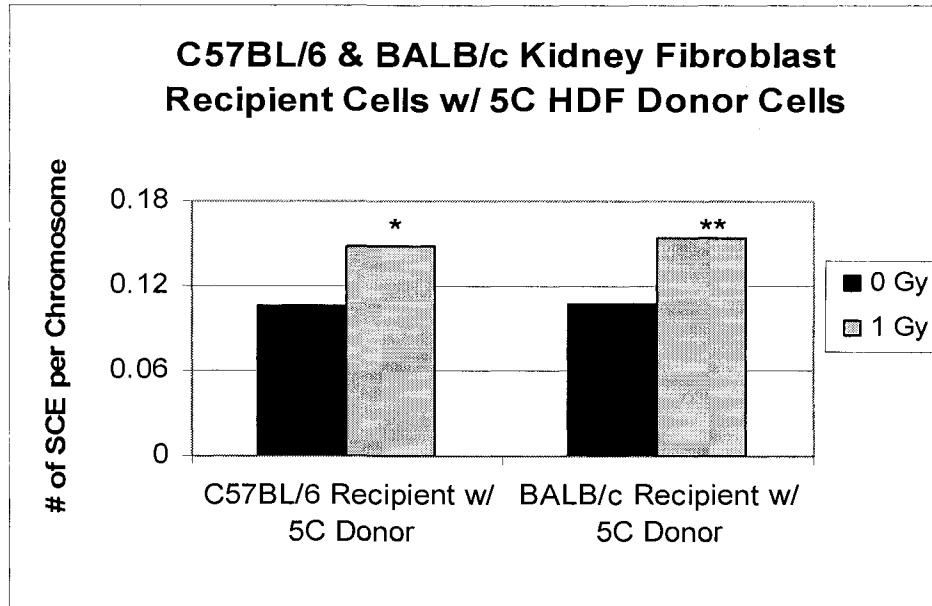


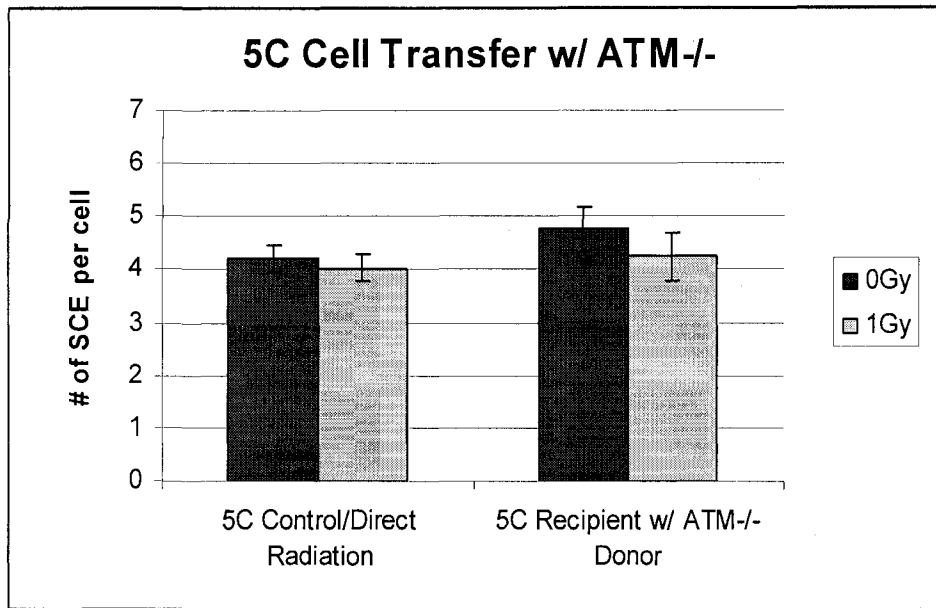
Figure 4A. Role of DNA-PKcs in generation, but not reception of bystander signals. Gamma-ray irradiation of both mouse C57BL/6 and congenic C.B6 (wild type *Prkdc*) cells produced a significant increase in SCE frequencies in bystander cells (5C HDF), while BALB/c and B6.C (*Prkdc^{BALB}*) did not. **B.** Reverse experiments demonstrate that DNA-PKcs is not necessary for the receipt of bystander signals. Both C57BL/6 and

BALB/c show significant increase in SCE when irradiated 5C HDF are added. (* \geq 95% confidence, ** \geq 99% confidence).

4.13 SCE/ metaphase (1 Gy). Our results utilizing these unique congenic mouse strains add additional mechanistic support for DNA-PKcs being involved in generation of bystander signals.

Reverse experiments were also performed in which irradiated or non-irradiated 5C HDF's were added to non-irradiated mouse cells. Both the recipient C57BL/6 and BALB/c mouse cells displayed significant increases in SCE frequencies after the addition of irradiated human donor cells (5C HDF). The C57BL/6 mouse cells displayed a SCE frequency of 0.106 SCE/chromosome (0 Gy) and 0.148 SCE/ chromosome (1 Gy) (Figure 4B). The BALB/c mouse cells displayed frequencies of 0.108 SCE/chromosome (0 Gy) and 0.154 SCE/chromosome (1 Gy) (Figure 4B). Note that SCE frequencies for mouse cells were calculated on a per chromosome basis as they do not have stable karyotypes (aneuploid). The somewhat lower number of mouse metaphases analyzed for SCE reflects the difficulty these cells seemed to experience in co-culture with human cells. However, results are statistically significant and represent a significant number of chromosomes scored. Others have also reported similar results in that DNA-PK is not necessary for the reception of the bystander signal (Mothersill *et al.* 2004; Kanasugi *et al.* 2007). Taken together, our results demonstrate that while DNA-PKcs is needed for the generation of bystander signals, it is not necessary for the receipt of such signals.

A.



B.

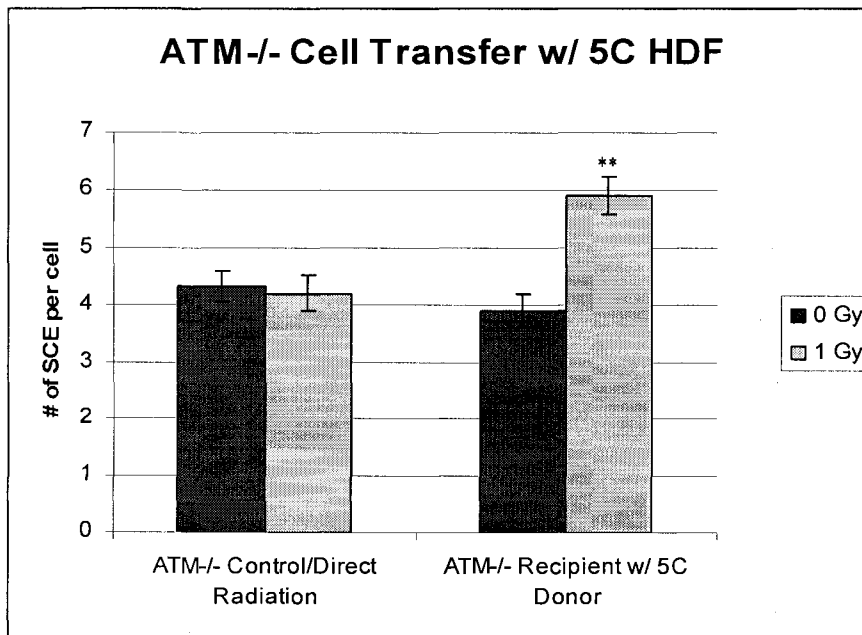


Figure 5A. Role of ATM in generation, but not reception of bystander signals. No increase in SCE frequency was observed following direct irradiation of 5C human fibroblasts. Irradiated donor ATM^{-/-} cells added to non-irradiated 5C HDF recipient cells, produced no significant change in SCE frequency. **B.** The reverse experiment revealed a significant increase in SCE in non-irradiated ATM^{-/-} (recipients) when irradiated 5C HDF donor cells were added, while no significant change was seen in the direct irradiation of ATM^{-/-} human fibroblasts. (* ≥ 95% confidence, ** ≥ 99% confidence).

Our focus then turned to ATM, another DNA repair and signaling protein in the same PI3K family as DNA-PKcs. A human dermal fibroblast line (AG04450) derived from an Ataxia Telangectasia patient was used to determine if ATM also plays a role in the bystander response. Similar to other 5C HDF controls, the 5C HDF cells did not show an increase in SCE frequency when directly exposed to γ -radiation; 4.2 SCE/ metaphase (0 Gy) and 4.03 SCE/ metaphase (1 Gy) (Figure 5A). There was also no significant increase in SCE frequency when ATM^{-/-} donor cells were irradiated and added to the non-irradiated 5C HDF recipient cells; 4.76 SCE/ metaphase (0 Gy) and 4.24 SCE/ metaphase (1 Gy) (Figure 5A). The reverse experiment, adding irradiated 5C HDF donor cells to ATM^{-/-} non-irradiated recipient cells, revealed a highly significant increase in SCE frequencies; 3.9 SCE/ metaphase (0 Gy) and 5.92 SCE/ metaphase (1 Gy) (Figure 5B). Like the 5C HDF, directly irradiated ATM^{-/-} human fibroblasts did not show a change in SCE frequency; 4.34 SCE/ metaphase (0 Gy) and 4.22 SCE/ metaphase (1 Gy) (Figure 5B). These data suggest that ATM, like DNA-PKcs, is necessary for generation of the bystander signal, but is not required for receiving such signals. Note all numbers are organized in Tables 1 (Figures 2 and 3) and 2 (Figures 4 and 5) demonstrating averages and statistical significance.

Summary Table for Figures 2 & 3

Cell Sample	Mean Frequency/Cell		p-value		Cells Scored	
	0Gy	1Gy			0Gy	1Gy
Figure 2:						
<u>5C HDF</u>						
Control	3.76	3.4	.532	NS	25	25
1:100	3.14	5.28	.0054	**	21	25
1:1000	3.68	5.48	.0018	**	25	25
Figure 3:						
<u>5C HDF</u>						
Control	4.2	4.03	.641	NS	40	40
0Gy Recipients (1:100)	3.9	5.03	.009	*	40	40
1Gy Recipients (1:100)	4.08	3.88	.614	NS	25	50

NS: Not significant
***: >95% confidence level**
****>99% confidence level**

Table 1. Summary of figures 2 and 3 SCE frequencies and statistical outcomes for all cell transfer experiments. (* \geq 95% confidence, ** \geq 99% confidence).

Summary Table for Figures 4 & 5

Cell Sample	Mean Frequency/Cell		p-value		Cells Scored	
	0Gy	1Gy			0Gy	1Gy
Figure 4:						
5C HDF with C57BL/6 MPF	3.72	5.33	.0001	**	50	30
5C HDF with BALB/c MPF	3.7	3.86	.6085	NS	70	78
5C HDF with SCID MPF	4.18	4.36	.6325	NS	50	50
5C HDF with C.B6 MPF	3.88	5.19	.0002	*	50	67
5C HDF with B6.C MPF	4.29	4.13	.5904	NS	65	76
C57BL/6 with 5C ^a	0.106	0.148	< 0.05	*	20	10
BALB/c with 5C ^a	0.108	0.154	< 0.005	**	30	20
Figure 5:						
ATM ^{-/-} HDF Control	4.34	4.22	.7568	NS	50	50
5C HDF with AT	4.76	4.24	.412	NS	50	50
AT ^{-/-} HDF with 5C HDF	3.9	5.92	.0018	**	25	25

NS: Not significant
 *: >95% confidence level
 **: >99% confidence level
^a: SCE/chromosome

Table 2. Summary of figures 4 and 5 SCE frequencies and statistical outcomes for all cell transfer experiments. (* \geq 95% confidence, ** \geq 99% confidence).

Discussion

DNA-PKcs and ATM are members of the PI3K family and each participates in multiple cellular processes. DNA-PKcs, the catalytic subunit of DNA-PK, orchestrates NHEJ in response to DSBs. It is also critical in V(D)J recombination, and is essential for effective mammalian telomeric end-capping function (Bailey *et al.* 1999; Ma *et al.* 2002; Meek *et al.* 2004; Dudley *et al.* 2005; Weinstock *et al.* 2006; Zhang *et al.* 2007).

Activation of ATM is an early event in response to IR-induced DSBs, and once activated ATM mediates downstream damage response pathways that include DNA repair, cell-cycle control, and apoptosis (Lavin and Kozlov 2007). ATM is reported to play a role in telomere maintenance as well (Kolomietz *et al.* 2002; Denchi and de Lange 2007). In addition to DNA-PKcs and ATM's well-established roles in repair and intra-cellular signaling, (Nagasawa *et al.* 2003; Collis *et al.* 2005; Nagasawa *et al.* 2005; Lavin and Kozlov 2007), our findings indicate a role for these proteins in inter-cellular signaling of the radiation-induced BSE.

We designed a cell transfer strategy that enables us to differentiate between the generation versus the reception of bystander signals. In our system, donor cells are irradiated (1 Gy γ -rays) and seeded at a very low concentration (1:100 or 1:1000) onto non-irradiated normal human fibroblast recipient cells. Using a low concentration of donor cells and ensuring that recipient cells were at low confluency, we reduced and/or eliminated any possibility of a bystander response transmitted via gap junctions. We then measured SCE frequencies in the normal human fibroblast recipient cells as an indicator of IR-induced BSE.

To validate our approach, we tested normal human fibroblasts (5C HDF) as both the donor and recipient cells to be assured that they were able to both generate and receive a bystander signal. Cultures were at low-passage (non-transformed) to circumvent any problem of decreased BSE with increasing passage. When directly irradiated, 5C HDFs do not display an increase in SCE frequency, in agreement with previous reports showing that direct low-LET IR does not influence SCE levels (Ardito *et al.* 1980). Our cell transfer strategy also demonstrated that 5C HDFs can generate a bystander signal, inducing significant increases in SCE frequencies in recipient cells. The observation that the irradiated donor cells at both dilutions were able to increase SCE levels in the non-irradiated recipient cells by approximately the same amount is consistent with previous data suggesting that the BSE operates through an “on/off” switch-like mechanism (Lehnert *et al.* 1997).

The data demonstrating that directly irradiated cells do not display elevated SCE frequencies suggest that directly irradiated cells are themselves refractory to bystander signals. To test this, we used our cell transfer assay to again show that directly irradiated cells do not show elevated levels of SCE (Figure 3A). Also in agreement with our other results, we show that by seeding irradiated donor cells with non-irradiated recipient cells, an elevation in SCE frequency in the non-irradiated recipient cells occurs (Figure 3A). However, when the reverse is done and *recipient* cells are irradiated (1 Gy γ -rays) before irradiated donor cells are added, there is no elevation in SCE frequency observed in the recipient population. This supports the hypothesis that once irradiated, “hit” cells become refractory to either *receiving* or responding to a bystander signal.

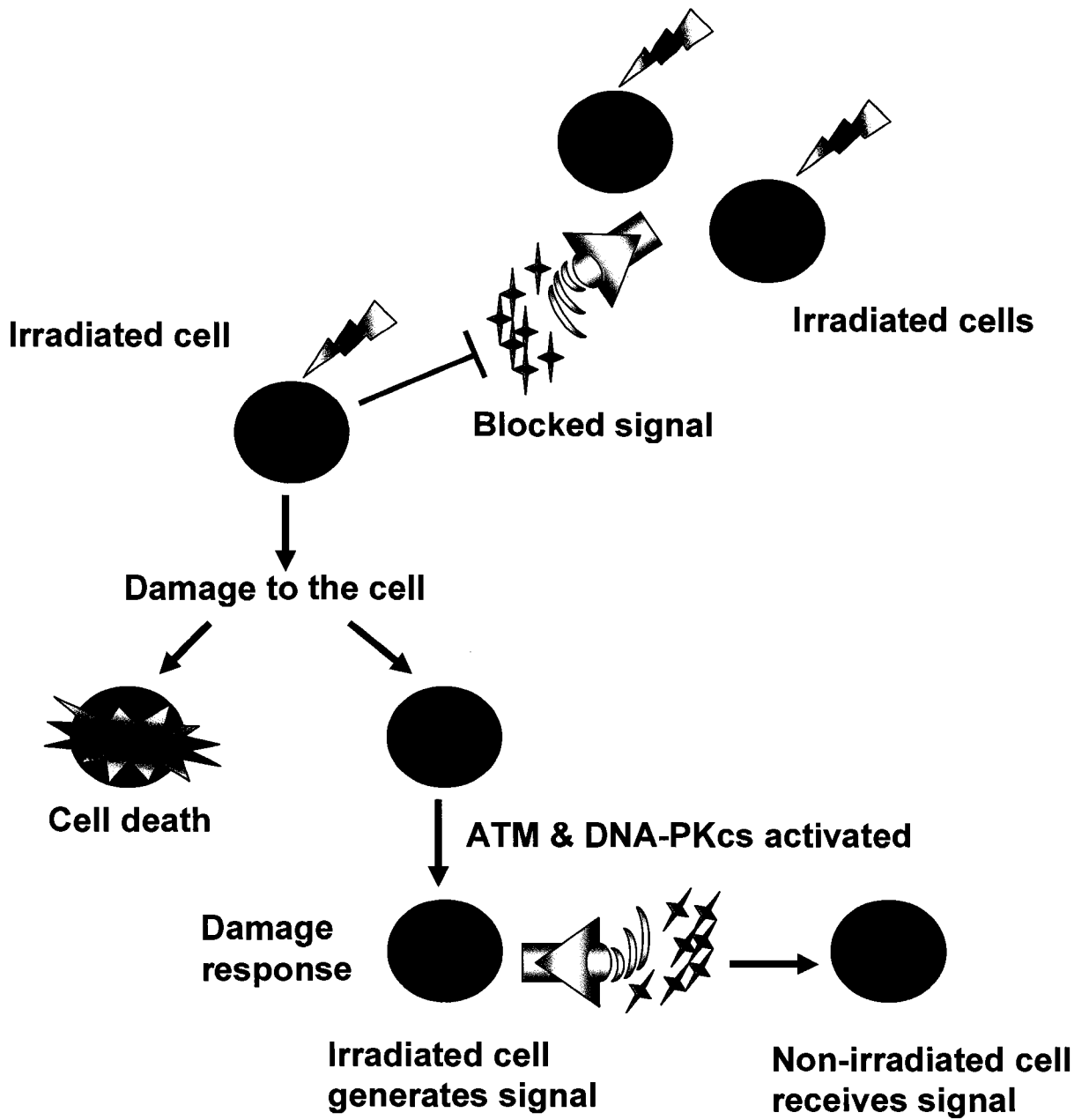


Figure 6. Proposed model for the function of DNA-PKcs and ATM in the generation of radiation-induced bystander signals.

We sought to determine whether the repair protein DNA-PKcs plays a role in the BSE. The BALB/c mouse strain contains two single nucleotide polymorphisms in the *Prkdc* gene, which produces a hypomorphic version of DNA-PKcs (Yu *et al.* 2001). We compared the wild type C57BL/6 mouse strain to the BALB/c strain for the ability to generate and/or receive bystander signals. Our results show that wild type C57BL/6 mouse cells are able to generate a bystander signal in response to IR. The irradiated C57BL/6 donor cells increased SCE frequency in the 5C HDF recipient cells by over 40% compared to the 0 Gy controls when seeded at a 1:100 dilution (Figure 4A). Similar results were observed when the C57BL/6 donor cells were seeded at 1:1000 (supplementary data). However, irradiated BALB/c donor cells were not able to influence SCE frequencies in the 5C HDF recipient cells, demonstrating that DNA-PKcs-deficient BALB/c mouse cells are unable to generate a bystander signal following γ -ray exposure. The reverse experiments revealed that DNA-PKcs is not necessary for receipt of and response to bystander signals (Figure 4B). We conclude that DNA-PKcs is necessary for the generation, but not the reception, of bystander signals.

To confirm that DNA-PKcs deficiency, rather than a coincidental mutation in BALB/c mice, is responsible for abolishing the bystander response, we utilized congenic mouse strains generated in our laboratory. The B6.C-*Prkdc*^{BALB} strain has a C57BL/6 background with the BALB/c variant of the *Prkdc* gene, while the C.B6-*Prkdc* has the BALB/c background with the C57BL/6 *Prkdc* gene. Interestingly, the C.B6-*Prkdc* showed a significant increase in SCE frequency, thus was able to generate a bystander response; however, the B6.C-*Prkdc*^{BALB} was not able to significantly influence SCE

levels. These results provide additional support for DNA-PKcs playing a critical role in generation of a bystander response.

Next we examined the role of the closely related protein ATM, in generating and/or receiving bystander signals. Again, we found no significant increase in SCE frequencies following direct irradiation of human ATM^{-/-} cells. By irradiating ATM^{-/-} cells (donors) and using our cell transfer approach, we found no significant increase in SCE frequencies in the 5C HDF recipient cells. However, when the reverse cell transfer was performed, the irradiated 5C HDF donor cells were in fact able to generate a response in the ATM^{-/-} cells, implying that ATM^{-/-} recipient cells can receive and respond to a bystander signal, but they cannot generate one. Therefore, like DNA-PKcs, ATM is necessary for the generation, but not the reception of bystander signals.

The role of DNA repair proteins in the generation of bystander signals may involve DNA-PKcs and ATM's capabilities as DNA damage sensors in signaling pathways. Such a damage response may initiate as yet undefined pathways that ultimately lead to the generation of a BSE in non-irradiated cells, and hints at a tissue-level response to radiation injury moderated by some of the same proteins that orchestrate the inter-cellular response to DNA damage. While an intra-cellular IR-induced signaling response has been demonstrated (Saretzki *et al.* 1999), it has also been shown that ATM and DNA-PKcs signaling activates NF- κ B via the p53-independent MEK/ERK/p90rsk/IKK signaling pathway in an anti-apoptotic response to DNA damage (Panta *et al.* 2004). In addition, DNA-PKcs is required for the activation of the stress kinases SAPK/JNK (Fritz and Kaina 2006). It has also been shown that DNA-PKcs activation can be induced by exposure to nitric oxide (Smith *et al.* 2003), which has been suggested as a possible

bystander signal. Taken together, these data support the idea that ATM and DNA-PKcs may regulate, or be regulated by, other kinds of signaling events, such as the BSE (Figure 6). This model suggests that the BSE is an active process in response to IR exposure, rather than a passive response to DNA damage.

While this model is currently speculative, our data do suggest previously unrecognized roles for the repair proteins DNA-PKcs and ATM in generation, but not receipt, of bystander signals. It should be noted that a previous study concluded that DNA repair proteins were not involved in generation of the bystander signal (Mothersill *et al.* 2004). Our conflicting results may reflect differences in experimental design including: cells used (primary fibroblasts versus various cell lines), endpoints examined (SCE versus clonogenic survival), and methods used (cell transfer versus media transfer). For example, the media transfer experiments limit the role of short-lived ROS, whereas in our cell transfer approach, the likelihood for continued ROS generation and interaction remains.

A better understanding of the underlying pathways involved in bystander signal generation and reception is an essential step to better understanding of the BSE. Moreover, because predominately low biologically/environmentally relevant doses of radiation elicit a bystander response (Nagasawa and Little 1992; Seymour and Mothersill 2000; Nagar *et al.* 2003), increased knowledge about this phenomena holds important implications for individual radiosensitivity and susceptibility to radiation carcinogenesis caused by inadequate DNA repair capacity, a condition relevant to human populations and health.

Some degree of exposure to radiation above the natural background level is an unavoidable consequence of living in the modern world. A better understanding of the radiation-induced BSE and its influence on radiation carcinogenesis will aid regulators as they seek to protect human health while avoiding undue economic hardship.

Acknowledgements. The authors would like to thank Dakim Gaines for technical assistance. Support for this research is gratefully acknowledged from the NIH/NCI, grants CA-09236-30 (RLU) and CA-043322-20 (RLU and SMB), the U.S. Department of Energy (DOE), grant DE-FG02-01ER63239 (RLU and SMB), and from the National Aeronautics and Space Administration (NASA), grant NNJ04HD83G (SMB).

References

- Ardito, G, Lamberti L, Piccotti F and Poggio G (1980). *Analysis of chromosome aberrations after exposure to ionizing radiation in "in vitro" cultures of human lymphocytes by means of BrdU incorporation* Boll Soc Ital Biol Sper 56(7): 719-24.
- Azzam, EI, de Toledo SM, Gooding T and Little JB (1998). *Intercellular communication is involved in the bystander regulation of gene expression in human cells exposed to very low fluences of alpha particles* Radiat Res 150(5): 497-504.
- Azzam, EI, de Toledo SM and Little JB (2001). *Direct evidence for the participation of gap junction-mediated intercellular communication in the transmission of damage signals from alpha -particle irradiated to nonirradiated cells* Proc Natl Acad Sci U S A 98(2): 473-8.
- Bailey, SM, Brenneman MA, Halbrook J, Nickoloff JA, Ullrich RL and Goodwin EH (2004). *The kinase activity of DNA-PK is required to protect mammalian telomeres* DNA Repair (Amst) 3(3): 225-33.
- Bailey, SM, Cornforth MN, Kurimasa A, Chen DJ and Goodwin EH (2001). *Strand-specific postreplicative processing of mammalian telomeres* Science 293(5539): 2462-5.
- Bailey, SM, Meyne J, Chen DJ, Kurimasa A, Li GC, Lehnert BE and Goodwin EH (1999). *DNA double-strand break repair proteins are required to cap the ends of mammalian chromosomes* Proc Natl Acad Sci U S A 96(26): 14899-904.
- Banaz-Yasar, F, Lennartz K, Winterhager E and Gellhaus A (2007). *Radiation-induced bystander effects in malignant trophoblast cells are independent from gap junctional communication* J Cell Biochem.
- Barzilai, A, Rotman G and Shiloh Y (2002). *ATM deficiency and oxidative stress: a new dimension of defective response to DNA damage* DNA Repair (Amst) 1(1): 3-25.
- Blunt, T, Gell D, Fox M, Taccioli GE, Lehmann AR, Jackson SP and Jeggo PA (1996). *Identification of a nonsense mutation in the carboxyl-terminal region of DNA-dependent protein kinase catalytic subunit in the scid mouse* Proc Natl Acad Sci U S A 93(19): 10285-90.
- Collis, SJ, DeWeese TL, Jeggo PA and Parker AR (2005). *The life and death of DNA-PK* Oncogene 24(6): 949-61.
- Denchi, EL and de Lange T (2007). *Protection of telomeres through independent control of ATM and ATR by TRF2 and POT1* Nature.
- Dudley, DD, Chaudhuri J, Bassing CH and Alt FW (2005). *Mechanism and control of V(D)J recombination versus class switch recombination: similarities and differences* Adv Immunol 86: 43-112.
- Fritz, G and Kaina B (2006). *Late activation of stress kinases (SAPK/JNK) by genotoxins requires the DNA repair proteins DNA-PKcs and CSB* Mol Biol Cell 17(2): 851-61.
- Grifalconi, M, Celotti L and Mognato M (2007). *Bystander response in human lymphoblastoid TK6 cells* Mutat Res 625(1-2): 102-11.
- Hu, B, Wu L, Han W, Zhang L, Chen S, Xu A, Hei TK and Yu Z (2006). *The time and spatial effects of bystander response in mammalian cells induced by low dose radiation* Carcinogenesis 27(2): 245-51.

- Iyer, R and Lehnert BE (2002). *Alpha-particle-induced increases in the radioresistance of normal human bystander cells* Radiat Res 157(1): 3-7.
- Jeggo, PA, Taccioli GE and Jackson SP (1995). *Menage a trois: double strand break repair, V(D)J recombination and DNA-PK* Bioessays 17(11): 949-57.
- Kanasugi, Y, Hamada N, Wada S, Funayama T, Sakashita T, Kakizaki T, Kobayashi Y and Takakura K (2007). *Role of DNA-PKcs in the bystander effect after low- or high-LET irradiation* Int J Radiat Biol 83(2): 73-80.
- Kashino, G, Prise KM, Suzuki K, Matsuda N, Kodama S, Suzuki M, Nagata K, Kinashi Y, Masunaga S, Ono K and Watanabe M (2007). *Effective suppression of bystander effects by DMSO treatment of irradiated CHO cells* J Radiat Res (Tokyo) 48(4): 327-33.
- Kolomietz, E, Meyn MS, Pandita A and Squire JA (2002). *The role of Alu repeat clusters as mediators of recurrent chromosomal aberrations in tumors* Genes Chromosomes Cancer 35(2): 97-112.
- Lavin, MF and Kozlov S (2007). *ATM activation and DNA damage response* Cell Cycle 6(8): 931-42.
- Lehnert, BE, Goodwin EH and Deshpande A (1997). *Extracellular factor(s) following exposure to alpha particles can cause sister chromatid exchanges in normal human cells* Cancer Res 57(11): 2164-71.
- M'Kacher, R, Bennaceur-Griscelli A, Girinsky T, Koscielny S, Delhommeau F, Dossou J, Violot D, Leclercq E, Courtier MH, Beron-Gaillard N, Assaf E, Ribrag V, Bourhis J, Feneux D, Bernheim A, Parmentier C and Carde P (2007). *Telomere shortening and associated chromosomal instability in peripheral blood lymphocytes of patients with Hodgkin's lymphoma prior to any treatment are predictive of second cancers* Int J Radiat Oncol Biol Phys 68(2): 465-71.
- Ma, Y, Pannicke U, Schwarz K and Lieber MR (2002). *Hairpin opening and overhang processing by an Artemis/DNA-dependent protein kinase complex in nonhomologous end joining and V(D)J recombination* Cell 108(6): 781-94.
- Meek, K, Gupta S, Ramsden DA and Lees-Miller SP (2004). *The DNA-dependent protein kinase: the director at the end* Immunol Rev 200: 132-41.
- Mothersill, C and Seymour CB (1998). *Cell-cell contact during gamma irradiation is not required to induce a bystander effect in normal human keratinocytes: evidence for release during irradiation of a signal controlling survival into the medium* Radiat Res 149(3): 256-62.
- Mothersill, C, Seymour RJ and Seymour CB (2004). *Bystander effects in repair-deficient cell lines* Radiat Res 161(3): 256-63.
- Nagar, S, Smith LE and Morgan WF (2003). *Characterization of a novel epigenetic effect of ionizing radiation: the death-inducing effect* Cancer Res 63(2): 324-8.
- Nagasawa, H, Huo L and Little JB (2003). *Increased bystander mutagenic effect in DNA double-strand break repair-deficient mammalian cells* Int J Radiat Biol 79(1): 35-41.
- Nagasawa, H and Little JB (1992). *Induction of sister chromatid exchanges by extremely low doses of alpha-particles* Cancer Res 52(22): 6394-6.
- Nagasawa, H and Little JB (2002). *Bystander effect for chromosomal aberrations induced in wild-type and repair deficient CHO cells by low fluences of alpha particles* Mutat Res 508(1-2): 121-9.

- Nagasawa, H, Peng Y, Wilson PF, Lio YC, Chen DJ, Bedford JS and Little JB (2005). *Role of homologous recombination in the alpha-particle-induced bystander effect for sister chromatid exchanges and chromosomal aberrations* Radiat Res 164(2): 141-7.
- O'Neill-Mehlenbacher, A, Kilemade M, Elliott A, Mothersill C and Seymour C (2007). *Comparison of direct and bystander effects induced by ionizing radiation in eight fish cell lines* Int J Radiat Biol 83(9): 593-602.
- Okayasu, R, Suetomi K, Yu Y, Silver A, Bedford JS, Cox R and Ullrich RL (2000). *A deficiency in DNA repair and DNA-PKcs expression in the radiosensitive BALB/c mouse* Cancer Res 60(16): 4342-5.
- Panta, GR, Kaur S, Cavin LG, Cortes ML, Mercurio F, Lothstein L, Sweatman TW, Israel M and Arsura M (2004). *ATM and the catalytic subunit of DNA-dependent protein kinase activate NF-kappaB through a common MEK/extracellular signal-regulated kinase/p90(rsk) signaling pathway in response to distinct forms of DNA damage* Mol Cell Biol 24(5): 1823-35.
- Perry, P and Wolff S (1974). *New Giemsa method for the differential staining of sister chromatids* Nature 251(5471): 156-8.
- Saretzki, G, Sitte N, Merkel U, Wurm RE and von Zglinicki T (1999). *Telomere shortening triggers a p53-dependent cell cycle arrest via accumulation of G-rich single stranded DNA fragments* Oncogene 18(37): 5148-58.
- Seymour, CB and Mothersill C (2000). *Relative contribution of bystander and targeted cell killing to the low-dose region of the radiation dose-response curve* Radiat Res 153(5 Pt 1): 508-11.
- Shao, C, Lyng FM, Folkard M and Prise KM (2006). *Calcium fluxes modulate the radiation-induced bystander responses in targeted glioma and fibroblast cells* Radiat Res 166(3): 479-87.
- Smith, TR, Levine EA, Perrier ND, Miller MS, Freimanis RI, Lohman K, Case LD, Xu J, Mohrenweiser HW and Hu JJ (2003). *DNA-repair genetic polymorphisms and breast cancer risk* Cancer Epidemiol Biomarkers Prev 12(11 Pt 1): 1200-4.
- Weil, MM, Brown BW and Serachitopol DM (1997). *Genotype selection to rapidly breed congenic strains* Genetics 146(3): 1061-9.
- Weinstock, DM, Nakanishi K, Helgadottir HR and Jasin M (2006). *Assaying double-strand break repair pathway choice in mammalian cells using a targeted endonuclease or the RAG recombinase* Methods Enzymol 409: 524-40.
- Yang, H, Anzenberg V and Held KD (2007). *The time dependence of bystander responses induced by iron-ion radiation in normal human skin fibroblasts* Radiat Res 168(3): 292-8.
- Yu, Y, Okayasu R, Weil MM, Silver A, McCarthy M, Zabriskie R, Long S, Cox R and Ullrich RL (2001). *Elevated breast cancer risk in irradiated BALB/c mice associates with unique functional polymorphism of the Prkdc (DNA-dependent protein kinase catalytic subunit) gene* Cancer Res 61(5): 1820-4.
- Zhang, Y, Zhou J, Cao X, Zhang Q, Lim CU, Ullrich RL, Bailey SM and Liber HL (2007). *Partial deficiency of DNA-PKcs increases ionizing radiation-induced mutagenesis and telomere instability in human cells* Cancer Lett 250(1): 63-73.

Chapter 6

Mouse Embryonic Fibroblasts Fail to Generate a Radiation-Induced Bystander Response

Mouse Embryonic Fibroblasts Fail to Generate a Radiation-Induced Bystander Response.

Abby J. Williams, R. Tanner Hagelstrom, Robert L. Ullrich, Susan M. Bailey and Kristin F. Askin*.

Department of Environmental and Radiological Health Sciences, Colorado State University, Fort Collins, CO 80523

*To whom all correspondence should be addressed.

E-mail: askink@mail.nih.gov

Phone: (301) 402-3789

Abstract

The bystander effect (BSE) is the process by which directly irradiated cells communicate with and impose an effect on neighboring non-irradiated cells. Despite strenuous efforts to elucidate the mechanism, much is still unknown about the BSE, including specifics on bystander signals, pathways and the purpose of the bystander effect. To complicate matters, it has been shown that a variety of primary cells and established cell lines can be either capable or incapable of producing a bystander effect. Here, we extend the study of the BSE by comparing mouse primary fibroblasts versus mouse embryonic fibroblasts (MEFs). We designed a cell transfer method in which γ -irradiated adult mouse fibroblasts or MEFs (donors) are co-cultured with unirradiated normal human fibroblasts (recipients). Sister chromatid exchange (SCE) frequencies were evaluated in the human cells as a marker of the BSE. Our results show that adult mouse fibroblasts are capable of producing a BSE, whereas MEFs of the same genotype are unable to generate a bystander signal. This is the first report that MEFs are incapable of producing a bystander signal.

Introduction

Ionizing radiation (IR) is a well known carcinogen and teratogen that directly interacts with DNA to produce multiple forms of damage including base damage, single-strand breaks (SSBs) and double-strand breaks (DSBs), which can lead to initiation of cellular transformation (Yokoya *et al.*, 2002; Collis *et al.*, 2005; Purkayastha *et al.*, 2006; Purkayastha *et al.*, 2008). Non-targeted effects of IR such as the bystander effect (BSE), have also been examined over the past few decades and have greatly impacted the field of radiation biology (Nagasawa and Little 1992; Mothersill and Seymour 1997; Ponnaiya *et al.*, 1997; Iyer and Lehnert 2002; Kovalchuk and Baulch 2008). The impact these secondary effects have in biological systems is currently unknown. Some would suggest that these effects are another mechanism by which radiation is detrimental to the cell and can potentially lead to carcinogenesis. This would indeed make sense, specifically if one considers the end-points used to study the BSE, i.e. clonogenic survival, micronuclei, apoptosis, etc. Another possibility is that these effects may have some benefit for the biological system as a whole (Prise 2003), such as promoting death of damaged cells and/or cells surrounding the area of insult to avoid possible future problems.

The BSE occurs when a directly irradiated cell imposes an effect on a non-irradiated cell, which can be measured by a variety of endpoints including SCE frequency, micronuclei formation, clonogenic survival, and apoptosis (Nagasawa *et al.*, 2005; Grifalconi *et al.*, 2007; O'Neill-Mehlenbacher *et al.*, 2007; Yang *et al.*, 2007). Currently, two models are accepted as mechanisms for bystander signaling. One requires cell-to-cell contact and utilizes gap junctions as a means to transport intercellular signals (Azzam *et al.*, 1998; Azzam *et al.*, 2001). Media transfer experiments suggest another

possibility in which signals are released from irradiated cells and are free-flowing in the media and able to interact with non-irradiated cells (Lehnert *et al.*, 1997; Mothersill and Seymour 1998). Proposed BSE factors consist of reactive oxygen species (ROS), nitric oxygen species (NOS), and cytokines (Shao *et al.*, 2003; Kashino *et al.*, 2007; Shao *et al.*, 2008). These observations suggest that the target for radiation response is likely greater than the actual volume of cells or tissues directly hit by IR and thus warrant further study.

Previous work has shown that not all cell types can generate a bystander response and that not all cell types respond to a bystander signal (Mothersill and Seymour 1997; Mothersill *et al.*, 2001; Nagar *et al.*, 2003). For example, Chinese hamster ovary (CHO) cells deficient in the homologous recombination (HR) proteins Rad51C, Rad51D, XRCC2, XRCC3 and BRCA2 were incapable of producing a bystander effect (Nagasawa *et al.*, 2008). In addition, we have previously shown that the DNA repair proteins DNA-PKcs and ATM are necessary to produce a bystander signal, but not receive one (Hagelstrom *et al.*, 2008). Here, we used a cell transfer method involving normal human cells, mouse primary kidney/dermal fibroblasts and mouse embryonic fibroblasts (MEFs). SCE frequencies were measured in the non-irradiated human cells to evaluate the generation of a bystander response from irradiated murine cells.

This study utilized a cell transfer method that allows for the co-culture of directly irradiated MEFs or corresponding primary “adult” mouse cells (donors) with non-irradiated normal human fibroblasts (recipients). Control or irradiated primary mouse fibroblasts (dermal or kidney) were plated at a 1:100 dilution with 5C normal human fibroblasts. The cell mixture was then cultured for 2 population doublings in the presence of 5'-bromo-2'-deoxyuridine (BrdU; Sigma) and then analyzed for SCE

frequency as a measure of the BSE. Despite genotypic diversity in the MEFs used, none were capable of influencing SCE levels in normal human fibroblast recipients, while their corresponding primary adult mouse cells were effective in producing a significant bystander response in normal human fibroblasts, as seen by increased SCE.

Materials and Methods

Cell Lines and Cell Culture. Kidney tissue from 8–12 week old female C57BL/6 (Jackson Laboratories) and CF-1 (Charles River Laboratories) mice were minced, and digested in 199 medium containing collagenase (Worthington Type III; 200 units/ml) at 37°C for 3–5 h with gentle agitation. Disaggregated cells were washed 6x in phosphate buffered saline (PBS) containing 0.5% fetal bovine serum (FBS) and cultured in α -MEM medium (15% FBS, penicillin/streptomycin). Media was changed after 3 days of incubation.

Adult Artemis +/+ and Artemis -/- (129SvEvTac/C57BL/6 background) mouse tail snips and corresponding MEFs were provided by Dr. JoAnn Sekiguchi (Rooney *et al.*, 2002). Tails were minced, placed into media and grown for two weeks before passaging. Artemis +/+ and Artemis -/- MEFs and low passage neonatal Human Dermal Fibroblasts (HDF C-004-5C; Cascade Biologics) were grown in α -MEM supplemented with 10% fetal bovine serum and antibiotics. The 5C HDF cells were counted using a Coulter Counter (Coulter Beckman, Fullerton, CA) and 4×10^5 human fibroblasts were plated into T-75 flasks, then co-cultured with 1:100 dilutions of either 0 Gy or 1 Gy γ -irradiated, exponentially growing mouse donor cells. Donor cells included wild-type MEF C57BL/6 (ATCC, #SCRC-1008; (Smiraldo *et al.*, 2005)), C57BL/6 primary kidney

fibroblasts, Artemis+/+ & Artemis -/- primary dermal fibroblasts (Rooney *et al.*, 2002), Artemis+/+ & Artemis -/-MEF (Rooney *et al.*, 2002), CF-1 primary kidney fibroblasts, and CF-1 MEFs (ATCC, SCRC #1040).

Irradiations were performed using a sealed-source Mark I ¹³⁷Cs γ -irradiator (J.L. Shepherd and Associates). 5'-bromo-2'-deoxyuridine (BrdU; Sigma) was added to cultures at a final concentration of 2×10^{-5} M and cells were allowed to grow for two rounds of cell division. Colcemid (Gibco) was added at a final concentration of 0.2 μ g/ml and cells were harvested approximately 2-3 hours later. Cells were trypsinized, centrifuged, then resuspended in 0.075M KCl for 15 minutes at room temperature and then fixed with 3:1 methanol: acetic acid.

SCE Staining and Analysis. Slides were prepared using standard cytogenetic techniques and then stained via Fluorescence Plus Giemsa (FPG) (Perry and Wolff 1974). Briefly, cells are grown for two replication rounds in the presence of BrdU. Slides are stained with Hoescht dye 33258 for 15 minutes at room temperature, rinsed with distilled water and exposed to UV light at 365nm for 25 minutes. Immediately slides are then soaked in 2x SSC for 30 minutes in a 60°C water bath. Following thorough rinses with distilled water, slides are allowed to air dry, then stained with 5% Giemsa for 10 minutes. Images were analyzed using a Zeiss Axioskop2 Plus microscope with a Photometrics Coolsnap ES2 camera and Metavue 7.1 software.

Statistical Analysis. Twenty five metaphases were scored for genomic SCE per sample and slides were blinded to the viewer. All experiments were performed a minimum of

two times. Error bars represent standard error of the mean (SEM) and a student's T-test was used to calculate statistical significance. Data from independent experiments were pooled if the means of identically treated samples were not significantly different.

Results

We designed a cell transfer approach that utilizes SCE frequencies as a marker of the IR-induced BSE, and importantly facilitates discrimination between the generation versus the reception of bystander signals. Immediately following IR exposure (1 Gy ^{137}Cs γ -rays), mouse irradiated (donor) cells were pelleted and rinsed in PBS to remove any remaining media. The irradiated donor cells were added to human (recipient) cells at low concentration (1:100 dilution) and co-cultured for two rounds of replication in the presence of BrdU. The cells were then harvested and scored for SCE frequency in human cells only.

Consistent with our previous work (Hagelstrom *et al.*, 2008), irradiated adult C57BL/6 mouse cells induced a bystander response in normal human fibroblasts as measured by a significant increase in SCE compared to non-irradiated donor C57BL/6 cells (Figure 1A). SCE frequencies in 5C HDF with adult C57BL/6 primary donor fibroblasts were 4.28 SCE/metaphase (0Gy donor) and 5.76 (1Gy donor), demonstrating a statistically significant increase in SCE levels. In contrast, when normal MEFs derived from C57BL/6 mice (C57MEF and MEF286) were used as the donor cells, no significant increase in SCEs was observed. The frequencies for the C57MEFs were 4.67 SCE/metaphase (0Gy donor) and 4.77 SCE/metaphase (1Gy donor); MEF286 frequencies were 4.38 SCE/metaphase (0Gy donor) and 3.96 SCE/metaphase (1Gy donor) (Figure

1A). Distribution graphs (Figure 1B) illustrate that this is an overall increase, rather than a few cells with many SCE skewing the data.

Figure 1A.

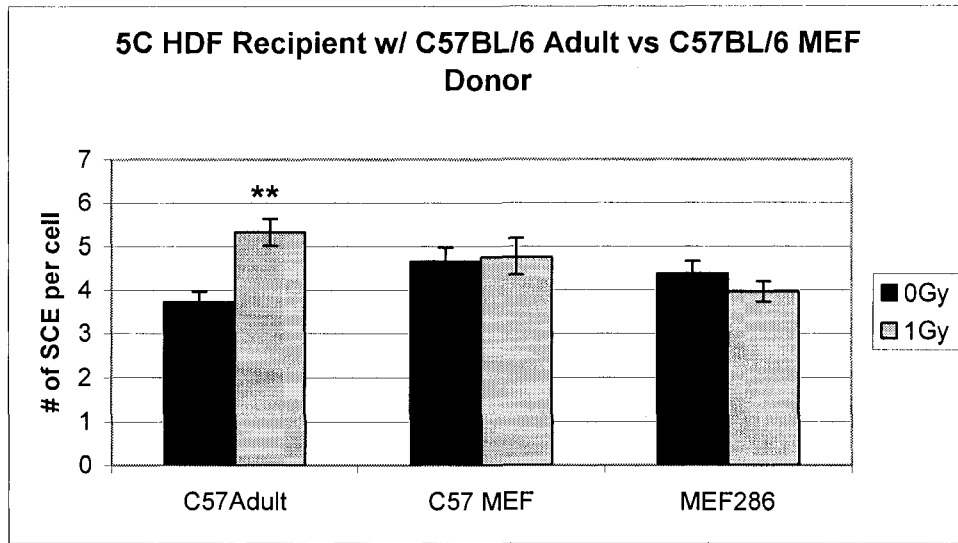


Figure 1B.

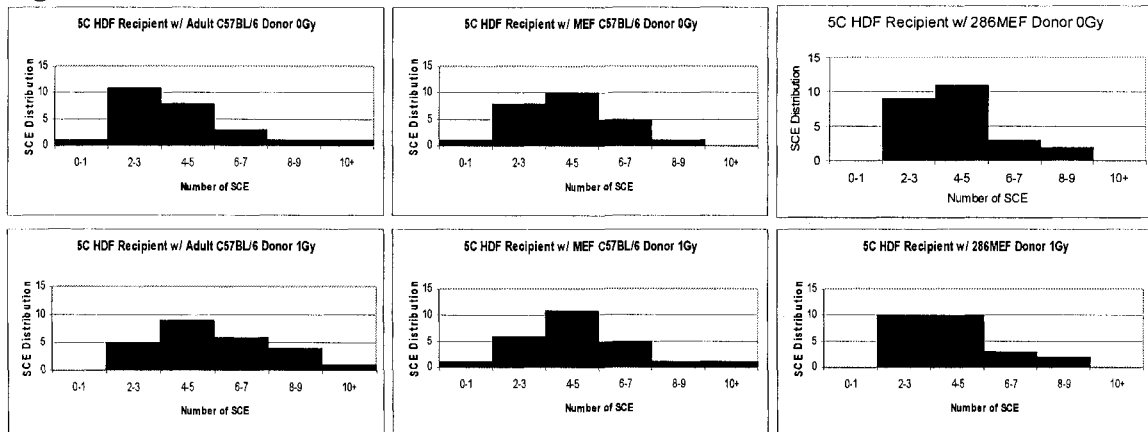


Figure 1. C57BL/6 mouse donor cells added to normal human fibroblast recipient cells. A. A significant increase in SCE is seen in recipient human cells when irradiated adult mouse fibroblasts are the donors, but no effect is seen when MEFs are the donors. B. The distribution of SCE number per metaphase illustrates an overall increase in SCE levels. * $\geq 95\%$ confidence, ** $\geq 99\%$ confidence

To further explore the hypothesis that MEFs are incapable of generating a bystander signal, we compared these results to other sets of mouse cells to determine if only C57BL/6 mouse strain failed or if it is a general phenomenon. Artemis^{+/+} or Artemis^{-/-} adult mouse dermal fibroblasts and their MEF counterparts on a 129SvEvTac/C57BL/6 mixed background were evaluated. Artemis is a DNA repair protein functioning in the NHEJ pathway that has single-strand exonuclease activity as well as endonuclease activity to open hairpin structures (reviewed in (Morio and Kim 2008)). Results demonstrate a significant increase in SCE numbers in normal 5C HDF recipient cells when either Art^{+/+} or Art^{-/-} mouse adult dermal fibroblasts were irradiated and co-cultured (Figure 2A and 2C). The adult Art^{+/+} frequencies were 3.60 SCE/metaphase (0Gy) and 4.86 SCE/metaphase (1Gy), and the adult Art^{-/-} frequencies were 3.64 SCE/metaphase (0Gy) and 4.92 SCE/metaphase (1Gy). Again, the MEFs did not generate a bystander signal; no significant increase in SCEs was observed when irradiated Art^{+/+} or Art^{-/-} MEFs were co-cultured with 5C HDF recipient cells (Figure 2A and 2C). Art^{+/+} MEF frequencies were 4.08 SCE/metaphase (0Gy) and 4.30 SCE/metaphase (1Gy), and the Art^{-/-} MEF frequencies were 4.28 SCE/frequency (0Gy) and 4.34 SCE/frequency (1Gy). Figure 2B and 2D show SCE distribution for both adult and MEF Art^{+/+} and Art^{-/-} cells. These results reveal that, 1) the DNA repair protein Artemis is not needed to generate a bystander signal and 2) MEFs derived from both C57BL/6 mice and 129SvEvTac/C57BL/6 hybrids are incapable of generating a bystander response.

Figure 2A.

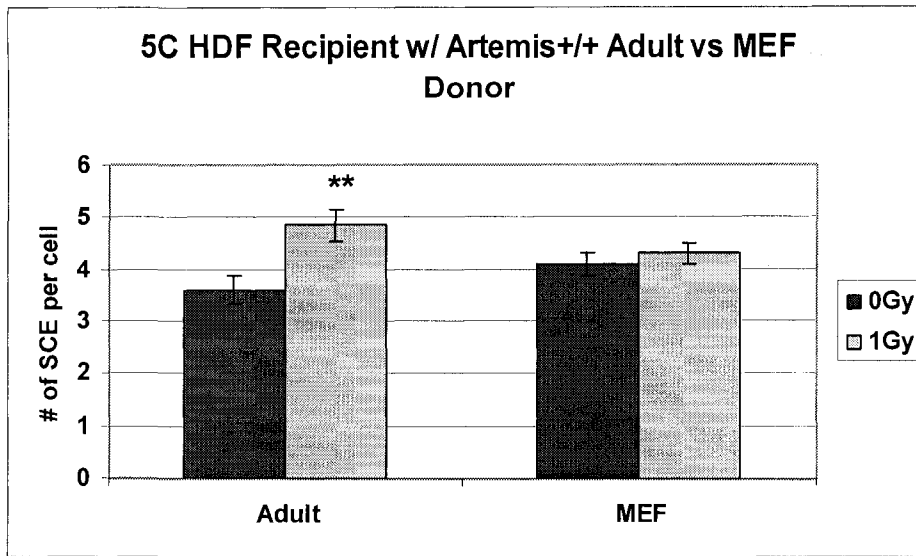


Figure 2B.

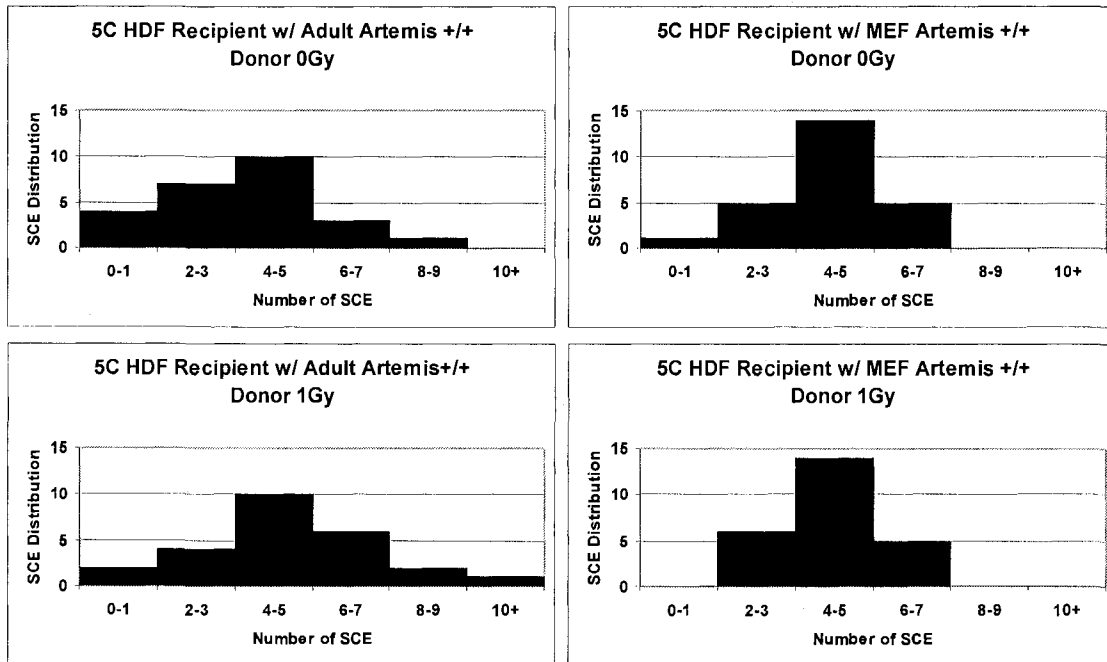


Figure 2C.

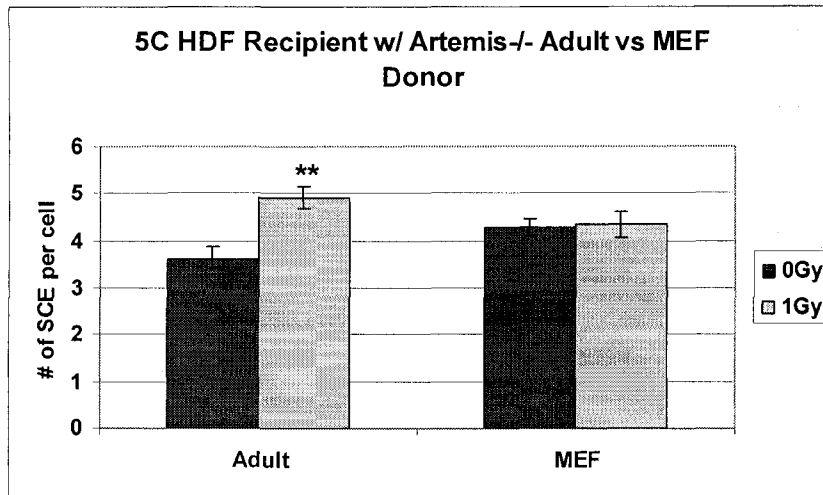


Figure 2D.

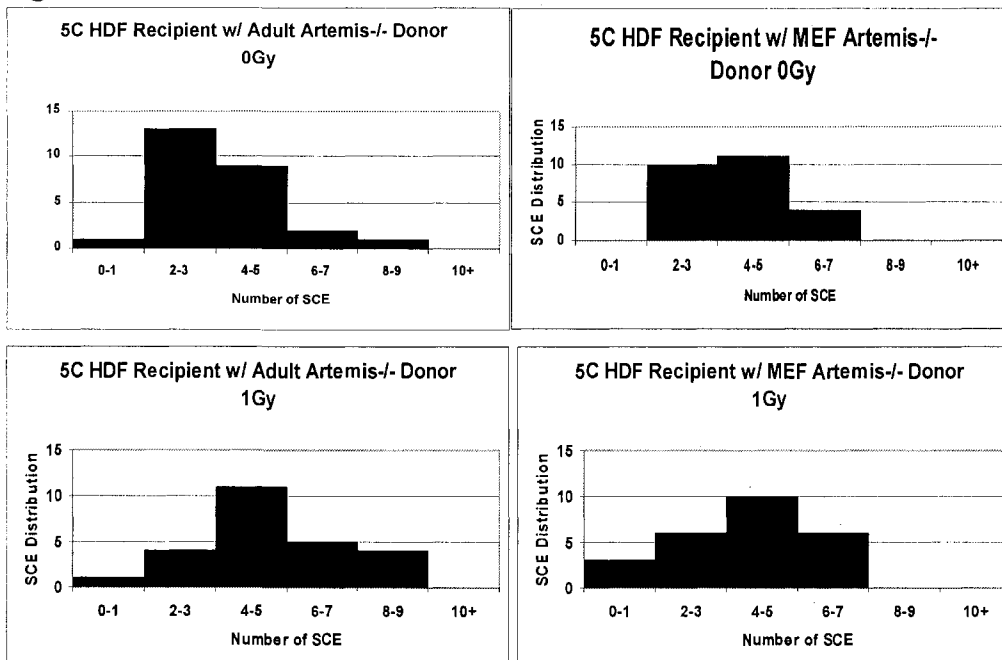


Figure 2. Murine Artemis donor cells added to human recipient cells. **A.** An increase in SCE frequency was seen in human cells with irradiated adult Art^{+/+} donor cells, but not with MEF Art^{+/+} donor cells. **B.** The distribution of SCE number per metaphase illustrates an overall increase in SCE levels. **C.** An increase in SCE frequency was observed in human cells with irradiated adult Art^{-/-} donors, but no increase is seen with MEF Art^{-/-} donor cells. **D.** Distribution graphs again illustrate an overall increase in SCE for the adult mouse Art^{-/-} donor cells. * $\geq 95\%$ confidence, ** $\geq 99\%$ confidence.

As mentioned, there were differences in the genetic background in the previous experiments; however, all of the strains used were inbred. Consequently, we examined an outbred strain, CF-1. Adult kidney CF-1 fibroblasts were either sham irradiated or exposed to 1Gy γ -radiation and added to normal 5C HDF recipient cells. SCE frequency in the 5C HDF for the 0Gy sample was 3.87, which significantly increased to 5.05 when irradiated CF-1 adult donor cells were added (Figure 3A).

CF-1 MEFs were also utilized as donor cells in the BSE experiments. Consistent with previous observations, the irradiated MEFs were incapable of significantly increasing SCE levels in 5C HDF (Figure 3A). Frequencies were 3.16 for the 0Gy samples and 3.44 for the 1Gy samples. Distribution for both experiments showed a general trend and was not skewed by a small outlying population (Figure 3B).

Note all numbers are organized in Table 1, which also reports averages and statistical significance.

Figure 3A.

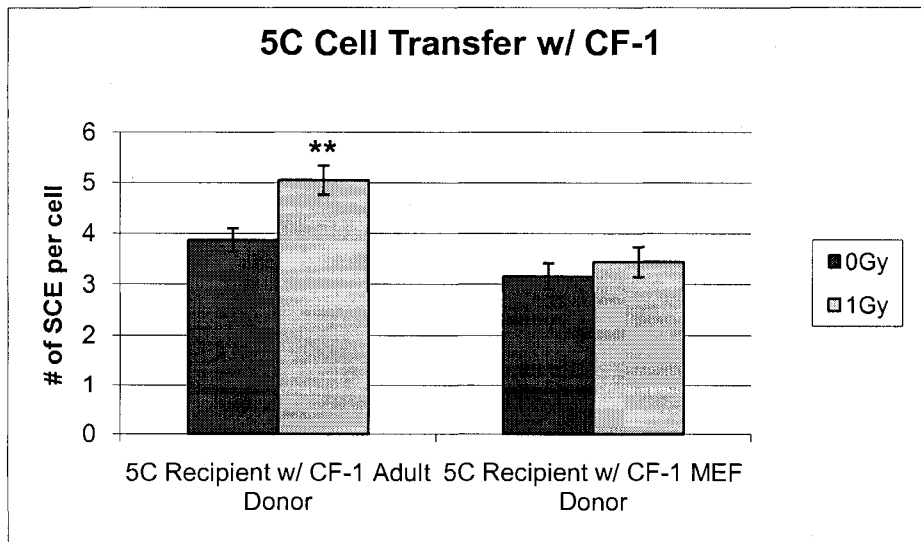


Figure 3B.

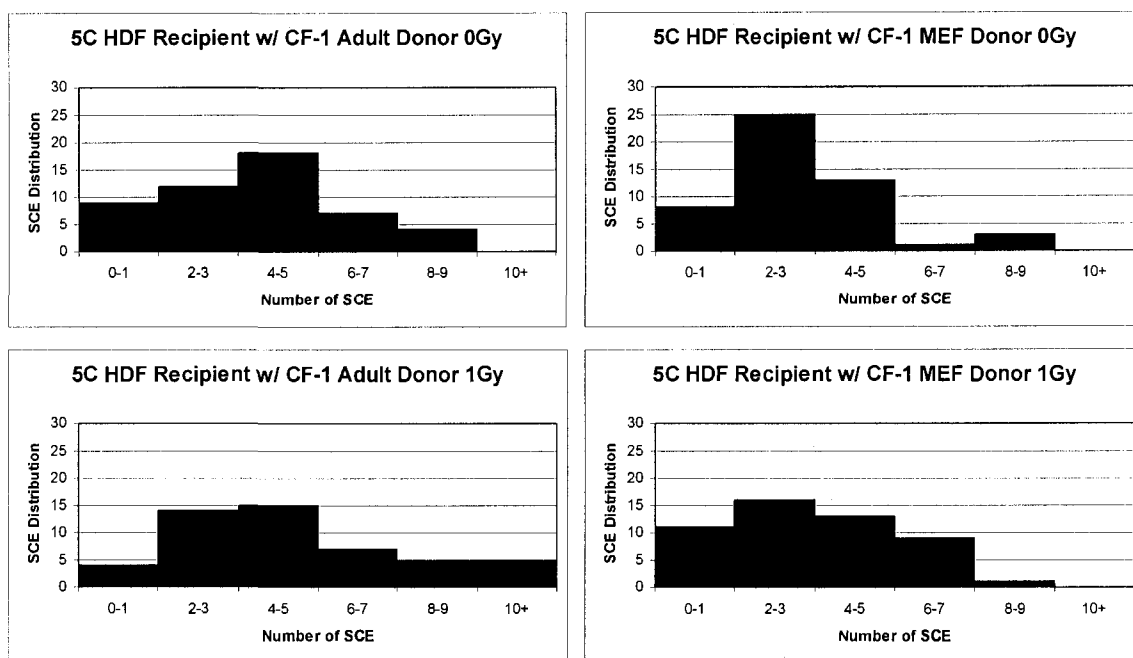


Figure 3. Both CF-1 adult and MEF donor cells were added to normal human 5C recipient cells. **A.** An increase in SCE frequency was observed in the human recipient cells when irradiated adult CF-1 mouse cells were added. The MEFs could not generate a response in that no significant increase was noted when irradiated cells were added. **B.** The distribution of SCE number per metaphase illustrates an overall increase in SCE levels. * $\geq 95\%$ confidence, ** $\geq 99\%$ confidence.

Table 1.

BSE Summary of Adult vs MEF Cell Transfer					
Cell Line	Background	Signal Generated	p value	metaphases scored	Figure
Adult C57	C57BL/6	yes	0.0001	50	1A
MEF C57	C57BL/6	no	0.3776	50	1A
MEF 286	C57BL/6	no	0.2542	50	1A
Adult Artemis +/+	129SvEvTac/C57BL/6	yes	0.0032	50	2A
MEF Artemis +/+	129SvEvTac/C57BL/6	no	0.4648	50	2A
Adult Artemis -/-	129SvEvTac/C57BL/6	yes	0.0004	50	2C
MEF Artemis -/-	129SvEvTac/C57BL/6	no	0.8622	50	2C
Adult CF-1	outbred	yes	0.0018	75	3A
MEF CF-1	outbred	no	0.4708	50	3A

Table 1. Summary and statistical outcomes for all cell transfer experiments.

Discussion

Despite numerous, sometimes contradictory, reports of the BSE, mechanistic details remain elusive. The present work is the first to demonstrate a significant difference in the induction of a bystander response in adult mouse cells versus their MEF counterparts. We have shown that wild-type C57, Artemis^{+/+}, Artemis^{-/-}, and outbred CF-1 adult mouse cells are capable of generating a bystander response in normal human fibroblasts as measured by SCE, but their matching MEFs do not. These studies also show that the DNA end-processing repair protein Artemis is not necessary for the generation of a bystander signal, as irradiated adult mouse Artemis^{-/-} cells elevate SCE frequencies in normal human fibroblasts.

MEFs have been widely used in a variety of studies; only a few of which note differences when compared to adult mouse cells. Several studies utilizing MEFs to examine signaling report no differences compared to adult cells (Wolff 1996; He *et al.*, 2008; Li *et al.*, 2008; Ocbina and Anderson 2008). In addition, no differences in apoptosis in MEFs compared to mouse adult fibroblasts (Vengellur and LaPres 2004; Masud *et al.*, 2007). MEFs were used to study the BSE (clonogenic survival) in one media transfer study and in contrast to our observations, they observed a bystander response (Shareef *et al.*, 2007). Perhaps differences in experimental design are responsible for these distinct results—primary fibroblasts versus lung cancer cell lines, dose of 1 Gy radiation versus 2-10 Gy, cell transfer (co-culture) method versus media transfer, endpoints of SCE versus cytokine production & cell survival, etc. However, one investigation has reported that wild-type MEFs, as well as MEFs with mutated Ku80, did not demonstrate an adaptive response (Raaphorst *et al.*, 2006). The adaptive response,

like the BSE, is a non-targeted effect of IR so in that sense, these results are consistent with our findings.

We have recently shown that the DNA repair proteins DNA-PKcs and ATM are required for IR-induced bystander signaling (Hagelstrom *et al.*, 2008). It has also been recently reported that DNA-PKcs levels are reduced in mouse embryonic stem (ES) cells compared to human ES cells (Banuelos *et al.*, 2008). Although MEFs are not the same as ES cells, MEFs do exhibit some chromatin marks that are similar to ES cells, suggesting impartial commitment to differentiated lineage (personal correspondence, JI Schemanti). If in fact, MEFs do have decreased levels of DNA-PKcs compared to mouse adult fibroblasts, this may provide an explanation for their inability to generate bystander signals.

Future studies (e.g. microarray studies) may provide additional insight into differences in regulation between MEFs and adult fibroblasts, as well as provide information regarding DNA-PKcs levels. However, it should be considered that radiation modifies gene expression predominantly at the translational level (Lu *et al.*, 2006), and therefore protein levels should be examined as well. It might also be worthwhile to perform clonogenic survival assays in addition to cell death analysis in MEFs. It is possible that apoptosis is occurring in the MEFs, which would inhibit the production of a bystander signal. Given that MEFs do not *generate* a bystander signal, it would also be beneficial to perform “reverse” cell transfer experiments to investigate whether or not MEFs are capable of *receiving* a bystander signal. Regardless, further studies are no doubt necessary to provide clues into the underlying mechanisms that are occurring here.

Although these studies alone are not entirely conclusive, our results open new doors to answer important questions raised here and highlight the need to further characterize MEFs. We believe this work points towards important differences in the stress response among developing cells (MEFs) versus those from an adult organism. Our results are among the first to guide research regarding non-targeted effects of radiation in new developmental-related directions.

Acknowledgements

The authors wish to thank Dr. Edwin Goodwin for his critical reading of the manuscript, Dr. Phillip Smiraldo (University of Texas Southwestern Medical Center) and Dr. Douglas Pittman (University of South Carolina) for the Rad51D MEFs, Dr. Penny Jeggo (University of Sussex) for the LigIV MEFs, and Dr. JoAnn Sekiguchi (University of Michigan) for all Artemis mouse cells used.

Supplementary Information

Table S1.

BSE Summary of Additional Cell Transfers Supplementary Data					
Cell Line	Background	Signal Generated	p value	metaphases scored	Figure
Adult p53 ^{-/-}	C57BL/5	no	0.3269	25	S1
Adult p53 ^{-/-}	C57BL/6	no	0.5526	25	n/a
*MEF p53 ^{-/-}	C57BL/6	no	0.9189	50	S1, S3
MEF p53 ^{-/-}	129SvEvTac/C57BL/6	no	0.7979	50	S2
MEF p53 ^{-/-} , LigIV ^{-/-}	129SvEvTac/C57BL/6	no	0.1708	25	n/a
MEF p53 ^{-/-} , LigIV ^{-/-}	129SvEvTac/C57BL/6	no	1.00	25	S2
*MEF C7: p53 ^{-/-}	C57BL/6	no	0.9189	50	S1, S3
MEF 288: Rad51D ^{-/-} , p53 ^{-/-}	C57BL/6	no	0.7794	50	S3

*same data for comparison purposes

Table S1. Summary and statistical outcomes for all cell transfer experiments.

Figure S1.

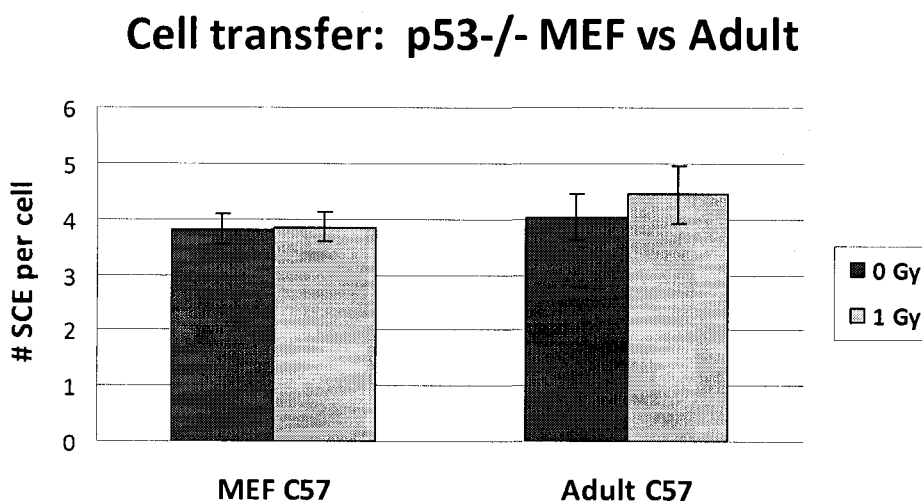


Figure S1. Cell transfer with adult or MEF p53^{-/-} donor cells and human recipient cells. No significant difference in SCE is seen when either type of donor cell is used.

Figure S2.

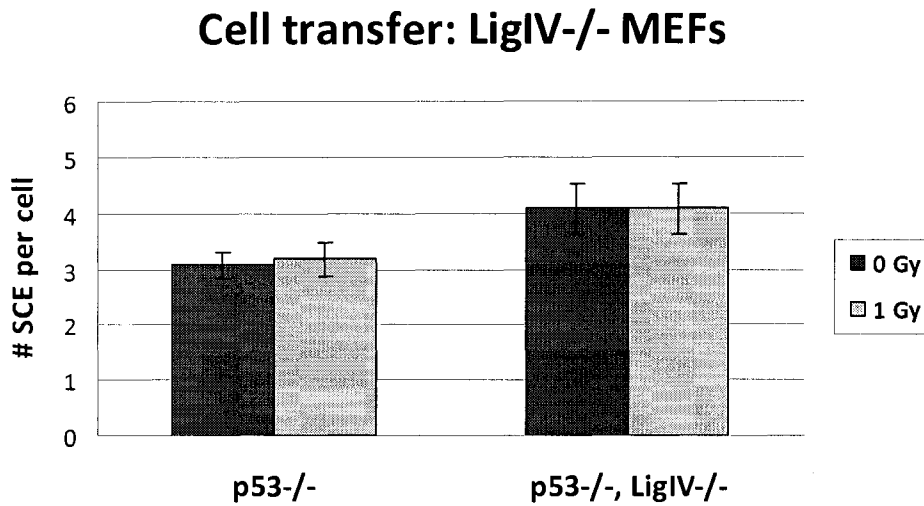


Figure S2. Cell transfer with p53^{-/-} MEFs and p53^{-/-},LigIV^{-/-} MEFs and normal human recipient cells. No significant difference is seen in SCE when using either donor cell.

Figure S3.

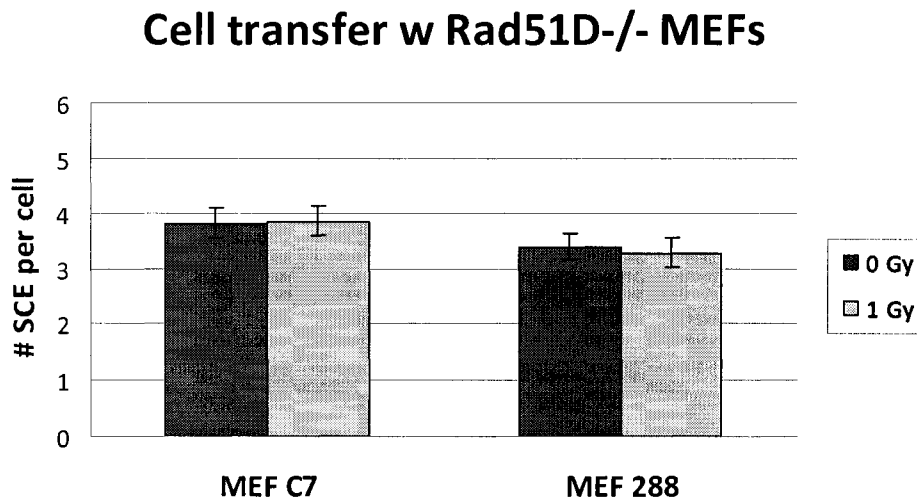


Figure S3. Cell transfer using MEF p53^{-/-} (C7) or MEF p53^{-/-},Rad51D^{-/-} (288) donor cells and normal human recipient cells. No significant difference is observed in SCE levels following radiation exposure with either donor.

Supplementary Methods

The same cell transfer method was used with normal human fibroblasts as recipient cells and the following mouse cells were used as donors: MEF C7 (p53^{-/-}) and MEF 288 (p53^{-/-},Rad51D^{-/-}) cells from a C57BL/6 background (Smiraldo *et al.*, 2005), Adult p53^{-/-} cells from a C57BL/6 background (Taconic, TSG-p53), p53^{-/-} and p53^{-/-},LigaseIV^{-/-} MEF and adult cells from a mixed background (Frank *et al.*, 1998).

Supplementary Results

Neither adult nor MEF p53^{-/-} cells from a C57BL/6 background were able to produce a bystander signal in normal human fibroblasts using our system. SCE frequencies for MEF p53^{-/-} were 3.82 and 3.86 for 0Gy and 1Gy, respectively while frequencies for Adult p53^{-/-} cell transfers were 4.04 and 4.44 for 0Gy and 1Gy, respectively (Figure S1, S3). In addition, p53^{-/-} and p53^{-/-}LigIV^{-/-} MEFs from a mixed background were both unable to produce a bystander effect (Figure S2), further validating our data that p53^{-/-} MEFs do not generate a bystander signal. The mixed background p53^{-/-} had SCE frequencies of 3.08 and 3.18 for 0Gy and 1Gy respectively, following cell transfer while the p53^{-/-}LigIV^{-/-} MEFs produced 4.08 and 4.08 for 0Gy and 1Gy respectively (Figure S2). Finally, p53^{-/-} and p53^{-/-}Rad51D^{-/-} MEFs on a C57BL/6 background did not create a bystander effect in 5C recipient cells either with SCE frequencies of 3.82 for 0Gy and 3.86 for 1Gy with the MEF p53^{-/-} and 3.38 for 0Gy and 3.28 for 1Gy using the p53^{-/-}Rad51D^{-/-} MEFs (Figure S3). An overview of supplementary results can be seen in Table S1.

Supplementary Discussion

Worthy of discussion is the fact that p53 deficient cells, both adult and MEFs, were not capable of producing a bystander signal using our protocol. This is interesting because previous reports show contradictory results regarding the status of p53 and the outcome of the BSE. For example, one article states there is no association between the p53 status and chromosomal instability induced by alpha particles in human lymphoblastoid cells (Kadhim *et al.*, 1996), while another group reports that p53 status does not affect either the production of or response to the bystander signal(s) following gamma-radiation exposure in lymphoblastoid cells (Zhang *et al.*, 2008). Furthermore, Ryan *et al.*, demonstrate the lack of a BSE with mutated p53 in human cells following media transfer experiments (Ryan *et al.*,) and Komarova *et al.*, observe the release of anti-growth factors by irradiated cells in a p53-dependent manner both *in vitro* and *in vivo* (Komarova *et al.*, 1998). Our results support the requirement of p53 for the generation of a bystander signal. Since no BSE was observed in the recipient cells without p53 in the donor cells, we cannot conclude whether or not LigIV or Rad51D is needed to generate a bystander response in our system. However, based on bystander studies in which CHO cells deficient in Rad51D and other HR proteins were irradiated using alpha particles, it seems that these repair proteins are needed in order to induce a bystander effect in neighboring cells (Nagasawa *et al.*, 2008). To date, we are unaware of any previous BSE work involving LigIV.

Given that the type of radiation used, the endpoint studied, and the type of cells used are just some of the factors that affect BSE results, clearly more research is needed to unveil specific molecular events surrounding this phenomenon. Nevertheless, these

data further validate the results in the main text of this work since none of the MEFs used for the supplementary work produced a bystander effect in human recipient cells.

References

- Azzam, EI, de Toledo, SM, Gooding, T and Little, JB (1998). "Intercellular communication is involved in the bystander regulation of gene expression in human cells exposed to very low fluences of alpha particles." *Radiat Res* 150(5): 497-504.
- Azzam, EI, de Toledo, SM and Little, JB (2001). "Direct evidence for the participation of gap junction-mediated intercellular communication in the transmission of damage signals from alpha -particle irradiated to nonirradiated cells." *Proc Natl Acad Sci U S A* 98(2): 473-8.
- Banuelos, CA, Banath, JP, Macphail, SH, Zhao, J, Eaves, CA, O'Connor, MD, Lansdorp, PM and Olive, PL (2008). "Mouse but not human embryonic stem cells are deficient in rejoining of ionizing radiation-induced DNA double-strand breaks." *DNA Repair (Amst)*.
- Collis, SJ, DeWeese, TL, Jeggo, PA and Parker, AR (2005). "The life and death of DNA-PK." *Oncogene* 24(6): 949-61.
- Frank, KM, Sekiguchi, JM, Seidl, KJ, Swat, W, Rathbun, GA, Cheng, HL, Davidson, L, Kangaloo, L and Alt, FW (1998). "Late embryonic lethality and impaired V(D)J recombination in mice lacking DNA ligase IV." *Nature* 396(6707): 173-7.
- Grifalconi, M, Celotti, L and Mognato, M (2007). "Bystander response in human lymphoblastoid TK6 cells." *Mutat Res* 625(1-2): 102-11.
- Hagelstrom, RT, Askin, KF, Williams, AJ, Ramaiah, L, Desaintes, C, Goodwin, EH, Ullrich, RL and Bailey, SM (2008). "DNA-PKcs and ATM influence generation of ionizing radiation-induced bystander signals." *Oncogene*.
- He, X, Chen, MG and Ma, Q (2008). "Activation of Nrf2 in Defense against Cadmium-Induced Oxidative Stress." *Chem Res Toxicol*.
- Iyer, R and Lehnert, BE (2002). "Alpha-particle-induced increases in the radioresistance of normal human bystander cells." *Radiat Res* 157(1): 3-7.
- Kadhim, MA, Walker, CA, Plumb, MA and Wright, EG (1996). "No association between p53 status and alpha-particle-induced chromosomal instability in human lymphoblastoid cells." *Int J Radiat Biol* 69(2): 167-74.
- Kashino, G, Prise, KM, Suzuki, K, Matsuda, N, Kodama, S, Suzuki, M, Nagata, K, Kinashi, Y, Masunaga, S, Ono, K, et al. (2007). "Effective suppression of bystander effects by DMSO treatment of irradiated CHO cells." *J Radiat Res (Tokyo)* 48(4): 327-33.
- Komarova, EA, Diatchenko, L, Rokhlin, OW, Hill, JE, Wang, ZJ, Krivokrysenko, VI, Feinstein, E and Gudkov, AV (1998). "Stress-induced secretion of growth inhibitors: a novel tumor suppressor function of p53." *Oncogene* 17(9): 1089-96.
- Kovalchuk, O and Baulch, JE (2008). "Epigenetic changes and nontargeted radiation effects--is there a link?" *Environ Mol Mutagen* 49(1): 16-25.
- Lehnert, BE, Goodwin, EH and Deshpande, A (1997). "Extracellular factor(s) following exposure to alpha particles can cause sister chromatid exchanges in normal human cells." *Cancer Res* 57(11): 2164-71.
- Li, SK, Smith, DK, Leung, WY, Cheung, AM, Lam, EW, Dimri, GP and Yao, KM (2008). "FoxM1c counteracts oxidative stress-induced senescence and stimulates Bmi-1 expression." *J Biol Chem* 283(24): 16545-53.

- Lu, X, de la Pena, L, Barker, C, Camphausen, K and Tofilon, PJ (2006). "Radiation-induced changes in gene expression involve recruitment of existing messenger RNAs to and away from polysomes." *Cancer Res* 66(2): 1052-61.
- Masud, A, Mohapatra, A, Lakhani, SA, Ferrandino, A, Hakem, R and Flavell, RA (2007). "Endoplasmic reticulum stress-induced death of mouse embryonic fibroblasts requires the intrinsic pathway of apoptosis." *J Biol Chem* 282(19): 14132-9.
- Morio, T and Kim, H (2008). "Ku, Artemis, and ataxia-telangiectasia-mutated: signalling networks in DNA damage." *Int J Biochem Cell Biol* 40(4): 598-603.
- Mothersill, C, Rea, D, Wright, EG, Lorimore, SA, Murphy, D, Seymour, CB and O'Malley, K (2001). "Individual variation in the production of a 'bystander signal' following irradiation of primary cultures of normal human urothelium." *Carcinogenesis* 22(9): 1465-71.
- Mothersill, C and Seymour, C (1997). "Medium from irradiated human epithelial cells but not human fibroblasts reduces the clonogenic survival of unirradiated cells." *Int J Radiat Biol* 71(4): 421-7.
- Mothersill, C and Seymour, CB (1998). "Cell-cell contact during gamma irradiation is not required to induce a bystander effect in normal human keratinocytes: evidence for release during irradiation of a signal controlling survival into the medium." *Radiat Res* 149(3): 256-62.
- Nagar, S, Smith, LE and Morgan, WF (2003). "Characterization of a novel epigenetic effect of ionizing radiation: the death-inducing effect." *Cancer Res* 63(2): 324-8.
- Nagasawa, H and Little, JB (1992). "Induction of sister chromatid exchanges by extremely low doses of alpha-particles." *Cancer Res* 52(22): 6394-6.
- Nagasawa, H, Peng, Y, Wilson, PF, Lio, YC, Chen, DJ, Bedford, JS and Little, JB (2005). "Role of homologous recombination in the alpha-particle-induced bystander effect for sister chromatid exchanges and chromosomal aberrations." *Radiat Res* 164(2): 141-7.
- Nagasawa, H, Wilson, PF, Chen, DJ, Thompson, LH, Bedford, JS and Little, JB (2008). "Low doses of alpha particles do not induce sister chromatid exchanges in bystander Chinese hamster cells defective in homologous recombination." *DNA Repair (Amst)* 7(3): 515-22.
- O'Neill-Mehlenbacher, A, Kilemade, M, Elliott, A, Mothersill, C and Seymour, C (2007). "Comparison of direct and bystander effects induced by ionizing radiation in eight fish cell lines." *Int J Radiat Biol* 83(9): 593-602.
- Ocbina, PJ and Anderson, KV (2008). "Intraflagellar transport, cilia, and mammalian Hedgehog signaling: Analysis in mouse embryonic fibroblasts." *Dev Dyn*.
- Perry, P and Wolff, S (1974). "New Giemsa method for the differential staining of sister chromatids." *Nature* 251(5471): 156-8.
- Ponnaiya, B, Cornforth, MN and Ullrich, RL (1997). "Radiation-induced chromosomal instability in BALB/c and C57BL/6 mice: the difference is as clear as black and white." *Radiat Res* 147(2): 121-5.
- Prise, KM, Folkard M, Michael, BD (2003). A review of the BSE and its implications for low-dose exposure. *Radiation Protection Dosimetry*. **104**: 347-355.
- Purkayastha, S, Milligan, JR and Bernhard, WA (2006). "An investigation into the mechanisms of DNA strand breakage by direct ionization of variably hydrated plasmid DNA." *J Phys Chem B* 110(51): 26286-91.

- Purkayastha, S, Milligan, JR and Bernhard, WA (2008). "An investigation into the mechanisms of DNA strand breakage by direct ionization of variably hydrated plasmid DNA." *J Phys Chem B* 112(13): 4152.
- Raaphorst, GP, Li, LF and Yang, DP (2006). "Evaluation of adaptive responses to cisplatin in normal and mutant cell lines with mutations in recombination repair pathways." *Anticancer Res* 26(2A): 1183-7.
- Rooney, S, Sekiguchi, J, Zhu, C, Cheng, HL, Manis, J, Whitlow, S, DeVido, J, Foy, D, Chaudhuri, J, Lombard, D, et al. (2002). "Leaky Scid phenotype associated with defective V(D)J coding end processing in Artemis-deficient mice." *Mol Cell* 10(6): 1379-90.
- Ryan, LA, Smith, RW, Seymour, CB and Mothersill, CE (2008). "Dilution of irradiated cell conditioned medium and the bystander effect." *Radiat Res* 169(2): 188-96.
- Shao, C, Folkard, M and Prise, KM (2008). "Role of TGF-beta1 and nitric oxide in the bystander response of irradiated glioma cells." *Oncogene* 27(4): 434-40.
- Shao, C, Stewart, V, Folkard, M, Michael, BD and Prise, KM (2003). "Nitric oxide-mediated signaling in the bystander response of individually targeted glioma cells." *Cancer Res* 63(23): 8437-42.
- Shareef, MM, Cui, N, Burikhanov, R, Gupta, S, Satishkumar, S, Shajahan, S, Mohiuddin, M, Rangnekar, VM and Ahmed, MM (2007). "Role of tumor necrosis factor-alpha and TRAIL in high-dose radiation-induced bystander signaling in lung adenocarcinoma." *Cancer Res* 67(24): 11811-20.
- Smiraldo, PG, Gruver, AM, Osborn, JC and Pittman, DL (2005). "Extensive chromosomal instability in Rad51d-deficient mouse cells." *Cancer Res* 65(6): 2089-96.
- Vengellur, A and LaPres, JJ (2004). "The role of hypoxia inducible factor 1alpha in cobalt chloride induced cell death in mouse embryonic fibroblasts." *Toxicol Sci* 82(2): 638-46.
- Wolff, S (1996). "Aspects of the adaptive response to very low doses of radiation and other agents." *Mutat Res* 358(2): 135-42.
- Yang, H, Anzenberg, V and Held, KD (2007). "The time dependence of bystander responses induced by iron-ion radiation in normal human skin fibroblasts." *Radiat Res* 168(3): 292-8.
- Yokoya, A, Cunniffe, SM and O'Neill, P (2002). "Effect of hydration on the induction of strand breaks and base lesions in plasmid DNA films by gamma-radiation." *J Am Chem Soc* 124(30): 8859-66.
- Zhang, Y, Zhou, J, Held, KD, Redmond, RW, Prise, KM and Liber, HL (2008). "Deficiencies of double-strand break repair factors and effects on mutagenesis in directly gamma-irradiated and medium-mediated bystander human lymphoblastoid cells." *Radiat Res* 169(2): 197-206.

Chapter 7

Discussion

Introduction

The data presented here emphasize the important roles DNA repair proteins play in maintaining genomic stability, regulating telomere function, processing damage, and in cell-cell communication involving non-targeted effects of IR, such as the BSE.

LCLs from Breast Cancer Cases & Controls

Potential biomarkers are important for identifying susceptible individuals as well as customizing cancer treatment plans. The studies here examine potential biomarkers using the following endpoints to predict whether women were at high risk for development of IR-induced breast cancer: G2 chromosomal radiosensitivity, telomere length and changes in gene expression. We analyzed twenty (20) LCLs from early-onset breast cancer cases and age-matched controls (10 of each), all of whom were radiologic technologists. We found no statistical evidence that any of the endpoints used (G2 chromosomal radiosensitivity, relative telomere length, or microarray analysis) were able to accurately predict the case vs. control status of each LCL. However, the investigation of the LCLs was intended as a small pilot study for which follow-up in a larger group would have been done if indicated.

Chromosomal Radiosensitivity

The G2 Assay has previously been used to study relationships between chromosomal radiosensitivity and carcinogenesis and most reports find an association between increased chromosomal radiosensitivity and cancer (Roberts *et al.* 1999; Scott *et al.* 1999; Baeyens *et al.* 2002). Surprisingly, though not statistically significant, our

results suggested a trend for reduced G2 chromosomal radiosensitivity in the cases compared to controls. This observation suggests more radiosensitivity in the controls, thus more cell killing and elimination from the population, while the more radioresistant nature of the cases allows damaged cells to survive, acquire additional mutations and continue advancing towards tumorigenesis.

Perhaps in support of this, it should be noted that the majority of the women diagnosed with breast cancer survived multiple cancer diagnoses and treatments. Perhaps the tumors of these women are sensitive to cancer treatment, despite the fact that they are susceptible to carcinogenesis, and thus exhibit an “amazing survivor” phenotype. This supports the idea that the breast cancer cases display lower G2 chromosomal radiosensitivity compared to the controls. It is also interesting to think about the ranges of radiosensitivity observed both within the breast cancer LCLs as well as the control group. Clearly considerable inter-individual variation exists that needs to be further dissected.

It would be predicted that LCLs from controls would be more radiosensitive compared to the cases. Other endpoints of cell radiosensitivity, such as processing of DNA damage and apoptosis, would test this hypothesis. Utilizing γ H2AX, phosphorylated histone variants that mark the sites of DSBs, would provide this kind of information given that this method allows for the evaluation of induction of DNA breaks as well as how the cell can repair the damage over time.

There is much interest in relationships between radiosensitivity and acute and late effects of IR. However, there is no relationship between any specific endpoint of radiosensitivity and acute reactions and late fibrosis. There has been less effort focused

on identifying late carcinogenic effects of cancer treatment and thus further investigations are needed. Iwasaki et al. conclude that no association exists between acute normal tissue reactions to radiotherapy *in vivo* and *in vitro* radiosensitivity assessed by telomere length, apoptosis, cytotoxicity, and cell cycle delay (Iwasaki *et al.* 2008). It should be noted that it may not be feasible to predict the response of distant tissues, such as skin or breast, based on studies from the blood since different tissues display different characteristics and regulatory mechanisms. Nevertheless, it is still important to investigate potential biomarkers in the blood due to the non-invasive nature of sample collection as well as the relatively low cost of the assays used for screening.

Telomere Lengths

Because of clear links between telomeres, DNA damage response and carcinogenesis, we evaluated relative telomere lengths in all 20 LCLs by using Telomere Flow FISH. We found that on average, a trend for telomere lengths to be longer in breast cancer cases compared to controls. While most previous reports suggest a relationship between shorter telomeres and breast cancer susceptibility (Meeker and Argani 2004; Meeker *et al.* 2004; Shen *et al.* 2007), a recent report found significantly longer telomeres associated with breast cancer cases compared to controls (Svenson *et al.* 2008). As suggested from our studies, another recent report identified abnormally long telomeres in a subset of clinically radiosensitive cancer patients (Sprung *et al.* 2008). Clearly telomere dysfunction plays a role in radiosensitivity and carcinogenesis.

If in fact, these cells from breast cancer patients have subsets of longer telomeres, this could contribute to telomere dysfunction as well as a pro-survival phenotype,

consistent with our hypothesis of persistent, damaged cells existing within the cancer cases. It is well known that tumor cells often use the enzyme telomerase to elongate their telomeric DNA which contributes to their survival. It should also be noted that our observation of higher levels of chromatid-type damage (i.e. G2 chromosomal radiosensitivity) in the controls does associate with the presence of shorter telomere lengths, consistent with previous investigations that have documented a relationship between decreased telomere length and increased radiosensitivity (Goytisolo *et al.* 2000; McIlrath *et al.* 2001; Cabuy *et al.* 2005). Based on the above studies, current ideas about telomere length and carcinogenesis may need to be reevaluated. Given the rapidly changing field of telomere biology, this is not unexpected. For example, for quite some time it was believed that telomeres were transcriptionally silent yet now we know this is not the case (Schoeftner and Blasco 2008).

To further elucidate potential telomere maintenance differences in breast cancer cases compared to controls, we should investigate individual telomere lengths in each of the cell lines used here, since only a few short telomeres are needed to initiate DNA repair mechanisms or senescence. Does telomere shortening occur on a specific chromosome in these breast cancer cases? If so, what genes are located closest to the sub-telomeric region and what does this mean for the cell? For example, a previous report observed telomere shortening is increased for chromosome 17q compared to global telomere shortening in the early stages of breast cancer (Rashid-Kolvear *et al.* 2007). Additionally, it is extremely important to investigate larger sample sizes to confirm or reject the results provided by these particular cell lines. From an epidemiological standpoint, a study consisting of 20 samples is substantially underpowered. From a

biological perspective, 20 cell lines are often sufficient to detect functional differences, if they exist.

Despite the fact that many reports demonstrate a relationship between shorter telomeres and cancer risk as well as shorter telomere length and increased radiosensitivity (Griffith *et al.* 1999; Wong *et al.* 2000; McIlrath *et al.* 2001; Meeker and Argani 2004; Meeker *et al.* 2004; Cabuy *et al.* 2005; Rodier *et al.* 2005; M'Kacher *et al.* 2007), our results and recent results from other investigators suggest that telomere lengths as a prognostic indicator is clearly more complicated than previously thought. It is possible to use telomere length in conjunction with other biomarkers comprehensively to assess an individual's susceptibility. An additional complexity to keep in mind is the concept of global versus specific chromosomal telomere regulation.

To further examine genomic and telomeric instability, spontaneous SCE levels in our LCLs may be a promising approach. One study identified increased SCE frequencies in the PBLs of young women (less than 40 years old) with breast cancer (early-onset) as well as their first degree relatives compared to age-matched controls (Cefle *et al.* 2006). They reported 7.17 SCE/cell in breast cancer patients, 6.44 SCE/cell in the first degree relatives, and 5.85 SCE/cell in controls (Cefle *et al.* 2006). Results from SCE studies could potentially identify young women with increased risk of acquiring breast cancer, especially since our cell lines are from early-onset patients (less than 35 years old). Furthermore, SCE frequencies can be evaluated in telomeric regions by using CO-FISH. A study like this in our cell lines may provide additional insight into telomere function among these individuals. Perhaps this additional endpoint would identify a difference

between breast cancer cases and controls. SCE analysis is certainly simple and inexpensive to perform.

Microarray Analysis

To provide more global analysis, we performed microarray analysis on all 20 LCLs using a “Telo Chip” approach. Interestingly, results showed only one gene that was differentially expressed between the two groups. *VIPR2*, Vasoactive Intestinal Peptide Receptor 2, is a G-protein coupled receptor found in the membrane of a variety cells and was down-regulated in the LCLs from breast cancer cases compared to controls, with a fold change of 0.422605. The fact that our microarray analysis did not show major differences between the cases and controls is a good indication that EBV transformation of the LCLs did not skew our results or cause major changes to the cells at the low passage we examined. We are currently performing Real Time PCR on the LCLs to confirm the decreased expression of *VIPR2* in the cases evaluated in the microarrays.

Given that *VIPR2* is a G-protein coupled receptor, down-regulation potentially has many functional implications. If there are fewer of these receptors in the PBLs of a patient, this could lead to alterations of signaling pathways associated with Ras, which can affect cell growth and the initiation of carcinogenesis. It is also possible that *VIPR2* down-regulation in lymphocytes may play a role in tumor progression, with reduced levels of *VIPR2* expression reducing immune response to tumorigenic cells, thus contributing to progression of the cancer. We know that cAMP and PKA are affected downstream of *VIPR2*. PKA can affect a number of substrates in lymphocytes, including NF κ B, MAPK, and CREB which can then modify immune response. Real Time PCR or

Western blots may provide information about changes in NF κ B, MAPK, CREB and/or Ras that would supply further insight into differentiating between these two possible scenarios.

RAD51D

It is becoming apparent that DNA repair proteins have multiple functions beyond repairing broken DNA structures. There is no doubt based on previous studies as well as the data presented here that Rad51d is an obvious example. It is clear that Rad51d is necessary for proper development and function given that Rad51d-deficiency results in embryonic lethality and we now know that this repair protein is needed to maintain proper duplex telomere length as well regulate the 3' ss-overhang, which is important for telomere end capping and thus protection.

While Rad51d is a repair protein that functions in the HR pathway, it also has a role in telomere function. Our goal was to define the telomeric role of Rad51d. Telomere length is decreased in Rad51d-deficient MEFs, yet they have increased length of the 3' ss-overhang. Rad51d may also be involved in carcinogenesis not only because of its function in DNA repair, but also because of a report that a variant in this gene, E233G, may be a low-penetrance breast cancer susceptibility allele (Rodriguez-Lopez *et al.* 2004).

Rad51d, DNA repair and Telomeres

Our studies confirm that Rad51d is indeed essential for maintaining genomic instability given that in its absence chromatid fusions, chromatid breaks, dicentric

chromosomes and detached centromeres are elevated in MEFs. Additionally, T-SCE levels increase without Rad51d, suggesting a role for this repair protein in suppressing excessive HR in telomeric DNA.

Increased levels of chromatid-type damage were observed, suggesting on-going instability among the Rad51d-deficient background since chromatid-type aberrations occur in G2 of the cell cycle immediately preceding the cell harvest. In addition, no telomere signal was seen at the point of chromatid fusions, suggesting that telomere uncapping is not occurring, but rather supports the telomere shortening phenotype reported previously. Further results demonstrate that spontaneous genomic SCE (G-SCE) levels are unchanged (Smiraldo *et al.* 2005) while T-SCE levels are elevated in Rad51d^{-/-} MEFs, implying that Rad51d is not needed for T-SCE to occur. More importantly, Rad51d preferentially regulates SCE recombination in telomeric DNA. However it should be noted that non-mammalian DT40 Rad51d^{-/-} (chicken) cells do have decreased levels of SCE (Takata *et al.* 2001). Based on these observations, it seems likely that Rad51d has a role in suppressing excessive SCE, at least in telomeric DNA, which is equally as important for maintaining genomic stability as suppressing chromosomal aberrations.

We know that telomere lengths decrease in the absence of Rad51d (Tarsounas *et al.* 2004). Interestingly, as mentioned previously, telomere length on chromosome 17q shortens more than global telomere length in the development of breast cancer—both RAD51D and BRCA2 are located on 17q in the human genome (Rashid-Kolvear *et al.* 2007). Could these observations be related? It is interesting to think about telomere shortening and specific chromosomes. Is a specific telomere shortened on purpose by

precise regulation or it is simply by chance? Given that a lack of Rad51d in mice causes decreased telomere length, it is important to determine whether this observation is consistent in humans, since murine studies do not always correspond with human studies.

In addition, CO-FISH using the C-rich telomere probe for the lagging strand should also be considered, as our studies only utilized the G-rich leading strand probe. Results of this study would provide insight into telomere fusions that we know are occurring in Rad51d-deficient MEFs. Furthermore, one could perform CO-FISH with both the leading- and lagging-strand telomere probes in human samples to confirm these initial results in a second species.

RAD51D and EZH2

EZH2 is often up-regulated in breast cancer, as well as other cancers, and is a histone methyltransferase (HMT) (Kleer *et al.* 2003; Zeidler *et al.* 2005; Ding and Kleer 2006). Because of reports that EZH2 down-regulates RAD51D in various cancers, we investigated expression changes in both *RAD51D* and *EZH2* following exposure to IR in human immortalized mammary epithelial and human primary dermal fibroblast cells. The overall trends were similar in both cell types and for both genes, with increases in relative expression at 2 and 8 hours post-IR. These results indicate that *EZH2* and *RAD51D* respond to IR in a similar manner, however further studies are necessary to evaluate the details of underlying mechanisms regulating this response. Analysis of protein levels and Co-Immunoprecipitation studies may provide clues to this regulation.

We know that HMTs are involved in chromatin silencing or chromosome condensation. It was recently reported that EZH2 is recruited to sites of DNA damage

and may function in returning chromatin to its initial state following completion of repair processes (O'Hagan *et al.* 2008). This may suggest that the changes in relative expression levels following radiation treatment are due to the presence of EZH2 at DNA damage sites. It may be that EZH2 is needed throughout the genome to signal the completion of the DNA repair process or to participate in regulating which sites are repaired, or in what order they are repaired. Perhaps RAD51D assists in the repair of telomeric DNA damage, specifically by restoring the protective t-loop structure after the repair process has concluded. Future studies may include repeating our Real Time PCR studies as well as western blots with additional radiation doses and perhaps different time points.

Clearly, chromatin structure, radiation sensitivity, telomeres, and DNA repair are all related; EZH2 regulates chromatin condensation which affects radiation sensitivity which then affects the amount of DNA repair needed by the cell (Laible *et al.* 1997; Tsukamoto *et al.* 1997; Ziv *et al.* 2006; Groth *et al.* 2007; Falk *et al.* 2008; O'Hagan *et al.* 2008). In addition, chromatin modifications are needed to allow DNA repair proteins access to the site of damage. We also know that some histone-modifying proteins (Sir) play a role in silencing of the telomeric DNA, at least in yeast (Martin *et al.* 1999). Therefore, it would be of interest to pursue investigations of relationships that may exist between chromatin modifications, telomere maintenance, radiation sensitivity and DNA repair in human populations.

Bystander Effect

The phenomenon by which irradiated cells influence non-irradiated neighboring cells, referred to as the bystander effect (BSE), is not well understood in terms of the underlying pathways involved. We sought to further explore what factors, particularly DNA repair related proteins, influence radiation-induced bystander responses. Recognizing what proteins play a role in the radiation-induced bystander response will broaden our knowledge not only regarding what criteria are needed in order for this phenomenon to occur, but also may be valuable for the fields of radiation therapy and DNA repair. Utilizing sister chromatid exchange (SCE) frequencies as a marker of the BSE, we performed cell transfer strategies that enabled us to distinguish between generation versus reception of a bystander signal. These studies allowed us to investigate the influence various proteins have on the BSE. We found a role for the DNA damage response proteins DNA-PKcs and ATM specifically in the generation of a bystander signal in addition to the observation that MEFs are incapable of generating a bystander response in non-irradiated neighboring cells.

DNA Repair Related Proteins

We have previously demonstrated the need for both DNA-PKcs and ATM in order to generate, but not receive, a bystander signal. We have also shown that Artemis, another DNA repair protein, is not needed to produce a bystander signal but p53 is. The role of DNA repair proteins in the generation of bystander signals may involve DNA-PKcs and ATM's capabilities as DNA damage sensors in signaling pathways. Such a

damage response may initiate as yet undefined pathways that ultimately lead to the generation of a BSE in non-irradiated cells.

Because we have shown a role for some but not all DNA repair related proteins in the generation of bystander signals, it would be interesting to complete cell transfer experiments using cell lines deficient in additional DNA repair proteins. Although it has been reported that no BSE was observed using Chinese hamster cells defective in Rad51D, XRCC2, XRCC3 and BRCA2 (Nagasawa *et al.* 2008), it is important to repeat the experiments using our system and Rad51d-deficient cells to both further validate our cell transfer method as well as confirm these initial results. Despite the fact that we performed cell transfer experiments using Rad51d-deficient MEFs, the fact that these cells are also p53-deficient prevents us from making any conclusions about Rad51D's role in the generation of a bystander signal.

MEFs

Using the same unique cell transfer method, we have also shown that MEFs do not produce a bystander signal while their corresponding “adult” cells do. The mechanistic basis for this difference is not known. This observation may be due to the relationship between embryonic development and the response to IR (although this is only speculation), adding yet another component to the complex network that surrounds the BSE.

It has been demonstrated the mouse ES cells produce p53 protein but it is generally inactive and further that murine ES cells undergo p53-independent apoptosis when cellular damage is present (Aladjem *et al.* 1998). In addition, early radiation

biology studies illustrate severe defects in irradiated embryos, despite exposures to different doses of IR, which relates to the organogenesis occurring at the time of irradiation (Hall 2006). Perhaps embryos “turn off” the BSE as protection, given that the BSE increases the number of cells affected by IR. This would make them more “radioresistant” in the sense that they eliminate all damaged cells from the population and do not transmit indirect effects from IR to neighboring cells. Although if enough damage occurs a cell or group of cells (i.e. from a large radiation dose, in this case) the fetus would not survive.

We have presented data suggesting that the BSE may be regulated differently during development versus an adult organism. Although most embryos will not be exposed to IR, it is possible that other environmental damaging agents may produce effects similar to a BSE or undergo similar regulation. Based on this idea, future studies should be conducted in order to fully understand how DNA damage responses are regulated during development and what these differences mean for the growing embryo. Is the “on/off” BSE switch under genetic control that is differentially regulated depending on the life stage of the organism? If so, mutations in what other genes will also disrupt the formation of a BSE, both in embryos or adults?

In light of recent work demonstrating deficient DNA-PKcs expression in murine but not human ES cells (Banuelos *et al.* 2008), it is important to investigate additional differences between these species and determine the applicability for humans of these animal studies. In addition, it may not just be related to DNA-PKcs or even DNA repair. For example, telomeric transgenes are silenced in adult mouse tissues as well as MEFs but are expressed in murine ES cells (Gao *et al.* 2007). Could this be related to important

genes located near sub-telomeric regions such as Rad51D as discussed above? Clearly it is critical that future studies continue to characterize MEFs given their extensive use in research.

Although more work is needed, there is clear evidence that the BSE does occur *in vivo*. For example, one report utilized a sex-mismatch bone marrow transplant protocol in mice and observed significantly increased chromosomal aberrations in the non-irradiated hemopoietic cells as a result of the gamma-radiated bone marrow donor (Lorimore *et al.* 2005). Also, bystander effects in the form of increased DNA damage, altered cell proliferation and apoptosis, have been documented in the spleen of both C57BL/6 and BALB/c mice following X-ray treatment only to the head while a medical-grade shield protected the rest of the body (Koturbash *et al.* 2008). These are just a few examples of *in vivo* investigations of the BSE that emphasize the need to further characterize the BSE not only to understand the cellular mechanisms that regulate this event, but also for applications to radiation treatment protocols and risks for secondary cancers.

Conclusions & Future Directions

Early work suggested telomeres as potential biomarkers. Results in these studies as well as others demonstrate a complex relationship between DNA repair and telomere maintenance. Because of this, telomeres are not useful when used alone but must be coupled with other markers to evaluate differences in other cellular functions such as cell cycle regulation, modes of cell death, transcriptional regulation, signaling pathways, etc.

Due to this complexity, it is not surprising that a single, reliable biomarker has yet to be identified.

These studies have provided additional data that support the need for Rad51d in maintenance of genomic instability as well as proper telomere regulation. Rad51d appears to play a role in suppressing excessive HR in telomeric but not genomic DNA, in addition to participating in the regulation of the 3' ss-overhang length that is so important for creation of the protective t-loop structure. Exactly how Rad51d regulates proper telomere function is not clear. Further studies are necessary to understand on a molecular level precisely how this protein participates in the HR process, telomere regulation and potentially mammary carcinogenesis.

The data reported here regarding the requirement of specific DNA damage response proteins to generate a radiation-induced bystander signal will help uncover the signaling mechanisms behind this phenomenon. Furthermore, our observation that MEFs do not produce a bystander signal is a novel finding. Despite the fact that BSE research has occurred for many years, exactly what conditions a cell needs to create or respond to a bystander signal are not understood. Our results suggest that the BSE is regulated in a different manner in embryonic cells than in cells from adult tissues. Future studies are no doubt essential to further define how the lack of a BSE may affect embryonic development.

Currently there is substantial information available regarding how the cell protects the ends of chromosomes from unnecessary degradation as well as how it repairs damage. Although it is clear that DNA repair proteins play a role in radiation effects, including the BSE, there is still much we don't know about cellular responses to IR. Telomere length

and chromatin condensation, among other factors, have been shown to influence radiosensitivity. In general, telomere dysfunction, decreased DNA repair capacity and increased chromosomal radiosensitivity correlate with increased cancer risk.

References

- Aladjem, MI, Spike BT, Rodewald LW, Hope TJ, Klemm M, Jaenisch R and Wahl GM (1998). *ES cells do not activate p53-dependent stress responses and undergo p53-independent apoptosis in response to DNA damage* Curr Biol 8(3): 145-55.
- Baeyens, A, Thierens H, Claes K, Poppe B, Messiaen L, De Ridder L and Vral A (2002). *Chromosomal radiosensitivity in breast cancer patients with a known or putative genetic predisposition* Br J Cancer 87(12): 1379-85.
- Banuelos, CA, Banath JP, Macphail SH, Zhao J, Eaves CA, O'Connor MD, Lansdorp PM and Olive PL (2008). *Mouse but not human embryonic stem cells are deficient in rejoining of ionizing radiation-induced DNA double-strand breaks* DNA Repair (Amst).
- Cabuy, E, Newton C, Joksic G, Woodbine L, Koller B, Jeggo PA and Slijepcevic P (2005). *Accelerated telomere shortening and telomere abnormalities in radiosensitive cell lines* Radiat Res 164(1): 53-62.
- Cefle, K, Ucur A, Guney N, Ozturk S, Palanduz S, Tas F, Asoglu O, Bayrak A, Muslumanoglu M and Aydiner A (2006). *Increased sister chromatid exchange frequency in young women with breast cancer and in their first-degree relatives* Cancer Genet Cytogenet 171(1): 65-7.
- Ding, L and Kleer CG (2006). *Enhancer of Zeste 2 as a marker of preneoplastic progression in the breast* Cancer Res 66(19): 9352-5.
- Falk, M, Lukasova E and Kozubek S (2008). *Chromatin structure influences the sensitivity of DNA to gamma-radiation* Biochim Biophys Acta.
- Gao, Q, Reynolds GE, Innes L, Pedram M, Jones E, Junabi M, Gao DW, Ricoul M, Sabatier L, Van Brocklin H, Franc BL and Murnane JP (2007). *Telomeric transgenes are silenced in adult mouse tissues and embryo fibroblasts but are expressed in embryonic stem cells* Stem Cells 25(12): 3085-92.
- Goytisolo, FA, Samper E, Martin-Caballero J, Finnon P, Herrera E, Flores JM, Bouffler SD and Blasco MA (2000). *Short telomeres result in organismal hypersensitivity to ionizing radiation in mammals* J Exp Med 192(11): 1625-36.
- Griffith, JK, Bryant JE, Fordyce CA, Gilliland FD, Joste NE and Moyzis RK (1999). *Reduced telomere DNA content is correlated with genomic instability and metastasis in invasive human breast carcinoma* Breast Cancer Res Treat 54(1): 59-64.
- Groth, A, Rocha W, Verreault A and Almouzni G (2007). *Chromatin challenges during DNA replication and repair* Cell 128(4): 721-33.
- Hall, EJ (2006). *Radiobiology for the Radiologist*.
- Iwasaki, T, Robertson N, Tsigani T, Finnon P, Scott D, Levine E, Badie C and Bouffler S (2008). *Lymphocyte telomere length correlates with in vitro radiosensitivity in breast cancer cases but is not predictive of acute normal tissue reactions to radiotherapy* Int J Radiat Biol 84(4): 277-84.
- Kleer, CG, Cao Q, Varambally S, Shen R, Ota I, Tomlins SA, Ghosh D, Sewalt RG, Otte AP, Hayes DF, Sabel MS, Livant D, Weiss SJ, Rubin MA and Chinnaiyan AM (2003). *EZH2 is a marker of aggressive breast cancer and promotes neoplastic transformation of breast epithelial cells* Proc Natl Acad Sci U S A 100(20): 11606-11.

- Koturbash, I, Loree J, Kutanzi K, Koganow C, Pogribny I and Kovalchuk O (2008). *In vivo bystander effect: cranial X-irradiation leads to elevated DNA damage, altered cellular proliferation and apoptosis, and increased p53 levels in shielded spleen* Int J Radiat Oncol Biol Phys 70(2): 554-62.
- Laible, G, Wolf A, Dorn R, Reuter G, Nislow C, Lebersorger A, Popkin D, Pillus L and Jenuwein T (1997). *Mammalian homologues of the Polycomb-group gene Enhancer of zeste mediate gene silencing in Drosophila heterochromatin and at S. cerevisiae telomeres* Embo J 16(11): 3219-32.
- Lorimore, SA, McIlrath JM, Coates PJ and Wright EG (2005). *Chromosomal instability in unirradiated hemopoietic cells resulting from a delayed in vivo bystander effect of gamma radiation* Cancer Res 65(13): 5668-73.
- M'Kacher, R, Bennaceur-Griscelli A, Girinsky T, Koscielny S, Delhommeau F, Dossou J, Violot D, Leclercq E, Courtier MH, Beron-Gaillard N, Assaf E, Ribrag V, Bourhis J, Feneux D, Bernheim A, Parmentier C and Carde P (2007). *Telomere shortening and associated chromosomal instability in peripheral blood lymphocytes of patients with Hodgkin's lymphoma prior to any treatment are predictive of second cancers* Int J Radiat Oncol Biol Phys 68(2): 465-71.
- Martin, SG, Laroche T, Suka N, Grunstein M and Gasser SM (1999). *Relocalization of telomeric Ku and SIR proteins in response to DNA strand breaks in yeast* Cell 97(5): 621-33.
- McIlrath, J, Bouffler SD, Samper E, Cuthbert A, Wojcik A, Szumiel I, Bryant PE, Riches AC, Thompson A, Blasco MA, Newbold RF and Slijepcevic P (2001). *Telomere length abnormalities in mammalian radiosensitive cells* Cancer Res 61(3): 912-5.
- Meeker, AK and Argani P (2004). *Telomere shortening occurs early during breast tumorigenesis: a cause of chromosome destabilization underlying malignant transformation?* J Mammary Gland Biol Neoplasia 9(3): 285-96.
- Meeker, AK, Hicks JL, Gabrielson E, Strauss WM, De Marzo AM and Argani P (2004). *Telomere shortening occurs in subsets of normal breast epithelium as well as in situ and invasive carcinoma* Am J Pathol 164(3): 925-35.
- Meeker, AK, Hicks JL, Iacobuzio-Donahue CA, Montgomery EA, Westra WH, Chan TY, Ronnett BM and De Marzo AM (2004). *Telomere length abnormalities occur early in the initiation of epithelial carcinogenesis* Clin Cancer Res 10(10): 3317-26.
- Nagasawa, H, Wilson PF, Chen DJ, Thompson LH, Bedford JS and Little JB (2008). *Low doses of alpha particles do not induce sister chromatid exchanges in bystander Chinese hamster cells defective in homologous recombination* DNA Repair (Amst) 7(3): 515-22.
- O'Hagan, HM, Mohammad HP and Baylin SB (2008). *Double strand breaks can initiate gene silencing and SIRT1-dependent onset of DNA methylation in an exogenous promoter CpG island* PLoS Genet 4(8): e1000155.
- Rashid-Kolvear, F, Pintilie M and Done SJ (2007). *Telomere length on chromosome 17q shortens more than global telomere length in the development of breast cancer* Neoplasia 9(4): 265-70.
- Roberts, SA, Spreadborough AR, Bulman B, Barber JB, Evans DG and Scott D (1999). *Heritability of cellular radiosensitivity: a marker of low-penetrance predisposition genes in breast cancer?* Am J Hum Genet 65(3): 784-94.

- Rodier, F, Kim SH, Nijjar T, Yaswen P and Campisi J (2005). *Cancer and aging: the importance of telomeres in genome maintenance* Int J Biochem Cell Biol 37(5): 977-90.
- Rodriguez-Lopez, R, Osorio A, Ribas G, Pollan M, Sanchez-Pulido L, de la Hoya M, Ruibal A, Zamora P, Arias JI, Salazar R, Vega A, Martinez JI, Esteban-Cardenosa E, Alonso C, Leton R, Urioste Azcorra M, Miner C, Armengod ME, Carracedo A, Gonzalez-Sarmiento R, Caldes T, Diez O and Benitez J (2004). *The variant E233G of the RAD51D gene could be a low-penetrance allele in high-risk breast cancer families without BRCA1/2 mutations* Int J Cancer 110(6): 845-9.
- Schoeftner, S and Blasco MA (2008). *Developmentally regulated transcription of mammalian telomeres by DNA-dependent RNA polymerase II* Nat Cell Biol 10(2): 228-36.
- Scott, D, Barber JB, Spreadborough AR, Burrill W and Roberts SA (1999). *Increased chromosomal radiosensitivity in breast cancer patients: a comparison of two assays* Int J Radiat Biol 75(1): 1-10.
- Shen, J, Terry MB, Gurvich I, Liao Y, Senie RT and Santella RM (2007). *Short telomere length and breast cancer risk: a study in sister sets* Cancer Res 67(11): 5538-44.
- Smiraldo, PG, Gruver AM, Osborn JC and Pittman DL (2005). *Extensive chromosomal instability in Rad51d-deficient mouse cells* Cancer Res 65(6): 2089-96.
- Sprung, CN, Davey DS, Withana NP, Distel LV and McKay MJ (2008). *Telomere length in lymphoblast cell lines derived from clinically radiosensitive cancer patients* Cancer Biol Ther 7(5): 638-44.
- Svenson, U, Nordfjall K, Stegmayr B, Manjer J, Nilsson P, Tavelin B, Henriksson R, Lenner P and Roos G (2008). *Breast cancer survival is associated with telomere length in peripheral blood cells* Cancer Res 68(10): 3618-23.
- Takata, M, Sasaki MS, Tachiiri S, Fukushima T, Sonoda E, Schild D, Thompson LH and Takeda S (2001). *Chromosome instability and defective recombinational repair in knockout mutants of the five Rad51 paralogs* Mol Cell Biol 21(8): 2858-66.
- Tarsounas, M, Munoz P, Claas A, Smiraldo PG, Pittman DL, Blasco MA and West SC (2004). *Telomere maintenance requires the RAD51D recombination/repair protein* Cell 117(3): 337-47.
- Tsukamoto, Y, Kato J and Ikeda H (1997). *Silencing factors participate in DNA repair and recombination in Saccharomyces cerevisiae* Nature 388(6645): 900-3.
- Wong, KK, Chang S, Weiler SR, Ganesan S, Chaudhuri J, Zhu C, Artandi SE, Rudolph KL, Gottlieb GJ, Chin L, Alt FW and DePinho RA (2000). *Telomere dysfunction impairs DNA repair and enhances sensitivity to ionizing radiation* Nat Genet 26(1): 85-8.
- Zeidler, M, Varambally S, Cao Q, Chinnaiyan AM, Ferguson DO, Merajver SD and Kleer CG (2005). *The Polycomb group protein EZH2 impairs DNA repair in breast epithelial cells* Neoplasia 7(11): 1011-9.
- Ziv, Y, Bielopolski D, Galanty Y, Lukas C, Taya Y, Schultz DC, Lukas J, Bekker-Jensen S, Bartek J and Shiloh Y (2006). *Chromatin relaxation in response to DNA double-strand breaks is modulated by a novel ATM- and KAP-1 dependent pathway* Nat Cell Biol 8(8): 870-6.

Appendices

Appendix I

List of Abbreviations

°C	degrees Celsius
α	alpha
γ	gamma
μg	microgram
μl	microliter
ABCFS	Australian Breast Cancer Family Study
Art	Artemis
ALT	alternative lengthening of telomeres
ATM	ataxia telangiectasia mutated
ATP	Adenosine-5'-triphosphate
ATR	ataxia telangiectasia and Rad3 related
ARRT	American Registry of Radiologic Technologists
BLM	Bloom syndrome gene product
bp	base pair
BrdU or Bu	5'-bromo-2'-deoxyuridine
BRCA1/2	breast cancer susceptibility allele 1/ 2
BRIP1	BRCA1 interacting protein C-terminal helicase 1
BSE	bystander effect
cAMP	3'-5'-cyclic adenosine monophosphate
CASP8	caspase 8
cDNA	complementary DNA
CHEK1/2	CHK1/2 checkpoint homolog
CHO	Chinese hamster ovary cells
CO ₂	carbon dioxide
CO-FISH	chromosome orientation fluorescence <i>in situ</i> hybridization
Cs	cesium
ddH ₂ O	distilled water
DAPI	4',6-diamidino-2-phenylindole
DCIS	ductal carcinoma <i>in situ</i>
DNA	deoxyribonucleic acid
DNA-PKcs	DNA-dependent Protein Kinase catalytic subunit
dNTP	deoxyribonucleotide triphosphate
DSB	double-strand break
dsDNA	double-stranded DNA
EBV	Epstein Barr virus
EtOH	ethanol
ES	embryonic stem
EZH2	enhancer of zeste homolog 2

FBS	fetal bovine serum
FGFR2	fibroblast growth factor receptor 2
FISH	fluorescence <i>in situ</i> hybridization
FPG	fluorescence plus Geimsa
g	gram
G0/G1	Gap0/1 (cell cycle)
G2	Gap 2 (cell cycle)
G5	generation 5
Gy	gray
H ₂ O	water
HDAC	histone deacetylase
HMT	histone methyltransferase
hr	hour
HR	homologous recombination
ICL	interstrand crosslink
IDC	invasive ductal carcinoma
IL1A	interleukin-1 α
IP	immunoprecipitation
IR	ionizing radiation
kb	kilobase
KCl	potassium chloride
kDa	kilodalton
L	liter
LCL	lymphoblastoid cell line
LET	linear energy transfer
LigIV	ligaseIV
LOH	loss of heterozygosity
M	molar
min	minute
MEF	mouse embryonic fibroblast
mg	milligrams
mL	milliliter
mm	millimeter
mM	millimolar
MRN	Mre11/Rad50/NBS1 complex
ng	nanogram
nm	nanometer
nM	nanomolar
NBS1	nibrin/Nijmegen breakage syndrome 1
NCI	National Cancer Institute

NHEJ	Non-homologous end joining
NIH	National Institutes of Health
NOS	nitric oxide species
O/N	over night
p53	tumor protein p53
PABL2	partner and localizer of BRCA2
PARP	poly-ADP ribose polymerase
PBL	peripheral blood lymphocytes
PBS	phosphate buffered saline
PCR	polymerase chain reaction
pen/strep	penicillin/streptomycin
PIKK	phosphoinositide 3-kinase-related kinase
PKA	protein kinase A
PNA	peptide nucleic acid
POT1	protection of telomeres 1
PTEN	phosphatase and tensin homolog
<i>Prkdc</i>	gene encoding DNA-PKcs
Rad51D	RAD51-like 3, DNA repair protein RAD51 homolog 4
<i>Rad51D</i>	gene encoding Rad51D
RNA	ribonucleic acid
ROS	reactive oxygen species
rpm	revolutions per minute
RT	room temperature
RT-PCR	real-time PCR
rxn	reaction
S	synthesis phase (cell cycle)
SCID	severe combined immunodeficiency
SCE	sister chromatid exchange
sec	second
SEM	standard error of the mean
SSB	single-strand break
ssDNA	single-strand DNA
SNP	single nucleotide polymorphism
TA	telomere association
TC	telomere DNA content
TDLU	terminal duct lobular units
Terc	telomerase RNA component
TFRC	transferrin receptor
TNM	tumor, node, metastasis cancer staging system
TRF1/2	telomeric repeat binding factor 1/2

USRT	U.S. Radiologic Technologists cohort
UV	Ultraviolet light
VIP	Vasoactive intestinal peptide
VIPR2	Vasoactive intestinal peptide receptor type 2
WRN	Werner syndrome
XRCC	X-ray Cross Complementing genes

Appendix II
Summary of USRT Patient Information
For LCLs

Patient	Patient Code	Status	Genetic group	Age at Blood Draw	Estimated Dose to Breast* (Rad)	Age at Breast Diagnosis 1	Age at Diagnosis 2	Type of Diagnosis 2	Age at Diagnosis 3	Type of Diagnosis 3	Race
1	0017	Case	Breast + Other	74	2.419	31	38	Thyroid	44	Breast	white
2	0060	Case	Breast + Other	55	0	22	36	Skin Melanoma	37	Skin Melanoma	white
3	10595	Case	breast	51	0.019	31	x	x	x	x	white
4	10600	Case	breast	70	0	33	35	Breast	x	x	white
5	10603	Case	breast	56	0	26	x	x	x	x	white
6	10727	Case	breast	59	0.853	33	63	Breast	x	x	white
7	10748	Case	breast	49	0	30	x	x	x	x	white
8	10759	Case	breast	47	0.033	32	33	Lung & Bronchus	46	Breast	white
9	10782	Case	breast	46	0	28	44	Breast	x	x	white
10	10789	Case	breast	55	0.589	33	x	x	x	x	white
11	15020	Control	Normal	58	0.072	x	x	x	x	x	white
12	15021	Control	Normal	47	0.052	49	x	x	x	x	white
13	15035	Control	Normal	50	0.163	x	x	x	x	x	white
14	15044	Control	Normal	48	0	x	x	x	x	x	white
15	15050	Control	Normal	55	0.061	x	x	x	x	x	white
16	15102	Control	Good Genes	80	1.74	x	x	x	x	x	white
17	15127	Control	Normal	61	0.053	x	x	x	x	x	white
18	15149	Control	Normal	60	0.068	x	x	x	x	x	white
19	15152	Control	Normal	61	0	x	x	x	x	x	white
20	15172	Control	Normal	77	1.115	x	x	x	x	x	white

*with lag time of 10 years

Appendix III

Genes Used in Microarray Analysis

<u>Plate Position</u>	<u>Oligo</u>	<u>Oligo sequence</u>	<u>GenBank</u>	<u>Symbol</u>	<u>Gene Name</u>
Subtelomeric genes from non single-copy regions					
A01	1	ACTGAGTCCAGCCTGGCTTA ACTCTTAAATATATGTGGTAT CTTTTCAGCATTAAACACAAC CCACACCC	BI829081		Homo sapiens cDNA, 5' end /clone=IMAGE:5171176
A02	2	GGGAGAGGAGGCAAAGGAG GTGAGAGCATTATGTGGCCA CTTATGTTTGCAATCTACCAT ACTTAGCCCT	BC031359		Homo sapiens, clone IMAGE:4778855
A03	3	GGAAAATGCACACATCCAAC TTTGAGAAGATGCCCTTGGG GGTGCTTCAAGGATCCTAGA TAATAACCCC	BQ012819		Homo sapiens cDNA, 3' end /clone=UI-1-BC1p-alk- h-09-0-UI
A04	4	TGAGACTGTCATTCCAGAGA GGGCCCTGCCCCACGTCCA GAGAAGAAAATGCTCAGAGA CGAAGACAAAT	BF437973		Homo sapiens cDNA, 3' end /clone=IMAGE:3703016
A05	5	TCCCCAGGAGCTGTCCAGTC TTATGTCATGTCTAGTCAGCA GAGTCCCAAAGAAGCTTGTC ATTCTCTAG	BI464772		Homo sapiens cDNA, 5' end /clone=IMAGE:5268125
A06	6	GCTCTAACACACCTGCTTCA CAGTGTAATTATGAGGATTTT ATAGAATTTGTATAGTGAGCG TTAGTTT	AI032307		Homo sapiens cDNA, 3' end /clone=IMAGE:1644210
A07	7	TCCCTCTGCTACTCTGTGGA GGGTTACATGCTGCAATATT TCTGTTCCAAGTAAAGATCAC AGGTTTTG	AA988133		Homo sapiens cDNA, 3' end /clone=IMAGE:1604649
A08	8	ATTCAATACATGCCTACTGAT ATGGTTAGGCTTTGTATCCCC ACCTGAATCTCGTCTTGAATT GTAATCC	AA780033		Homo sapiens cDNA, 3' end /clone=IMAGE:462019
A09	9	TTACATGCTGTACGAAGTACA TGTTGACATGTGAGCATATAA TAAATGGGCTGGAGGCCAGA GGATTGCC	BQ028050		Homo sapiens cDNA, 3' end /clone=IMAGE:3106576
A10	10	CAGCTCCAGTTTTATGTGAAA TAGAGTTTTAGATTTATGTA GCATGGAAAGTTTAATACGT CAGAGTT	BF939606		Homo sapiens cDNA, 3' end /clone=IMAGE:3577418
A11	11	CACATACTGTTGATTGTGAAA TGCCAGTTGAAGCATATGTC CTGCAAGCTTAGGGGTGCTA CAAGTTGAC	AL137655		Homo sapiens mRNA; cDNA DKFZp434B2016 (from clone DKFZp434B2016) /cds=UNKNOWN
A12	12	CAAGCTCATGACTCACAAATG GCCTATTTAGGCCCATACCC TACGTCACGGCAGTCTCCGC AGATGAGGC	AL137733		mRNA; cDNA DKFZp434M0420 (from clone DKFZp434M0420)
A13	13	ACCATGCAATGCACACGTGT GGCTGCACGTCAGCGAGACT GTATTTTATTAGTAGTAGTAG TATTGTTG	AI911319		Homo sapiens cDNA, 3' end /clone=IMAGE:2328152
A14	14	ATTAGATGGGAATATTGCTCA AGCCCTGAAGGTTGAGGCTG CAGTTAACTGTGATTGCACCA CTGCAGTC	BF870283		Homo sapiens cDNA
A15	15	GAGCCAGAGTATGCTACTCC CTAGCAGGAAATCAACAGGA	AW273831		Homo sapiens cDNA, 3' end

		TGACCTATTAACACCATTCA GAAGATGCT			/clone=IMAGE:2814076
A16	16	CGGGAAGCAAGGGGCTAGA CTCTAGATATGCACTTTTTAT TAAATAGTACAGCAGCCTGTA GCCACATGT	AV757131		Homo sapiens cDNA, 5' end /clone=BMFAKG04
A17	17	AAAGTGGGACAAAAGCATT AAAGGAAAGCAGCAGCCCAC TTTTTCCTGCCATGATGCACA TCAGAGTAG	AI393386		Homo sapiens cDNA, 3' end /clone=IMAGE:2111668
A18	18	CTGGCCCTTAGGTACGCCAG TGGTCACGTGTTAAGTTGTC TGGTCCCCATCCCAGTTGA GCCCCAGGA	BQ181476		Homo sapiens cDNA /clone=IMAGE
A19	19	AGTCAGGACACCTCTCAGTT TGGCCTCACTGCTCAAGATT GAGCTGAATTCATGACCATAA TTC AAGCAT	AW119138		Homo sapiens cDNA, 3' end /clone=IMAGE:2604791
A20	20	AAACTCGGGCAGTGCATGCC TCCCCTGCAGAGAAATCCTG TGTTTCACTAGATATTTGTA ACACCTACA	T91839		Homo sapiens cDNA, 3' end /clone=IMAGE:116571
A21	21	TGAAACTACCTTGATAAGCA TATCAAGACCCTTCAGAGATT CTAAAACATGTTCAAGCACTT CTGGTAC	AW297229		Homo sapiens cDNA, 3' end /clone=IMAGE:2731629
A22	22	TTCTTGTC AAGAACGATGAC CGGCAAATAAGCAATTTAGT TCCTTGATTTGAGCACCACT CTTGCAT	AI697700		Homo sapiens cDNA, 3' end /clone=IMAGE:2341255
A23	23	CCCATATGATCCCCGAATG GAACTTCACAAGTTCGAATTC ACTGGGTCACAGTGTGATAG CGTGAAGAT	BG619940		Homo sapiens cDNA, 5' end /clone=IMAGE:4731800
A24	24	AATGAGGAGGCCCTTGACCGT CAGTAGCAGAGAGGGCAGCA GAAGCCTAATTC CAAATTC TTAGATGG	NM_024796		Hypothetical protein FLJ22639
B01	25	ATGACCGCCGTGTGGTAAAC TGATGAACCCTGACCCATTA GGCTTTGGCTACAGAATGTG GAAATAAGT	AK026873		clone IMAGE:4431274, mRNA, partial cds
B02	26	TGGGAAGCACAGGTTAGCGT GTCACCTTGGGCAAAGCTCT CAGCATTGTGAGCCTCTGTT TCTACTCTG	AA701668		Homo sapiens cDNA, 3' end /clone=IMAGE:433604
B03	27	GGTGGCTGCTCACTGTGGGA TGCTGTGCGATTAGACAGTT ACTATCTTCCCTGGTTGACG GATTAGAGT	AI051839		Homo sapiens cDNA, 3' end /clone=IMAGE:1659132
B04	28	GATTCTTAAACTGGTTCAGTG GAGCTAGGCCAGGCTCCCTC TGAGCAGATGTTGGTCCCTT TGCAGGCCT	BE222239		Homo sapiens cDNA, 3' end /clone=IMAGE:3166120
B05	29	TGGACTCCAGCCTCCCCAGC AACATAAGAGATCAAAAGCA TCGTTGAGGAAGCAGCTTGC TGAAACGCT	BC015393		Homo sapiens, clone IMAGE:4431274
B06	30	GCACTCCAGACCGTGTCCC TTCACCTGCCATGATCACATCA CAAACAGCGAGGCTTGGAGA GGACTTAAG	AL079648		Homo sapiens cDNA, 3' end /clone=DKFZp434N1629
B07	31	CAATGAAGGAACACGCAAGA GGACCTTGTGCATGAATAAT CTTGTTCCATATTACCACGA GTGGGTAAC	BI524892		Homo sapiens cDNA, 3' end /clone=IMAGE:5201580

B08	32	AGCTTCCCCTGTTAGGAATTA AGTCAGGAGTCAAACCTGAG ATGGGCTAACCTCGCTGCAG GTGGAGCAA	BQ016214		Homo sapiens cDNA, 3' end /clone=IMAGE:5715297
B09	33	ACGATTTCTGGGCATATCTAT GAGGGCGTTTCTGGAAGACA CTGAGATAACCATGACCCAA TGTGGATG	AK055264	L23aL1	Ribosomal protein L23a- like 1
B10	34	GTGGTTGGCGTTGATGTTGC GTTTTCTCAACGGCGGCATC CGAGGAGTTCGTCTCACCA CTGCGCGCCG	BI458592		Homo sapiens cDNA, 5' end /clone=IMAGE:5265912
B11	35	GACCCACCCACACTGACATG GTCCATTTTCATTGCTGCATG GTCTCTCGTTGTCTGAGGGG AGCATGGGA	AA921816		Homo sapiens cDNA, 3' end /clone=IMAGE:1543505
B12	36	TCTACAGCTGTGCGACCCTC AAACAAAAGAAACACCAGCT CCTCTCTGGGTCTGCAGCTG CAGGAACCTC	BG231764		Homo sapiens cDNA, 3' end /clone=IMAGE:4142476
B13	37	TCTGGTGACCCAGGGCTCCC TGCCACAAGAAGTGTCTGTTG GATCTCTTAGAATCAATAATT GGCACTGAG	AA609920		Homo sapiens cDNA, 3' end /clone=IMAGE:1031125
B14	38	AAAAATACTTTGATCGACCCA TCTCTTTGTACATGAAGCTG GAAACACTAACAGAGGCTGT TGGAAAGA	AI221124		Homo sapiens cDNA, 3' end /clone=IMAGE:1842507
B15	39	TTTAGGCCCCAGCTCATTCTC ACGTCGGCCATTCCAGGCC CGTTTTTCCCTTCCGGCAGC CTCTTGCC	AV704704		Homo sapiens cDNA, 5' end /clone=ADBAPD04
B16	40	TGTTCTTCATTGGTGAGTAA AAGCTCCTGTCCACGGCCCT GAGTGCCAAGGAGTGAGTCT TTAGAGCAC	BF908880		Homo sapiens cDNA
B17	41	CAGCTTCAAGATATGATTACT TAGCTAAGCGGAAATGGGA CGTGACTGCTGCCTCATTCC CAGGCCTCT	AA431778		Homo sapiens cDNA, 3' end /clone=IMAGE:782526
B18	42	GGCTTGACAGTTGTTCTCAG GGAGCAGAACAGAAGTGGG CATTTTCATTCTGGTTACACC ATCAGCGATA	BM980877		Homo sapiens cDNA, 3' end /clone=UI-CF-EN1- ade-k-16-0-UI
B19	43	ATCTCTCTGGATCTTTCTAAG TGAGTCCTGTGTTTCACCACA GCTCCCCGACACAGTTGAG CAGCTGTA	BQ000584		Homo sapiens cDNA, 3' end /clone=IMAGE:5712356
B20	44	TTCAGAAGTGTGGCGGTCG TTGCTAACATGAGATCCAACA AGAAATGGTGAAAATGCACA ATGCCTCAG	BQ185095		Homo sapiens cDNA, 3' end /clone=UI-E-EJ1-ajo-f- 10-0-UI
B21	45	AAAAATGTCAGTCACCTTAC TGGGAACAACACAGCCGTCC AGGAACTCAAGCGGTCTCA GAGCAGTT	NM_020040	TUBB4Q	Tubulin, beta polypeptide 4, member Q
B22	46	AGTACAGACACTAACAAAAG ACAATGCATTCTGCTCTTGT TTTCTGAGGATGTCCAACCT GTAATGGA	AI911402		Homo sapiens cDNA, 3' end /clone=IMAGE:2328335
B23	47	TTTCGTCTCTTTGTCAGTCTC TGCCAAATAGACCCTCAGGG GCTCTCTGTCTCTTGATG AACACTCT	AA974764		Homo sapiens cDNA, 3' end /clone=IMAGE:1578879
B24	48	CAGTCTAGCAGCAAAGGGGA TAGACATGCAAAGACATGAT GTGCAGTTCAGATGGTGGAG TGACACTAGA	AW592902		Homo sapiens cDNA, 3' end /clone=IMAGE:2944708

C01	49	CACTTTGACACTTAATTCTAG ATTTCCCAGATGAACTGAAGT GTGTTGCTCTGTCTTGTGGT GCTTTTCC	AI223429		Homo sapiens cDNA, 3' end /clone=IMAGE:1838953
C02	50	GGCCTCAACAATCACAAAAT ACCCAGTCCGTTAATAACTGA GGAAGGACCCAACTTGCCAG AAATCAG	NM_032263		Hypothetical protein DKFZp434B227
C03	51	TCATGCAGGCTGAGTTATGTT TTCAAATATCTTTTATTCTT GTGGTAGGAACTTACCCTC AAGTGTAG	AL137527		Homo sapiens mRNA; cDNA DKFZp434P1018 (from clone DKFZp434P1018); partial cds /cds=UNKNOWN
C04	52	TGCTGTCTGGCGTCTTCTCT GGGAAAGCTTTCCGGAGCC TGATGGAGGAAGACAGAGGA AAGAGACCTG	AA534508		Homo sapiens cDNA, 3' end /clone=IMAGE:926233
C05	53	GACCAAGCTCTGTAGGAAAA TATCACAGCACGCTGGCCTC GAAAGGCCACGACGTGGCC CTAAACTGTTC	BI261493		Homo sapiens cDNA, 5' end /clone=IMAGE:5087677
C06	54	CCCATTACATGTCAGCCGTG GGAGGTTTTCCAACTGTGG TCCCTGGCATGTCATGGATA ACACGTTCCG	BI056753		Homo sapiens cDNA
C07	55	TAAATGTTGACCACAGTGGAT GCAAATGGCTCTGTGCATCG TCTGTTCAATATGGTCAGGTG ACCACCC	AK055127		cDNA FLJ30565 fis, clone BRAWH2005008
C08	56	AGTCAAGGCCAGACTAGATC AGCCTAAGCCCAGCCACGCC ATGGGTGCAGGAGTGAAGAG CAAATGCTAA	AI744451		Homo sapiens cDNA, 3' end /clone=IMAGE:2362767
C09	57	AACTTAAGGTTCTATTGTATG TAGCCGAACAATACAATCTG GAAACCAGCATGAAACTCTAT TATTCACA	AV656976		Homo sapiens cDNA, 3' end /clone=GLCEWH12
C10	58	AGGTCTAATATAAATGGGCCT GGGACACCCAGGCCACGTAA TCGACCAAAGGTTTTCTGTG AGCCCC	NM_019853	PP4R2	Protein phosphatase 4 regulatory subunit 2
C11	59	AGCGATCCTCAGCCATGTCC CTAGCCTCTGGCTTCCGGCT GATTTTTAAATTTTTGGTAGA GGCGGGATC	AI885212		Homo sapiens cDNA, 3' end /clone=IMAGE:2432252
C12	60	GAGATTTAGATGCAGAGGGT TAGTGTCTTTTTCCCAGGG GGATGGCGTGATGATTTGTT CAAGATTGTG	BG563892		Homo sapiens cDNA, 5' end /clone=IMAGE:4712617
C13	61	CACTTGATGCCACTCACAGA CCACCAACTTCAGAATATCTA GGTGTAAGCTCTGTACAAA AGTTATAAC	AW665984		Homo sapiens cDNA, 3' end /clone=IMAGE:2981415
C14	62	GGGATTAAGAGAAGTAAGTA CAGTTAGTGAGCAGAGCAAG CCAGCGTGGTGAGGGCCTTT CCTAGGTGAG	AA804519		Homo sapiens cDNA, 3' end /clone=IMAGE:1184924
C15	63	ACAGAGATACACAACCTGCCA AAGTCAGCTCTTAGGGGTGT TGTACCAGGAGGTGGTGTA ACAGATCTGG	AW051978		Homo sapiens cDNA, 3' end /clone=IMAGE:2555418
C16	64	GTAAAGTTGTATGTGGTACTA TAAGGCACAACATGCCTCTA CTTTGAAAAGAATAGCCACCA AGTCCTGA	BF510521		Homo sapiens cDNA, 3' end /clone=IMAGE:3086690
C17	65	GAAAAGCAACAGCTGGATTA AGGACATGATCTTGAACCTCC AGACATCTGAATTTCACTACA	BF514678		Homo sapiens cDNA, 3' end /clone=IMAGE:3082494

		CACTGGAT			
C18	66	TAATCGGCCCTCAACCCTTA CTGTACACAAGCGAATTCATA CTGGCAAGGAACATAGTTGA ATGACATT	AK056302	ZNF91	cDNA FLJ31740 fis, clone NT2RI2007133, moderately similar to ZINC FINGER PROTEIN 91
C19	67	TGGGGTCTCGCTCTGGTCTT CTACGTGGAATGAACGAGA GCCACACGCCTGCGTGTGCC AGACCGTCC	NM_033178		Double homeobox, 4 DUX4
C20	68	GGATCAGGGAAGTGCTAATG AGACAGAATGGCCATTGAAG CCAAAAGGTCTGAATTCAGG TAGATAATTT	BM544412		Homo sapiens cDNA, 5' end /clone=IMAGE:5728143
C21	69	ATCTCCGTGCTCCACGGGT GCCCCGATCCCCGGGTCT AGGTCAACCGACAAAATTATT TTAAATGGG	AA883831		Homo sapiens cDNA, 3' end /clone=IMAGE:1467508
C22	70	ATGGGTACCCTTCTCCATAAT AAGATTCCGGGAGGAGTACC CCGACCGGGATCATAAAACA CATTCAAGA	BM552383		Homo sapiens cDNA, 5' end /clone=IMAGE:5549661
C23	71	TGAGACGCTTCTGGACAGGA GAGCCAAATTGAAAGCCGAC AGATACTGCAAGTGACTGGG ATTTTGT	NM_004477	FRG1	FSHD region gene 1
C24	72	TACAAATGCGTGTACCCGA CCTGGTAATCTGCTTCTTGA AATTTATCTTCAGGTCCACC GCACATCT	AI675425		Homo sapiens cDNA, 3' end /clone=IMAGE:2313802
D01	73	TCACCGGGAGCCATCAAGAT GAGAGACCACCCAGCCCTTG TGACTTGACTAAGAAATTA TCCATGTTA	BF968931		Homo sapiens cDNA, 5' end /clone=IMAGE:4358378
D02	74	TTTTAGGGTATTTCTGCTTG TTTCTGCACACACAGTCGC GCGAGGCGCAGTCTGAGT GACCCACGCA	AW303588		Homo sapiens cDNA, 3' end /clone=IMAGE:2813736
D03	75	TGATAAATGTGTCATGGTTAT ATAACACGCTACAATTAGGG GAGACTGGGTGGAAGGCTTA CTGGAACCC	AW163194		Homo sapiens cDNA, 3' end /clone=IMAGE:2784216
D04	76	TCTTCCATGTTGTAGCAG TTGTCTCTACGTGACAGTCTG TCTTGTGAGGTCGAGCTCCC TGAAGGCA	AA824343		Homo sapiens cDNA, 3' end /clone=1391837
D05	77	GACAGACAGCCGGCTTGCTC ATGATTCCGCCTTCTCTGTTA TTGGCAACAAGCCGTCCTG GAACCTTGT	BF064100		Homo sapiens cDNA, 3' end /clone=IMAGE:3323600
D06	78	CACAGCCGGGCGAGTCTGA GACAGAGTGGAGCTGTCCC GAGCTGCAGTTAAAGCATC ACTGGGGTTG	AI017200		Homo sapiens cDNA, 3' end /clone=IMAGE:1627958
D07	79	TGGAATGGAATCGAGGCCA CTGGGAACGGCTGCGTCGAA GAGTAACTTGGGAACGCATA GGGATTCA	AA922263		Homo sapiens cDNA, 3' end /clone=IMAGE:1544093
D08	80	ACATGGTAGGGTTAATGCTA CACGGAACATGAACTCTGAA GACCCCTATTTGGTTCCAT GAAGGTGGT	BC029568		Homo sapiens, clone MGC:39584 IMAGE:4838327
D09	81	CTGAACTGTACAGTAGCTTGT TGTAACATTTATTTCTGGGC AAGGCCAGCTCCACGGCTAC ACGATCAG	AW511060		Homo sapiens cDNA, 3' end /clone=IMAGE:2912217

D10	82	CTGAACTTGATTTACGCCAT CACCTTCCACCTTTAACCAG CATCTCCTGGACAGTCAGCC GAGTGT	AI479320		Homo sapiens cDNA, 3' end /clone=IMAGE:2157777
D11	83	CGGTGGTACTCCATGAATTT CACCCAACATCTGAGAAACG GCTGGTTCAGCAAGCTAACA GCATACAGAT	AI004124		Homo sapiens cDNA, 3' end /clone=IMAGE:1620575
D12	84	GCCCGTGGCACAGCATGGA GCGAAATGGTCCAGTGACCT TTTCAGACACTCGGGCAATG CGTGGTATAGT	AI001820		Homo sapiens cDNA, 3' end /clone=IMAGE:1638104
D13	85	GTTGTCTTTGGTCGGGCATG TGCCCTGAGCATCGAAGAGT CATGCAGGCCTGGAGATAAA GTCCCTCCA	NM_004168	SDHA	Succinate dehydrogenase complex, subunit A, flavoprotein (Fp)
D14	86	AACAGAGAAGTCAGGCGTGA CAACCAGCCTGGCCTACTT CCCTCTCTGACCTGCAGC ACAGACACCC	AL539168		Homo sapiens cDNA /clone=CS0DF034YM16
D15	87	GGTGGGACTCAGCCCCACCC CTGCATTTTCTCTGCATTTTC TTTCGTTGCCCGAAAGTAA ATCCAAAA	BG008300		Homo sapiens cDNA
D16	88	CACGGTGGCCGCTGTGTCTA AAATATTCAGTCCCGTGCAGT AGACACGGTGGCCGCTGTGT CTAAGATAT	AI912163		Homo sapiens cDNA, 3' end /clone=IMAGE:2337022
D17	89	AAGACAAGATTCCTCAGATA ACTAAGCCATTCCCTGGCCA TCAGTCACTACAGTTTCGGA CATTGGTG	BM713521		Homo sapiens cDNA, 5' end /clone=UI-E-EJ0-aho-j- 13-0-UI
D18	90	GAGCAAATGCCAACTGTCCA TGACAGTGACTTTCAAAGGG GCGTGTCAATGTGCCTCATCC CAGCAACAG	AK024175		cDNA FLJ14113 fis, clone MAMMA1001715
D19	91	CCTACGCATCCCAGGCAGAA TGTTGTGCAAAAACACACC AGGATTCGTACATGCCAGAG GACTGAACTT	AW576422		Homo sapiens cDNA, 3' end /clone=IMAGE:3073531
D20	92	TTCTTTTGGAGGTGAAATCTA ATTATTGGTGAGAGTCTTGG GAACAGGCTGTTCCAGTCT CAAAGCAG	BC029040		Homo sapiens, clone IMAGE:5181522
D21	93	AGCTGCAGGACTTTGAAATG ACCCTGTCTCAGCCTGGAG GATGCGGTATTCTGATTGTCT GGTGCTGTG	AV728229		Homo sapiens cDNA, 5' end /clone=HTCADD01
D22	94	AATTCAGAGAACACCTGTGG GATAGTAAACAAGATGCCCA TTCTAAGGCATCCACAGTC ATTAGAATAG	AL050200		Homo sapiens mRNA; cDNA DKFZp586E1423 (from clone DKFZp586E1423) /cds=UNKNOWN
D23	95	CTGAAAGTCTCGTATTAGGTC TATGGGGTATCTAGGACATA ATATTGGGTCAAGATTGTGTT GTGGGTCG	BF247769		Homo sapiens cDNA, 5' end /clone=IMAGE:4069508
D24	96	ACGTGTTCTGTTCTGGGGAA GGGGCAAAGGCAGGGTGA ATCACTTTCTAAAAAGTATA GCTCAAGTTG	AW964023		Homo sapiens cDNA
E01	97	TTTGCATTTCTAGAATGATGG CGCCGAACACTCCATGCTGT CTTTTAGTTGGTGCAGCAGG AGGGGTAGC	AA601705		Homo sapiens cDNA, 3' end /clone=IMAGE:1099517
E02	98	CACTTCTATAATAGATCAGAA TTCACATGGTGTAGAACTCTC AATGACATGAATGGAGGGTA	BC026190		Homo sapiens, similar to zinc finger protein from gene of uncertain exon

		GTCCTCAG			structure; similar to Q99676 (PID:g3025333), clone MGC:33349 IMAGE:4837032
E03	99	ATACCGTTCTCAGACGGAT GGGACATCATCACCTTAGGC CAGGTGACCCCCACGTTGTA TATGCTTAG	NM_012173	FBXO25	F-box only protein 25
E04	100	ATATATATCTCCACTTACATG AGGCACCCACTTACATAAGG CACTTACATGAGTAGTCAAAC TCGTAGAG	BQ017262		cDNA, 3' end /clone=IMAGE:5717210
E05	101	GGTCACAATGGAATCAAGGA CAGAGACCAAAAACGTAGCT GTCCTGACAGCCGTGAAGAG CTTCTTCATT	BE784712		Homo sapiens cDNA, 5' end /clone=IMAGE:3876673
E06	102	ATGGATCTGTTCCGGTTTCAGA GCCCTGCTTTCTTTCACTG GAATGTGCTCTTCGCTTAGC CCTTTTT	AK021796		cDNA FLJ11734 fis, clone HEMBA1005443
E07	103	GTAACCTTTCAGCTTGGGGT ACGAGGAAGGTCAGAGTGT GTTCCAGGGATTGAACAAG GACCGAAGGA	BE560888		Homo sapiens cDNA, 5' end /clone=IMAGE:3679471
E08	104	CTAAGCGTGACATCCAGCAC GTGGTCAGTGAATCCAGTA TTCCTACCCACCTCTCTAGTC TCCCCTCCA	BM686056		Homo sapiens cDNA, 5' end /clone=UI-E-CK0-aap-c-05-0-UI
E09	105	CATGTCCATCTACGAAGGGC TGTGGCAAGCCATATACACA AAGATGCCTGTTTCTGTCTT CTCGGTTA	AK000939		cDNA FLJ10077 fis, clone HEMBA1001864
E10	106	TTCTCCCTCTGCCCTTTCCT CTCTGTCTGTAAGTAGAAG CACCTTTTGGCATAGACCCAT ATCCCAGT	BM974070		Homo sapiens cDNA, 3' end /clone=UI-CF-EC1-abz-d-17-0-UI
E11	107	GAACATGAAGATGGGATCTA CTCACAACCCCCAGAAGTGA GGGGTCTGATAACACATTA TTCACCCTC	AW104157		Homo sapiens cDNA, 3' end /clone=IMAGE:2598679
E12	108	TAAGCAACCCACAGATTGCT CCCTGTGAAGAGGAGCCTGC CAGGGGAGCAGCATTCCACC AGACCCTGAT	AA732814		Homo sapiens cDNA, 3' end /clone=IMAGE:399374
E13	109	CTAGTTTCCAAGGATAGACG GCAGTGAGGAGTCGGGTATC TAGATGGAATTTCTGTTGGTT TGGATTCCA	AW070358		Homo sapiens cDNA, 3' end /clone=IMAGE:2567941
E14	110	AGGGTCTGGCGTCGCCACC GGGAGGCGGATGCATCTCTT TCAGCATTGAGAGTATCATG CAAGGGGTCAG	NM_012184	FOXD4	Homo sapiens forkhead box D4 (FOXD4)
E15	111	GATTGTCCAGGGTGCCATG AGCTCTATGATCTGGAGGAG ACTCCAGTGAGCTGGAAGGA TGACACTGA	NM_018491	LOC55871	COBW-like protein
E16	112	AGCAGTGGACAACACGTTTC CAAGAAGATCAAGTTTGACA TAACACTAGAGGCATTTCTTA TCAAAGG	A1144241		Homo sapiens cDNA, 3' end /clone=IMAGE:1706875
E17	113	TTAGGATAACTTCTTTGTTCC TCTTAAACCCTGAGGGGTG GAGTGGGGGATGTGTAAGTG AGCAGTGTG	AA811613		Homo sapiens cDNA, 3' end /clone=IMAGE:1337075
E18	114	GCGGTATGGCTGTACAGTAT AGAATCACCTGAAGAGCTT ATTAAAAACAGCTTGCTTGAC CCCCTCCCT	AF068294		Homo sapiens HDCMB45P mRNA, partial cds /cds=UNKNOWN

E19	115	GCAGTGTGAAGGGACTTCA AGCAAATAGTGTGATGCCTG TGGGTGCAATGTTACTCCTTC CCTTAGGTT	AI369029		Homo sapiens cDNA, 3' end /clone=IMAGE:1992325
E20	116	TCACCTGCTAGTCATCTTCAG TATTCTGGAGAGGAAATATTC TTTCTGTCCCTTACAGTGGTT GTATATC	AA857001		Homo sapiens cDNA, 3' end /clone=IMAGE:1474670
E21	117	ACCGCCCATAGCTGGAAGGG ACTTGTCTTGTCTCGGACTGA AACTTTGGACTTTGCCCTGTG CCTTTGAG	BG675417		Homo sapiens cDNA, 5' end /clone=IMAGE:4755272
E22	118	GGGGGTTTCGTCATGATATTT CTGTACATAAGATAGCTCCTG TGATCTGTGAGTAGCCGTTTT TACTGCTT	BM980996		Homo sapiens cDNA, 3' end /clone=UI-CF-EN1- ade-d-24-0-UI
E23	119	AAGGGAGAAATGTTTAAATCT GTCTATGCCATATGTGCCTCT GGCTTATTGCCCAATTAATTG TAGACTC	AL365511		Homosome 22 /cds=(290,484)
E24	120	ACTTCCTAGTCCACTCCTGTA AGTTTCTCTTGAGTACATACT AGCAATGAATATGCTGAGTC ACTGCATA	AL038019		Homo sapiens cDNA, 3' end /clone=DKFZp566B081
F01	121	ATTCCCTAAGTGGTGATGCTA TCAGGATCCCCATCTGCGTT TCAGGAACCTGGGCAGGGAA GGGTAACAC	AA572685		Homo sapiens cDNA /clone=IMAGE:914177
F02	122	CCAGAAGCAGCGAGGAGCTT CGACTTCCTCAGGGCAGCAC GGGGGTCGCGTTAACTTGGT GTTCTTCATT	BI911504		Homo sapiens cDNA, 5' end /clone=IMAGE:5213069
F03	123	CGGTGCCTAAGTGGACCTCA GACATGGCTCAGCCATAGGA CCTGCCACACAAGCAGCCGT GGACACAACG	AY026938	RYD5	Homo sapiens putative ligand binding protein RYD5 mRNA, complete cds /cds=(20,307)
F04	124	CAGGTAACCCCTCAGGGACA TGGAAGCAGAGACCCTGCCC TTTTCCCTAGACACTGTGACA GCTACTACT	AL133658		Homo sapiens mRNA; cDNA DKFZp434A0527 (from clone DKFZp434A0527) /cds=UNKNOWN
F05	125	GAAATTTTTCTCACAGTTCT GGACTTGGGGGATCTTTCT TGAACCTGAACCTCGCTGA CCAGATGTT	BI480944		Homo sapiens cDNA, 5' end
F06	126	CATGAGCTAAGCTGATGCCA TTCAGCTGGGTAGCATCGCA GTCACTGTGCAACTTTTAAAC ATACAGCTG	AW206096		Homo sapiens cDNA, 3' end /clone=IMAGE:2723455
F07	127	CCTGGTCAGCACCTGACCTT GACAATGGTGATGCATAAGG GAATGGGGAGGGGAAGTA GAGCTGAGAAT	BC024764		HomoHomolog, clone MGC:30156 IMAGE:4940063
F08	128	AGAAACGTGTAATGACCCC GAGTGTGACTGGGAAGGAGA ACTTATTCCTTACCAGGAAAC TGAAGCT	NM_023011	UPF3A	Similar to yeast Upf3, variant A
F09	129	TGTGTCTTGGGGAACGCAGT GCTTTGAGCATTTC AAGAGC AGTTTTTCTGAAAGTCAGAT CCCAGAGT	W94343		Homo sapiens cDNA, 5' end /clone=IMAGE:358807
F10	130	AACTTGTTACAGGCTTGACA GAAATGTAGAGTGATTTCCA GTTTTGACAAAAGAAATGGCAA GATGGCAGC	AA306761		Homo sapiens cDNA, 5' end /clone=ATCC:160858
F11	131	AGGTTCTTCAGCCAAGCTCT GAGCATTGCACCGGAAGACC CTTTGTTATGCATGAGGTCG	NM_003903		HomoHomolog (S. cerevisiae) (CDC16)

		GCGTGGTTG			
F12	132	CCACTGAAAGACTGAAAACA AGAAAAAACTCAGGTCCCT CACCCAACTGGGCAGTGGT GGTCAGGCTT	AI021939		Homo sapiens cDNA, 3' end /clone=IMAGE:1655403
F13	133	TGTCCTTAGTGTTCAGTGA GGTGCGCAGTGCCAGTG GCACTCACCAGTGATCTGAG TGCTGAGCAC	BQ028188		Homo sapiens cDNA, 3' end /clone=IMAGE:3106544
F14	134	CCTGACACAGCTGGGATTAC AGGTGTACAACACCATCCCC GGCCAATTTCTGTATTTTAG CAGAGATGG	AV651561		Homo sapiens cDNA, 3' end /clone=GLCCRB03
F15	135	GATGGTTCAACACCTACACT GGGAACCCCAACATATGCCCA GGGCTTCACAGGACGGTTTG TCTTCTCCAT	BC032733		Homo sapiens, similar to immunoglobulin heavy chain variable region, clone MGC:45495 IMAGE:5552881
F16	136	TGTAGGAAATGACGCAGCTG CATCAGCTCCATTCTGGCCT CTGTCATGTGACAGTTTTTTG TGGATTTGC	AA437248		Homo sapiens cDNA, 3' end /clone=IMAGE:757468
F17	137	CATCTATCCTGGGAACTCTG ATACCAGATACAGCCCATCC TTCCAAGGCCACGTACCAT CTCAGCCGAC	BC002792		Homo sapiens, clone MGC:3963 IMAGE:3621362
F18	138	TCCCAGCCCCTAAGGCAACT GTATAGGGGACCTGACCATG GGAGGTGGATTCTCTGACGG GGCTCTTGTG	X58397		Human CLL-12 transcript of unrearranged immunoglobulin V(H)5 gene /cds=(39,425)
F19	139	ATCAGGAGCTGCTCAGAATC ACCAGACGGCGGCTGGGCG CGGTGGCTCACGTCTGTAAT CCCAGCACTTT	AW261871		Homo sapiens cDNA, 3' end /clone=IMAGE:2747206
F20	140	TTTGGGATTCAGATTGGGAC CAAGAGGGAGGCTCACCCAG GGCCAGGTCTTAGAATCC TGACAGTTTT	AL043142		Homo sapiens cDNA, 5' end /clone=DKFZp434E1423
F21	141	AGAGTAAGGTGTGTTCTCAT GTACAACTTCCAGGGTTCC CATACTGATCCACACTCTA CCAAGGCTG	AI479376		Homo sapiens cDNA, 3' end /clone=IMAGE:2157842
F22	142	CATGGCTCTCAGTCAAGTCTT GACGCTCCTGCTTCTACAGA CAGGATTTTTTTCGATGCTCC CGCACTGG	AW183711		Homo sapiens cDNA, 3' end /clone=IMAGE:2664165
F23	143	CGGAAAGGAATACCGTGCCT GTGGAAATAGACAGAGCTTA AGTATTTTGTAACTGGTGAA CATACTGCC	BG390749		Homo sapiens cDNA, 5' end /clone=IMAGE:4524641
F24	144	CAGACTAATACCACATAACTC TGTTAGTGCTGTCCCCTGGA TGGAGAATTAGCCTCCTGAG GCTGGGCAC	AI923527		Homo sapiens cDNA, 3' end /clone=IMAGE:2449664
G01	145	TCTTGTGATCGAACCCACTC GAAGAACCCTGTTGTGCTTCA AGATAGTTTAGACTTGGTATG CCAAGGGA	AK058096		cDNA FLJ25367 fis, clone TST01791
G02	146	ATGGTAAATGCTATGAAAGC CTAAACGGCAGATGTGGACT AGGGTGAGATTCCTGGGGAC CTACACTCCG	AW137117		Homo sapiens cDNA, 3' end /clone=IMAGE:2715033
G03	147	ACACTGAAATCATCCCTATCA TACTATTACAGGCAATAATGC CAAGCATAACCCACTATCACA CCCCATC	AW205123		Homo sapiens cDNA, 3' end /clone=IMAGE:2719992

G04	148	CTCACCAATATGTTTTGTGGA CTCTGACGAGCCAAATCTGA CATCAGTTCTGGAACATCTAG AAGATACT	AI417995		Homo sapiens cDNA, 3' end /clone=IMAGE:2114218
G05	149	AGCATGACTATTTTTAGAGAC CCCCTGTCTGTCACTGAAAC CTTTTTGTGGGAGACTATTC CTCCCAT	AK057285	MGC13005	Hypothetical protein MGC13005
G06	150	AGTCACCGGTGCATGTGAC TGAACCTTTCACCCAGTCT GTGGCTTTCCCGTTGCAGTG AGAGCCACG	AK024481		cDNA FLJ31670 fis, clone NT2RI2004984
G07	151	TATCTCAGTCTGGTCACAGC CCTAACTAGGCAGATGATCC CAATGTCAGCCCAAAGCCCA GCAGTCAGGC	AW975445		Homo sapiens cDNA
G08	152	CTCTCAGCTGTTCTGCCCTC ATACCCTTAAAGGGCCAGCC TGGGCCAGTGGACACAGGT AAGGCACCAT	NM_002186	IL9R	IL9R (and pseudogenes, X is real)
G09	153	TTCATGCCCCCTGGGTGGGA GGAGGGGGAGAGGGAGAGC TCCAGTGAGTGGTCTCTGGT TTTTCCCTCA	AW293057		Homo sapiens cDNA, 3' end /clone=IMAGE:2725919
G10	154	TCAACTTGGGGTGAAGAGGA GGGGAGGAGCTAGAGCCAG ACGTGTGTGTGCACATGCTG ACATGCACATG	AI809467		Homo sapiens cDNA, 3' end /clone=IMAGE:2386652
G11	155	CCCTAGTGTGTGCTTGCCCT GTCCCTCGGGGTAGATGCTT AGCTGGCAGTATGAGTTGTG TGCCCTGAG	NM_016310	POLR3K	Polymerase (RNA) III (DNA directed) polypeptide K (12.3 kD)
G12	156	GCCCTCTGTGTACGTATCTG TGTGAGTGTGGGGGTTTCAA GGGTGTATTAGGAATAACGC TCAAAATCC	NM_052996	PRDM7	PR domain containing 7
G13	157	TACAGCTCACTTCTGTGGTTC TGACTATTCAACAAGAATTCC TAGGTCTGTCCCTGTACCAT ATTGTTA	AW189701		Homo sapiens cDNA, 3' end /clone=IMAGE:2674316
G14	158	TGCGCCACTGTGTTCTTCTCT AAAGAGGCTTCCAGAGAAAA TGGCACACC	BC015400		Similar to RIKEN cDNA 1110049F14 gene, clone IMAGE:4156973, mRNA, partial cds
G15	159	GATATCTGTAGTTTTTCTCTA TTGAATTCTTAAAGGGGGT GGGAATAAGCAGATCACAA GGGAGCTGC	AK056232		Homo sapiens cDNA FLJ31670 fis, clone NT2RI2004984 /cds=UNKNOWN
G16	160	GTGCAAGGGTAGGAGGCAG GGCCGCTGCCACCCCTGGG CCGGCACATTGTAATTCTGTC CTGCCTTTTTC	AL559019		Homo sapiens cDNA /clone=CS0DJ008YJ19
G17	161	CAGAGAGTTAGTTTCTCAG CTGGCTGGAGTTCAGCTGGG ATGCTTTAGTTATTTGATGGG AGGAAAAAT	BI044492		Homo sapiens cDNA
G18	162	GCTTTCGAGAATGTAAACCG TGCACTCCAGGAAAATGCA GACACAGCACGCCTTTGG GACCGCGGTT	AW118867		Homo sapiens cDNA, 3' end /clone=IMAGE:2605571
G19	163	AACTGGACTCATACGATATCT GTAGTTTTTCTCTATTGAATT CTTAAAGGGGGTGGAACT AAGCAGAT	BM450745		Homo sapiens cDNA, 5' end /clone=IMAGE:5494478
G20	164	TCACATCCACACAGCAATAAC TCCTCAAAGCAACTTTTGGC CGAGGCGGGAGGATCGCTT GTGCTTAGG	AW449392		Homo sapiens cDNA, 3' end /clone=IMAGE:2734680

G21	165	GCTTCCTCACTGGAAGGAGA TGGTGCTCTTCTTTTTCTTT CTGAATTGTGGCCACCTTCAT ACCACTCT	BG403551		Homo sapiens cDNA, 5' end /clone=IMAGE:4526461
G22	166	GCACTGGACAAGCTAGTGGG CTTTTCGTTGTCCATGGGCTT TTTCGGTGGGGATGTGACCA GCTTTGAAC	AK024448		Homo sapiens mRNA for FLJ00038 protein, partial cds /cds=UNKNOWN
G23	167	AGAGAAGGTACAATAATATG CATAACAACCAATGATCCACT GGTGCTATAAGTTGATGCGG CCGCGAATT	BF477289		Homo sapiens cDNA, 3' end /clone=IMAGE:3261003
G24	168	TTGCTCCTGATTATGATGGCT TCGATGGTGTAAACAAAATTG GGATCACTAAACTGAGTCCA CTGGCTTAC	BF340769		Homo sapiens cDNA, 5' end /clone=IMAGE:4185636
H01	169	CATTTTCCTGTGGAAGATGA GTCGGCCCTGGGTCAAAGC CGCCGGAGACCTCTGACCC TATTGCTCG	AK000827	MGC2752	Hypothetical protein MGC2752
H02	170	TCCAGGGGACTCTTGATATTA CTTAGATCTGACTGTGCTACT CCAAGGTGAAAGCTCTCCA ACCCATCT	BQ212012		Homo sapiens cDNA, 5' end /clone=IMAGE:6095516
H03	171	GCTCCAGCCGGGACGCACT GTGTCCGCCATGGTCTCTCC CTGGTTATTGTGAGGCTGGC GATTACATAA	NM_003422	ZNF42	Zinc finger protein 42 (myeloid-specific retinoic acid- responsive)
H04	172	CTCAGACTGGCTGGGGTTC ATCTGCAGGGTCTACACCC TCATCACCTGCTGCTTGAA CACGAGAAC	BF512338		Homo sapiens cDNA, 3' end /clone=IMAGE:3068810
H05	173	TCCATGGTGACGGAGGTGGC AATGACATCATCAAGGTGAG AGGGTAAATTCCTAACAGGA GACCACAAAG	NM_004535	MYT1	myelin transcription factor 1 (MYT1)
H06	174	CATGGTATTCTAAGGTGTTGA CACCTCCATCCTCAGAGCA GGTCGAAAATATTAATAGAC TGGGACT	NM_018257		chromosome 20 open reading frame 36 (C20orf36)
H07	175	ACCGCTTACGGGCGAAGACT TGCTTGTCCGTGTCCTTGCC ATCTAAGTGGAGAGCCTACG ACTAGATTT	BC010172		clone MGC:19912 IMAGE:3937944, mRNA, complete cds
H08	176	TTCTCCTGAGGTAATGATTTA CCCCCCACCCACAGCTGAG TCTGTGAGGCCCATCCTTT CCCTACGTT	NM_007081	RABL2B	RAB, member of RAS oncogene family-like 2B (RABL2B)
H09	177	AGCTGAGATCACAGGAACAG CAGGTGACAGGCCTAGCTAT AGTTAGGAATACACAAGCCG TAAATCGAG	A1765198		Homo sapiens cDNA, 3' end /clone=IMAGE:2398874
H10	178	GAAGTGGATCGCCTCCAAGA TTGGTTCAAGACCTTTGCGA CTTTCTTTTGCCAAGCGCCTA CAGCAGCTC	AA429889		Homo sapiens cDNA, 3' end /clone=IMAGE:781136
H11	179	GAAGTGGATCGCCTCCAAGA TTGGTTCTAACGCTTTGCGTA TGATTCAATCGGCCACCCT CCACCGCC	NM_001097	ACR	Acrosin
H12	180	GTCCCCACTGCCAACCGTTG CTGTCTATTCTATTACTCAG ACAGATTGTAGTGCCTAGCT ATATCTTG	AW070632		Homo sapiens cDNA, 3' end /clone=IMAGE:2567341
Unique subtelomeric genes					
H13	181	TCTTGAAGCCCAAACTTCCT CAAATCAGCCCTTTGCGTAAC	AK024248		1p36.33 similar to hypothetical protein

		TTCTGTCTACTGTCCGACTCT ACAGGCC			DKFZp434F142
H14	182	AGGGGAGCCAGCAGGGATT CCAGAGTTCCTGCCATAGGC CGGCCTTTGGCCATCAGGGA AAGCCAGCTA	AK096776		cDNA FLJ39457 fis, clone PROST2011105
H15	183	GGCTTTATTATTTATTTTTCAG CATGAAAGACCAAACGTATC GAGAGCTGGGCTGGGCTGG GCTGGTGT	NM_015658		DKFZP564C186 protein (DKFZP564C186)
H16	184	CACTCAGAAAACACCTGTGA GAGCCCCGCAGGCATGCAG GGCACTGTCTGTGAGCACACC AGTGGGGACA	AK056486		Similar to hypothetical protein FLJ11267, clone IMAGE:3350725, mRNA
H17	185	CAGGTACCTGCCCTCTAA CCCATTCAAATTACAAGTCA GGTCTGAACCCAGTGTGAT GGGGGAGT	NM_032129	DKFZP434 H2010	Hypothetical protein DKFZp434H2010
H18	186	CAGGTGGCTGGGTAGGAGG GTGGCCAGATTCACAGATGA GAACACAGGGCATTCCGTTA ATTTCAGACA	NM_032722	MGC13275	Hypothetical protein MGC13275
H19	187	GCGCCGAGCGGTATTAACG AGAGCCTCGCTCAGCTCAA ACCCTCATCTGGACGCCCT CAGAAAAGA	NM_021170	Hes4	BHLH factor Hes4
H20	188	GGAGCTAAGGGCCTCCACCA GCATCCGAGCAGGATCAAGG GCCGGAATAAAGGCTGTTG TAAGAGAAT	NM_005101	ISG15	Interferon-stimulated protein, 15 kDa
H21	189	AACTTGTTGCTTTTGTATAT GATTTTCTTGCTGAGTGTG GCCGGAGGGACTGCTGGCC CGGCCTCC	AF016903	AGRN	Agrin
H22	190	GTGCCTCACAGGCGGCCCTG ATGCTCTGTGCTCAAATCTC TGCAGGACTGGATTTCCGCC GGACAGAG	BE218262		cDNA, 3' end /clone=IMAGE:3175497
H23	191	GGAAATTCAGTTTGGCTTCC AGTGTATCGACTGTGCCTCG GGACCTTCTCCGGGGGCC ACGAAGGCC	NM_004195	TNFRSF18	Tumor necrosis factor receptor superfamily, member 18
H24	192	AAGGAAAGACTTTTATGTCAG AAGTTGGTGCCTGTACCGTC AACCCCGCTGCTGCCCGTGT TTAAACGCA	NM_080605	B3GALT6	UDP-Gal:betaGal beta 1,3- galactosyltransferase polypeptide 6 (B3GALT6)
I01	193	ATCTGTATTGAGTCCCTGTGC CAGCGCCACACGTGCCTGGA GGCCGTCTCAGGCCTGGAGA GCAACAGCA	AI634846		cDNA, 3' end /clone=IMAGE:2297512
I02	194	ATTTTATTAGATGTGGTCACT TAGAAATGCAAACCTTGCTGC CGACCGCGGGCTGCTCCTG CGTTCTTG	NM_058167	Ubc6p	Ubiquitin conjugating enzyme 6
I03	195	TAGGTGAACAGGGGCTGCCG CATCAGAGCCACAGACAGAG GAGCAGCCTGGCCAAAATCA ACATCGTCT	NM_002978	SCNN1D	Sodium channel, nonvoltage-gated 1, delta
I04	196	GCCCTAGTTTGTACCACAATT ACCTTCAGGGTTGGTAAGGC CGATTATTGGGCACACCCTC AGAGTTTCT	BE858544		cDNA, 3' end /clone=IMAGE:3304817
I05	197	AAAATATTTGAAGCAGAGAGA ATGGCATGTGCAAATGCTCT GAGGCGAAGCAAGCCTAGCA CATTGAGA	AI017184		cDNA, 3' end /clone=IMAGE:1627587

106	198	AGAACCAGATGCCAAATAATT TCAGGCTAGAACTCCAAGC GCCCATGATTAATGGATACAA GATAAGAA	AA774570		cDNA, 3' end /clone=1344020
107	199	ACAGTGTTCAGCCACCGT AGCAAAAGTCACCCAGCCCT GCTTCTAGCCCCTCAAGAGT CACCCAGTGG	NM_017865	FLJ20531	hypothetical protein FLJ20531 (FLJ20531)
108	200	ATGGAGATTTGGGAAAAGAC GATGTGGCCTCCTACCTTTC CAGTTTCTGTTGGCAGCCCT TCACGTAGC	NM_024836	FLJ22301	Hypothetical protein FLJ22301
109	201	GCCACAGATGATCAATGAGT GTTTGCTGACCCGCATATGA CAACACGGATTAAGGAAGAC AAATCTGGTA	BF975214		cDNA, 5' end /clone=IMAGE:4335701
110	202	AGAACCTCATCTTCCGGCA GGTGAAGGGATGTGGCAAA CAGTGCACAGGGTCCCAAG ACTTGTCCCT	BF222646		cDNA, 3' end /clone=IMAGE:3649945
111	203	GTGTATTGAATTCTCTGGCAT CATAAACACAGGTATTCGTGA CGTAGCCATTGAAATGAAGA GATGCACA	AI016270		cDNA, 3' end /clone=IMAGE:1641285
112	204	TCTCCATTCTCCTGCCTTAGC TAGCACCTTCTCGATCTTCCC TCTACAAAACCTCCTTCAGTTC ACATTGC	AI004800		cDNA, 3' end /clone=IMAGE:1626115
113	205	AGATTCATGCCACAGCTCCA TATCTTGAGTATGTGTAAGAG GTGAGTTCCTTCTCAGCCA GGGGCGGT	AL137761		mRNA; cDNA DKFZp586L2424 (from clone DKFZp586L2424) /cds=UNKNOWN
114	206	TACACTAAGACCATGTACCTG TATTTTCCACACACGCGTTC AGTTTGTGATCATATGTGTGA CATGTTT	AA909879		cDNA, 3' end /clone=IMAGE:1523863
115	207	TACACACACCCGTGCATTTG CCTTTTTATTGATTATACCTTC TTAAGACATGGAGAAGGAGA ATGAAGAC	BE222018		cDNA, 3' end /clone=IMAGE:3132997
116	208	CACAGCAGTCATCTGCACCA GTCCAGCTGAACTCTGGCTC TCAAAGCAACAGAAATGAATA TAAGCTCT	NM_015677	DKFZP586 F1318	Hypothetical protein
117	209	ATTCCAACCTTATCTCTGATAT TGAGAGGATGGATCAATTAA GCACAGAAATGTAAACAGCC ACAAAGCCC	AW811976		cDNA
118	210	GGAAGAGAAATGCTGGCAGA AGCCTCTCCTGTGGATATACT GCAGCCCTGACCAGGGGCT GGGGGAAGGA	BC030778		Similar to hypothetical protein DKFZP586F1318, clone MGC:26291 IMAGE:4825726
119	211	GTAATTTGATCTCATGAAGT TGATTTGAAAAGCCTACACTG AGAGGCAGTATTTAACTATT CTGAGAT	AI208700		cDNA, 3' end /clone=IMAGE:1839168
120	212	TACTCTAAAAGATCAGACCAG TGTGGCATGTGTGGAAGTGC TCTGTACCAAGATCACACTCT TCAGTTGG	BM480034		cDNA, 5' end /clone=IMAGE:5577457
121	213	CACTTTCCTCTGAAACTTAA TTACATCCAGAAAGAAGGAC ACTTGATGCTAGTCTATGGT CAGTTGA	NM_004300	ACP1	acid phosphatase 1, soluble (ACP1), transcript variant a
122	214	ATGTCATGGGAGTGTGACG AAATACAGTCTTTTCTAGCTA CTGGAAGTGCATACTAAAAG CCAAAGTTT	H08291		cDNA, 5' end /clone=IMAGE:45389

I23	215	GCCGACATATAATTCTCATGT GTGATGTAGAAAGATGGTCC CGTTACTTTAGGGGTAGTTAC AGATCTCT	AI077540		cDNA, 3' end /clone=IMAGE:1677144
I24	216	TGAATACACAAGGCCTGAAG ACACAGCGTTCAGAGGAAGG AGCTCAGACCTCCCCGATCA AATGGTATCT	AA127376		cDNA, 3' end /clone=IMAGE:565433
J01	217	TCACGCAGTTAATCCAGAGC CCCTTAGAGAGGTTTACAAC GGAGCTGCTATTTAAAGGCC TAGATGAGA	BF513468		cDNA, 3' end /clone=IMAGE:3070996
J02	218	GTAAGCCTGCCAGTCCATGG TGTTTTGTTCCAACTGCCCA ATACAATGGTCTCCCCCAGG GAAATGGAA	AW973703		cDNA
J03	219	GGAGGCAGGTCTGGAACCA GTTCCCCCATGCCCTGTGCC CCTAGTCAATATGGACATTTA TTTCTCACAG	AW974431		cDNA
J04	220	GGCATCGATATTTAGATGCA CCCGTGTGTGAAAAATGTAG AGCACAATGGAATTATGCTG GAAGTCT	NM_006614	CHL1	HomoHomolog of L1) (CHL1)
J05	221	TTAATGTTGCCTTAACTATCA GGTTTCTGATAGCCCCACAT AGCCAAGTGGGACCCTGGTC AAGAAGTT	AK055236		cDNA FLJ30674 fis, clone FCBBF1000748
J06	222	AGTTGTTTCAGGCAACAAG ACCTCAGATGTCTTCACCTC AACCACTCTGGGATACTGA AGGGTATTG	AI241341		cDNA, 3' end /clone=IMAGE:1869217
J07	223	AACCAAAAGCCCAAAACCCC ACTAATGTTGGGAAGCAGGA ACATCTTTAATTACCTGGTTA TATAATCGC	BE048481		cDNA, 3' end /clone=IMAGE:3131844
J08	224	TCTTACAGCATGACACTTTCT GGATTGCAGTAAAATAAAGA AACAGCAACATGCATGCTTG CTTGAAGGA	AI017718		cDNA, 3' end /clone=IMAGE:1638622
J09	225	CATGGAAAGAGGGGCCTTTG TATTCTGCTAGAACACAGAG CATAGTAGTAGATCACTTTTC TGAAGAGC	BC008625		clone IMAGE:4183899
J10	226	TGTTGTCTCTCATGCTTCTTG AGTTGCTTCATGGTTTATGCT CGCCATGGAAAGCTATCAGT AACAGTT	NM_032288	DKFZp761 B1514	hypothetical protein DKFZp761B1514 (DKFZp761B1514)
J11	227	TATGTACCCAGGATGAACAC AAATCTCAGTTTGAACACCAC CATGAACACCAAGGAAACAG ACTGAAATA	AA805445		cDNA, 3' end /clone=IMAGE:1340887
J12	228	CTTGAGTTTATAAAAAGCGG AGTTTTTTTATTTTTGAGAC GGAATACTCTGTACCCAGG CTGCAGTGC	BG546142		cDNA, 5' end /clone=IMAGE:4701687
J13	229	TGACACGATGCCGTCTCAC CTTCCAAATACCCAGTTATTT ATTCAAGAGGGGGGAAGTGG GTAGAGGA	D86979	KIAA0226	KIAA0226 gene product
J14	230	TCCAGTATACCACTGACTC CCCATAGCTGGAAAACCCCA TGGGGCTCTCTGTTTGCCC TTATATCAGG	AI090019		cDNA, 3' end /clone=IMAGE:1696594
J15	231	CACCCACCTCGGCCTCCCAA AGTGCTGGGATTACGGGTGT GAGCCATCGTACCTGGCCAC TTTAATTATT	AI470295		cDNA, 3' end /clone=IMAGE:2144113

J16	232	TCTGGTTAGTAGATTTAGTGA GCAAGGCCCAAAAAGGAGAA AAAGGAAGACAAAGGCCAGG GATCCCAAC	BE082843		cDNA
J17	233	GGCCTGTCTCTGGACTCCTG CACATTCCGAACCATGGAAG GTAGGCAAACCATGATCT CCAGCTGTTT	AA994705		cDNA, 3' end /clone=IMAGE:1625463
J18	234	TTCTTAACAGTCTCTAATCAC TTGCCCTACCTACTTTCTGTA TTTAACTGCACTGCTGCTCC TGAAACA	BM987769		cDNA /clone=IMAGE
J19	235	TCGGCACGAGGCAGGCAT TCATTCTGAACAAAACCTTTA CAAATGTGAAGAATGCAGCA AAGCCTTTA	AW291262		DNA, 3' end /clone=IMAGE:2724618
J20	236	GCACCCCAAGAGAAGTCT TTCAGTGGCATGTTTCTGATG GTGACAGGCCTGGTTTGTAA AACCTCTAA	AI143189		cDNA, 3' end /clone=IMAGE:1705626
J21	237	TGAAAACGTGGCAGAGCCT TCAGACCATCCCAAACCTTT ATGAAAATTCATATTTGAGAG TAGAAGA	NM_003441	ZNF141	zinc finger protein 141 (clone pHZ-44) (ZNF141)
J22	238	ATGTCTCCAGATGCCCTTTC TTGTAATACCCAAGCATCTG GTAACCAGCATTCTACTCTCT GGCTTAT	BF111809		cDNA, 3' end /clone=IMAGE:3523447
J23	239	AAAGAGAAGAGAAATAAAG ATGCACCAGGAAAATCTGAG CAGAGAGGCTTTTAGTGGTT GACTTACTGA	AB075862		mRNA for KIAA1982 protein /cds=UNKNOWN
J24	240	CATAACATTTGGGTTAATGCG CTTACACTGCAGGAGAGGTC ACCAGGAACATCCAATCATC AGAAAGTCC	AA868350		cDNA, 3' end /clone=IMAGE:1408510
K01	241	AGACTGAGACAGGACGCTCA GGTACATCATACTGAGACAG GACTCTCAGGTACATGATAT GAGACAACAA	AI765360		cDNA, 3' end /clone=IMAGE:2399021
K02	242	TGGAGAGACTTTTCGCGGCT TTGGCCTGAAAGTGACACAT ATTGCTTCTGCTCCCGTTTCC TGGGCCAGA	AI688800		cDNA, 3' end /clone=IMAGE:2330669
K03	243	GTAGTACTTTCCACAGTAGC CCCAGCAAATCAATACAGGG CCTACAGGCATGGATTTCTG TTCCAGTTA	BF436754		cDNA, 3' end /clone=IMAGE:3645541
K04	244	GCAGACCTCGACGGCTCCTT TCCCTACAGCCATGGTGACT GGATCTGCTTCCGTGAGAGG CTGGAACACT	AW245715		cDNA, 5' end /clone=IMAGE:2822673
K05	245	GACTGACAGACAGATGAGAG GGGCCTTAGGGCATTGGCT GACACAATTTTGGCAGGTCA AGAGCCCCA	AB067496		mRNA for KIAA1909 protein, partial cds /cds=UNKNOWN
K06	246	GCTTGAGGCTTAGACTGACG GGAGCTATTCGGGTGTTTA ATTGAAGGTCTAGCACTGA CCAGCCCCTG	BM676744		cDNA, 3' end /clone=UI-E- EJ0-ahu-e-23-0-UI
K07	247	CAGTGCTTAAAAGGAAGGA CTTTTGCGGGGAGGGGTTGA GATTGACTTTCTAATTTCCG TTGCTTCAG	AA781880		cDNA, 3' end /clone=1375775
K08	248	TGTTGGGGATATGGTTTCTTG AAGCATTTTATAGGCTGCCAGT ATTGTATTAAGCAGAACAGTA TAACCTC	NM_145265	sRIKEN	similar to RIKEN cDNA 0610011N22 (LOC133957)

K09	249	TCCCTGCCTTTAGAAACGCG GGACAGCTGATTGCTCTCCT TGGCCACACGTGCTCCTTTT AGCTGCACGG	NM_007277	SEC6	Homo sapiens similar to S. cerevisiae Sec6p and R. norvegicus rsec6
K10	250	GAGTGCAAAGAAGCCTGGGC TCTTCAGGTCTTCTGTTCTAA CATTTTGCCGGACTTGCTTTA CTCTATAG	BE887251		cDNA, 5' end /clone=IMAGE:3910094
K11	251	TTACATCTTCCAGTTTGCCA TCCCATGAGTTAGAGTTCGT CTTGACTCTGCAAGCTAGAAT CAAAGAA	NM_032765	MGC16175	Hypothetical protein MGC16175
K12	252	ACACCTCCTGTGGCTACCCA ACTTTTCACACATCTTACTGA TTATAGGCCTTGCTGTGAATG CTTCTT	NM_022907		hypothetical protein FLJ23053 (FLJ23053)
K13	253	TCTGGAGGCAAGGATGGCCA GGCCATGTTATGGGATCTCA ACGAAGGCAAACACCTTTAC ACGCTAGATG	NM_006098	GNB2L1	guanine nucleotide binding protein (G protein), beta polypeptide 2-like 1 (GNB2L1)
K14	254	CTCCTGGGGAGGAGGGATT TAACTTTCCTTCCGTCCTCA ATTTCTACCTCCATAGACCGG CCAGAATT	AK074052		mRNA for FLJ00123 protein /cds=UNKNOWN
K15	255	TTCGCATCCGAGGTAGAAA AACCAACCGGACACTGTCTC ATGGTTTAGATGAAC TTCCT AACTGCCCA	BM272169		cDNA, 3' end
K16	256	CTGACTGGGAAGGGTGCCTG GCTCCCTAAAACAATGTCAAA GCCAGTCTGCTGTTCTCTG TTGCCAGG	AF396655	TRIM7	Tripartite motif-containing 7
K17	257	GGAGTTCATCACTCCTAAGG GGAAAGTGCCTCGCAACAGA CCAACCTGGTGAGGGAGGC GGGGGGAGCAC	H99640		cDNA, 3' end /clone=IMAGE:262823
K18	258	TTCCCCCTAAACTCAGAACCT GCCATGGCTTCTCCTTACC GTCAAAATCAGCATT CAGTAT GGCCTAAA	AI187167		cDNA, 3' end /clone=IMAGE:1741285
K19	259	AGCCCTTGGTGTGGTTTTA TCTCTGGTTTTGTGTTCTCCGT GGTGAATTGACCGAAAGCT CTATGTTTT	NM_020185	MKPX	mitogen-activated protein kinase phosphatase x (MKPX)
K20	260	GCCAGGTGTTGTGCTAGTGG GTGAGGAGGGAGGCAAAGG GAGTACAGTGGTAAATGACC CAAAGATTCTT	BM991695		cDNA, 3' end /clone=IMAGE:5698325
K21	261	CACGCTTGATTTATATATGT ACTTAACAAGAAATCACCAAG ACTGCAGCGGGCAGTTCCTC TTCCCTTT	AV693098		cDNA, 5' end /clone=GKCFGA04
K22	262	TTTTACATGCCCGTTTTTGA GACTGATCTCGATGCAGGTG GATCTCCTTGAGATCTGATA GCCTGTT	NM_002460	IRF4	Interferon regulatory factor 4
K23	263	AGATTATAGGGAGCATGGGT GAAGCACTTGAGGAAGA GGATTCCATGGCAAACATG AATCCAGGGA	NM_002598	PDCD2	programmed cell death 2 (PDCD2)
K24	264	GGGAACATGGTCATATCAAA GATTAAGGATAAGGATTA GGCCATGTCAGAACTCAAG CAACATGAA	AW237443		cDNA, 3' end /clone=IMAGE:2689710
L01	265	CGTGACTGTGAGTTGCTCAT ACCGTGCTGCTATCTGGGCA GCGCTGCCCATTTATTTATAT GTAGATTT	NM_003194	TBP	TATA box binding protein (TBP)

L02	266	GGATCTGCATAGTGACCAAA GAGGGCATCAGGGAGGAAA CTGTTTCCTTAAGGAAGGACT GATCTGTGT	AK023290	PSMB1	Proteasome (prosome, macropain) subunit, beta type, 1
L03	267	ATCCCTGTTCCAGCCTTTCC GCCCTCAAAGTGCTGCTTT TGGTTTCTGCTTCTAGCCTG CAAGATGGC	BM685066		cDNA, 3' end /clone=UI-E- EJ1-ajl-m-12-0-UI
L04	268	GTGTCCATGGAATCAGTTG GTGCGGTGAGCGGCAGGTC TGATATGAAAGCTACTCGCA CTTCCCGTCTG	BM662952		cDNA, 3' end /clone=UI-E- CI0-aaa-d-12-0-UI
L05	269	ACGAGCCTGAGAGCAGATTG CAAAGCAAAGCGTGTAGTGC AATCCAACCTTTGAAAGAAA AATAAATCC	AI192009		cDNA, 3' end /clone=IMAGE:1738644
L06	270	AGGTGGCATCAACAGGTTTG GAGCAAACCTGAGTGTCTCC CGGTTGGTCACATCTCAACT GACGAAATCC	AI352120		cDNA, 3' end /clone=IMAGE:1940490
L07	271	TCATCCCCAGAGGGCTTGGT AAGGGGACTGTTTGACAGAGA CATAGGCAGAGGGCTGAAA ACTACCAAAA	AK024243	FLJ14181	cDNA FLJ14181 fis, clone NT2RP2004300 /cds=UNKNOWN
L08	272	GTGGTCTTCCCTGAGCACAT CCTGGCCAAGGATGCTGCC CCAGGAGATTTGAGAAGTCC TGTAAGGATC	AI823386		cDNA, 3' end /clone=IMAGE:2384469
L09	273	TGTGAGAAGCCTAGAAGTGC TTTGCTGTCGTTTCTCACTT AATAAAGACAGCAAATCAGC CTCACACTG	AI245369		cDNA, 3' end /clone=IMAGE:1869832
L10	274	CCCAGGCCACATAAGGCTG GTGTTCTCTCATGGACGGTG GAGGTTCCCCAGGCCTCAG TGCTAGGTG	AA968456		cDNA, 3' end /clone=IMAGE:1580183
L11	275	TATTGCGTGGTTTGCAGATAC TCACGATTCTTGTCTTGAA TGTGCCCGTCCGTGAATGAT TTCATGTG	BM661683		cDNA, 3' end /clone=UI-E- CK1-abm-b-01-0-UI
L12	276	AAGCTCACACATCCTGTCAG TGTCACCTTGGTTTGCAAAAC CCATATCCCCGGTAAAATGA GGCCGGACA	NM_003382	VIPR2	vasoactive intestinal peptide receptor 2 (VIPR2)
L13	277	TGTAGTAAATCTGTTTGTCTA GATTGCCCTTCCAAAAGGCTG AGACAGCTGACAGCTGCACG TGGGATCAC	AI025211		cDNA, 3' end /clone=IMAGE:1639824
L14	278	TGCAGGACGACACATCCAAC ATCTACATCTGGGACCTCCT CCAGAGCGATCTGGGTCTG TCGCCAAACA	NM_018051		hypothetical protein FLJ10300 (FLJ10300)
L15	279	TCATGAATGTAATTGGAATAC CCCTTTGATTTTACTGGTGAC GTATACCCACTAGTGTACTGA GACGGAA	BI492977		cDNA, 3' end /clone=IMAGE:2485078
L16	280	AATTTTAAAAGGGCGCATCC CACACAAGAAGCCCAGTTGA GTTTGATGTCTGTGAATCAC GATATGTC	BM987252		cDNA /clone=IMAGE
L17	281	ACACTACCTCGACTTTAGCC CAAACCCAGATGGCAGAGTC TCCTCCAGGTGGGAAAGTA GCCATAAGCA	AI680858		cDNA, 3' end /clone=IMAGE:2272203
L18	282	TCCCATCTGGGAGACTGTAA ACATGGATTCCACTGTCTCG GACAGTGAGACGATCCCAG TCTTTTCTG	BF513645		cDNA, 3' end /clone=IMAGE:3070959

L19	283	CACCAAGGCTACGTAAGGCA CACCGCTAAGATATATCTTCG GTTTATTCTTTTTCTTATGAGT ACTAGA	AK024566		cDNA: FLJ20913 fis, clone ADSE00630
L20	284	ATTCCTTTAGGTTGCCACAG ATAGACGTTACCTGCAGCCA ATATACATGCTTGTGCTAGCA GAGGGATG	AI652777		cDNA, 3' end /clone=IMAGE:2310279
L21	285	TAGAGAAGTACAGTTCCTCC AGGATGTGACTGCTGTGTGC TGTGACCAGAAAGTAATTGTA CTCTACTAG	BQ189084		Homo sapiens cDNA, 5' end /clone=UI-E-EJ1-aju-l- 02-0-UI
L22	286	AATTCACCCAGCTCTTTGCC TGCAGGCTGATCCAGGGACT TAGAGCTTGTACCCAGTTAC AACTTCTT	AK027662		cDNA FLJ14756 fis, clone NT2RP3003193, moderately similar to ZINC FINGER PROTEIN 135 /cds=UNKNOWN
L23	287	ACTGCCTACATCCAGTGGCC ACATAGCCTGGGACCCTCCT TTGAAACATCCTTACAGGCT CCCTTCTC	NM_006958	ZNF16	zinc finger protein 16 (KOX 9) (ZNF16)
L24	288	ACAAGCAGCCTTCAGCCCAA GAGAAGTCTCTGTAACTCTA TAGGAAGCTTTTCTTTGGCGA TTCAGTG	AK054888	LOC58500	Zinc finger protein (clone 647)
M01	289	TGGTCAATAACTAAAATTG TTGCCATGCCCTTTAAGGGT CCCAATTTTTGGGAGTTTGG TAGCTTTG	W69913		cDNA, 3' end /clone=IMAGE:344264
M02	290	GTTCAGACTAGTGTGCTGT GATCATACTATCTAGCCTGGA CAACAGAGAGAGACCTTGTC ACAAAAAT	AU155388		cDNA, 3' end /clone=OVARC1001838
M03	291	AGAGGGCACCTCTGCTGAGG TCAGACATCTCCTTGATGTCT GTGATCAAACCATGACAGGA TGCAACCAC	NM_014066	HT002	HT002 protein; hypertension-related calcium-regulated gene (HT002)
M04	292	GAGAATACACACTAGGGCCC AGTGGTTTTACGAATATGGG AATGCCCTGGAAGGGTCCAC CTTTGTGAG	NM_003416	ZNF7	Zinc finger protein 7 (KOX 4, clone HF.16)
M05	293	GGAGGTGGCCGAATTGACAA ACCCATCTTGAAGGCTGGCC GGGCGTACCACAAATATAAG GCAAAGAGG	NM_033301	RPL8	Ribosomal protein L8
M06	294	TGTCAGGTAGTTTAGTAACTT TTCAGTACTGGTTAGGTA CCCCGCCCCCAATGCCAC CAAATATC	BF589631		cDNA, 3' end /clone=IMAGE:3253940
M07	295	TCACAACCTGGCGTGAATGC TTTTCTCCGGAGAAACTGA AGGCGGCGTTCTTGCGATTC AAGGGTAC	AK055720		cDNA FLJ31158 fis, clone KIDNE1000008
M08	296	AGAGATGGCTGGGCTCAAAA CCTGACCGAACACTCACGGA AAAAGCCCAGTTCTGTGAC CAGAGATGGC	BQ024665		cDNA, 3' end /clone=UI-1- BB1p-atm-d-09-0-UI
M09	297	TGTGAAGAGAATGCATTA TGTACCAGGTAACACAGCAG CAGGTGGCACACTGCAATTC AAATCCAGG	AW969060		cDNA
M10	298	CAAAGCACTGATGTAGGAGA TACACGGTACTTGGAGCAGT CAGCCAGAAATCACAGATAC TGCTTTCATC	AK074081	FLJ00152	mRNA for FLJ00152 protein /cds=UNKNOWN
M11	299	CCTCGGGATCCATCACTGCA GGATGTTGTGAAAAGTACTC GCGATGGCAGCCAGGTAGCA	BQ233723		cDNA, 5' end /clone=IMAGE:5769589

		AGCCCTTGCC			
M12	300	CCGTGACCGCTCAGACGCCT GCATGCAGCAGGCGTGTGTT CCAGTGGATGAGTTTTATCAT CCACACGG	NM_000718	CACNA1B	calcium channel, voltage- dependent, L type, alpha 1B subunit (CACNA1B)
M13	301	ATGTTTTACCATTTAAATAAT GGGGCCAGGCACGTGTGTC ACGCCTGTAATCCCAGCACT TCGGGAGGC	AA209434		cDNA, 3' end /clone=IMAGE:648350
M14	302	CAGGCCAGTCAGTGAGTTC CACTGAACCTTCAAATATAA ATTCCCTATAGAAATGCTCTC TAACTCA	AB058779	FLJ12879	Hypothetical protein FLJ12879
M15	303	AACAGGCAGTTCCGGCGAGG GGGGAGCCTCAGCAGGATTG CTGTGTGAAAACCGAGCTGC TGGGAGAAGG	AW628783		cDNA, 3' end /clone=IMAGE:2974682
M16	304	ATCATCCTGACACTCAGCAG TGATGCTGCAACGGGATAAT TGAGGGCTAGGCATGGGGG AAGCTCTCGCA	BF196963		cDNA, 3' end /clone=IMAGE:3528030
M17	305	CCGGAGTCACCCGATGATT ACTCTTTTCAGACACAGCGG TTTTTGTTCCAAGAAGCCAA AATTGTTT	NM_006624	BS69	adenovirus 5 E1A binding protein (BS69)
M18	306	TCTCATCCTCCCCACTAGAGT GGGAGCTTCTGAGTGCACAG GGTCCAAGTCTCGTCTAC AGCCGCCAC	AI244299		cDNA, 3' end /clone=IMAGE:1865867
M19	307	AGGCTCCACCTCCAGCATGT GCATTGCTCCCAAGTTCTTAA GTGTTGCTGACGGGAACATC CTTTGAGAA	H61890		cDNA, 5' end /clone=IMAGE:204132
M20	308	ATCTATTTGGGAGAGGAAAA GTCTCTTGCAATGGGAGGA ATACAGGGAGAGACTACACA CAAGCCAACC	AW297156		cDNA, 3' end /clone=IMAGE:2731329
M21	309	ATGCAGCTCTCCTTGAATGTC TGATACATTTTCATCCTTTAA AATGAAGCCGATGGGTGACA GGAAGCG	AA047791		cDNA, 5' end /clone=IMAGE:380267
M22	310	GCACCGGCCTGGGACCTCTG CTGTCCCGTGTAGGGGTGCC CTGCAAATATGTGATGAATAA GTGAAGAAA	AW976645		cDNA
M23	311	ATTCTTCAGTCAGTCCAGGA CAGACGAGTTCTCTAAGATG CAGTTAATCATACCTGTCTTA AACAAACTG	NM_130784		hypothetical gene supported by AY027807; AY027808 (LOC93426)
M24	312	TCCTTTTAGGGGCTTGGGAC TGGCCTGCAGGAGGTTAGTG TCCAGGGTGGGAATTAACAC CCATCCCCAT	AW063892		cDNA, 3' end
N01	313	ATCCCACCACGTTACAAACTC TGTGTCATTCGCCGCTCATG AGTGTGTGGAGGACACCCTG AACCCCCC	NM_000773	CYP2E	Cytochrome P450, subfamily IIE (ethanol- inducible)
N02	314	AGATACATCTACAGGGCACC ATTGTGGCACCTTTTGTAA TAAATAGTTGGGAAACCATT TGAATTGT	AA932853		cDNA, 3' end /clone=IMAGE:1570267
N03	315	ATCTCAGCCCAGGACGCCAA GCAAGCAGGTCTTGTGACGA AGATTTGTCCTGTTGAGACAC TGGTGGAA	NM_004092	ECHS1	Enoyl Coenzyme A hydratase, short chain, 1, mitochondrial

N04	316	GTATCCACAGTGCCCGAGTT CTCGCTGGTTTTGGCAATTAA ACCTCCTCCTACTGGTTTAG ACTACACT	NM_021932	RIC-8	likely ortholog of mouse synembryn (RIC-8), mRNA
N05	317	TCCCTGACACCAGTAAACC AAAAGGACTCTGGGGGCTC AGTGTGAGAGCCAGGGTTAC CTACTCTGC	AK022958	LOC51238	cDNA FLJ12896 fis, clone NT2RP2004194, weakly similar to Rattus norvegicus Golgi SNARE GS15 mRNA /cds=UNKNOWN
N06	318	GATTTGCCTCTGGTCCAGTTT CTCATCTCTGGACTGCAACG GTCTTCTTGTGCTAGAACTCA GGCTCAG	AK026897	LOC60626	Hypothetical protein from EUROIMAGE 1987170
N07	319	TGGGAAGCTTGATGGACCAG ACAAATAGGATGATGGCTGC CCCCACACAATAAATGGTAA CATAGGAGA	NM_012239	SIRT3	Sirtuin silent mating type information regulation 2 homolog 3 (<i>S. cerevisiae</i>)
N08	320	GTTCTTGCTCTAAAACAGGA CTGTCCCTGATGGGAGCCAG GCCACAGGGAGGAGGCTTCT TTGTGGGT	NM_002817	PSMD13	Proteasome (prosome, macropain) 26S subunit, non-ATPase, 13
N09	321	TCTGTGGAGCTGAGCGAGCA GTCACTACAGGAGCTTCAGG CTGTGAAGAGAGCAAAGCCG GATCTGGTCA	NM_138329	PYPAF5	Homo sapiens PYRIN- containing APAF1-like protein 5 (PYPAF5)
N10	322	TGCTGACTGAAAGTGTGCTGAC GGAGTTCATAAGCTAGTCAG GGGCCGCAGCTTTAAGGCTG GTTCTGGTC	AW665857		cDNA, 3' end /clone=IMAGE:2979994
N11	323	GCGGTGGTGGCTTTCCTGAG CCCTGTTTGTCTAATGTAGGC CCGGTTCGCACTGTTTCATTC ACTCTGCTC	BM055176		cDNA, 5' end /clone=IMAGE:5674412
N12	324	TCTCCCTAACACTGACAATCG AGCTCTTTTCATGTGTTGCCT GGGGAAATCTCAGGCAATGA ATCTTATT	A1867771		cDNA, 3' end /clone=IMAGE:2307946
N13	325	TAGCAAAGCAAATGGACGAA GACAGAGGACTCTGGTTGAG AGCTCCGATTCTCCATCTTCA CACTTCTCA	A1373619		cDNA, 3' end /clone=IMAGE:2030602
N14	326	AGCCACCCAAGCTTTCCTTACA TCACTCTGTCTACACATAAGC TGCAGGTTGTCACATTTGACA AATTGTT	AA164928		Homo sapiens cDNA, 3' end /clone=IMAGE:632364
N15	327	TAAACTGCATTACCGAATAC CCTGGACTAGAGAAAGCTTA GATGTTCTCTGTTGGCATCTC TCACTTGTT	AA829703		Homo sapiens cDNA, 3' end /clone=IMAGE:1415064
N16	328	AATAAACAGATTGAAATGCTA GAACATAAGTACGGCGGTCA CCTGGTGTCCCGGCGCGCC GCTTGCACCA	BI712372		cDNA, 3' end /clone=IMAGE:5086346
N17	329	CTCCTGATTTGATCCATTTCGG CCCCAACTCCAGAGTCGGGA ATGGGAGATGAAACTAGTTTT CCACCCA	AB029033	KIAA1110	mRNA for KIAA1110 protein, partial cds /cds=UNKNOWN
N18	330	GGGTCTCAAAGTGAAGTATG CATTGGGATTGCGTGGCGGG GTTTATTAATGCACGGATTGC TGGGGCCCC	BM805297		cDNA, 5' end /clone=IMAGE:5728585
N19	331	CACCCGGGGGATGCACGATC ACACAAACCCACGCAGTGAT GAATGTGCACATACAGCAGC TTCTGTGAGC	A1026900		cDNA, 3' end /clone=IMAGE:1644783
N20	332	GGTGGAGGTATTAATCAATG CCTCCCCAGCCCAGACTCACC	N73382		solute carrier family 6 (neurotransmitter)

		ATTTTACCAATTTCAAGAGAT ACAATTA			transporter, GABA), member 13 (SLC6A13)
N21	333	GATCCTTCCTTAGGCTTAACG ACAGAGGCAAGCCTTTGCAT GCCGTCAGTCTGGAGTTTCC TCCGAGTCT	NM_003044	SLC6A12	Homo sapiens solute carrier family 6 (neurotransmitter transporter, betaine/GABA), member 12 (SLC6A12)
N22	334	GCTGAGCTGGAGGCCTCCCA CTGCAACTTTTCAGCTCAGG GGTTGTTGAACAGATGTGAA AAGCCAGT	NM_016615	SLC6A13	Solute carrier family 6 (neurotransmitter transporter, GABA), member 13
N23	335	GTATCAGGAAAACCCAGAGA GACATTTGAGGCATCAGCTT ATTCATACTGGAGAAAACCC TATGAGTG	NM_015394	ZNF10	zinc finger protein 10 (KOX 1) (ZNF10)
N24	336	TCTCGGAGACCTAACTGCAG TCATTTCTAACCTAATAACAC TTGTTGGCTGGCATTCTGGG TGACATCCT	AA844106		cDNA, 3' end /clone=IMAGE:1388347
O01	337	GCTTGGTTAGGACTGGAATT TACACTCTAATTTTGCCCGAG TGATCTTGAACAGATTGAG CATCTCAA	AI185207		cDNA, 3' end /clone=IMAGE:1742100
O02	338	GCATGCTGCTTGATTTCGAG TCAGACTGTACACTATTGTAA GATAAATCAGCCTCTCTGAAA CAACTCTT	BQ441574		cDNA, 5' end /clone=IMAGE:6105847
O03	339	ACTCTTGGAAAGAAGCCTTAT GTGAAAGTGATGACTGTGAA GTAATATGGCCACACTTTAT TCACCAC	NM_003440	ZNF140	zinc finger protein 140 (clone pHZ-39) (ZNF140)
O04	340	CGTCCTCCGCTCTTTTGCGC ACGGTCGCTAGAGGTTCTGG GAAGTGATGTTGCCTGAAGC TCGTGTTCTT	AI300487		cDNA, 3' end /clone=IMAGE:1908956
O05	341	CAGAAGTCAAGTCTCTTAAG CTATTAGAAATATCCACTGG GGATGAGGGAAAACCCCATG AATGCGGG	NM_003428	ZNF84	zinc finger protein 84 (HPF2) (ZNF84)
O06	342	CCATATCTTGTTCCTAACTCC TCCTAATATTCTACCATTAAG AAGCACACTGGCTTTACGGT TAAAATCC	AI811226		cDNA, 3' end /clone=IMAGE:2265245
O07	343	CATTGATTGACATGAGCACC CCTGTTTTCTCTGGAGAAATA CCTCCCCTCTCTGGGGTGCT TCCTGTGG	NM_019591	ZNF26	Zinc finger protein 26 (KOX 20)
O08	344	GAAAGACGGGAATGATGTCC CATACTCCCCAGCTCTAAA GTGTTATGCTGTACAATTA ATACCCC	AK027873		cDNA FLJ14967 fis, clone THYRO1000242, moderately similar to ZINC FINGER PROTEIN 84
O09	345	ATTCGTCCTCGGGGAGAAG AGACCCCAAGAGTGTTGAGC AGCCCATCGTGCTTAAAGAA GGGTTTCATG	NM_007368	GAP1IP4B P	RAS p21 protein activator (GTPase activating protein) 3 (Ins(1,3,4,5)P4- binding protein) (GAP1IP4BP)
O10	346	CTGCAGGAAGAGAATCACAC TCTTTAGACCGGGGTCTCAG ATTTAGCCGGACGGGAAT CTCTGCAGGG	AA666317		cDNA, 3' end /clone=IMAGE:859187
O11	347	GTGTTGGTAGATCTGTTTGGT GAGGGTCTCGGTTTTTGA AACAATTTAGGGACATATGTT AAGATGCT	BF197414		cDNA, 3' end /clone=IMAGE:3134783
O12	348	ACCGTAGGACTGCATATCCC CGGGGGGTCCAGGACAGGA AAGCTGAAATGCTTTTTGAGT	AK000385		cDNA FLJ20378 fis, clone KAIA0536

		GGGGGCGTGG			
O13	349	TTATAGCCCGCATTAGGCTTC AGACAGGTGAGTAAGGCCAT CATAGACCCTCCAACCCAG TCAAGCTGC	BE674181		cDNA, 3' end /clone=IMAGE:3278904
O14	350	CATGAATCCTGCCATTGGGT AATTTTAAAGACCTTGTGTAA CTTCGAAGACCTTGCCTACT ACTCCTAAT	AI218886		cDNA, 3' end /clone=IMAGE:1841663
O15	351	TGAACGTGTAGTGACATGC ACGAAGTTAATTTACTCATG TCCACGGGGGACGTTTAGAG GGCACGTG	AK056653		cDNA FLJ32091 fis, clone OCBBF2000824, moderately similar to THREONYL-TRNA SYNTHETASE, CYTOPLASMIC (EC 6.1.1.3) /cds=(45,2168)
O16	352	TTCATACCTAATGGGGGCCA CATGTTTTCTCTGTGCTTAGG CAAAGGTGAGAAACGCCATG TGTCTCGTG	BM968250		cDNA, 3' end /clone=UI- CF-DU1-aao-o-14-0-UI
O17	353	AGAGGTGAGAGAGATAACTG ATGGTTAGTACTGTGTTTTTC CCCCTATAAAAGAACATATAG GCTGGGTG	AW769221		Homo sapiens cDNA, 3' end /clone=IMAGE:3005055
O18	354	TCTCTTGACTTCTCTGGGGCT AATCCATATTCGTAGACTGCG AGAGCATAAAGTGAATTATAC CGTGCTT	AW003500		cDNA, 3' end /clone=IMAGE:2476255
O19	355	CTACGGCATCCGGAATCGAG ACGAGGTTTCTTCATCAAAA AGCTGAGGCAAAAGTGAGCC TCCAGACA	NM_024571	FLJ22940	Hypothetical protein FLJ22940
O20	356	GAAAGTCACTTCCCTGCTG AATGTCTCCCACCCCGCC TGCTACTGACTACAGGATCTT GCACTGCC	AK056708		cDNA FLJ32146 fis, clone PLACE5000115
O21	357	AACCAAAGCAGTTTTGCCGA CGGATGGGGCAAAAGAAGCA GCGACCAGCTAGAGCAGGG CAGCCACACA	NM_002434	MPG	N-methylpurine-DNA glycosylase (MPG)
O22	358	GAATGTGCAGAAACACTTGT GTGGCCTGTCCTGTCTCTC TGACAGCCTTCCATTTGTGAA GTGCCCTG	NM_012075	CGTHBA	Homo sapiens Conserved gene telomeric to alpha globin cluster
O23	359	ATGTCTTGACCAAGACTGA GAGGACCATATTGTGTCCA TGTGGGCCAAGATCTCCACG CAGGCCGAC	NM_005332	HBZ	Homo sapiens hemoglobin, zeta (HBZ), mRNA
O24	360	GACAAGTTCCTGGCTTCTGT GAGCACCGTGCTGACCTCCA AATACCGTTAAGCTGGAGCC TCGGTGGCC	NM_000558	HBA1	Homo sapiens hemoglobin, alpha 1 (HBA1), mRNA
P01	361	TTATTCCTGCCCTGGGACC TCTTCTGAAACGTAGCTGGG TGCGAAGAATCAAATTGGAA ATTATGGAAT	BC021245		clone MGC:20817 IMAGE:4334866
P02	362	GTCCTCGTAGAGTCTATTGCT GCCTGGACACCTTTCTTTTG GGAGCTCAAAGCAAGTGAGC TCACCTAC	NM_001481	GAS11	growth arrest-specific 11 (GAS11)
P03	363	GAAGCGGACAGGGAGACGG GCAGCAGCTCACATGCTGGG ACAACGCAGTGTTCAATCCAT TCTCCATCC	NM_001214	C16orf3	Chromosome 16 open reading frame 3
P04	364	TCCCCAAATGAGATTCAAATC TGGGCAAACACTCTATCCCC TGGGCCTCACTACCCCCACC	AA815423		cDNA, 3' end /clone=1375333

		CGCCACCT			
P05	365	AACCAGTCGTTGGGTTATTGT TGGAGCAGAAATCCCTGAA GTCCCATAGGAAGCCTTCCA CAATTGGGC	AI366786		3' end /clone=IMAGE:1935582
P06	366	ACAGCCACCGGCATAGGCCA ATCTCAGCCAGAGAGAGTGA ACTGGGACACCATTACAGTG ATGGGCCAG	NM_024992	FLJ12547	Hypothetical protein FLJ12547
P07	367	TCCATTCCCTCCTTAGCTCAG AACACCAAATATCACCAGACT GCCTAAGAGACTTGATGACA CCTCCCG	NM_024043	MGC3101	Hypothetical protein MGC3101
P08	368	CATCTTGCTGCCGACACCCT GCTTTCCCATCGCCCTAGG GCTCCCTTGCCGCCCTCCTG CAGTATTTA	NM_006086	TUBB4	Tubulin, beta, 4
P09	369	CAGAGGTGACCGAAAAGCCG TATGATGATGTTCCCGATTTT TCTGTTGGTCCGAGTCGGCC AGTTGCCT	NM_014972	KIAA1049	KIAA1049 protein
P10	370	AACCGCCGGCCACACTGGTC ACAGGCAAAGTCCAGCTCAG TCTCAGCCTTGTGTTTGGTCA TGTGGTAC	NM_000135	FANCA	Fanconi anemia, complementation group A
P11	371	GTA AACCTGACGGTGGGCC TGGCACACGCCTGTATTCCC ACACCAGGTCTTCCGATCAG TGGTGTCTG	NM_003674	CDK10	Cyclin-dependent kinase (CDC2-like) 10
P12	372	GGGGTCTGCCTGGCCTGTG GGTTCTGCCGGTGGGGCTTC AGGAGTAATAAAGTGCACC CTATCCTTGT	NM_014427	CPNE7	Copine VII
P13	373	GAGTGAACCTCCCGATGCAT GGACTCTGGCTGTGCTCGAC GCAGACTCTCGTGCATGCT TAACCCCGTT	BM703179		cDNA, 5' end /clone=UI-E- CL1-afd-a-05-0-UI
P14	374	ATGGGTAAATTGGCACATGC TTCACCTCAATGATTCCACAAG CCCTGGGGGTGAATGAGACA CAGGCCT	NM_003585	DOC2B	double C2-like domains, beta (DOC2B)
P15	375	CACAGGTACAGGGCCTTGGC AGGCTCAGCGGTGAGGACGT CCAGGTCTCATCTCCAGTCT GCCTCTTGT	BM702416		cDNA, 5' end /clone=UI-E- CQ1-aez-e-05-0-UI
P16	376	TCTCTGCCTGCTGGAACCT TCTGGGGCTCCCAGGGTCTG GGGAACAGTTCGAAGACCAC TGGGTCTAAG	BQ186063		cDNA, 5' end /clone=UI-E- EJ1-ajn-k-03-0-UI
P17	377	CTGAACCAGAAAACCTCCC CTAGAGTTTGGGGCTGGCG TGCAGCTGCTCACATTTTAT CTTGCTAAA	AI825739		cDNA, 3' end /clone=IMAGE:2310904
P18	378	CTCCGTTGCTATATTAATGGC AAGACTAAATGAAACCTAGG GCACGGCCTCCGAAGCTGC GTGTGGCCC	NM_006987	RPH3AL	Rabphilin 3A-like (without C2 domains)
P19	379	CACACACCCGGCAGCCTGAG CTATGTGGCTGACAGGTGCT CATGACTAACGTGTCCTCGG AAGGGCACC	AK054757		cDNA FLJ30195 fis, clone BRACE2001374 /cds=UNKNOWN
P20	380	GCACCAGACACTCACAAAGG TGACTTTGTGCCCGTGAAC CGGCTGCAGCCCACAGTTT GCCTTGCTGC	AW063448		cDNA, 3' end

P21	381	GAAATAATTACAGGGGGTC AGAGTCAGGAATCCTGGATA AAACGCCAAATCCATGATCCT AGTTCAGC	AW072307		cDNA, 3' end /clone=IMAGE:2566992
P22	382	ATTGCCTGTAGTCTCATTCC ATTCCGAGTGCCCCAGGGA GAGTCAGCCACCTTATGTAG AGAGGCAA	U79265		Human clone 23614 mRNA sequence
P23	383	CCCATACCTCACCCCTGCCT GGTGAGGATGTCTTGTTCCT GAGGGAGGCCGGTGTGGAA AGCCTTGAC	NM_005993	TBCD	tubulin-specific chaperone d (TBCD)
P24	384	CTTCTCTGGAAAGAGCTGG TCCTCTCATGATCCC GCCGC ATTTGTGCGGGTTCATCTATA AAACGGAG	AK054838	FN3K	Fructosamine-3-kinase
Plate: Telomeric Array 2					
A01	385	AGCGTTGTCCACTTTGTGGG GCTTTGTAGGTAGACGGAGC CACACTACAGGCAGGGTATG AGCAGAGGG	NM_024619	FLJ12171	Hypothetical protein FLJ12171
A02	386	TCAGTGCTGCTGTCCATCCC ATGGAAACATGGGCACAATC AAGTATTTGTCCAGCCTATTG CAGGCTTT	NM_005151	USP14	ubiquitin specific protease 14 (tRNA-guanine transglycosylase) (USP14)
A03	387	AAATTAAGAGAGCCCAAGGA ACTCCCGTTCTTTACGTTTTA TGCATAAAAGCCAATTCGCA CCAATGAAT	BG196289		cDNA
A04	388	ACGGATTCAGCTCTTTTGGC CAGGCTTTTCCCTCTGTCTGA GAAATCAGGTCTTAACCTGCA GAGTCA	NM_005131	p84	nuclear matrix protein p84 (P84)
A05	389	CAGGATTCAGACGCAAGCTT TGAAAATGTTCTAATTTCTTT AGAAGGAAGGGCCCTTCTTA ATAGCACA	AW444448		cDNA, 3' end /clone=IMAGE:2733635
A06	390	TGCACATGGACTGAATCACA TAGATTCTCCTCCGTCAGTAA CCGTGCGATTATACAAATTAT GTCTTCC	NM_030781	COLEC12	Collectin sub-family member 12
A07	391	ACAAGTCTCAGACCTTGCGA TTCTACGATTGCAGCGCAGT GGAAGTCAAGAGCAAGTTTG GGCGGAAT	NM_032510	Par6	Homolog gamma (C. elegans) (PARD6G)
A08	392	GACAGTTGCAAGATGACGGA GCCCTGCGACCAGGAACCTG ACTCTTCAGCTCAAATCTTGG TTTGAAGG	BF197266		cDNA, 3' end /clone=IMAGE:3528059
A09	393	TCTGTGAGGTCACCTGGATT CACTGCAGCCCGCAGTTCC TCAGAGCGTCAACATAGAG TTGCCCTAGG	U55964		cDNA /clone=45432
A10	394	TATTAACCTACTTTAGGGTCC TGTTTCTGGACTCAGTGGAC TCAAGTGTAGCCAGGTCCAA TCTGTGCAC	AK056304		cDNA FLJ31742 fis, clone NT2RI2007214 /cds=UNKNOWN
A11	395	TGCCTAGACAACGAGAAGGC CCTAGCACAGGCTCTGGCAC ATGCTCCAGGCAGCAGGGTT AATGCACCCT	BE674650		cDNA, 3' end /clone=IMAGE:3282050
A12	396	GTGTTCAAGACGCTGGGTAC AAACCCTGTGATGTATGTATA AGGCTCCCTGAGGATGCACT GCATTAAC	NM_014913	KIAA0863	KIAA0863 protein (KIAA0863)
A13	397	GAGTAGATGGAGAGGCTCTG CCCATCCCACATTTGCAGGG	NM_024805	FLJ21172	Hypothetical protein FLJ21172

		AAAAGCATTGGCACGCAACG CAGCATGTG			
A14	398	TTGATAACATGGTCTTAACTC ACCGAAATAACAAGCACGT GGTGAGAGGAGCAGGCCTA CTTGTTTGT	NM_006701	DIM1	Similar to <i>S. pombe</i> dim1+
A15	399	GCCCTCAGTCTCGGTCCACG CTGCTTTCTTCCAAAGGACA TGTATATTTGCAGAGCTCCAC ATACAGA	NM_004715	CTDP1	CTD (carboxy-terminal domain, RNA polymerase II, polypeptide A) phosphatase, subunit 1
A16	400	GAGGAACTGTCTCGGCCCAA GAGATTCTACCTGGAATATTA CAACAACAACAGGACGACTC CTGTCTGG	NM_016585	THEG	testicular haploid expressed gene (THEG)
A17	401	GCGCTGTATGTGCAGGCACG ACTCTGTTGGAAGTGGGCAC GGCTGCTGCGACCCACAGTC CAGTTCTTC	NM_003712	PPAP2C	phosphatidic acid phosphatase type 2C (PPAP2C)
A18	402	GACTTTATTTGCAACTGTGGA CGGGAGTATGGCTCAAGGGC TGGCCTTGATCTCACCTGAC TGGACATTC	BF000499		cDNA, 3' end /clone=IMAGE:3317433
A19	403	ACAACTTTTAGCCCATTTGG ATGAATAAAGAAAACCTGATTG CCGGACCGTGTGATGAGACC GTGTTTA	AB033019	KIAA1193	KIAA1193 protein
A20	404	CATCATGGCAAAGACTTGG TGCGCACCCGGCGTTATGTG CGCAAGTTTGTATTGATGCG GGCCAACAT	NM_014453	BC-2	putative breast adenocarcinoma marker (32kD) (BC-2)
A21	405	GCCGTGTCTGCCAGAAGCCA GGCGATCTGGTTATGTGCAA CCAGTGTGAGTTTGTTCCTCA CCTGGACT	NM_005762	TRIM28	tripartite motif-containing 28 (TRIM28)
A22	406	ATGTGTTGATGCCACCTGTAT GTGCAGGTGTGACCTCAGGT GTGTGAGTATCCCTCATACC CCTTATCAT	NM_138781		similar to envelope protein (LOC113386)
A23	407	ATATATGGGGGCTGGGCCTC GGGACTCTCGCTCTAATAAA GGACTGTAGGCCATGGGGC CTAAACCACG	NM_032792	FLJ14486	Hypothetical protein FLJ14486
A24	408	AGAACGTGTCCACGCACGAG GTGGAGGGCGTGTTCGCA GGTGACTTCTTGCAACAGG TTAACGTGT	NM_012254	VLCS-H2	Very long-chain acyl-CoA synthetase homolog 2
B01	409	GTGGAGCCCCACATGTTCCC TGAAGAGCCCTGGCCCTTTC ATACAACTGGACTTGATCCT CCCACGCAC	AA745270		cDNA, 3' end /clone=IMAGE:1283013
B02	410	ACCTGGGATGACTACTAGCG TCTTCCCTGTTGCCGGTGCC TGCCACAGTGAAAAAGCCT GCAGAGACA	NM_014347	ZF5128	Zinc finger protein
B03	411	TGGTGAGGTCTCCCTATTCT GTTGCTTGGCTGGTCCCTAT CCTGCCAATAGTAATGGGCC CTTCTTCA	NM_003433	ZNF132	Zinc finger protein 132 (clone pHZ-12)
B04	412	GTAGGAACAAGCTATCATGC TGCATTTCTATAATACACAT GAATATACTCGACGACCAGC ATTTCCTGT	NM_153325	DEFB125	defensin, beta 125 (DEFB125), mRNA
B05	413	CCTTACTCACTGCCAACTGA TTTGGACCAGGATTTCACTCT TTATTCTCAGCAGTGAAAATG CTGCATT	BQ011406		cDNA, 3' end /clone=UI-1-BC1p-asc-e-01-0-UI

B06	414	AAACCTGAAGAGATGCATGT AAAGAATGGTTGGGCAATGT GCGGCAAACAAGGGACTGC TGTGTTCCA	NM_030931	C20orf8	epididymal secretory protein ESP13.2 (ESP13.2) (DEFB126)
B07	415	ATCATTGCAATTCTGCTGTTT CAGAAACCCACAGTAACCGA ACAACCTAAGAAGTGCTGGA ATAACTATG	NM_139074		defensin, beta 127 (DEFB127)
B08	416	CAACAAAGCATAGCAGCTGG TCCCAACTACCCTGAACAAA CCTATCTAACCTCAGGACCC AAACAGTGG	AI954794		cDNA, 3' end /clone=IMAGE:2473057
B09	417	CTATCTTTGCCAGCCTCATGC TACAGTACCAGGTGAACACA GAATTTATTGGCTTGAGACG CTGTTAAT	NM_080831		defensin, beta 129 (DEFB129)
B10	418	GACGTGCTGGCCGTGCCGG TGAAAGTGACCGACAGGTTT GGGATCTGGACCGGGGAGT ACAATGCGAG	NM_033089	C20orf99	Chromosome 20 open reading frame 99
B11	419	GTGGAACCTTACACAGCCGA GCCTTTGTGTTTCACTATTT AGGATGCAAACCTGAGCAAG AACTGATAC	BF509219		cDNA, 3' end /clone=IMAGE:3086431
B12	420	CACCTTGTCTCCACCTCCA TGCTTGTATGGCTGCCTTTAT TCAGACCGTGGTGACTTGGG CTTGGGTCT	AL137285		mRNA; cDNA DKFZp434D2416 (from clone DKFZp434D2416) /cds=UNKNOWN
B13	421	ACCCTCTTAAGAAAGGAAG CTTAAGACTATACCTTGCTGT TGCACTTACAAGCAGGGAT CTGTTGGGG	AI684833		cDNA, 3' end /clone=IMAGE:2303035
B14	422	GTTCTGCCCTTCTTCTTTT GCTGGCGTCTACAGCAACGA GCTGCAGGTCCCAAGCTGTG GGCTGAGC	NM_005286	GPR8	G protein-coupled receptor 8
B15	423	CAGAACCTCCGCATCGTGTA GTTTTGTGACATAAGGAGAC CTCCTACTTGAGCTGTCTGTA CCCCAGAA	NM_005873	RGS19	Regulator of G-protein signalling 19
B16	424	AGCTAAGGTGGCGATGTATG CGATGGGACTCTGCATGGGA TAGTACAGTTGTGTAGACGT CTTCCAAT	NM_001535	HRMT1L1	HMT1 hnRNP methyltransferase-like 1 (S. cerevisiae) (HRMT1L1)
B17	425	TCCTCAGTCATAAATGTGATG TGCTTCCCTTGACTTGGGAC CTTCTGAAGGATGCAAGGTG GACCAAAG	AJ003313		cDNA /clone=MPIp145K22
B18	426	ACCTAGCTTCAGTTCAGATA AGATGGAGAAGGCATACTCC TTTCATGTCTCCCACTGAATG CAGCTAT	AK055950		cDNA FLJ31388 fis, clone NT2NE1000023
B19	427	TCTAGCTTTAGTTCTACTGCA ACGTTTACAGAGCAGGCCATA GTCTTACAGGCCAGAGCTCC TCTGTTGTA	BM682781		cDNA, 3' end /clone=UI-E- EJ1-ajf-g-02-0-UI
B20	428	GGGCTTGCAGCCTAGTAGGA GCTGAGCTTCCAGCCGTGT TGTAGCTAATTAGGAAGCTTG ATTTGCTT	NM_006272	S100B	S100 calcium binding protein, beta (neural) (S100B)
B21	429	ACATTATTCAAGCAAGTTAGC ATGAGGCAAGCCTAGAGCTT TTACACAGGGCTGGATGTTG AGCAGAGAG	AW293016		cDNA, 3' end /clone=IMAGE:2729239
B22	430	CGGGACTCGCCCTTCTGTG CTCTTACAGATCCCTCTCAAC AATCCCCGCATCTCCTTTAG AAAGCACT	AF490768	KIAA0184	KIAA0184 protein mRNA, complete cds /cds=(88,4791)

B23	431	ACCTTTATGCATGACTGCAAA GCCAGCTGGAGCATTTTCTA TGGAGCCTCCGATGTTTTA GGCCCATG	NM_006031	PCNT2	pericentrin 2 (kendrin) (PCNT2)
B24	432	GGGGTGTACCTGTGAGAGCA CCCTGTCTCCTCTTCCAAAGA AAGTCAGAGGCCATCCTGCA CCCTGGGT	AB051437	ProSAP2	mRNA for KIAA1650 protein, partial cds /cds=UNKNOWN
C01	433	ACATGAACCCATCCAGAGAT CAGAATTTTGCAGGAAGTACT GAGTAAAAGAACAGACATCA CGTAGGGGT	AI198827		cDNA, 3' end /clone=IMAGE:1753849
C02	434	TTCCTCTGGCGGCTTGGAGC ACACTGACTCCTTTTCTTTTG GGGGATCTGCCACTAAGTCC CTATTTCCC	BG820812		cDNA, 5' end /clone=IMAGE:4934124
C03	435	GCCGTATCCCAGCGGCAGAG AGCGCGCGCGCTCCATGATC ATCCTGCAGG	AI857655		cDNA, 3' end /clone=IMAGE:2423212
C04	436	GTTCAGGGTGGAGAACAGCT ACCAACGTCCATTGGGCTGA CGTGGTCAGAATTTTACCAT AGCTATTCC	BF510814		cDNA, 3' end /clone=IMAGE:3088078
C05	437	CGTCCTACCCAGACGAGGTC CGTGGGGTTTTTGTGTGCG GACTGGAAAGTACAAGGCTC ACTTCTTCA	NM_000487	ARSA	Arylsulfatase A
C06	438	TTTTATAGTGAATCTCAAGGG ATCATCCCATCCTTGACCACA GGGACAAGAGGGGCCCCCT CGCCCCAG	NM_012324	MAPK8IP2	Mitogen-activated protein kinase 8 interacting protein 2
C07	439	CATTGACGACATAGCGGCC CCGGTCCGGTTACAAATAC ATCTACAGATATTTTCAGGGA TTGCTTCA	NM_000451	SHOX	short stature homeobox (SHOX), transcript variant SHOXa
C08	440	GGCCACGTCAGCAGTGGG AGCATCTGTGGATACCGCAG AGTCTGGGACAGCTGGGC GTTTAACCGAAA	AW291358		cDNA, 3' end /clone=IMAGE:2724337
C09	441	TGGGAAAAGTGTTCATTCT GGGAAAAGCCCAAACCGAAT ACGGTCAGCAGTCAACTCCA GGGTTTGG	NM_005638	SYBL1	synaptobrevin-like 1 (SYBL1)
C10	442	CTGATAGCATGTAAACAGATT GAACACTTGGTGTAGGTCGT ATGTGCCTTTAATCTGAGGTT GGCCTCAG	BM685155		cDNA, 3' end /clone=UI-E- EJ1-ajl-b-16-0-UI
C11	443	TAGGCCAGAATTCTTGCTTT ATAGTACACTGCTTCTATCTC TACCCTATTCCCTCTGAGC CTTTGCT	AI659452		cDNA, 3' end /clone=IMAGE:2252580
C12	444	CATAAATACTATCTTCAACTT AAAGAAAGAAGATTTGAGGT GCAGTAGTGGGAGCTAACC AGCAAAAAG	X92108	Subtel	mRNA for subtelomeric repeat sequence
C13	445	CATATACCTTGGAGGGACCA TGCTATGAGGGAAAGTGTA ATCTAGAAATGAGAAACCCCT AGGGAAAA	AF317549	ZNF268	Zinc finger protein 268 (NM_003415)
C14	446	ATCAGCAACTCAGCCTACGG CAAATTCGGGAAGCTCTTCC AGGATGAACGGACGCCACA GAGGCCTG	NM_012227	PGPL	Pseudoautosomal GTP- binding protein-like
C15	447	ATAAGATAGTTATACATAGCA CCATATGGGAAACTGCAGTA TGGAGTTTCTCCCATGGGGA GGTTATCA	AK055180	PDCD2 (RP8)	Programmed cell death 2 (RP8)

C16	448	GCCCTCCACCCTTGATGAG GGACTCTTTCTCCGACGCCA GGAGGCTGCAGCCACAGTG CAGCTGTTTCA	in AY028079	FRG2	FSDH region gene 2
C17	449	TTGGCTGCTGATGTGGGCAA GGGCGCCGCCAGCGTGAG TTCCATGGTCTGGGCGACTG TATCATCAAGA	J04982	ANT1	ANT1
C18	450	GTCCTTCAGATAGCATGTACA GGTGGCAGCATAGGGCCTGT CCCTAGTGAGAGTGCAGGGA ACTCAGCAC	XM_088704		Distal X ORF
C19	451	GCCTGTACCTTAGAATCACAA CCAGCTGCAATTCAGGATG GAGTTCAAATAATTGTGGG GGCATGTGC	NM_145177	DHRXS	DHRXS
Random controls					
C20	452	TGGGGAGAAATCTCGTGCCC AAACCTGGTATGGATCCCT TACTATTTAGAATAAGGAACA AAATAAAC	NM_000015	NAT2	N-acetyltransferase 2 (arylamine N- acetyltransferase)
C21	453	GCTTTGAACCTGGAGCCTTC GATGGCCTGAAGCTCAACTA CCTGCGCATCTCAGAGGCCA AGCTGACTG	NM_001711	BGN	Biglycan
C22	454	GCCTGAAGAGTCCTGAAT GAACCTTCTGGCCTCCACACA GACTCAAATGCTCAGACCAG CTCTTCCGA	NM_001838	CCR7	Chemokine (C-C motif) receptor 7
C23	455	CTGCCATCCTGGCTACGGTC TTCCAAAAGTCCGTCAGACC ACAGTTACATGTACGGAGAA TGGCTGGTC	NM_021023	FHR-3	Complement factor H related 3
C24	456	AGTTCCTAGTTAACACCAAT GGAAGTGGGTTCACTTCTGAA TCCTGGAGGAGCTTCTCGT GCCACCCA	L78132	LGALS8	Lectin, galactoside-binding, soluble, 8 (galectin 8)
D01	457	TGCTTAACTGTTGCTCTGTCA AAACAGCTATGCAGTGGAGT TGCATTTGATGTTCTAGAGTT TGATTAC	AB014733	AF140225	Hypothetical protein AF140225
D02	458	GAAAGGTTGAGAAAGGAATG GTTTGATATTTACCACAGCGC TGTGCCTTTCTACAGTAGAAC TGGGGTA	NM_012328	DNAJB9	DnaJ (Hsp40) homolog, subfamily B, member 9
D03	459	ACACTCGTGCGTGTGCGCGC ACACAGAGCTTACCTGACTT GCTCTGCTTGAGTCATGCAG TTACAAAAA	AB029551	RYBP	RING1 and YY1 binding protein
D04	460	TGTGTGAATATGATGTGTGCA CATGCTTAATGAGCGTGCAA GTGTGCACACGTTTGTGGAG AGGAGGGT	AK021925		Homo sapiens cDNA FLJ11863 fis, clone HEMBA1006926
D05	461	CAGATTCTCAGGCCTCAACC GTACACCACCCCCACACA CGTACTAAATCAAGAATATGT GCAGAAGG	AL137294	ATP11	Hypothetical protein FLJ22351
D06	462	GGAAGGTAGTAACTTCAAAA AGAGGGGGAAAAGGGGGAA TCAGTATAATGCCACTGGAT CAGTTCTCA	AF131770		Homo sapiens clone 25153 mRNA sequence
D07	463	ATTGGGTAGTCCCTGATTT GGAGCCAGCTGTTTCCAGTT GTTACTGAAGTTATCTGTGT ATTTGGAC	L21934	SOAT1	Sterol O-acyltransferase (acyl-Coenzyme A: cholesterol acyltransferase) 1
D08	464	AAGACATGAAGCGGTATAAA CTGAGAAGTCTTGTCCCAC	AL390214		Homo sapiens mRNA; cDNA DKFZp564O2423

		AACCCACGTGCCAGGTACA CATAACCAT			(from clone DKFZp564O2423)
D09	465	GGGAGTATTTGCTTGGGCAG AGGAAGTGCTACCAGTCTCC TCAGATCATCTGTTCTTTTGA CAGAGAGC	AK057708	NLVCF	Nuclear localization signal deleted in velocardiocardial syndrome
D10	466	AACTCAAACGGGCCGTTCTT TCTAAGGTGTCGGTATGTGG GGAGTGGTACAAAATGGTCT GATGCTCCT	NM_005088	DXYS155E	DNA segment on chromosome X and Y (unique) 155 expressed sequence
D11	467	TCCACAACGTTGCTACAAGA CGATTAAGTGGCTTCCTGAG GACACTTGCAGACCGGCTGG AGGGCACC	NM_032778	FLJ14393	Hypothetical protein FLJ14393
D12	468	CACAGATATAGCATAGGGCA GTGGGTTTTTGTATTAATTA TGGCGTACTTTGTTTATCCAT TGGCCAA	AK027829		Homo sapiens cDNA FLJ14923 fis, clone PLACE1008244, weakly similar to VEGETATIBLE INCOMPATIBILITY PR
D13	469	TTTTTCCCTGCTGGGTAGCAT TTTGTATGGAACGGTTGGAAT TTTCTGGGCCAGTCCAC GTGCCTT	NM_017829	CECR5	Cat eye syndrome chromosome region, candidate 5
D14	470	TCTGCTCTGACTGAGTTGAA GGAATTGTAAGTTTCAGTTGC TGAATATATCAGTATATCTGA ACTCCGG	NM_018178	FLJ10687	Hypothetical protein FLJ10687
D15	471	TCCTGAACGCTGGGCAAAG GTTGGGCAGAGACTTCTGGG TGTGCCTTGGCTCCCAAGGT GGCACTGTG	NM_002405	MFNG	Manic fringe homolog (Drosophila)
D16	472	AGAAGCATCACCATGCATGG TGGCGAATGCCCCAACTC TCCCCAAATGTATTTCTCCC TTCGCTGG	NM_000131	F7	Coagulation factor VII (serum prothrombin conversion accelerator)
D17	473	TCTTCTGCGAATTCTGTGAGC CAAGCAGACCTTCCCTCTCA TCCCAAGGAGCCAGATCCT CCCAAGAT	NM_005227	EFNA4	Ephrin-A4
D18	474	AATGTGTGTTCTGCGAATGA CTCGAGCTAGACGTTCCAG GTAGAACAGCAGCAGTCAT CACTGTTGA	NM_014109	PRO2000	PRO2000 protein
D19	475	TCACGGTTCTCATCTTCTCC ACCAGGGAGGGCAGAGAGA TGCACAAGTTCTCCAGTCC ACGTACAAC	AF119045	LOC92235	Hypothetical cardiac/skeletal muscle- expressed ORF
D20	476	TTTAAGAAAATAATCATGATT GGAGATGGTGCCACAGATAT GGAAGCCTGTCTCCTGCTG ATGCTTTC	NM_004577	PSPH	Phosphoserine phosphatase
D21	477	CCACTACAAGTTTATAACGAC ATTGCTGGATGCTACACTCC ATGTCTCTTTGTGGACCCA GGCTCATG	AK001853		Homo sapiens cDNA FLJ10991 fis, clone PLACE1002072
D22	478	AACTTTGAAGTGTGGGAACG ACCTCTCTCAGGCTTAGCCT GGGCTGTAGCTATGATAAAC CGGCAGGAG	NM_000169	GLA	Galactosidase, alpha
D23	479	ACCCTGAGGTCAGACCAACT TCAGCCGTGGCTGCCTGAGA CCTCAATACCCCAAGTCCAC CTGCCTATC	NM_000040	APOC3	Apolipoprotein C-III
D24	480	AAGTCTGACTACATCCGGAA GATAAATGAACTGATGCCTAA ATATGCCCCCAAGGCAGCCA GTGCACCG	NM_006010	ARMET	Arginine-rich, mutated in early stage tumors

E01	481	ACCTGGCTACTGTTTCAGCAA GTTTACAAAAGTGTTCAGTC TGAACAGGAACCGTTTTCAAT CCTTTAT	AK055873	DRG2	Developmentally regulated GTP binding protein 2
E02	482	CCTGCCTGCGGAACAGGGTA TGTGCCTGGAAGGCCTGCCA CAGGCCCCACAATTGAAGAA GTAGATTAA	NM_005527	HSPA1L	Heat shock 70kD protein 1- like
E03	483	TGTTTTTATAATCCATGTATA GTTGGTGTACACTCAAACCT GTCCCCGGCAGCCAGTGCTC TCTGTA	NM_006145	DNAJB1	DnaJ (Hsp40) homolog, subfamily B, member 1
E04	484	TCTCCATTATTCGCTTCTAAG CCAGAGACCCTTATCCACTG CTCCTCTAGGTGGCCCATTT ATGGTTTG	NM_002066	GML	GPI anchored molecule like protein
E05	485	CTCTGCTCCTTATCCAGTG TTCCATTTGAACCAAGTATCC ATGTCCTGAAAAATGCTCAAT CTCAGC	NM_015596	KLK13	Kallikrein 13
E06	486	TCCCCCTCCCATTTAACTGTC CTCACAGGCCCTTGCCTAGG ATGGATGACCAACTGCAC TCAATGAG	AB046839	SEMA4G	Sema domain, immunoglobulin domain (Ig), transmembrane domain (TM) and short cytoplasmic domain, (se
E07	487	GTTGCTTCTATATACTAGAGG CCCCAGATGGCAGGCCCTTGG GCTACGTCTGGCTTGCATGG TCTCCCAA	NM_006598	SLC12A7	Solute carrier family 12 (potassium/chloride transporters), member 7
E08	488	TATTGCTATCAATCGCAGTAG TCTTTCCCCTGTGTGAGCTG AAGCCTCAGATTCCTTCTAAA CACAGCT	NM_006986	MAGED1	Melanoma antigen, family D, 1
E09	489	CACATCACGCAGAGCTAGTG ATCGAGTTTGCACAATTACAC CAACAGTCTGCCCCACGTGG GAACCATT	U66589	RPL5	Ribosomal protein L5
E10	490	ATAAGTATAACCCACAAAACC CAACAGATTTTGGGGCACC TCTAACAGGGTCTTAAGAC CAAATGT	AF161337		Homo sapiens HSPC074 mRNA, partial cds
E11	491	GGACAGGATTGCAGGGACAG GGGACATGGGAGGAAGACA GAAAAATTCAAAACCGCAG ATGCCACTAC	AK021425		Homo sapiens cDNA FLJ11363 fis, clone HEMBA1000251
E12	492	GATAGAGGAACAGGGAGACC TGTCTAACTTTGCCCTGTCC AGGAACAGGGAAGTCATATC TGCTAAAG	NM_025049	FLJ22692	Hypothetical protein FLJ22692
E13	493	TGGGTGACGGAGCGAGACC CTGTCTCAAGAAAAAAGGA GAAGCTACTGAATTGCAGTA AAACCGTGTG	AK022174		Homo sapiens cDNA FLJ12112 fis, clone MAMMA1000043
E14	494	ATGGAGCTGCAATTCTTGTG GCGACATCTCCGCTCTGGT TTGTTGATGACACCTTCTAGA TGCTCCAT	AK056799		Homo sapiens cDNA FLJ32237 fis, clone PLACE6004966
E15	495	ATAAGTGGAGTACAGGCTGG ATTTAGCCCTAACCACCCG CTCCCCCAGGACATGGTAC AGTACACAA	AK023464		Homo sapiens cDNA FLJ13402 fis, clone PLACE1001456
E16	496	CTCAGGATGTCACGGAGAAT CTATCTAATCCCACTGTATTA AGAGGGGAAACCGGGCCAA GCGCAGTGG	NM_017638	FLJ20045	Hypothetical protein FLJ20045
E17	497	ATTTGAGGGTTATGACTCCAT CGACAGCCCCAAGGCCATCA CATCTCTGAAGTACATGTTGC	NM_002815	PSMD11	Proteasome (prosome, macropain) 26S subunit, non-ATPase, 11

		TGTGCAA			
E18	498	GCAAATGGAGATTCAGGTAT TGGGGATGCAGGTTGTGGG GAGCTGGCCTGGCAGAGTAG GGGTAGTTGG	NM_024681	FLJ12242	Hypothetical protein FLJ12242
E19	499	ATTAAGAGGAGTTAGAGCT GGGCCTTGAGGCTCTTCACT TCTTTCAACAGATATTTAATAT GTACCTA	AK000532		Homo sapiens cDNA FLJ20525 fis, clone KAT10610
E20	500	TCCACCTCGCGGCGGAACCC GAGGAGAGGAGCCTCAGATG AAAGAAACAA	NM_001207	BTF3	Basic transcription factor 3
E21	501	CAATGTCCAGCCACTAAATG AACAGGAGTCGCTACTGAGT CGTTACCAACGTGGGGACAA ACAAGGGTT	NM_003323	TULP2	Tubby like protein 2
E22	502	ATCCAGTCCTCTGGCCCTTG CCTAGCCCTGAATTGCTTCTC TAAGCTGGTGTTCCTCATGCA CAGGGCCA	NM_032548	BPOZ	BPOZ protein
E23	503	GCCGCCTGCATAGCATATAT TAGGCTCACACAGTACATGG ATGGCAGTGAATGCCAAAG ACAATGCAG	NM_001221	CAMK2D	Calcium/calmodulin- dependent protein kinase (CaM kinase) II delta
E24	504	CCTGAGGTCACAGAATGAAT AGATCACCAAGAGTATGAGG CTCCTGCTCTGATTTCTCCT TTCCTTC	NM_013247	PRSS25	Protease, serine, 25
F01	505	TTTTATGAACATGATACACTT TGGTCTTCTTTCCCCAGCG CCCCTGAGGGCCAGAGGCA GATGTGGGC	NM_030928	CDT1	DNA replication factor
F02	506	CTTCCTGTTCAAAACAGGATT TGATTGCCTTATGTGACAAGC CCAAGATCTGTGACAGTTGG AGCTCAA	NM_024753	FLJ11457	Hypothetical protein FLJ11457
F03	507	TTGCAGAAACCACACACT GTTGCTGGATCTTGAGTCCC ATTAGCTGTGAGATGCCTGT GAGAGCCTT	NM_004977	KCNC3	Potassium voltage-gated channel, Shaw-related subfamily, member 3
F04	508	GAACAGGAGCTGGGGTACTT GAGGTAAAAGAGGCCTGCC CAAATGTGGTCATTTTCTCGA AAACATAA	AK022993		Homo sapiens cDNA FLJ12931 fis, clone NT2RP2004861
F05	509	CTGCTGCTACTTCCACTGTTT ACAGACATTCTATCATCTTCA CCCCAGTGACTAATGAATTT CTATAG	AF070586		Homo sapiens clone 24528 mRNA sequence
F06	510	AATCTTCCCTTGTACTGTG GGATGATCCCACATCCAAGC GAGAACAATGGTTTAGGTTTT CCACTGA	NM_052933	TSGA13	Testis specific, 13
F07	511	GTTCCAGGAGGGTTTCGGGT TGCTCTGAAGACTTTTGAATT AAATGGATACCAGATTCCCAA GGGCTGG	NM_057157	CYP26A1	Cytochrome P450, subfamily XXVIA, polypeptide 1
F08	512	GGGTGCCATGGTCTCCAGCA ATTACAGCACTACAGTTTGTCA ACTACCCAACCTCAGGTCCTT GGTAAATC	NM_005827	UGTREL1	UDP-galactose transporter related
F09	513	CTTCATTACGCCTGCAAACCT GGTGTTCGTGTACCTGCTGT GCCGCGAGTCGCTGCGTGG	NM_003936	CDK5R2	Cyclin-dependent kinase 5, regulatory subunit 2 (p39)
F10	514	AAAACCCAAAGACTCTTTGG CAATTGGCAGTCAACTCAG CCAGGCTCTCAGACTGGAGG TGTTGTTGG	NM_032867	FLJ14966	Hypothetical protein FLJ14966

F11	515	TGACAGATGGGACCCTCCTC TGGCCAAATGTACCTCTCGT GCACATGATGCTCTCATAGTT GGCACTTT	NM_000651	CR1	Complement component (3b/4b) receptor 1, including Knops blood group system
F12	516	CCTCGAAACTTGACATGGGG CCAGAAGGGCCTGGGTTGAA GTAGTAATTGGGCTTCCTTG GAGCTAGTC	NM_004594	SLC9A5	Solute carrier family 9 (sodium/hydrogen exchanger), isoform 5
F13	517	GAGCTTCTTTATGTAGCTA CACTCCATGATTCCAAGAGC CCAGCAGCCGGGGCTGGCC TGTTCCTAG	AK001064		Homo sapiens cDNA FLJ10202 fis, clone HEMBA1004929
F14	518	ATGTCTCTGAGGTGGCCAAC ATTAGTCCTTCTATAGCCAGA TTAGCAATCTTAGAGCCTGGT CAGGCAC	AK021634		Homo sapiens cDNA FLJ11572 fis, clone HEMBA1003373
F15	519	CATCTTGGGGCAGTACAGAT CAACTTAAGGAGGTCAGAAA AATGGTTCTAAGATAGTGGG TGTGGAAT	AB053315		Homo sapiens ALS2CR13 mRNA, partial cds
F16	520	GGGCAGGGGCAGGGGCTAG CAGTTGTGTTAAGCAAATC TGCAGGTGCTTTTCTATCCT AGTTTGAG	AK023557		Homo sapiens cDNA FLJ13495 fis, clone PLACE1004425
F17	521	ACGTGCTGGTTGGCAGGAAG AACCTCAGGCTCCTGGACGA AATGAGGAGACTCTCCCCTC ACTTTTGTC	NM_032093	HTIFN	Pregnancy-associated interferon
F18	522	ATCCTCTTCCCAGGCATGAC CAAGACTGGCATAGACCCTT ATTGTCAGCCCACGCTACG GCCATGTAA	NM_004189	SOX14	SRY (sex determining region Y)-box 14
F19	523	CTGCTCGGGGTGTGCTGCAT TACTCGCTCTTCAACGTCAT CTCCATCCTCATCAAGCAGG TGCTCAAC	NM_022055	KCNK12	Potassium channel, subfamily K, member 12
F20	524	AAATCCTAAAGGCCGCGGAG TCGGCGGTGTTGTAGGTAGC GGTACCTTGAGTGGCAACAG AATTCGATT	NM_016632	LOC51326	ARF protein
F21	525	AAAGAACCTATGGCACTTCT GAGCCCTACAGTGTATGACT ACTTCCATATTTCCACAGAAT CTCCTCT	AK001299		Homo sapiens cDNA FLJ10437 fis, clone NT2RP1000581
F22	526	CAAACGACGCTCATCAACA GAGACCTCCTCCTCCAAGT CAAGGACAATAAGCCTCTGG TTGAACGGT	NM_014230	SRP68	Signal recognition particle 68kD
F23	527	ACAGAAACAGCCATGAAGGC AGTTTCTGGGATAGTCCATAT GCAAGCAGCTCCAAAGGAGG AATGTGCC	NM_005525	HSD11B1	Hydroxysteroid (11-beta) dehydrogenase 1
F24	528	TACCACTGCTAGGACGCTGG CAGAACGCACCCATAACTTG GCAACACTCGGAGGATGGAT GGCAAATAA	NM_017618	FLJ20006	Hypothetical protein FLJ20006
G01	529	CCAGGACTGCTCAGAGGGG CGATTCCCTCGTCAATTTGG GTTGTGTCATCATAATGTTT CGCCTTATT	NM_021794	ADAM30	A disintegrin and metalloproteinase domain 30
G02	530	TTCACAGAGTGTAGTTAGATC CCAACCTCCATGACCTCTGG CTTCAGTGGTGGGTGGGCA GGCCAGAT	NM_030971	BA108L7.2	Similar to rat tricarboxylate carrier-like protein
G03	531	GGTTGTACCTCGCCCGTAGG AGCTTCATCATCCAGAATATT CCGGGCTTCTGGGTCAACGC CTTCTCTGA	AL121897	TSPYL3	TSPY-like 3

G04	532	AGAAGTACACACCAAGGGGG AATCAAATACACTTCAAGATA CCTCTGTCATTCCAACCCAT AGGAGAC	AL117560		Homo sapiens mRNA; cDNA DKFZp566P2324 (from clone DKFZp566P2324)
G05	533	AAGAAGCTCTAATGCTTCTGT TACATGTGTCTATGTGGACA GTAAGCCACTTACTTGGGGG ATCCTTTT	AK024862		Homo sapiens cDNA: FLJ21209 fis, clone COL00396
G06	534	GCATCCATCTACATTTAATAC CACTCATTTTTCCCATGGATC TCTTCCCAGCATTAGACCTC AGATGC	NM_033060	KAP4.10	Keratin associated protein 4.10
G07	535	GAATCCACGTGGTTGACGTT AGAACCTCCCTTCTGCAGAC TGTTGCCTGTCATCTAAGCG AATTGGAAA	AB051514	KIAA1727	KIAA1727 protein
G08	536	TGTCGCCTTGAAGCACATGC CCCCTAACTTACAGAAGGTG GACCTCTTTCGGGCAGTTCC CAAACCAGA	NM_032336	MGC14799	Hypothetical protein MGC14799
G09	537	GTAAGTGCACCATCCCTTAAG CAGCATCTGTAAGTGGCCAG CTCATTAAGCCCTTCCCCTA GTTTGCA	BC007266		Homo sapiens, clone IMAGE:3138608, mRNA
G10	538	AATGGACGTGACTTTTTCTCT AAGGTGCTCTTGTCTGCATA GTACGCTGTCCCAAAGGGTC AAGGGTCA	BC009393		Homo sapiens, clone MGC:15307 IMAGE:4135946, mRNA, complete cds
G11	539	ATCTCAATGGTGGTAACAGT GACCTGGTCAGGGATGAGAA ACGGCTGACCCTGGGTCACA GCAAACCTGG	AL121753	C20orf128	Chromosome 20 open reading frame 128
G12	540	AGTGGAAATCAAGAGATTTTT TTCCACGGGGAAGTCTTTTT ACAAAGCGTTGATTTCTTGGC ACCCCG	BC009950		Homo sapiens, clone IMAGE:3833021, mRNA, partial cds
G13	541	AGCAGGAAGCTGGAGTAAC GCCACAAGCTCCAGGAGGGA GTGTCTAGAACATCCACGTTT TGCAGCAG	AK057425		Homo sapiens cDNA FLJ32863 fis, clone TEST12003615
G14	542	GAAAATGTAAAGCCATTAGCT TGTTAGCAATCATGATTCTGG TTGGGGACAGCTGCATAAT TTTGCA	AK055061		Homo sapiens cDNA FLJ30499 fis, clone BRAWH2000443, weakly similar to Human breast cancer, estrogen
G15	543	ATGGATTCCTTGCTTAGGAA GTGAGGCAGGTACCAGGGA CATGGACAGGAGCCTGCCCA AGCAGGCTTT	AK055850		Homo sapiens cDNA FLJ31288 fis, clone KIDNE2007222
Housekeeping genes					
G16	544	TGAAGAGGGGAGGGGCCCTA GGGAGCCGCACCTTGTATG TACCATCAATAAAGTACCCTG TGCTCAACC	NM_002046	G3PDH	GAPDH
G17	545	TTTTGAATGATGAGCCTTCGT GCCCCCCTTCCCCCTTTT GTCCCCCAACTTGAGATGTA TGAAGGCT	AF111848	B-Act	Beta Actin
G18	546	CAGCACTTTATGCACGTATTA TTGACATTAATACCTAATCGG CGAGTGCCCATCTGCCCCAC CAGCTCC	NM_002627	PFKP	Phosphofructokinase, platelet
G19	547	AGGAGGGCTGGCAACTTAGA GGTGGGGAGCAGAGAATTCT CTTATCCAACATCAACATCTT GGTCAGAT	AK026463	B2M	Beta-2-Microglobulin

G20	548	AGGATAAAGTCAGCCATGTG AGCACTGGGGGTGGTGCCA GTTTGGAGCTCCTGGAAGGT AAAGTCCTTC	NM_000291	PGK1	PGK1
G21	549	TGTCGTCTGTGAATGCTAAGT CCATCACCCCTTCCGGCACA CTGCCAAATAAACAGCTATTT AAGGGGG	NM_000034	ALDOA	ALDOA
G22	550	CAGAGCTGAGTGAAAAGGGG ACCGAGGAGGCCAAGCGGG GAGCCAAGGCCATCAAGGAT GCCAAGATGG	NM_000290	PGAM2	PGAM2
G23	551	CGAGGCTGAAGAAGGTGAAG AATACTGAGGGGAGGGTGTG GTGGGTTCTCCACTCCACTG CCACCCCA	BC011721	TUBA2	TUBA2
G24	552	AGAAAAGCAGACGCAGCAGC TGGGACCCCTTCCAACCTCA ATGCCCTGCCATTAATCCG CAAACAGCC	NM_000402	G6PD	G6PD
H01	553	TCACTGAACATGCCTAGTCC AACATTTTTCCAGTGAGTC ACATCCTGGGATCCAGTGTA TAAATCCA	NM_005566	LDHA	LDHA
H02	554	GAAACATCTGGAGTCTATT GACATCGCCAGTAAATATC AATGTTCTAGTTCTGTGGCCA TCTGCTT	NM_000194	HPRT1	HPRT1
H03	555	AACTTTGCCGTTGAAGCTGC TAACTACCAAGACACTATTGG CCGCCTGCAGGATGAGATTC AGAATATG	NM_003380		Vimentin
Known to change with cellular age					
H04	556	TTCTACTTGGATGAAGAGAG GACCGTGAGGGTCCCCATGA TGTCGGACCCTAAGGCTGTT TTACGCTAT	NM_002615	EPC-1	Serine (or cysteine) proteinase inhibitor, clade F (alpha-2 antiplasmin, pigment epithelium derived factor)
H05	557	TGCAGTCACTGGTGTCACCC TGGATAGGCAAGGGATAACT CTTCTAACACAAAATAAGTGT TTATGTT	NM_002421	MMP1	Matrix metalloproteinase 1 (interstitial collagenase)
H06	558	CTGCTTAGCTTGCACCTTGTC ACATAGAGTGATCTTCCCAA GAGAAGGGGAAGCACTCGTG TGCAACA	NM_002422	MMP3	Matrix metalloproteinase 3 (stromelysin 1, progelatinase)
H07	559	ATGAGCCAAAATGGTTAATTT TTCCTGCATGTTCTGTGACTG AAGAAGATGAGCCTTGCAGA TATCTGC	NM_002425	MMP10	Matrix metalloproteinase 10 (stromelysin 2)
H08	560	TACTCAGGCAGATCTCAGCC CTCTACTGAGTCCCTTAGCC AAGCAGTTTCTTCAAAGAAG CCAGCAGG	X59405	MCP	Membrane cofactor protein (CD46, trophoblast-lymphocyte cross-reactive antigen)
H09	561	TTCGGATTGTCTCCCATTTTC CCAGGTGGGGCCTGCCTGG GGAAAGCTTGTGGCCGGAAG AGAAAATGA	NM_000501	ELN	Elastin (supravalvular aortic stenosis, Williams-Beuren syndrome)
H10	562	AGGGCTGCTAATCTCAAGGA GCTTCCAGTGCAAGGGGAAAT AAATGCTAGACTAAAATACAG AGTCTTCC	NM_003266	TLR4	Toll-like receptor 4
H11	563	ACACACGTATTTATATTTGGA AAGAGACCAGCACCGAGCTC GGCACCTCCCGGCCTCTCT CTTCCCAG	NM_000597	IGFBP2	Insulin-like growth factor binding protein 2 (36kD)

H12	564	TGATCCACATTGTTAGGTGCT GACCTAGACAGAGATGAACT GAGGTCCTTGTGTTTTGT TCATAAT	NM_000089	COL1A2	Collagen, type I, alpha 2
H13	565	GATGGAGTGGGAGCCGTGAA TATCTCTGTGATGAATCCAC TGGTGGCAGTAGCAGTGGCG GTGGCATT	NM_005556	KRT7	Keratin 7
H14	566	GTTTTGCTGCACTTTTTACTT TTTTGCGTGTGGAGCTGTATT CCCAGACAACGAAGCGTTG GGATACT	NM_003247	THBS2	Thrombospondin 2
H15	567	TAGTTATATTAGCAGCCCTCT GAGATGGCGTATCTATCGGA AGGATTTCAAACACCAATTGC TTTACCT	NM_001334	CTSO	Cathepsin O
H16	568	ATTATGATTACTATCCGAG GAGCAACAACCACTTTCTCT GCAGTGGAAAGGGATCGCCA GTGGAAGT	NM_001937	DPT	Dermatopontin
Known to change with organismal age					
H17	569	CAAGCACCTAGATACCAGCA CAAGTCGGTTAATCCCTGTCT GGACTGAGCCTCCGTTGGCT TCTGAACT	NM_002105	H2AFX	H2A histone family, member X
H18	570	GCTTTTATGTGTGCTGGTGCT ATGTGTGTTTCATGTCCGCGG CAGCTGTCTTTTTGCTACTAT AAGGGAA	NM_001761	CCNF	Cyclin F
H19	571	CTGCATCCATGGTGACGGAG GTGGCAATGACATCATCAAG GTCAGAGGGTAAATTCCTAA CAGGAGACC	AB020642	MYT1	Myelin transcription factor 1
H20	572	TGCCTTGCATACCCAAACCA GGTGGGAGCGTTTTGTTGAG CATGACACCTGCAGCAGGAA TATATGTGT	NM_021874	CDC25B	Cell division cycle 25B
H21	573	GTGGGCCGTATTCATCGACA CCTAAAATCTAGGACGACCA GTCATGGACGTGTGGCGC GACTGCCGCT	NM_002106	H2AFZ	H2A histone family, member Z
H22	574	AAGAGAGGCTCACAAACAAG TAACTTGTGAGAAATCTCCAA AGTCTCCTAAAGTGACTGGA ACAGCTTC	NM_001813	CENPE	Centromere protein E (312kD)
H23	575	GCCCGCATGCAGCTTACCT CCCCTTCCAGGCGCCACTG TTGAGAAGCTAGAGATTGTAT GAGAATAA	NM_005804	DDXL	Nuclear RNA helicase, DECD variant of DEAD box family
H24	576	GTGGGGTGTCTTCTTGGGA CCCCACTAAGACCCTGGTC TGAGGATGTAGAGAGAACAG GTGGGCTGT	NM_000962	PTGS1	Prostaglandin- endoperoxide synthase 1 (prostaglandin G/H synthase and cyclooxygenase)
I01	577	CTTAGGATAGGCCTATGTGC TAGCCCACAAAGAATATTGTC TCATTAGCCTGAATGTGCCAT AAGACTG	NM_000963	PTGS2	Prostaglandin- endoperoxide synthase 2 (prostaglandin G/H synthase and cyclooxygenase)
I02	578	TAAGCTCTGAGCTGAGGAAA CAAGGTGTCTCCATCCCCC AGTGCCTTCACATCTTGAGG ATATGCTTC	AF119841	HSA250303	Peroxisomal trans 2-enoyl CoA reductase; putative short chain alcohol dehydrogenase
I03	579	AGGAGGATGTGGTTAATCTG TTTACCTGGTTTGTCTAAG GCCATAGTTAAAAAGTACCA GCTCTGGC	NM_002023	FMOD	Fibromodulin

I04	580	AAGGGGTGCCGTCCTGAG GGGGAAGTGAGAAGGGCTC AGAGAGGACAAAATAAAGTG TGTGTGCAGGG	NM_000095	COMP	Cartilage oligomeric matrix protein (pseudoachondroplasia, epiphyseal dysplasia 1, multiple)
I05	581	TCCTCTCAGCTCCTAAAGCA CAACTGTGTGAGATGTGAT AAGTCCCCGAGGGCGAAGG CCATTGGGTT	NM_001323	CST6	Cystatin E/M
I06	582	ATGTATGATCTTCCATGTTTT GACGTTTGAGTCACACACA ACACCTTAGTTCCTCTAGGG GCTGTACA	NM_005328	HAS2	Hyaluronan synthase 2
I07	583	CCTCAGTAGAAAGCCCAAGC CAGACAGTGACGTGACTCAG ACCATCAATACAGTCGCATAC CATGCGAG	NM_000465	BARD1	BRCA1 associated RING domain 1
I08	584	ACCTTCAAAGCAAGATAATTC TATTTGAAGCATGCTCTGTAA GTTGCTTCCTAACATCCTTGG ACTGAGA	L23808	HME	Human metalloproteinase (HME) mRNA
I09	585	AGGAGGTGTTATGACAGGGA GAACTGGACATGGAGGCCCA CAGTTTGTGGCAGATCATCC TTTTCTTTTT	M31551	PAI-2	Human urokinase inhibitor (PAI-2) gene, exon 8
I10	586	TCCTTAGGATAGGCCTATGT GCTAGCCCAAAAGAATATT GTCTCATTAGCCTGAATGTG CCATAAGACT	in U04636	hCox-2	Cyclooxygenase 2
I11	587	GCAAGACTTTTGCCCGCTAC CTTTCATTCCGGCGTGACAA CAATGAGCTGTTGCTCTTCAT ACTGAAGCA	D21063	HUMORFA AA	Homo sapiens KIAA0030 mRNA
I12	588	AGTCTGCTAGCCAGGATCCA CAAGTCCTTGTTCCACTGTG CCTTGGTTTCTCCTTTATTTT TAAGTGAA	Y00787	HSMDNCF	Human mRNA for MDNCF (monocyte-derived neutrophil chemotactic factor)
I13	589	CCAGGGGTGCTCCTGTGCTC ACCCTCTCTTGGTGCAATTTT TTGGAAGAATAAAATTGCCTC TCTCTTTG	X13293	B-Myb	B-Myb
I14	590	GACTGTTCTGCTCCTCATAG CTCCCTGCTGCCTGATTATG CAAAGTAGCAGTCACACCC TAGCCACTGC	U74612	FOXM1A	Homo sapiens forkhead box M1A (FOXM1A) mRNA
Additional known to change with hTERT overexpression					
I15	591	ATGCCTTCCGGCTGAGTCCT GCTCCTTCCAAAACACTTATG GACAACTATGAGGTCTTGG GGGTACAG	NM_003998	NFKB	Nuclear factor of kappa light polypeptide gene enhancer in B-cells 1 (p105)
I16	592	TGGCAAACATTTGTATGACT CATAATAAGTCTTCCCAGC TGACCAAAGCAAAGGCGAGG GCGATCT	NM_005037	PPAR gamma	Peroxisome proliferative activated receptor, gamma
I17	593	TCCAAGCATCACCTGGGAG TTTCTGAGGGTTTTCTCATA AATGAGGGCTGCACATTGCC TGTCTGTC	NM_002026		Fibronectin 1
I18	594	TCTTCGGCAAATGTAGCATG GGCACCTCAGATTGTTGTTG TTAATGGGCATTCTTCTTCT GGTCAGAA	NM_000600	IL6	Interleukin 6 (interferon, beta 2)
I19	595	GCAGGGCAAAGATGGCATCG GCCACAGACTCGCGCTATGG GCAGAAGGAGTCTCGGATC AGAACTTCGA	NM_002866	RAB3A	RAB3A, member RAS oncogene family

I20	596	AGGAAGCAGGGATGTCGCAG GAATCCGCTGGCTAACATCT GCTCTTGGTTTCTGCTGCC TGGAGCCTG	NM_003285		Tenascin R (restrictin, janusin)
I21	597	AAACAGACTCGATTTCATATTG AATATAATATATTTGTGATTT AACAGGGAGGGGAAGAGGG GCGATC	NM_002229	JunB	Jun B proto-oncogene
Additional cell cycle related					
I22	598	CTGAGGCTATGGAGGGTCCT CCTCCATCTTTCTACAGAGAT TACTTTGCTGCCTTAATGACA TTCCCT	NM_000075	CDK4	Cyclin-dependent kinase 4
I23	599	ATGCCCCATAATTATTATTTTC CAGTGTTTGGGATGACCAGG ATCCAAGCCTCCTGCTGCC ACAATGTT	NM_001798	CDK2	Cyclin-dependent kinase 2
I24	600	TACGTGCCACCACGGCGTTG TACCTGTAGGACTCTCATTGG GGATGATTGGAATAGCTTCT GGAATTTG	NM_053056	CCND1	Cyclin D1
J01	601	TATTTTTAATTGGTTTAGTTCT TAACTGCTGGCCAACTCTTAC ATCCCCAGCAAATCATCGGG CCATTG	NM_001759	CCND2	Cyclin D2
J02	602	GAATAGTCTAGATGGTCCT CTCAGTACTTTGGAGGCCCC TATGTAGTCCGTGCTGACAG CTGCTCCTA	NM_001760	CCND3	Cyclin D3
J03	603	AGACGGGGAGCTCAAACTG AAGCACTTCAGGGGCGTCGC TGATGAAGATGCACACAACA TACAGACCC	NM_001238	CCNE1	Cyclin E1
J04	604	TGGCCAGAAACCTTGCTGC ATTTACAGGGTATTCATTAAG TGAAATTGTGCCTTGCTGA GTGAGCTT	NM_003914	CCNA1	Cyclin A1
J05	605	TATCTGAGACAACCTGAGGA AGAGCAAGCAGTCAGACCAA AATACCTACTGGGTCCGGAA GTCACTGGA	NM_031966	CCNB1	Cyclin B1
J06	606	CAAATAAGTGTTCAAACCAA ATGTTTCAAGATTGAAATGGA TTGTTTCTGGGCGTACTGCA CGGCAAT	NM_004060	CCNG1	Cyclin G1
J07	607	GGGCCCAGACACCAGCCTAG CCTGCTCTGCCCCGAGACG GTCTGTGTGCTGTTGAAAAT AAATCTTA	NM_004305	Bin1	Bridging integrator 1
J08	608	ACTGCACTCCGCCACCCCCC TACCAGCCGACCCAGCCT CGTCAGTTTTTAAACAGGATT GGGGTGTC	NM_005427	p73	Tumor protein p73
J09	609	TAAACCACTCCAGAATGGCC ACCAGGCTTCCAGAGTTCT ATGGTCTTCTTCCCAAGAGA GTTTTAAT	NM_006565	CTCF	CCCTC-binding factor (zinc finger protein)
J10	610	GAGGACTTGTTCGGAAACG ACGAGAACAGTTGAAACACA AACTTGAACAGCTACGGAAC TCTTGTCG	NM_002467	Myc	V-myc myelocytomatosis viral oncogene homolog (avian)
J11	611	AATACCAAGAGCAATTTACCT GGTACTAAACCCGCACCCCA GTGCGGACCCCTCCAGCCC TCATCCCA	BC003525	Max	MAX protein
J12	612	GCCACCGCCACCCAACCTCAG TCATCCACCTGCCCTTCATCA	NM_007111	DP1	Transcription factor Dp-1

		TCGTCAACACCAGCAAGAAG ACGGTCAT			
J13	613	TAATTTGGGAGTTCTCGATTT GATCCGCATCCCCTGTGGTT TCTAAGTGTATGGTCTCAGAA CTGTTGC	NM_005375	Myb	V-myb myeloblastosis viral oncogene homolog (avian)
Telomeres and telomerase related					
J14	614	AGCTTTTCCTCACCAGGAGC CCGGCTTCCACTCCCCACAT AGGAATAGTCCATCCCAGA TTCGCCATT	NM_003219	hTERT	Telomerase reverse transcriptase
J15	615	CGCTGTTTTTCTCGCTGACTT TCAGCGGGCGGAAAAGCCTC GGCCTGCCGCCTTCCACCGT TCATTCTAG	U85256	hTR	Telomerase RNA
J16	616	AGTGTTAGTGACAAACAGTCT GCGGTAACGAATCCTCAGA GGGTACAGTATCCTTATTGA GGTCTACA	NM_017489	TRF1	Telomeric repeat binding factor (NIMA-interacting) 1
J17	617	GGGATGAGAATTTTGGGCAA CCTCCTTCGACGTGGGGGAG GTCCCATTTCCACTTCATCAC TGTTGGAG	NM_005652	TRF2	Telomeric repeat binding factor 2
J18	618	GGCTACTTCCGCCTTCTTAG CGTCTGGTCAGAGAGCTGAT GGATATCCCATTTGGTCCCG ACAAGATGA	NM_018975	hRap1	TRF2-interacting telomeric RAP1 protein
J19	619	AGTAGTTTGATTCTGGTTTTCC CTCATACAGTGTGCCTCCG TCTCTGTGCAGCTCCGTCATT ACCATAG	NM_012461	Tin2	TERF1 (TRF1)-interacting nuclear factor 2 (TINF2)
J20	620	CAACAGCACTCGGAGTAGTA ATTGTGTTTTCTCATTGTGAT GTTGGTCTGTGTAGCAACC AGTGTAGT	AF082557	TANK1	Tankyrase, TRF1- interacting ankyrin-related ADP-ribose polymerase
J21	621	AATTAAGTGGCCCTTTCAGT AAGTTGTACATAAAGTGCTAG AAAATCATGTTCTTGTCCCTG AGTAAG	NM_025235	TANK2	Tankyrase, TRF1- interacting ankyrin-related ADP-ribose polymerase 2
J22	622	GCTACAGTGTACTTTAAGTAG AAATGGCAAAGTTGCTTTGTT GGGGTGCTGATACTGATGAT TTAGGA	NM_015450	hPot1	Protection of telomeres 1
J23	623	ACTCCAGAGCAGGTGGGCAA GATGAAGGCTATCGTTGAGA AGCTTCGCTTCACATACAGAA GTGACAGC	NM_001469	Ku70	Thyroid autoantigen 70kD (Ku antigen) (G22P1)
J24	624	GTGGGAAGGGGAGCACAATT TCCCTTCATACTCCTTTAAG CAGTGAGTTATGGTGGTGGT CTCATGAA	NM_021141	Ku80	X-ray repair complementing defective repair in Chinese hamster cells 5 (double-strand- break rejoining)(XRCC5)
K01	625	GTCAAAGGTCGTAGATTTAA AGGAAAAGGAAAGGGTAATA AAGCTGCCAGCCTGGGTCT GGTAAAGG	NM_003142	La	Sjogren syndrome antigen B (autoantigen La) (SSB)
K02	626	TTCTCAAGCTGGCTCACTCA GACACATTGGGACAAACCCT GGACAGCCATGCCAGAGAGA GGCCTTTGA	NM_017453	Stau	Staufen, RNA binding protein (Drosophila)
K03	627	CGCCCCCCTCACTGGCCTT GTGACGGTTTATTCTGATTGA GAACTGGGCGGACTCGAAAG AGTCCCCT	NM_006037	HDAC4	Histone deacetylase 4
K04	628	ATTAAGCCCTAAGGTCCTAA GGCATCTATCTGTGCTAGGT TAAATGGTTGGCCCCCAAAG ATAGACAGG	U63139	Rad50	RAD50 homolog (S. cerevisiae)

K05	629	CATATTGATGCCCTCGAAGA CAAAATCGATGAGGAGGTAC GTCGTTTCAGAGAAACCAGA CAAAAAAAT	NM_005591	MRE11	MRE11 meiotic recombination 11 homolog A (<i>S. cerevisiae</i>)
K06	630	TCTGGCTGCTGCAGGTGGA ACTCCAGCTGCAAGGGAGTT AGGGAATGAAGTCTTTTTT TAAAAGCT	NM_002485	NBS1	Nijmegen breakage syndrome 1 (nibrin)
K07	631	CCAAAACGAAATCCTCCAGC ATCATTGGATCCAGTTCAGC CTCACATACTTCTCAAGCGAC ATCAGGAG	NM_000057	BLM	Bloom syndrome
K08	632	AGGAAGAAGTAGGCATCAAT ACTGAGACTTCATCTGCAGA GAGAAAGAGACGATTACCTG TGTGGTTTG	NM_000553	WRN	Werner syndrome
K09	633	AGTGCACACCCAACTCCTG GCCTTCTGTGGTTTTCCCTTTG CTCCAGAAACACAGATGTGT CTAAAAAA	NM_002725	PRELP	Proline arginine-rich end leucine-rich repeat protein
K10	634	TGTTGAGGTCCTAGGCAATT AATGCAGCAGTTGCGATAAA TAAAAACATCTCACCTAAGTC TCCTTTTC	AK057820	p23	Unactive progesterone receptor, 23 kD
K11	635	TGACCATTCCATTATTGAGAC CTTAAGGCCAAAAGGCAGAGG CTGATAAGAACGACAAGTCT GTGAAGGAT	NM_005348	hsp90 alpha	Hsp90 (HSPCA)
K12	636	CCGCCTGCTGGTGTCTAGTG TTTTTTTCCCTCTCCTGTCT TGTGTTGAAGGCAGTAACT AAGGGTGT	NM_007355	hsp90 beta	Heat shock 90kD protein 1, beta (HSPCB)
K13	637	TCCATGTGAAAGGTTCTTTGC AAGAGGAAAGCCTTAGGGAC AAGATTCCTCGAAGAGGACAG GCGCAAAA	NM_002155	HSPA6	Heat shock 70kD protein 6 (HSP70B')
K14	638	CAGCTTGCCGTGGGAGACGT GCAGGGCAATGTGTACTTTC TGAATTGGGAATGAAGATGT GCCACTCGG	NM_007110	TEP1	Telomerase-associated protein 1
K15	639	CTCTGTTTGAGTTGGGAAGC CTCACCTTCAGACCCAGTAA CTGTCCGCAGCTGTCTGCTA GTGGTTGTC	NM_001363	DKC1	Dyskerin
K16	640	CAACCTGCTTGGGTGGAGAA GCCATTGTCTTCGGAAACCTT GGTGTAGTTGAACTGATAGTT ACTGTTGT	NM_002136	hnRNP A1	hnRNPA1
K17	641	TTCCCATGTTCAATTCAT ATTGCCCCGCGCCTAGTCCC ATTTTCACTTCCTTTGACGCT CCTAGTA	NM_031314	hnRNP C1/2	Heterogeneous nuclear ribonucleoprotein C (C1/C2)
K18	642	TGAACGGAAAAGCTGGGAAC CTTGGTGGAGGGGTGGTGAC CATCGAAAAGGAGCAAGAGCA AGATCACCG	NM_000983	RPL22	Ribosomal protein L22
K19	643	TCCCTCTTCTGGTCTGGCT CAGGGGGCTGGGATTTTGAT ATATTTTCTAATAAAGACTT TGTCTCGC	AK056851	B4GALT3	UDP-Gal:betaGlcNAc beta 1,4- galactosyltransferase, polypeptide 3
K20	644	GAGCTGGAAGGTCAACATC TTTTACATTCTGCAAGCACAT CTGCATTTTCACCCACCTT CCCCTCC	NM_000546	p53	Tumor protein p53 (Li- Fraumeni syndrome)
K21	645	GCTGGAGGTGTGTTACAGA GCCCAAAATAAACAATGCA ACCAGGTCAGACCAGCGGTT CTCACACAG	AB032968	PAK4	P21(CDKN1A)-activated kinase 4

K22	646	TCGGAGTTAATAGCACCTCC TCCGAGCACTCGCTCACGGC GTCCCCTTGCCTGGAAAGAT ACCGCGGTCC	NM_000077	p16	Cyclin-dependent kinase inhibitor 2A (melanoma, p16, inhibits CDK4)(CDKN2A)
K23	647	CCTCGTGCTGATGCTACTGA GGAGCCAGCGTCTAGGGCA GCAGCCGCTTCTCTAGAAGAC CAGGTCATGAT	NM_058195	p14	ARF
K24	648	AAGCTTCCTTTCCGTCATGCC GGCCCCACCCTGGCTCTGA CCATTCTGTTCTCTCTGGCAG GTCATGAT	NM_058196	p16 var2	Cyclin-dependent kinase inhibitor 2A (melanoma, p16, inhibits CDK4)(CDKN2A)
L01	649	CGCGCGTACAGATCTCTCGA ATGCTGAGAAGATCTGAAGG GGGGAACATATTTGTATTAGA TGGAAGTCA	NM_058197	p16 var3	Cyclin-dependent kinase inhibitor 2A (melanoma, p16, inhibits CDK4)(CDKN2A)
L02	650	TTTGGGAAGGTTTGTGTTTTTC TCTGGAATGGTACATGTCTTC CATGTATCTTTTGAAGTGGCA ATTGTC	NM_000321	Rb	Retinoblastoma 1 (including osteosarcoma)
L03	651	CTGCGGAAGCTGAACCCTCC TGATGAGAGTGGCCCCGGCT GCATGAGCTGCAAGTGTGTG CTCTCTGA	NM_005343	HRas	V-Ha-ras Harvey rat sarcoma viral oncogene homolog
L04	652	CAGTTAATFACTCAGCAGAAT GGTGATCACTCCAGGTAGTT TGGGGCAAAAATCCGAGGTG CTTGGGAG	BC001971	CDKN1B	Cyclin-dependent kinase inhibitor 1B (p27, Kip1)
L05	653	CCCCAGGATGGATATGAGA TGGGAGAGGTGAGTGGGGG ACCTTCACTGATGTGGGCAG GAGGGGTGGT	NM_005225	E2F1	E2F transcription factor 1
L06	654	TTGGCAACTTTAAGGAGCAG ACAGTGATTGCCGTC AAGGC CCCTCCGCAGACGAGACTGG AAGTGCCCCG	NM_004091	E2F2	E2F transcription factor 2
L07	655	ATCTAGTTTGCCCCTTAATGC CATTGAACCTTGTGTGATTTG TCAAGGTCGACCTAAAATG GTTGCAT	NM_002392	MDM2	Mdm2, transformed 3T3 cell double minute 2, p53 binding protein (mouse)
L08	656	AATACCTGAGTACCCATGGG AATAATAGACACTGGGGAGG TAGGGTGGGGAGCGGGACG AAGAGCTGAAA	NM_003218	Pin2	PIN2 (TRF1 with 60 nucleotide deletion)
L09	657	GAACATGCGTCGCAAACCTCT TTGGGGTCTTGCGGCTGAAG TGTCACAGCCTGTTTCTGGAT TTGCAGGTG	in NM_003219	hTERT	Telomerase 3'UTR (endogenous)
L10	658	CCTTCCACCCCAACATCCA GGTGGAGACCCTGAGAAGGA CCCTGGGAGCTCTGGGAATT TGGAGTGACC	in NM_003219	hTERT 3UTR	Telomerase 3'UTR (endogenous)
L11	659	CTGACTCTCAACATTCTACTC CTCCAAAAAAGAAGAGAAA GTAGAAGACCCCAAGGACTT TCCTCAGA	S79054	SV40 LT	SV40 large T antigen (partial)
L12	660	AGGATCCAACACGGCGACCC TACAAGCTACCTGATCTGTG CACGGAACTGAACACTTAC TGCAAGACAT	in M20324	E6	Human papillomavirus E6
L13	661	ACTTGCCATGGGCAGGAAAC CACAGATTCTCGGACAAGA AGGAAAAGAAATCTTTAGCC TTGAGGAA	NM_017884	PinX1	PIN2-interacting protein 1
Miscellaneous					
L14	662	GATGGTGTGGCCGATGTGTC TATTGAAGATTCTGTGATCTC	NM_000454	SOD1	Superoxide dismutase 1, soluble (amyotrophic

		ACTCTCAGGAGACCATTGCA TCATTGGC			lateral sclerosis 1 (adult)
L15	663	GCCTTATTCCTACTGCTGGGG ATTGATGTGTGGGAGCACGC TTACTACCTTCAGTATAAAAA TGTCAGGC	NM_000636	SOD2	Superoxide dismutase 2, mitochondrial
L16	664	TGAAGGCCTCCATTTGTACC GAAACACCCCGCTCACGCTG ACAGCCTCCTAGGCTCCCTG AGGTACCTT	NM_003102	SOD3	Superoxide dismutase 3, extracellular
L17	665	GGGCCCTGCACCTGTGCAGC GAAGCTTAGCGTTCATCCGT GTAACCCGCTCATCACTGGA TGAAGATTC	NM_001752	Cat	Catalase
L18	666	GGGGGGGTTTTTCATCTATGA GGGTGTTTCCTCTAAACCTAC GAGGAGGAACACCTTGATC TTACAGAA	NM_000581	Gpx1	Glutathione peroxidase 1
L19	667	AGCTGAATATTGAACTGGAA GCAGCACATCATTAGGCTTTA TGACTGGGTGTGTGTTGTGT GTATGTAA	NM_005746	PBEF	Pre-B-cell colony- enhancing factor
L20	668	TTGAGGTGATCTCGCAAAGT TATTCTTCCACCATGGCCAAC AACGAAGGACTTTTTCTCCCT GGTGGCGA	NM_006169	NNMT	Nicotinamide N- methyltransferase
L21	669	TCTGAATCCCGGGCTAAGAA TGCAGACTTTTCAGACTGAC CCCAGAAAATTCTGGCCAGCC AATCTAGAG	AF217965		Prostaglandin E synthase
L22	670	GAATTGCCTTAAGGCCACAC TGGCATCTCCCTGACCTTCT CCAGGGACAGAAGCAGGAGT AAGTTTCTC	NM_000961		Prostaglandin I2 (prostaglyclin) synthase
L23	671	TATATTGTTGAAGAATGGACG GGACCCTGGGGAAGCGCGG CCAGATATCACCCACCAGAG TTTGCTGAT	NM_006331	C2F	C2f protein
L24	672	GAAAGACCAGTAGACGCTCC TCTACTCTTTGAGACATCACT GGCCTATAATAAATGGGTAA TTTATGT	AK023419	RPL37a	Ribosomal protein L37a
M01	673	AAAAACGCTGAGTTGTGAAG TCCAATCAGGCACTTCTAACT CACCCCAAGCTCGCCATCTG GAAAAACA	NM_004576	PPP2R2B	M - Protein phosphatase 2 (formerly 2A), regulatory subunit B (PR 52), beta isoform
M02	674	ATTAGGGTTGGCATTCCCTAG CAGAAGAACCCACTTCCCTGC TTAGTTGAGATAGTTGAATCT AGCATTCG	NM_002717	PPP2R2A	M - Protein phosphatase 2 (formerly 2A), regulatory subunit B (PR 52), alpha isoform
M03	675	ATGGAATTAGATGACACTTTA AAATATTCCCTTCCCTCAATTT GACCCGGCGCCTCGTCGTG GTGAGCCT	NM_004156	PPP2CB	M - Protein phosphatase 2 (formerly 2A), catalytic subunit, beta isoform
M04	676	AACCAGTTCATTGCATGCTGA AGCGACATTGTTGGTCAAGA AACCAGTTTCTGGCATAGCG CTATTTGT	NM_002715	PPP2CA	M - Protein phosphatase 2 (formerly 2A), catalytic subunit, alpha isoform
M05	677	TTGGAGGAAAATCACCTGGG GGGAGGGGACTTCTTGTGTT AAGAGCAAGTGCAGGTATGA AATGCCAAG	NM_002719	PPP2R5C	M - Protein phosphatase 2, regulatory subunit B (B56), gamma isoform
M06	678	TGTAGCCACATCTCTCCCGC TCCCTAAGGGTAACCTAGCC AATGGAAGCTGGCCTTTGGG TAGGTGCTG	NM_021131	PPP2R4	M - Protein phosphatase 2A, regulatory subunit B' (PR 53)

M07	679	AGCAACTCCTTACTTCGGTTC CTCTGATTTCAAGGCCATATT TTAAAAATCAAAGGCACTG TGAAC	NM_005502	ABCA1	M - ATP-binding cassette, sub-family A (ABC1), member 1
M08	680	GAGAGTAGTTCAGACACGGA AAGAAGAGCCTCTGCCCCCG GCCACGAGCCAAAGCATTCC GACCTTCTAC	XM_171248	LOC256664	M - LOC256664
M09	681	AGGTATGTGCAGTTCGCCGGC CCCTGCCACCCAGCCTCATG CAAGTCATCCCCGACATGAC CTTCACGACC	XM_029744	PPP2R2C	M - protein phosphatase 2 (formerly 2A), regulatory subunit B (PR 52), gamma isoform (PPP2R2C)
M10	682	CACTGGGCCTTCCAACCTTG CTGGCAAGCTCTGGTAACCT CCCTGACTGTGGATCTTATAT AAAATCTCA	NM_002718	PPP2R3A	M - protein phosphatase 2 (formerly 2A), regulatory subunit B", alpha (PPP2R3A)
M11	683	TTCAGTCATAGTGGGCGGTA CATGATGACCAGAGACTTAC CTGTCCGGTGAAGGTGTGGGA CCTCAACATG	NM_018461	MDS026	M - uncharacterized hematopoietic stem/progenitor cells protein MDS026 (MDS026)
M12	684	CAGGCTGGCAGAGGGGCTG GTGCCCTGGAGAAAATAAG AGAAGGCTGGAGAGAAGCC GTGCTTGGTGAA	AF250238	ABCA7	M - macrophage ABC transporter (ABCA7) mRNA
M13	685	AGCAGTCACACGAGGCAGAA AAGTGCAGAAGGAAGGGAAG ATCAGCTATGCCACTTTGTC TGTTTTT	NM_013239	PR48	M - Protein phosphatase 2A 48 kDa regulatory subunit
M14	686	CCACGAACCCACAGCGCAA TCAACACGTTCTGTGAATAA ATAAAAGTTTATCATTCCGTA CAAACGCA	XM_210090	LOC286529	M - similar to hypothetical protein
M15	687	AGCACAGCAGCATCTTCAA CATGTACAAAATCGATTGGCT TTAAACACCCTTACATACCC TCCCCC	NM_000612	IGF2	insulin-like growth factor 2 (somatomedin A) (IGF2)
M16	688	ACTACCCCTGATCCTTACGCT AACATTAGTCTGGATGGTGA GACGTTCCCTTTGGACCGG GATTTCA	NM_001618	ADPRT	ADP-ribosyltransferase (NAD ⁺ ; poly (ADP-ribose) polymerase)
M17	689	CTTTATGCATAAAACCCAG CTAGGACCATTACTGCCAGA GAAAAAATCGTATTGAATGG CCATTTT	NM_012238	SIRT1	Sirtuin silent mating type information regulation 2 homolog 1 (S. cerevisiae)
M18	690	CTGTGGCTAAGTAAACCATA CCTAACCTACCCAGTGTGG GTGTGGCCTCTGAATATAA CCACACCC	NM_012237	SIRT2	Sirtuin silent mating type information regulation 2 homolog 2 (S. cerevisiae)
M19	691	ACTGTAACATTTGGGGGGTG GGCCAGGGAGGAAAAGTAAC AATAGTCCACATGTCCCTGG CATCTGTTT	NM_002140	hnRNP K	Heterogeneous nuclear ribonucleoprotein K (HNRPK)
M20	692	AGATCACATGACCTTCTGTC AGCGGGTGAAGAACATGCTC ATTGCCTTTTACAGAACCTT CTGTGCCA	NM_000463	UGT1A1	UDP glycosyltransferase 1 family, polypeptide A1
M21	693	CGGAAGGGAGAGCAGGGGA GAGAAGGCCTCATCTCTCTA TATTTATACATAACCCGGGG AAGACACAG	NM_006819	STIP1	Stress-induced- phosphoprotein 1 (Hsp70/Hsp90-organizing protein)
M22	694	CACCCTACTCTGAATGCAGA TGACCAAGAATGCAAACGAA ATCTCAGTGATATTGACCAGA GTTTCGAC	NM_000051	ATM	Ataxia telangiectasia mutated (includes complementation groups A, C and D)
M23	695	GTTTCTGAGAACATTCCTGA TCCTACATCATGGTACAGTAG TAGATCAGCTTACTGCCGTTT CACTGC	NM_001184	ATR	Ataxia telangiectasia and Rad3 related

M24	696	GCCTGGGGGCAGCCTCTCC CCAGCCTCCCCGTGCCAAA ATCTTTTCATTAAGAATGTTT TGGAACCTTT	NM_005572	LMNA var2	Lamin A/C (variant 2, C)
N01	697	GTGCGCTCAGTGACTGTGGT TGAGGACGACGAGGATGAG GATGGAGATGACCTGCTCCA TCACCACCAG	NM_170707	LMNA var1	Lamin A/C (variant 1, A)
N02	698	GATGCTGAGAACAGGCTGCA GACCATGAAGGAGGAAGTGG ACTTCCAGAAGAACATCTACA GTGAGGAGC	NM_170708	LMNA var3	Lamin A/C (variant 3, Adelta10)
N03	699	CCTGGCCTGCTCACCAACAC CATGGATGTGTTTGTCAAGG AGCCCTCCTTTGATTGAAAA ATTTTGAAC	NM_006904	DNAPK	Protein kinase, DNA-activated, catalytic polypeptide (PRKDC)
N04	700	TGTATGTGTTGTAAGTGTGAA GCCAGAATTAAGCTAGTAGT AGAAAGCTCAGCAGACGACC TTCGAGCAT	in M20324	E7	Human papillomavirus E7
N05	701	GGAGAGGGCGCTCCTCTCTG CACACCTACTAGTCACCAGA GACTTTAGGGGGTGGGATTC CACTCGTGT	NM_002165	ID1	Inhibitor of DNA binding 1, dominant negative helix-loop-helix protein
N06	702	CATCTCCCGGAGCAAACCC CTGTGGACGACCCGATGAGC CTGCTATAACAACATGAACGA CTGCTACTCC	NM_002166	ID2	Homo sapiens inhibitor of DNA binding 2
N07	703	CCCTGGGGTCAAGAAATTAC TGCCCCACTTGTCAAGTTCA GCCACCATCTGTTTGAACAT TATATGAA	NM_005537	ING1	Inhibitor of growth family, member 1 (p33)
N08	704	TGCGGCGGTATCTGACCTCA GAGGACAGGAACACCACCA GCTCTTCGATCTGATTGAAAG CATGCTAG	NM_003993	Clk2	CDC-like kinase 2
N09	705	GTGATATCAACCCAAGGTCC AAAGCCAATGAGAAGCTCAC AGCTAATGCAGAGCAGCGGC CGCTCTGGA	NM_002518	NPAS2	Neuronal PAS domain protein 2
N10	706	GGAGGGACTTTGTTTCAGGAA GAAATCCGTGTCTCCAACCA CACTATCTACCCATCACAGAC CCCTTTCC	NM_002084	GPX3	Glutathione peroxidase 3 (plasma)
N11	707	GGCAAGACCCGAAGTAAACTA CACTCAGCTCGTCGACCTGC ACGCCGATACGCTGAGTGT GGTTTGCGG	NM_002085	GPX4	Glutathione peroxidase 4 (phospholipid hydroperoxidase)
N12	708	ACAGCGCAATATCCTGAAGT AAATGCACTCCAGGAGGAGC TGAAGCCCTATGGTCTAGTT GTGTTGGGC	NM_001509	GPX5	Glutathione peroxidase 5 (epididymal androgen-related protein)
N13	709	CTCAGCGCCGGGGCTTCACC AAGACCTACACTGTTGGCTG TGAGGAATGCACAGTGTTC CCTGTTTAT	NM_003254	TIMP1	Tissue inhibitor of metalloproteinase 1 (erythroid potentiating activity, collagenase inhibitor)
N14	710	GGATCCCTCAACCAAGAAGA ATGTTTATGTCTTCAAGTGAC CTGTACTGCTTGGGACTAT TGAGAAAA	M35878	IGFBP3	Insulin-like growth factor binding protein 3
N15	711	AATGTTCTTGGCCCATCATGA CATTGGGTAGCATTAACTGTA AGTTTTGTGCTTCCAAATCAC TTTTTG	NM_003406	YWHAZ	Tyrosine 3-monooxygenase/tryptophan 5-monooxygenase activation protein, zeta polypeptide (14-3-3)
N16	712	ATTCTCGTATCCAACCCAAG GACCTTTTGAATGACTGGG	NM_002662	PLD1	Phospholipase D1, phosphatidylcholine-specific

		GAGGGCTGCAGTCACATTGA TGTAAGGAC			
N17	713	GACAGAGACTCAGATGAGGA CAGAGTGGTTTCCAATGTGTT CAATAGATTTAGGAGCAGAA ATGCAAGG	NM_000602	SERPINE1	Serine (or cysteine) proteinase inhibitor, clade E (nexin, plasminogen activator inhibitor type 1, PAI1)
N18	714	AAATTGGTTTTGGATAAGTTT GAGCCCTTGACCTTAATTTCA TTGCTACCACTCTGATCTCTT AGCACA	NM_002048	Gas1	Growth arrest-specific 1
N19	715	CAGACGATGAGACCGACGAT CCCAGGACGTATCAGAAATA TGGTTACATTGGAACACATGA GTACCCTC	NM_016816	OAS1	2',5'-oligoadenylate synthetase 1 (40-46 kD)
N20	716	GCATGCTCAAGTTTGAGAAC CGCTGCTCTCATAGACTGCT CCTCCAAGGGGAAGCAGTGT GGAACAGCA	NM_033238	PML	Promyelocytic leukemia
N21	717	TGACACAGTTGTAGGGTTAC AGAGACCTATGTAAGAATTC GAAGACCCCTGACTCATCAT TTGTGGCA	NM_004938	DAPK1	Death-associated protein kinase 1
N22	718	GCATCTTTTATAGACGCTCTT TTCTAAGTGGCGTGTGCATA GCGTCCTGCCCTGCCCTCGG GGCCTGT	NM_005157	ABL1	V-abl Abelson murine leukemia viral oncogene homolog 1
N23	719	CAGAAATGATTGTTAAAATTC TCCCAACTGGTTGACCTTT GCAGATACCCATAACCTATGT TGAGCCT	NM_005180	BMI1	B lymphoma Mo-MLV insertion region (mouse)
N24	720	CGATGAGGACGAAGACGACC CTGACAAGCGCATCTCGATC TGCTCCTCTGACAAACGAATT GCCTGTGA	NM_004964	HDAC1	Histone deacetylase 1
O01	721	GAGATGAAGATGGAGAAGAT CCAGACAAGAGAATTTCTATT CGAGCATCAGACAAGCGGAT AGCTTGTG	NM_001527	HDAC2	Histone deacetylase 2
O02	722	TTTGCCTTTAGGATTCTAGAC AGACCTAAGGGAAAAAGAAC TGAAAACATATTTGCCCCCA CCCCAC	AF130111	HDAC3	Histone deacetylase 3
O03	723	AAGCCATTGGCTTGGAGATC AAGCTTTGTATGTTGGCCAAA GCCCCGAGAGATGCCTCAGC TAAAATAA	NM_001379	DNMT1	DNA (cytosine-5-)- methyltransferase 1
O04	724	TGTCGAGTTACTGTGCACCA ACTATAAACTTTGAAAGGTC TGAGAGACATTTGCTTACAA ACTGGTA	AJ223333	DNMT2	DNA (cytosine-5-)- methyltransferase 2
O05	725	CTCCGCTGAAGGAGTATTTT GCGTGTGTGTAAGGGACATG GGGGCAAAGTGGAGTAGCGA CACAAAGTT	NM_022552	DNMT3A	DNA (cytosine-5-)- methyltransferase 3 alpha
O06	726	CCCAGATGAGAAGTCTGCTA CCCTCATTTCTCATCTTTTTA CTAAACTCAGAGGCAGTGAC AGCAGTCA	NM_006892	DNMT3B	DNA (cytosine-5-)- methyltransferase 3 beta
O07	727	TCAGCCAGGCAGATGCACTT GGCCAGGTTTCTGCGGATGC TTCTGCGACTCGCTGATGAG TTTGGTGA	NM_002875	RAD51	RAD51 homolog (RecA homolog, E. coli) (S. cerevisiae)
O08	728	GCTGCATAAAGTGTGTATGC CTGGTGCTTTGCGACTTGTG ACACGAGGTCACGTGTGGAA TTTTCCAC	NM_002879	RAD52	RAD52 homolog (S. cerevisiae)

O09	729	CATCGGAAAGCTGTGTGAGA GGCACTCTCACTCACTTATGT TTGGATCTCCGTAACACATT TTTGTTC	NM_006791	MRG15	MORF-related gene 15
O10	730	GTTGGGCACCCAGCTACTCA ACAAATTTGAGAGACCACAG TATGCCGAAATTTTGCAGAT TGTCGGAT	NM_006792	MORF4	MORF4
O11	731	CAGTTGTGGTCATCGGAGCT GTGGTCGCTGCTGTGATGTG TAGGAGGAAGAGTTCAGGTG GAAAAGGAGG	U29057	HLA-B7	Human MHC class I antigen HLA-B7 variant (HLA-B) mRNA
Elledge					
O12	732	CCTGCTTCCAGAATTTGAAA TCCTAGTTTCTCTCCTTCGT ATCCCGAGTCTGGGACACAA AACTCCG	NM_000244	MEN1	Multiple endocrine neoplasia I (Menin)
O13	733	TCCTCAGATTGCTGAATCCCA TCAGGCTGTTATTATGAAGGA ATTTGATTGCTTTGCTGCACA GCAGGA	NM_002031	FRK	Fyn-related kinase (RAK)
O14	734	GTCTCAGTCCAGCTTGCCG AACAGAGCTTCTGTTCTCCA GGGAGGAGGCGGACACGCT CAGGTTGAA	NM_003550	MAD1L1	MAD1 mitotic arrest deficient-like 1 (yeast)
O15	735	CAACCCGCCCTGAAGGTTA TTCCCAACACTTCAATGGCA ACAGCAACAAGTGGCACAGT TTTCAACT	NM_003616	SIP1	Survival of motor neuron protein interacting protein 1
Cohen Fibroblast					
O16	736	ACGTAGGGCTAAGGGAGGG GGCGCTGGAGCTTCCAACCC GAGGCAATAAAGAAATGTT GCGTAACTCA	NM_002256	KISS1	KISS-1 metastasis- suppressor
O17	737	TGAAAGTGAACACGAGGATG CAGTGCTTCTCGGTGACGGA GAGAGGCTCTTTCTACCCCG GGAGCGGCT	NM_000820	Gas6	Growth arrest-specific 6
O18	738	TTACAGTGGTTGATGCCTTAC ATGAAATACCAAGTGAATAAAG GTGAAGGTGCCGAGCTATAA ACCTCCA	NM_001553	IGFBP7	Insulin-like growth factor binding protein 7 (MAC25)
O19	739	CTCAGGGATGTCGGAGAGGA ATGACCTGTTTCTTTCTGAAG TGTTCCACCAAGCCATGGTG GATGTGAA	NM_002575	SERPINB2	Serine (or cysteine) proteinase inhibitor, clade B (ovalbumin), member 2
O20	740	GGAAATGCCTGCCAACTAAT CTTGATAGATTCTTTAAGGC ATTCCACTTAGCTTGCCAGTT GAGACAA	AL136877	SMC4L1	SMC4 structural maintenance of chromosomes 4-like 1 (yeast)
O21	741	TGGAGTTGGGGCTCTTGGCT TTCAGAGTTTGGTTAATCAGT GTTGATTCTAGATGATCAACA TAATGGA	NM_003472	DEK	DEK oncogene (DNA binding)
O22	742	CCAGTCTCGCCGGCCGACGA CAGCCTGAGCAACAGCGAGG AAGAGCCAGA	NM_000474	TWIST	Twist homolog (acrocephalosyndactyly 3; Saethre-Chotzen syndrome) (Drosophila)
O23	743	GGAAGATTCAGCTAGTTAGG AGCCATTTTTCTTAATCTG TGTGTGCCCTGTAACCTGAC TGGTTAAC	NM_005228	EGFR	Epidermal growth factor receptor (erythroblastic leukemia viral (v-erb-b) oncogene homolog, avian)
O24	744	CCTGACCATCTGACCAGTTG CGTCCGGCCTGATGTCCGTG TTTCTCCGAGTTTCAGTCAGA ACTGTTTG	NM_006209	ENPP2	Ectonucleotide pyrophosphatase/phospho diesterase 2 (autotaxin)

P01	745	CATGCCCCAGAAAGGGATGT ATGTCGCTGTCCAAGAGAAG GCTGTGGAAGAACCTATACA ACTGTGTTT	NM_002097	GTF3A	General transcription factor IIIA
Cohen HMEC					
P02	746	TGATAGTGTGGTTTATGGACT GAGGTCAAAATCTAAGAAGTT TCGCAGACCTGACATCCAGT ACCTGA	NM_000582	SPP1	Secreted phosphoprotein 1 (osteopontin, bone sialoprotein I, early T- lymphocyte activation 1)
P03	747	CGCTTGCTATTTATTTTACAA ACTGGACTGGCTCAGGCAGG GCCACGGCTGGCTCCAGCT GCCGGCCC	NM_004207	SLC16A3	Solute carrier family 16 (monocarboxylic acid transporters), member 3
P04	748	CCCCCCAGCCTGGCCCCG GCCTTTATGTTTTTTGTAAGA TAAACCGTTTTTAAACACATAG CGCCGTGC	NM_002135	NR4A1	Nuclear receptor subfamily 4, group A, member 1
P05	749	CCGTCTCTGCTTATCCGTTAG CCGTGGTGATTTAGCAGGAA GCTGTGAGAGCAGTTTGGTT TCTAGCAT	NM_002462	MX1	Myxovirus (influenza virus) resistance 1, interferon- inducible protein p78 (mouse)
P06	750	CAAGCTCCTGCCACGGTCTT GAAGTTCTGTTCTTATGCTCT CTGCTCACTGGTTTTCAATAC CACCAAG	NM_000240	MAOA	Monoamine oxidase A
P07	751	AGACTTGGGTAAGCTCTGGG CCTTCACAGAATGATGGCAC CTTCCTAAACCCTCATGGGT GGTGCTGA	NM_002083	GPX2	Glutathione peroxidase 2 (gastrointestinal)
P08	752	TGACCGGCAAGGAGCTCCGA GTTGCCACCCAGGAAAAAGA GGGCTCCTCTGGGAGATGTA TGCTTACTC	NM_004867	ITM2A	Integral membrane protein 2A
P09	753	TGACATGCAAGATGATTTTAT CTCTCCATGTGGGCCTGCA GGCAAGTCATGAGAGAGTTT GGCACCAA	NM_001785	CDA	Cytidine deaminase